



University of Évora

ARCHMAT

(ERASMUS MUNDUS MASTER IN ARCHaeological MATerials Science)

Mestrado em Arqueologia e Ambiente

6<sup>th</sup> Century BC Glass Beads from Southern Ukraine: Raw  
Materials and Technology

Oleh Yatsuk

Professor José Mirão (University of Évora)

Doctor Pedro Barrulas (University of Évora)



Évora, October 2018





To my parents

## Acknowledgements

This work was possible only with help of great number of people. Here the author will make an attempt to mention and thank to at least the half of them. The idea is the essence of any undertaking and there would be none if not the counsel and help of my former supervisor from Odesa I.I. Mechnikov National University (Ukraine) Oleh Lugovyi who suggested places to search and people to talk about the topic. Following his lead, it was great pleasure to talk again with Dmytro Kiosak from same university who later took part in our small sampling expedition. In this way of search, it was advised to address Anjelika Kolesnichenko who is associate of Odesa Archaeological Museum of National Academy of Sciences of Ukraine.

The author is deeply grateful to her most of all for her trust and will to make it real. She offered very interesting material of significant importance and helped to develop the first grasp of the problem. Her input is also measured with amount of information provided by her to establish archaeological context of the site and artefacts. We forgot to mention her participation in sampling of sediments and showing the archaeological site of Yahorlyk. Portion of thanks belongs to Dr. Bruyako, the Odesa Archaeological Museum director, who kindly allowed to bring samples to Portugal.

Regarding the sand collection, we would not go far without help of Serhii Kadurin whose advises were needful to establish representative set of sampling areas. Sand collection was not a pleasant work. It was great to have Ivan Ponomarov and Yurii Ponomarov helping with that. It was long way and lots of pits, but we were through only within two days because of them. The most hospital Zhukov's family, who hosted us during the expedition. The fastest driver of Ivanivka village, who knew every turn and bump also deserves a big thank. All these people represent Ukrainian side of the project and all of them were incredibly helpful in their own way. Thanks go to my family and friends who forgive rare visits on the regular basis and whose emotional support is perceptible even thousands of kilometres away.

To supervisors who were so kind to take this project that was quite big and made so much more work for them to do. To main supervisor, Prof. Mirao, who was most helpful every time when we faced crossroads and whose decisions saved us from defeat. Thank You for faith in it, for so precious time and sorry for bringing more questions than answers. To the co-supervisor Dr. Barrulas, whose competence in ICP-MS let us all stand on the solid basis of data. Especially, for giving special skills of laboratory work. Sorry for panicking every time we have seen an obstacle.

If one set a task for himself to list all the big and small but so important things made by Mafalda Costa for this project, it would stretch for as many pages as this work has. Her experience with glass analysis that she generously has shared and skills of work with the equipment she translated cannot

be paid back easily. The author is indebted infinitely for her psychological support as well. Only thanks to her the work has been done in time.

People in Hercules laboratory who were great company all the time. Special thanks go to Luis for help with the preparation for the XRF analyses, Prof. Moita, Ana, Massimo and Yigit for answers to countless questions that aroused every day, Miguel for hand-grinding of some samples, Alvin for helping with TGA, Soraya for helping with fastest preparing of ICP-MS batch for analysis and all the good people who make this place great.

To all the ARCHMAT people that stayed in Evora, namely, Sima (here special thanks for days in library), Sriradha, Mercedes, Arif, Roshan, Ilya, Alvin and those overseas who remained in contact. They are the best group of people that author had a pleasure to study with. Thank You for two years.

And the last but not the least, to the ARCHMAT consortium for covering all the laboratory expenses in the Hercules laboratory and personally its coordinator Prof. Schiavon for encouraging to bring self-developed project and its approval in the very beginning.

# TABLE OF CONTENTS

Acknowledgements .....	iii
Table of contents .....	v
List of tables .....	vii
List of figures.....	viii
Abstract .....	xiii
Resumo.....	xiv
CHAPTER I. INTRODUCTION .....	1
<b>1.1 General approach, aim and objectives of the study</b> .....	1
<b>1.2 Historical and archaeological context of the analyzed material</b> .....	2
1.2.1 Greek colonization and North Pontic steppe population .....	2
1.2.2 Origin of glass industry. Evidences on Glass production in Ancient Greece .....	5
1.2.3 Yahorlyk settlement .....	7
1.2.4 Archaeological typology of glass beads from Yahorlyk settlement .....	10
<b>1.3 Geological and environmental context of the possible raw materials</b> .....	13
1.3.1 Geological structure of Dnipro river estuary and surrounding formations .....	14
1.3.2 Main predetermining factors of sediment deposition in Dnipro river Estuary and North Black Sea region .....	17
CHAPTER II. METHODOLOGY OF THE STUDY .....	22
<b>2.1 Sampling</b> .....	22
2.1.1 Sampling of glass fragments .....	23
2.1.2 Sampling of sand .....	26
<b>2.2 Justification of selected methodology</b> .....	29
2.2.1 Methods of glass analysis .....	29
2.2.1.1 <i>Optical microscopy (Stereomicroscopy)</i> .....	30
2.2.1.2 <i>Scanning electron microscopy coupled with an energy dispersive spectrometer (SEM-EDS)</i> .....	31
2.2.1.3 <i>X-ray fluorescence (p-XRF)</i> .....	32
2.2.1.4 <i>Micro X-ray diffraction (<math>\mu</math>- XRD)</i> .....	33

2.2.1.5 Laser ablation inductively coupled plasma mass spectrometry (LA-ICP-MS) .....	34
2.2.2 Methods of sand analysis and corresponding sample preparation .....	37
2.2.2.1 X-ray diffraction (XRD).....	38
2.2.2.2 X-ray fluorescence (XRF) .....	39
2.2.2.3 Inductively coupled plasma mass spectrometry (ICP-MS).....	39
 CHAPTER III. RESULTS AND DISCUSSION .....	 42
 <b>3.1 Results</b> .....	 42
3.1.1 Glass analysis .....	42
3.1.1.1 Optical microscopy (Stereomicroscopy).....	42
3.1.1.2 X-ray fluorescence (Portable XRF) .....	47
3.1.1.3 Variable pressure scanning electron microscope coupled with energy dispersive X-ray spectrometry (VP-SEM-EDS).....	50
3.1.1.4 Micro X-ray diffraction ( $\mu$ -XRD).....	56
3.1.1.5 Laser ablation inductively coupled plasma mass spectrometry (LA-ICP-MS).....	57
3.1.2 Sand analyses and their interpretation .....	63
3.1.2.1 Powder X-ray diffraction (PXRD) .....	63
3.1.2.2 X-ray fluorescence (XRF).....	64
3.1.2.3 Inductively coupled plasma mass spectrometry (ICP-MS).....	67
<b>3.2 Discussion</b> .....	68
3.2.1 Glass batch .....	68
3.2.2 Technology of producing glass beads .....	72
3.2.3 Colour .....	74
3.2.4 Possible raw materials .....	77
 CONCLUSIONS AND FUTURE WORK .....	 85
REFERENCES .....	87
ANNEXES .....	I

## LIST OF TABLES

<b>Table 1:</b> Compositional analysis of sand from “Shabivske” sand deposit (Хлебников, 1988).....	20
<b>Table 2:</b> List of Yavorlyk glass samples.....	24
<b>Table 3:</b> Minimum recommended sample size for trace elements analysis based on the biggest estimated grain size in sediments and loose samples (Smodis et,al. 2003).....	27
<b>Table 4:</b> List of samples from the vicinity of the Yavorlyk archaeological site.....	28
<b>Table 5:</b> Instrumental settings for the analysis of Yavorlyk glass.....	36
<b>Table 6:</b> Instrumental settings for the analysis of sand samples.....	40
<b>Table 7:</b> The summary of stereomicroscope observations of the Yavorlyk glass artefacts. (the number of + corresponds to the relative amount of bubbles; *- the eye part is free of bubbles). ....	46
<b>Table 8:</b> The VP-SEM-EDS results of selected areas (%). (<DL - below detection limit).....	53
<b>Table 9:</b> Yavorlyk glass REE concentrations (ppm) (Ce/Ce* - Ce anomaly; Eu/Eu* - Eu anomaly).....	60
<b>Table 10:</b> The results of XRD analyses of Yavorlyk sand samples (+++++ - main constituent; ++++- very abundant; ++ - small abundance; + - very small abundance; Vtg. – vestigial; - - not detected). ....	64
<b>Table 11:</b> The average values of elemental concentrations of Yavorlyk sand samples obtained by XRF. ....	64
<b>Table 12:</b> Concentrations of trace elements in sand samples obtained by ICP-MS (ppm) (Ce/Ce* - Ce anomaly; Eu/Eu* - Eu anomaly). ....	67

## LIST OF FIGURES

- Figure 1:** Map of Greek colonies on Northern Black Sea coast circa 450 BCE Olbia and Berezan settlement (Borysthene on the map) are northernmost points on the Black Sea shore. (image MapMapster).....3
- Figure 2:** Greek colonies on the Banks of Dnipro-Bug estuary. 1 - Olbia (Ольвия); 2 - Berezan (Березань); 3 - Yahorlyk settlement (Ягорлыцкое) (Крижицкий, 1985).....4
- Figure 3:** The layout of Yahorlyk settlement: 1 – iron smelting furnace remains; 2 – iron melting furnace remains; 3-7 – bronze items and slugs finds; 8 – glass industry finds; 9 – ceramic furnace remains; 10-11 – lead items finds; 12 – surface ceramic finds. (Островерхов, 1981)..... 8
- Figure 4:** Blue round bead (Ya-1).....11
- Figure 5:** Eyed bead type 25 (Ya-12).....11
- Figure 6:** Bead type unknown (Ya-10).....11
- Figure 7:** Dark bead (Ya-9) .....12
- Figure 8:** Yellow biconical bead (Ya-21) .....12
- Figure 9:** Biconical colourless glass bead (Ya-18)..... 12
- Figure 10:** Main geological structures of Ukraine. Ukrainian shield is marked yellow (1); North-Black Sea depression is in pink (9) (Wikipedia). .....14
- Figure 11:** The transversal section of Dnipro mouth area. Quaternary depositions. Green: aI, aII – lower and middle Quaternary alluvial, alluvial-lake depositions of 3 and 4 terraces of Dnipro river; aIII – upper Quaternary alluvial depositions of 1 and 2 terraces of Dnipro river; aIV – Holocene alluvial depositions of Dnipro river mouth. Blue: LmIV – estuarine-marine depositions. Orange: vdI, vdII – lower and middle Quaternary aeolian colluvial depositions; vdIII – upper Quaternary aeolian-colluvial depositions, vIV – Holocene aeolian sands. Purple: pre-quaternary depositions (Novodran et al., 1978). .....15
- Figure 12:** Distribution of Litho-tectonic complexes over geoblocks of the Ukrainian Shield (Bobrov et al., 2006).....16
- Figure 13:** Geographical outline of the Dnipro mouth region. 1.- Dnipro-Bug estuary; 2 - Yahorlyk bay. Yahorlyk settlement is marked with orange arrow (Google)..... 18

<b>Figure 14:</b> Sand arenas in the Dnipro mouth region: 1. Kakhovka; 2- Kosachelagera; 3 – Oleshky; 4 – Chalbass; 5 – Zburjivska; 6 – Ivanivka; 7- Kinburn.....	19
<b>Figure 15:</b> The map with pointed places of sampling (left) and the table of sand samples with description (right).....	26
<b>Figure 16:</b> Photograph of the Qua-2 sampling pit. The 20 cm ruler is placed for the scale.....	27
<b>Figure 17:</b> Schematic layout of scanning electron microscope (Janssens, 2013). ....	31
<b>Figure 18:</b> Interaction of electrons with semi-infinite sample suitable for SEM (Janssens, 2013).....	31
<b>Figure 19:</b> Schematic drawing of handheld XRF device (Janssens, 2013).....	33
<b>Figure 20:</b> Schematic representation of $\theta/2\theta$ diffraction in Bragg-Brentano geometry (Birkholz, 2006).....	34
<b>Figure 21:</b> Schematic layout of LA-ICP-MS machine (Janssens, 2013).....	35
<b>Figure 22:</b> Stereomicroscopy images. a. surface of Ya-1 at magnification 50X; b. surface of Ya-2 at magnification 50X. Dark grains are marked with arrows.....	43
<b>Figure 23:</b> Stereomicroscopy images. a. Ya- 4 section surface at magnification 50X. An empty collapsed air bubble (left arrow); a bubble filled with quartz grain (right arrow); b. -Ya-5 surface at magnification 50X. ....	43
<b>Figure 24:</b> Stereomicroscope images. a. - Ya-11 white glass (50X); b. Ya-16 dark base glass (50X); c.-Ya-12 eye (50X).....	44
<b>Figure 25:</b> Stereomicroscope image of sample Ya-14 at magnification 125X; bubbles underneath the surface are marked with arrows. ....	44
<b>Figure 26:</b> Stereomicroscope image of sample Ya-9 (50X); the iridescence effect is marked with an arrow. ....	44
<b>Figure 27:</b> Stereomicroscope image of the rough surfaces of green non-beads: a. sample Ya-17 (125X); b. sample Ya-8 with some grains in the matrix (50X). ....	45
<b>Figure 28:</b> Stereomicroscope image of the light-colored layer of sample Ya-7. (magnification 50X).....	45
<b>Figure 29:</b> Stereomicroscope images. a. surface depositions on sample Ya-19 (120X), b. sample Ya-18 at magnification 50X.....	45

**Figure 30:** Stereomicroscope images. a. dark grain on the surface of sample Ya-22 (50X); b. slight roughness of sample Ya-20 with superficial deposits visible (50X) .....46

**Figure 31:** Yahorlyk glass Cu against Co binary plot. Every colour is attributed to a specific group. Sample Ya-5 is marked with the arrow. ....47

**Figure 32:** Yahorlyk glass Al against K binary plot. Two clusters can be noticed. Sample Ya-3 is marked with an orange arrow. ....47

**Figure 33:** Yahorlyk glass Al against Fe binary plot. Sample Ya-3 is marked with the arrow. Two groups can be noticed. ....48

**Figure 34:** h-XRF bi-plots. a - Yahorlyk glass Ti against Fe binary plot; two trendlines are represented with arrows; b - Yahorlyk glass Co against Fe binary plot. Ya-7 light side position is marked with the green arrow..... 48

**Figure 35:** Yahorlyk glass Ti against Zr binary plot; two trendlines are represented by arrows, samples from group 8 are in the circle. Sample Ya-23 is marked with the yellow arrow..... 49

**Figure 36:** VP-SEM images. a - the backscattered image of sample Ya-2 showing step structure inside the collapsed bubble; b. – Ya-1 backscattered image demonstrating the roughness of the surface (light spot is the zircon grain trapped inside one of the collapsed bubbles). ....50

**Figure 37:** VP-SEM images. a - backscattered image of the surface of sample Ya-9; b - backscattered image of the surface of sample Ya-14. ....51

**Figure 38:** The backscattered image of the surface of sample Ya-21. The fine cracks area by the edge.....51

**Figure 39:** Backscattered image of sample Ya-11 representing all three colours. the tilted lines are put to distinguish between them: blue-white - border between blue and white glass; white and dark - border between white and dark parts..... 52

**Figure 40:** VP-SEM-EDS data. a - map of Cu distribution on the surface of sample Ya-11; b - backscattered image of the same area. The blue eye can be identified by different texture and higher amount of Cu. ....52

**Figure 41:** Backscattered image of a tin inclusion found in sample Ya-10 and a table generated after quantification of EDS data..... 55

**Figure 42:** Backscattered image of monazite inclusion detected in sample Ya-15 and a table generated after quantification of EDS data..... 56

<b>Figure 43:</b> Backscattered image of apatite inclusion found in sample Ya-13 and a table generated after quantification of EDS data. ....	56
<b>Figure 44:</b> X-ray diffractogram of the sample Ya-7 (Light part): q- quartz; d-diopside; m - microcline; h- hematite.....	57
<b>Figure 45:</b> The LA-ICP-MS values of Yahorlyk beads binary plot. Na <sub>2</sub> O against MgO. Groups 1,3,7,8 and groups 2,4,5,6 cluster respectively. ....	58
<b>Figure 46:</b> The LA-ICP-MS values of Yahorlyk beads binary plots: a - Al <sub>2</sub> O <sub>3</sub> against Fe <sub>2</sub> O <sub>3</sub> ; b – K <sub>2</sub> O against MgO. The two groups can be noted. Sample Ya-8 is marked with the blue arrow (b). ....	59
<b>Figure 47:</b> The LA-ICP-MS values of Yahorlyk beads binary plots: a - TiO <sub>2</sub> against Fe <sub>2</sub> O <sub>3</sub> ; b – TiO <sub>2</sub> against Zr. ....	59
<b>Figure 48:</b> Linear plots of chondrite normalised values of REE determined for Yahorlyk glass fragments and divided by groups: a- group 1, b - group 2, c -groups 3 (Ya-14 and 15), 4 (Ya-10), 5 (Ya-9), d - group 6, e - groups 7 (Ya-18 and 19) and 8 (Ya-20, 21 and 23).....	61
<b>Figure 49:</b> IvQ-2 diffractogram: q- quartz, a -albite, m – microcline, r -rutile. ....	63
<b>Figure 50:</b> Yahorlyk sand binary plots: a - Na <sub>2</sub> O against Al <sub>2</sub> O <sub>3</sub> ; b - K <sub>2</sub> O against Al <sub>2</sub> O <sub>3</sub> , c – Fe <sub>2</sub> O <sub>3</sub> against MgO, d – Fe <sub>2</sub> O <sub>3</sub> against MnO. Plots c and d do not include Iv-S sample. ....	65
<b>Figure 51:</b> The linear graph of element concentrations in sand samples. Logarithmic scale. ....	66
<b>Figure 52:</b> ICP-MS results. The line graph of chondrite normalised values of REE of sand samples.....	68
<b>Figure 53:</b> Ternary plot of the system CaO-Na <sub>2</sub> O-MgO+K <sub>2</sub> O. Glass families are put after Gratuze, Janssens, 2004. Sample Ya-8 is marked with a green arrow. Sample Ya-6 is marked with a blue arrow. Data of the LA-ICP-MS analyses. ....	70
<b>Figure 54:</b> Yahorlyk glass scattered biplot of CaO against Sr. Data of the LA-ICP-MS analyses. ...	71
<b>Figure 55:</b> Yahorlyk glass biplots: a- CaO against Na <sub>2</sub> O; b- CaO against SiO <sub>2</sub> ; c - SiO <sub>2</sub> against Na <sub>2</sub> O. Clustering of groups 1,3,7,8 on one side and 2,4,5,6 on the other is observable. ....	72
<b>Figure 56:</b> Phase diagram of the system SiO <sub>2</sub> -Na <sub>2</sub> O-CaO (after Shugar, Rehren, 2002) and position of Yahorlyk samples on it. Group 6 (blue oval) temperature range is too high for ancient furnaces. Rest of the soda plant-ash groups (2,4 and 5) are also in the high range. ....	73

- Figure 57:** Proportion of Fe (expressed as ferric oxide) and Cu (expressed as cupric oxide) shown as the normalized to 100%. Cu is prevailing in blue coloured glass (samples 1-6 and blue parts of the eyes), Fe in green (samples Ya-7, Ya-8 and Ya-17). .....75
- Figure 58:** Comparison of appearance of two kinds of base glass that was used in eyed beads: a – Ya-16 (50X magnification); b - Ya-14 (50X magnification). .....76
- Figure 59:** The relationship between Ca and P oxides in the beads of group 2. Values of each oxide concentration together with calculated ratios and correlation coefficient are put in the table on the left. ....76
- Figure 60:** The concentrations of elements from La-ICP-MS analyses of Yahorlyk glass compared with such found in sands by means of XRF (orange lines for min and max value): a - Al<sub>2</sub>O<sub>3</sub> (the max value of sand is 10,8% - not depicted), b - TiO<sub>2</sub>, c - Zr. The groups: group 1 – Ya-1, Ya-2, Ya-4, Ya-5 and Ya-6; group 2 – Ya-3, Ya-11, Ya-12, Ya-13 and Ya-16; group 3 – Ya-14 and Ya-15; group 4 – Ya-10; group 5 – Ya-9; group 6 – Ya-7, Ya-8 and Ya-17; group 7 – Ya-18 and Ya-19; group 8 - Ya-20, Ya-21 and Ya-23. ....78
- Figure 61:** Chondrite normalised linear plots of Yahorlyk glass and sand: a - groups 1,3,7 in comparison to Qua sample of sand; b - group 2 in comparison to all the Qua subsamples; c - group 6 in comparison to Iv-S sample of sand; d - groups 4,5,8 in comparison to Qua sample of sand. The groups: group 1 – 1,2,4,5,6; group 2 – 3,11,12,13,16; group 3 – 14,15; group 4 – 10; group 5 – 9; group 6 – 7,8,17; group 7 – 18,19; group 8 - 20,21,23.....79
- Figure 62:** 1000\*Zr/TiO<sub>2</sub> against Cr/La binary plot of Yahorlyk glass (rounds) compared with the ones reported in Shortland et al. 2007. Nuzi and Tell Brak are Mesopotamian sites (squares) while Amarna and Malkata are Egyptian (triangles). Group 8 is in the blue circle. The orange line is separating groups 2 and 4 from the Mesopotamian samples. ....82
- Figure 63:** Binary plots of Yahorlyk glass compared with the ones reported in Shortland et al. 2007 and Blomme et al., 2017: a – Cs-La plot (group 8 is absent due to the absence of Cs values); b – Lu-Th plot with two different trend lines (one follows sand samples (blue arrow), another Pieria samples (orange arrow)). Pieria is a Greek site (diamonds). Nuzi and Tell Brak are Mesopotamian (squares) sites while Amarna and Malkata – Egyptian (triangles).....83

## **Abstract**

The aim of this study is to establish the nature of the remains of the glass industry found at the ancient Greek archaeological site on the Yavorlyk bay shore (North Black Sea region, Ukraine), dated to the 7<sup>th</sup>-5<sup>th</sup> centuries BCE. A multi-analytical, non-destructive approach that compares the chemical and mineralogical composition of glass fragments with that of sand collected in the vicinity of the archaeological site was used in order to determine the local or non-local origin of the glass artefacts. To this end, a comprehensive characterization of all the materials was performed by means of XRF, VP-SEM-EDS, LA-ICP-MS and XRD. In parallel, an attempt was made to reconstruct the manufacturing process of the glass objects with an emphasis on the recipe used and how the colour was achieved. The results will contribute important new information to the literature concerning glass circulation in the Black Sea region.

## **Resumo**

Com esta dissertação pretendeu-se determinar a natureza dos objetos remanescentes da indústria vidreira encontrada no sítio arqueológico localizado na costa da baía de Yahorlyk (região do Mar Negro Norte, Ucrânia), datado dos séculos VII a V a.C. e com ocupação Grega. Neste estudo foi usada uma abordagem multi-analítica e não-destrutiva, que permitiu comparar a composição química e mineralógica dos fragmentos de vidro com a da areia recolhida nas proximidades do sítio arqueológico, a fim de determinar a origem local ou não-local dos artefactos de vidro. Para este fim, os materiais foram caracterizados por FRX, MEV-EDS, LA-ICP-MS e DRX. Paralelamente, tentou-se compreender a técnica de fabrico dos objetos de vidro, dando particular ênfase ao processo de manufatura usado assim como na forma de obtenção da cor. Os resultados contribuirão com novas informações sobre a circulação de artefactos vítreos na região do Mar Negro.

## CHAPTER I. INTRODUCTION

### 1.1 General approach, aim and objectives of the study

Every day we are more and more away from previous societies that dictated their reality to people who lived and worked thousands of years ago. Modern researchers have to order and reproduce tangible and intangible elements of culture by putting them into a certain time frames, organizing our system of knowledge about the past. These words are particularly concerning to archaeologists, who often deal with material remains not mentioned in ancient texts. However, it is possible to extract information revealing details of the past that were left out by the ancient societies.

Archaeometric studies greatly extend the methods to reconstruct the reality of ancient people, analysing artefacts using the tools of physical and live sciences. This study is intended to shed light on some aspects of the old technology, and, provided that its results are placed into a greater picture, to clarify some details of relations between different groups of the ancient populations. Such ambitious goal requires study the objects at different angles, with the maximum coverage of all sources of information that the researcher may have at his disposal.

This implies the need for an interdisciplinary approach, because only by combining historical, archaeological, technological and raw materials contexts it is possible to fulfil the purpose of the work. Glass beads and other fragments of the manufacture process, presumably, from the time of the Ancient Greek colonization of the North Black Sea coast constitute the body of materials to be studied. Technology comes to a certain area with people who distribute it and are more likely to be involved into the production of these goods. We can definitely say that all the information obtained during the study will also characterize different details of the ancient society life, which is, probably, not possible to achieve in another way.

This chapter is meant to show the objects of the study in the entirety of the context of the archaeological site. The context of the finds is the nameless settlement on the shore of the Yavorlyk Bay (Yavorlyk settlement in the historiography (Островерхов, 1974)) with the remains of glass production as well as synchronous archaeological sites (Greek colonies, such as Olbia, Berezan settlement) that could have connections with it. The historical context is the process of the Ancient Greek colonization and the interaction of the foreigners with the local nomadic population. Above that, it seems useful to add all the information about glass production that we can find in historical sources. What is referred to herein as the raw material context concerns mostly questions about the origin of the main ingredient for making glass, namely sand. Information about the regional geology, as well as the processes of sediments deposition in a certain area of the Dnipro river estuary and the

Yahorlyk Bay will help to answer one of the most important issues raised during the study, namely, were these fragments of glass were made exactly?

Two other chapters are dedicated to the experimental part of the study and to the interpretation of the results aiming to conclude about development of glass manufacturing technology on the North Black Sea coast. Among other research objectives, we distinguish gathering information about other components of the glass material, such as flux, colorants, modifiers, etc. which is extremely important for the characterization of the manufacturing technology. To achieve these goals, it is necessary to use various analytical methods to characterize the materials. These methods and the results of experiments will be discussed in the relevant section. But all the information that we initially have in our disposal should be given in the first place.

## **1.2 Historical and archaeological context of the analyzed material**

In this section, an attempt will be made to reproduce the historical and technological conditions for glass production on the northern shore of the Black Sea. It is necessary to give a very brief description of the archaeological site of Yahorlyk and its place in the political and economic landscape of the region. It is proposed to move from general to partial, namely after the characterization of some features of the region, proceed to the characterization of the settlement itself. The accent will be on the archaeological evidences of glass production and its final products.

### **1.2.1 Greek colonization and North Pontic steppe population**

Relevant details of archaeological context are to be sketched roughly here. Without aiming to entirely comprehend the phenomenon of Greek colonization, we will be satisfied only with the guidance on its important details for the further presentation of the material. A small reconnaissance in literature on the Ancient Greek colonization shows that this movement was quite large (Gagarin, 2010). The colonies of individual Greek poleis were based on the remote shores of the Mediterranean (Morris, 1900). The Greeks did not neglect the Black Sea as well (Иессен, 1947; Гайдукевич, 1955; Morris, 1900).

The colonization process of distant lands from Greece itself has begun in the eighth century BCE, since the founding of Al-Mina (White, 1961), which has been a trading port with the Phoenicians and Cumae (Graham, 2001), that has played the same role in relations with the Etruscans. If we focus on the Black Sea region, we must agree that the development of the colonies was carried

out later, due to some deterrent factors, such as the difference in climate and the difficulty of overcoming the straits. The oldest known settlements to occur are, most likely, only from the seventh century BCE (Graham, 2001).

Typically, the formation of the colony was preceded by close trade links. As an evidence of such connections on the northern Black Sea coast one can mention the limited number of fragments of Greek ceramics from the graves of noble Scythians (Tsetschladze, 1998). This nomadic population was inhabiting the surrounding steppes. The reasons for the foundation of colonies could be different. In historiography, trade interests are mentioned as the main goal of the creation of colonies. Indeed, quite often, the emporions (Roberts, 2007) (*εμποριον* - gr. more or less permanent Greek merchant point) were followed by the creation of apoikias (Roberts, 2007) (*αποικια* - gr.), that were independent settlements "homes out of the home" for emigrants from the Balkans or Ionia. However, there are discussions about the specific content of these terms (Tsetschladze, 1998). Such settlements helped to transfer "production facilities" closer to the consumers of Greek goods - the surrounding tribes, or proto-state formations. Often, lack of fertile land in Greek realms, which forced a part of the grown population to settle on another place is mentioned. Sometimes researchers state political motives to establish a polis different from the metropolis political system. Most researchers of this issue agree with the complexity of its causes (ЛАПИН, 1966; Гайдукевич, 1955; White, 1961; Graham, 1999).

It was widespread practice before leaving Greece to consult with the Delphic oracle. Usually, the "expedition" was led by the oikist - a man who organized the life of the colony and the distribution of new land in the first years of its existence (Graham, 1999).

On the colonization of Northern Black Sea region. Among the colonies founded here in the 7-6<sup>th</sup> centuries. B.C. the settlement on the island of Berezan was probably the first permanent settlement of the Greeks on the North shore of Black Sea. Dwellings at the place of Olbia, Tyras, Panticapaeum



**Figure 1:** Map of Greek colonies on Northern Black Sea coast circa 450 BCE Olbia and Berezan settlement (Borysthenes on the map) are northernmost points on the Black Sea shore. (image MapMapster).

were also founded one of the first in the region (Гайдукевич, 1955).

Regional leadership in the colonization process belongs to the Ionian Greeks, in particular, those from Miletus. According to Pliny the Elder (1<sup>st</sup> century CE), Miletus founded more than 90 cities (Pliny, 5.31). Such a number of incepts creates doubts about the veracity of

his words, but it has been established



With the foundation of Olbia, the settlement at Berezan began to lose its significance, eventually being incorporated into the agricultural area (*chora*) that was under control of the Olbian polis (Christodoulou, 2016; Крижицкий 1985). Olbia was one of the largest centres on the northern coast of the Black Sea. At its heyday, the city area reached 50 hectares, and the population 15 thousand people (Крижицкий, 2010). The surrounding lands on the banks of the Dnipro and Bug estuaries were pointed with numerous agricultural settlements, even at the early stages of the city-state existence (Крижицкий, 1989). It is clear, that local artisans produced goods both for domestic needs and for sale. Expectedly, traces of metalworking were found in the region (Лапин, 1966). The question of Olbia's trade ties with the local tribes and Greece itself is controversial (Noonan, 1976; Одрін, 2010), but there is no doubt that intermediary trade, as well as trade of polis' own goods, was taking place from the very first years of settlements (Гаврилюк, 2008).

This is confirmed by the finds in Scythian burial mounds (Гречко, 2010). The early start of casting, and then minting of their own coins in the sixth century BCE also partially confirms that fact (Каришковський, 1988; Зограф, 1955). Thus, the Yahorlyk settlement, most likely, was one of many settlements based on the territories adjacent to the Dnipro and Bug estuary, though its location is somewhat secluded, its connection with Olbia and Berezan is undeniable. One of the arguments supporting the statement above is the disappearance of many settlements of the Olbia's *chora* in the 5<sup>th</sup> century BCE and the accumulation of population in the city coincides with the disappearance of the Yahorlyk settlement (Крижицкий, 1989; Островерхов 1981).

Thus, the world of artefacts considered in this study emerges in its general features as a zone of cultural, but not to a lesser degree technological contact between the Greek settlers and the steppe population of the northern Black Sea coast. In this paragraph, we do not discuss the finds from Yahorlyk settlement, mentioning here only its position and period of existence. The site description will be given below. The technological level of the Greeks in the field of glass production, seems more convenient to describe in the next section.

### 1.2.2 Origin of glass industry. Evidences of Glass production in Ancient Greece

In this section, the attention will be focused on the evidences of what the ancient populations could have known about the glass production and what were the artisans' traditions in Ancient Greece. The need for it arises from the need for gathering contextual information about the glass beads and as we already mentioned the ones from the Yahorlyk settlement are associated with the Greek context (Островерхов, 1974). It is also important to make reconnaissance in the mass of historical sources, and to reveal written information about the old techniques of glass manufacturing.

In the literature we can find different definitions of the term “glass”. Here, we define glass as an artificially vitrified material, which in general corresponds to the definition of Paul: “glass is a state of matter, which maintains the energy, volume and atomic arrangement of a liquid, but for which the changes in energy and volume with temperature and pressure are similar in magnitude to those of a crystalline solid” (Pollard, Heron, 2008). Such a broad definition allows to call glass such materials that are commonly discriminated in archaeology, namely glass, glaze and enamel. Even natural “glasses” will be included (Goffer, 2007). Such terminological differences hinder interdisciplinary dialogue.

In the framework of this paradigm, the first vitreous material made by man can be attributed to third millennium BCE. However, the origin of glass is difficult to locate in a specific place between Egypt and Mesopotamia (Henderson, 2007; Галибин, 2001; Reren, Freestone 2015). We will not go into this discussion, but we consider it worthwhile to note that the history of the vitrified materials production by the 6<sup>th</sup> century BCE was already up to 2000 years old. Batch formulas have already been tested and different methods of glass production have been known, as well as various techniques for the shaping objects. It should be mentioned that beads are the oldest artefacts made of glass, apparently due to the simplicity of their manufacturing (Henderson, 2013).

The oldest list of ingredients for making glass has survived from the second millennium BCE (Brill, 1972). Detailed studies of the Mesopotamian cuneiform plates were made by Oppenheim. His work showed knowledge of ancient people about the addition of various fluxes, effects of metals as arsenic (As), antimony (Sb) and lead (Pb) were mentioned (Oppenheim, 1973). However, the author himself acknowledges the uncertainty of the terms used. The middle of the second millennium BCE is thought the time when the technological achievements of ancient people have made technology more elaborated and widespread in the world (Oikonomou et al., 2012).

Greek artisans were using mostly recipes borrowed from the Middle East and Egypt, including the addition of natron (Egypt) or plant ash (Syria, Mesopotamia) as the main flux (Oikonomou et al., 2012). Beads were the most abundant category of products realised in glass. The beginning of the glass industry in Greece dates back to the times of Mycenaean civilization (Kalliopi, 2006). After the Dorian invasion, the technology, probably, has been lost and reintroduced to these territories only before the beginning of the archaic period (Oikonomou et al., 2012).

Unfortunately, we do not have much information in written sources about this period, but, as is known, glass played a significant role for making jewellery. It is mentioned among the offerings in the Athenian temples from the classical period, where it is sometimes called the “poured stone” (Stern, 2007), famous are cases of the combination of glass and precious metals such as gold or silver in jewellery (Stern, 1999). This leads to the conclusion about the high value of glass among jewellery production materials.

Quite often, in ancient times, the production of glass and the manufacturing of goods were different types of craft activities that were not necessarily placed under the same roof. Glass chunks or ingots were traded in the Mediterranean since ancient times, and from the classical times the division of glass production sites and workshops, where the final products were made, was the most common practice. In Classical period, for example, no glass production traces were found on the territory of Greece, whereas the number of secondary workshops was large (Stren,1999; O’Hea, 2005).

Unfortunately, we do not have information about the glass batch formulas or at least the description of products that were dated to 7<sup>th</sup> – 6<sup>th</sup> century BCE from Greece itself or its colonies. The technology was relatively well described in Roman times (Stern,2007), in particular, by Pliny the Elder, which, as it is widely known, wrote his *Historia Naturalis* in the first century CE. By this time, technology has been already at the high level of standardization, the market has grown and connected a dense network of secondary artisans’ workshops, having only a few primary workshops, working with raw materials and producing large quantities of glass (Pliny, 36).

Due to the scanty written evidences on the development of the glass industry in the archaic period in ancient Greece, archaeology and, especially, archaeometry can fill the gaps in our knowledge of this important milestone in the history of civilization. Taking into account the information above, the Yahorlyk settlement and the information that we can collect based on archaeometric methods is going to be very valuable for understanding the whole situation about "flows" of glass in the ancient world. What type of workshop existed on the shore of the Yahorlyk Bay? What "recipes" were used by ancient artisans? What was the purpose of creating a workshop of glass production in such a remote region? These questions cannot be answered without reference to the archaeological context of the site itself, to which we proceed in the following section.

### 1.2.3 Yahorlyk settlement

The Yahorlyk settlement, located on the shore of the bay that gave its name to it<sup>1</sup> 4 km north-east away from the Ivanivka village of the Gola Prystan district, Kherson region, Ukraine. Discovered in 1973 (Островерхов, 1974), archaeological activities were conducted intermittently until 1977. Excavations were not systematic. The vast majority of items were collected from the surface (Загний,

---

<sup>1</sup> No historical sources mention the settlement, thus impossible is to say what was its original name and whether it was called in a specific manner at all.

1977; Буйских, Островерхов1978). After this, no information about any kind of archaeological excavations of the settlement appears.

The site was severely damaged due to the plowing before the afforestation in its territory. The sea, which from time to time floods the area with water, wash out the material remains (the whole territory is not more than 2m above the sea level). No actions were made to preserve the site. (Оленковський, 2013).

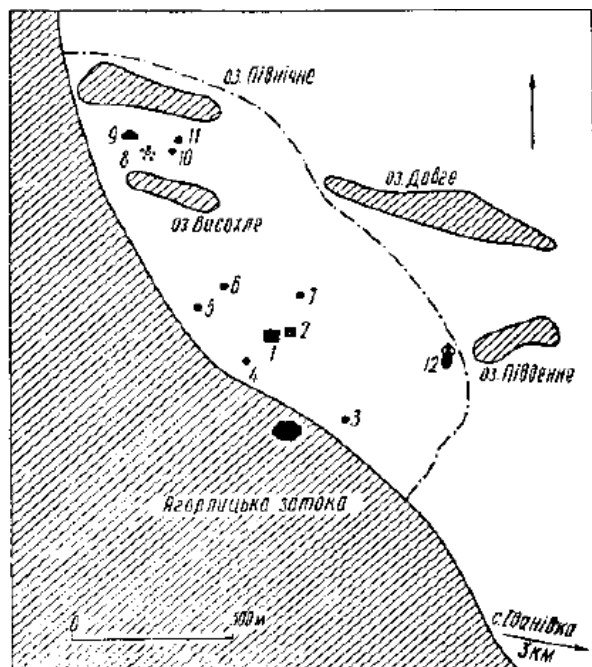


**Figure 3:** The layout of Yahorlyk settlement: 1 – iron smelting furnace remains; 2 – iron melting furnace remains; 3-7 – bronze items and slugs finds; 8 – glass industry finds; 9 – ceramic furnace remains; 10-11 – lead items finds; 12 – surface ceramic finds. (Островерхов, 1981).

The large territory of the settlement included several clusters with a cultural layer. It stretches for 1 km along the shoreline and is over at 400 m from the coast (Bezborodow, Ostroverhov, 1978). There are several small lakes on the territory of the settlement (Fig. 3)

The remains of the dwellings (Загний et al., 1977), as well as the fairly large composition and dating of the ceramic complex, is what allows researchers to declare that the site was a settlement of people. Ceramic materials also support the Greek origin of the population and the connection between this place and different cities in the Greek territories, especially, Ionian (Рубан, 1983). These same materials, can be used to date. According to Ruban, the settlement existed from the end of the 7<sup>th</sup> to the

middle of the 6<sup>th</sup> century BCE (Рубан, 1983). Instead, Kuznetsov restricts the foundation of the settlement only in the first half of the 6<sup>th</sup> century BCE. The same opinion is held by the Buiyskikh (Драган, 2010) and, together with Ostroverhov, they defend the continue occupation of the settlement to the 5<sup>th</sup> century BCE (Загний et al., 1977). Ruban's opinion is supported by Olbia's growth as a manufacture centre and the possible transfer of production facilities to the city. His opponents emphasize the synchronism of the Yahorlyk settlement disappearance, along with many settlements of the Olbia's *chora* in the 5<sup>th</sup> century BCE. To conclude, it is a recognized as a fact that Yahorlyk settlement was one of the oldest Greek settlements in the region (Крижицкий, 1989; Островерхов 1981; Рубан, 1983).

Was it permanent? The arguments in favour of temporality are quite ponderable. First, only about two residential structures were unearthed, these were small ground level structures (sand does not allow the construction of semi-dugouts as on Berezan or Olbia) with adobe walls and clay floors with hearths (Крижицкий 1989, Загний et al., 1977; Рубан, 1983). Secondly, there was no

agricultural conditions for maintaining an independent population. The settlement was rooted on sand, which, moreover, was covered with forest. Herodotus refers to this area on the Dnipro's left bank as Woodlands (gr. Η Γλαίη trans. by Godley) (Herodotus, 4.18.1). Some researchers agree the settlement was seasonal. (Крижицкий, 1989; Tsetskhladze, 1998; Марченко, 1980)

Despite the fact that the settlement was not of an independent nature, its uniqueness is doubtless. It was quite isolated from other centres, even during the time of the growth of the small agricultural settlements on the shores of Dnipro and Bug estuaries (Figure 2). But the greatest interest to researchers is the remains of the manufacturing goods in metal and glass.

Even though, in this work we are more interested in the remains of glass production, a few words on metal smelting and working should be given, because this craft production was clearly the main activity during the entire existence of the settlement. Obviously, the settlers were engaged in manufacturing of a wide range of metal articles. Such objects as details of weaponry (arrowheads, axes) and decorations (bracelets, buckles) were found on the surface. Different metals were used: bronze (arrowheads), iron (nails, awls, arrowheads) (Крижицкий, 1989; Tsetskhladze, 1998; Марченко, 1980; Островерхов 1978) and lead (spindle whorls, rings) (Виноградов, Фоняков, 2000). The evidences of the metal smelting and its processing are the remains of the forge for the smelting of iron and the furnace (Fig. 3, points 1 and 2). They were surrounded with slag and pieces of raw materials (Fig. 3, points 3-7) (Островерхов, 1978). Perhaps, the iron was smelted here with the addition of lime. Blacksmiths used pipes to reach required temperature (Островерхов, 1978). The stones used to shape or anneal products were of Mediterranean origin (Островерхов, 1978).

Metal artefacts found on the settlement have "barbaric" characteristics. For example, most arrowheads are early-Scythian (Виноградов, Фоняков, 2000; Дараган, 2010). Vinogradov writes about the tight connections of settlements with the regions of central Europe and the western Black Sea coast (Виноградов, Фоняков, 2000). The idea about the participation of Scythian artisans in articles production was stated (Ольговський, 2012). Thus, Yahorlyk settlement is thought to be a rather significant metallurgical centre, serving to a geographically large market, but not only to the colonies.

Now we can familiarise with the evidences of glass production at the site. There were found some fragments of ceramic crucibles, some with glass mass, pieces of frit and clusters of glass beads. A significant amount of glass beads had no fully perforated aperture, was chipped, deformed, etc. Presumably, it was defective waste of production. Moulds for bead manufacturing were also among the finds (Островерхов, 1981). The beads were different in colour and shape. There were round beads of various shades of blue, dark glass (a lot of them with "eyes"), biconical ones were mostly green, yellow and transparent. Their sizes in diameter usually does not exceed 1 cm (Островерхов, 1981). Most of the materials found are stored in the Kherson Historical Museum.

Such materials are extremely rare for the age of the settlement, even in Greece itself, without even mentioning the European territories far from the Mediterranean world. It was already mentioned that according to researchers, the glass was mostly produced in the regions of the eastern Mediterranean and was a valuable product, transported in chunks or ingots to the secondary workshops where the final products were made (Rehren, Freestone, 2015). Was the same pattern working in the Northern Black Sea region? It is difficult to answer without a thorough study of the archaeological materials from the settlement. Interesting is the fact that Olbia and the settlement on the island Berezan had a certain connection with Naucratis (a famous Greek centre in Egypt, where, among other things, glass was made), as evidenced by some imported products (Островерхов, 1978). It is possible that this connection will become more evident after the study of the glass materials from the Yavorlyk settlement.

Thus, the Yavorlyk settlement is an extremely interesting archaeological site that provides invaluable material for the understanding of the first centuries of the Greek colonies existence in the Northern Black Sea coast. Probably it was not permanent occupation, it certainly did not exist for a long time and it was mostly craft-oriented. Perhaps, there also were not only Greek people who used the workshops on the settlement.

#### 1.2.4 Archaeological typology of glass beads from Yavorlyk settlement

Finding the place of the analysed glass samples in the general picture of the artefacts distribution map, is the task that we set ourselves in this section. In order to do this, it is necessary to determine the types of beads that will be presented in this study. For specialists in ancient archaeology of the Northern Black Sea it is widely known the publication "Ancient beads of the northern Black Sea region" (*"Античные Бусы Северного Причерноморья"* – rus.) by Alexeyeva, containing the typology of glass beads and other materials that were found in this region, their dating and a list of Greek and Roman sites they were found. We will use that work to provide information systematically, and to make descriptions adaptable for different purposes of the current research. It is extremely difficult to provide accurate quantitative information about such characteristics of beads as colour and transparency. So, to have a system determining the features of every bead type is crucial. The system developed in the above-mentioned edition will continue to be used below. Regrettably, the author does not "register" artefacts from the Yavorlyk settlement, probably, for the reason that materials from the site have not been published yet. The finds of glass on the sites attributed to various, non-Greek cultures are not usually reconciled with the catalogue available for Greek sites, that is why it is difficult to interpret such data.

Bearing in mind all above, we can distinguish at least six types of glass beads among the fragments that were provided for our archaeometric analyses: round blue beads, two types of round eyed beads, dark beads, colourless and yellow beads. Non-identified fragments of glass that are in the scope of current research are omitted in this section.

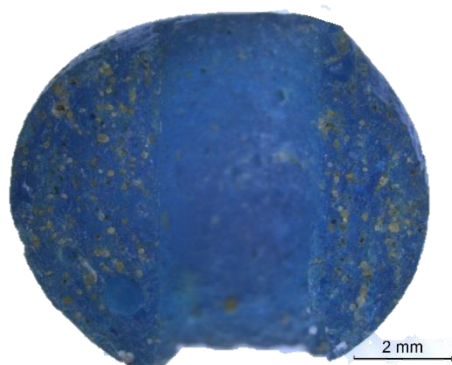


**Figure 4:** Blue round bead (Ya-1).

Round, blue, semi-translucent beads up to 1 cm in diameter (type 15 of monochromatic glass according to Alekseeva, 1975) are common on the northern Black Sea coast from the 6<sup>th</sup> century BCE. However, they were more popular there later. Similar beads were made in all the ancient centres of glass production; archaeologists find them in Greece in the Mycenaean strata (Polikreti et al., 2011). They appear on sites along all the northern Black Sea coast. The Eastern Black Sea region is known for their findings as well (Turmanidze, 2005). The mention of a similar glass necklace can be found in the archaeological descriptions of the Scythian burials (Махортих, Тупчієнко, 2011; Фіалко, 2010).

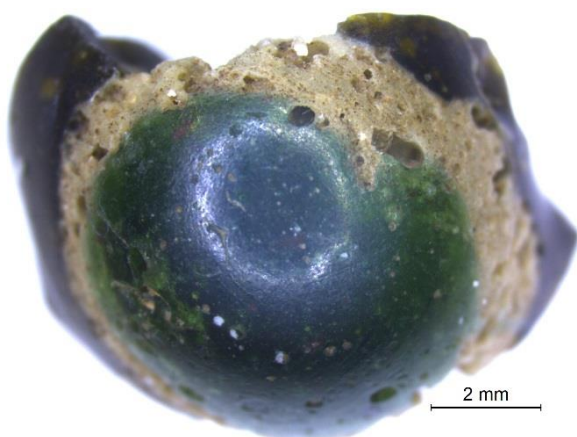


**Figure 5:** Eyed bead type 25 (Ya-12).



**Figure 6:** Bead type unknown (Ya-10).

Polychromatic beads with eyes is a complex group of artefacts (Fig.5,6). Representatives of at least 2 types (according to Alexeyeva) will be processed in this work, although several dozens of types are known in total. The earliest ones present on Greek sites are dated back to the 6<sup>th</sup> century BCE (Алексеєва, 1975). The first type of eyed beads that is shown in the study are ones made of very dark opaque glass with two or three eyes. The eyes are made of layer of white opaque glass on the surface of the body with a drop of green or blue glass in the middle (Fig. 5) (type 25 variant “Ж”) (Алексеєва, 1975). Such beads were found in Olbia and Berezan (Островерхов, 1981).

Another type of eyed beads is difficult to identify, because they are only available to us in small fragments, and therefore it is not possible to determine the size or number of “eyes” (Fig. 6). The discriminating characteristics of these beads are: dark but with a purple tinge colour of the body;

slightly different texture of the glass (smoother) and the matter of eyes execution. The layer of white glass is either very thin and sometimes completely offset or forms a "spiral" as it is shown in the Figure 6. The eyes are blue. Some beads of Egyptian origin in the museums of the world have similar description (Eisen, 1916).

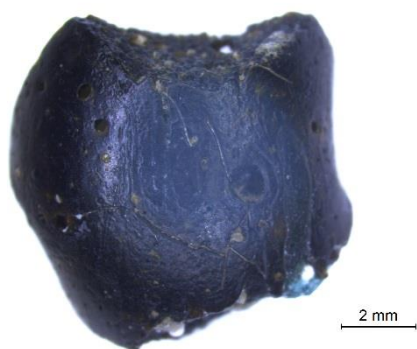


**Figure 7:** Dark bead (Ya-9).

The next type of beads (Fig. 7) that was identified is round monochromatic beads made of a very dark, opaque glass, similar to that used to form the body of some eyed beads. They belong to type 1 of monochromatic beads, which is not numerous in the northern Black Sea coast at all stages of the ancient poleis' existence. The most abundant these beads are in strata from first centuries CE (Алексева, 1975).

Beads made of translucent glass have biconical shape and slight blue or yellow hues (Fig. 8, 9). The dimensions do not exceed 12 mm in the largest measurement, cone-shaped aperture. First mentioned to appear in the 5<sup>th</sup> century BCE (Type 96) (Алексева, 1978). Fragments available for research are fairly short in the axis of the aperture.



**Figure 8:** Yellow biconical bead (Ya-21).



**Figure 9:** biconical colourless glass bead (Ya-18).

The last type of beads presented in this study is biconical beads made of translucent yellow glass and non-symmetrical, cone-shaped apertures. Finds are known in some archaeological complexes of 6<sup>th</sup> century BCE and more recent ones (Type 90) (Алексева, 1978). The biconical beads are relatively numerous, besides the Greek sites they were also found on the hinterland sites of Scythian time (Bezborodov, Ostroverhov, 1978), in the Northern Caucasus and Greece itself (even from the 8<sup>th</sup> century BC) (Островерхов, 1981, Oikonomou, 2018).

In this section, we do not aim to provide a complete list of samples with their images and particular features, this is mere attempt to give an idea of the material about to be discussed after. In the framework of this study, attention is not restricted to beads exclusively. There will be presented other fragments of glass, which now remain unidentified in the corresponding section. As one can

see, most of the bead types found in the Yahorlyk settlement have analogues in a wide range of sites from Egypt to the Ukrainian Forest-steppe zone. In the neighbouring Scythian territories, they are not often encountered, but they are known (Петренко, 1978). It is not necessary that all of them could be made at the workshop on the shores of Yahorlyk Bay, so it is evident that the aesthetic taste and the technology itself were common to a wide range of cultures in the middle of the first millennium BCE.

We complete the exposition of the historical and archaeological context of glass samples from the Yahorlyk settlement and now it is high time to summarize what has been said. Settlement on the shore of the Yahorlyk Bay has been inhabited for about one hundred years starting from the end of the 7<sup>th</sup> - early 6<sup>th</sup> centuries BC at the time of the Greek colonization of the northern Black Sea coast; along with similar settlements around the island of Berezan and Olbia. However, the nature of human activity there was different from the more agricultural nature of the known small settlements synchronous to it. The production of glass and its final products is a complex craftsmanship requiring qualification and a rather specific raw materials list, with a frequent import of many components from afar. The Yahorlyk settlement is a fairly distant point of this craft, and such remoteness should be reflected in the production. The brief time of the settlement existence makes to face some questions: was the workshop moved somewhere, or disappeared altogether? Whether only the glass beads were made locally or the glass itself? Types of beads found in the settlement are quite common in large areas, which adds value to the study. Even if they were not produced in same place, they, expectedly, share technological features of production, making the ancient world a smaller place.

### **1.3 Geological and environmental context of the settlement and possible raw materials**

The one of main tasks of this work is to determine the origin of the glass from the Yahorlyk settlement. As previously mentioned, there are enough reasons to think that the glass itself was produced locally and to prove this, the provenance research methodology that includes a comparison between the chemical composition (mainly minor and trace components) of the artefacts with that of possible raw materials is going to be implemented. When working in glass provenance, almost everything is reduced to analysis of only one but main component – sand (Goffer, 2007). Other components of the batch formula must be taken into account, but the sand analysis is decisive, because it is difficult to imagine it being imported when there is the opportunity to produce the glass locally; export of ingots or chunks for subsequent reworking seems more practical.

In this section, we have merged all known information about the sediments, which can be found around the Yahorlyk settlement. As it is known, sand is a product of weathering and its formation requires the action of different natural forces. If so, we must consider different environmental factors.

Therefore, in addition to describing the geological structure of the region, there will be made an attempt to mark important changes in the region environment from the Ancient Greek times until nowadays.

### 1.3.1 Geological structure of Dnipro river estuary and surrounding formations

The geological structure of the region is very important in order to understand what impurities should be sought in the sand from which the beads from the Yahorlyk settlement were probably made. Defining trends, by identifying "geochemical fingerprints" (content of some elements) that will make up a unique "chemical signature" of a certain type of sand in all products



**Figure 10:** Main geological structures of Ukraine. Ukrainian shield is marked yellow (1); North-Black Sea depression is in pink (9) (Wikipedia).

made from it, will allow one to understand where the origin of the object lays (Degryse, 2014). Since the Dnipro river is the main environmental factor in the settlement area, it is necessary to describe the structures up the stream. After all, the river brings sediments from the whole drainage basin in the process of erosion (Goffer, 2007).

Consequently, we will focus on two geological constructions in the Black Sea drainage basin: the Black Sea depression, which directly includes the territory of the

Yahorlyk settlement and makes a major part of Northern Black Sea region (number 9 on the Fig. 10), and the so called Ukrainian shield, where the valleys of the Dnipro and the South Bug are located (number 1 on the fig 10).

The Black Sea depression is a large geological structure within the East European Craton, on its border with the Sarmatian Craton. It is a prominent slope south of the Ukrainian shield, formed at the beginning of the Cretaceous period after the separation of these two cratons. It was formed simultaneously with the transformation and slight elevation of the Black Sea basin (Robinson et al. 1995). The sedimentary cover is significant, with a thickness of up to 7-8 thousand meters (Білецький, 2007) (1500 m beneath the estuary). Also, there are distinguished older, isolated, and so-called autochthonous layers that lie deeper. The presence of autochthonous layers permitted the identification of the structure as a graben type (Чекунов et al., 1976).

The relief of the Black Sea depression is flat, the elevations are insignificant (2 - 50 m above the sea level), the altitude is increasing in the northern direction (Blagovolin, 1984). In Geomorphological terms this depression corresponds to the Black Sea lowlands. There are silt, clay, limestone, marl and sandstone deposits in the sedimentary cover. In the most recent Pliocene layers in the surroundings of the Yavorlyk Bay, mainly sandy and silty clays lay (Чекунов et al., 1976) .

It is reasonable now to look at the scheme of the quaternary deposits in the area of the Dnipro mouth (Fig.11). As one can see, the Dnipro's right bank is high and steep, formed mainly by aeolian-colluvial loam, sometimes with palaeosoil, which was accumulating there throughout the Quaternary period (orange). On the left bank alluvial deposits (sand, sandy loam) brought by the Dnipro (green) took part in the formation of four terraces of Dnipro. Closer to the surface some aeolian and aeolian-colluvial deposits appear. The Yavorlyk settlement itself was located on the Holocene layers of aeolian sand (Novodran et al.).

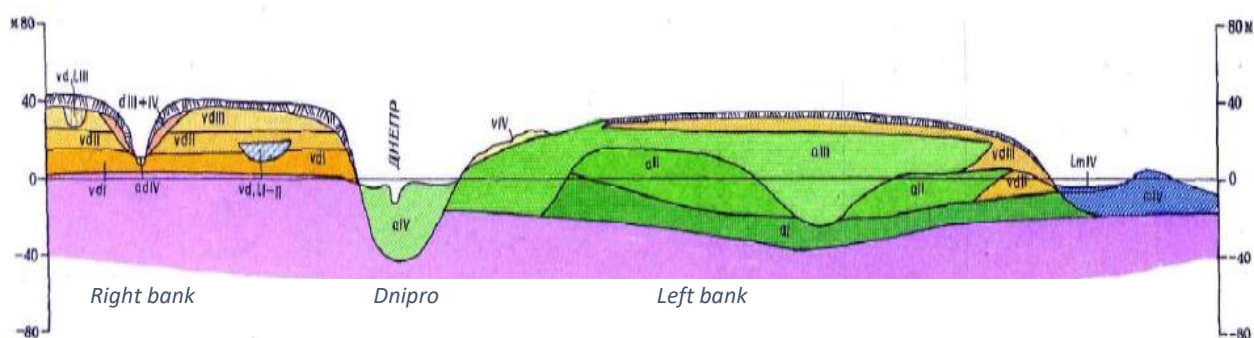


**Figure 11:** The transversal section of Dnipro mouth area. **Green:** aI, aII - lower and middle Quaternary alluvial, alluvial-lake depositions of 3 and 4 terraces of Dnipro river; aIII – upper Quaternary alluvial depositions of 1 and 2 terraces of Dnipro river; aIV – Holocene alluvial depositions of Dnipro river mouth. **Blue:** LmIV – estuarine-marine depositions. **Orange:** vdI, vdII – lower and middle Quaternary aeolian colluvial depositions; vdIII – upper Quaternary aeolian-colluvial depositions, vIV – Holocene aeolian sands. **Purple:** pre-quaternary depositions (Novodran et al., 1978).

As already mentioned, the sedimentary rocks were brought there by the river, or rather by two, the Dnipro and the Southern Bug. The values differ from month to month, but certainly, the Dnipro's discharge of water varies from 400 to 6000 m<sup>3</sup> of water per second, and Southern Bug from 80 to 1000 m<sup>3</sup> (Margvelashvily et al., 1999). The Dnipro river is very much affected today by dams constructed in the second half of the last century (Linnik, Zubenko, 2000). These major rivers have an extensive drainage basin, from which they take small particles and accumulate dozens of meters of sedimentary deposits in thickness over large areas during the time of their valleys existence (Pettijohn et al., 1987; Matoshko, 2002).

Quartz sand, as it is known, forms during the erosion of rocks with quartz (Pettijohn et al., 1987). The most significant geological structure that could provide such quantity of "raw material" for quartz sand formation within the drainage system of the Dnipro and the Southern Bug is the so-

called Ukrainian shield or Ukrainian crystalline massif (number 1 on the Fig. 10). This is an ancient Precambrian structure, which is the uplift of the crystalline foundation of the East European platform. Its linear dimensions are 1000 km in Northwest - Southeast direction and 250 km in Southwest - Northeast direction. It occupies most of the middle and lower parts of the Dnipro valley and almost the entire basin area of the Southern Bug (Білецький, 2013). It is divided by meridional faults into 6 zones, which are horizontally divided into units according to lithotectonic complexes (LTC) (Bobrov et al., 2006). Figure 12 allows us to familiarise ourselves with their localization and variation of rocks within the different LTCs.

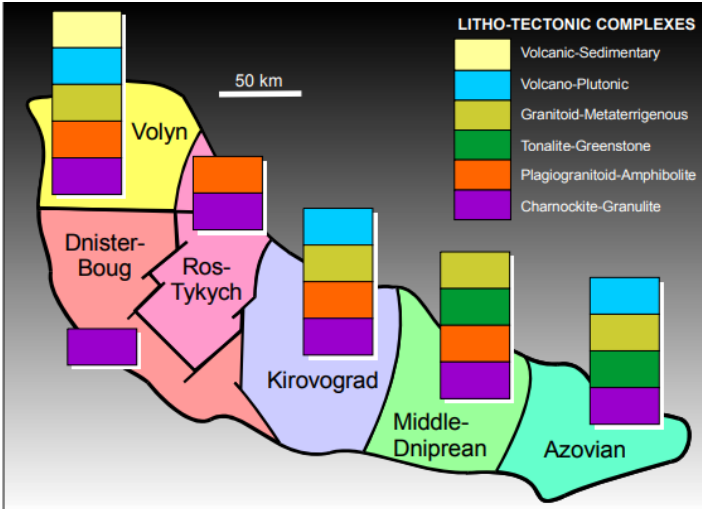


**Figure 12:** Distribution of Litho-tectonic complexes over geoblocks of the Ukrainian Shield (Bobrov et al., 2006).

The oldest structures of the Ukrainian Shield date back to 3.75-3.1 billion years ago (Claesson et al., 2014). In the Mining Encyclopedia it is said that up to 90% of the rocks of the Ukrainian Shield are metamorphic (migmatites, gneisses, granite-gneisses, crystalline slates) and magmatic (granitoids, gabbro, diabase) (Білецький, 2013). The Ukrainian Shield is extremely rich in valuable minerals. Here are ores of black, practically all non-ferrous and noble metals (Starostenko et al., 2010).

It is proved that a granite shield in its various zones contains rare earth metals in significant quantities (Esipchuk et al., 1993). We do not set ourselves the task of describing the geological structure of the Ukrainian Shield, it is described well in great detail by other authors (Shcherbak et al., 1984; Thybo et al. 2003; Grad, Tripolsky, 1995).

Of course, the Dnipro basin is not limited to the Ukrainian Shield and is also covered by sedimentary deposits (Яценко et al., 2009). But this structure (Ukrainian Shield) is the most indicative to demonstrate that the alluvial deposits of the Dnipro, may contain a wide variety of impurities at the level of minor and trace elements. Thus, the sand that could serve as a glass raw material for the ancient Greeks may have a unique “chemical signature” that will be reflected in the artefacts. This is the very important connection between glass and raw materials that we must find.

### 1.3.2 Main predetermining factors of sediment deposition in the Dnipro river Estuary and the North Black Sea region

One can only agree that sand deposition is a process in which various environmental factors take part. Small particles can be carried by the flow of water or with help of wind, deposition spots are largely determined by the morphology of the territory (Wright, 1977). According to the estimates, the Dnipro River along with the Southern Bug carry more than 2.5 thousand tons of solid material into the Black Sea annually (Ross et al., 1978). A certain percentage of this number remained in the Dnipro-Bug estuary, but most of it can be found on a sea shelf that is quite broad in the north of the Black Sea (Ross et al., 1978).

It should not be forgotten that every kind of rock has individual tolerance to weathering, because the minerals that make up these rocks weather at different speeds, interacting with water in different ways, some of them dissolve and travel with the flow in form of individual ions, and some, like quartz, are quite durable and therefore are deposited as particles. For this reason, the proportion of minerals in the composition of sediments rarely corresponds to the mineral composition of the rocks, from which this sediment was formed (Pettijohn et al., 1987). The Dnipro River sediments are not exclusive in this matter.

As it is widely known, beaches are quite dynamic systems, where the particles constantly interact with water and with themselves, but the tides disturbance in these beaches is not significant, as experiments have shown (King, 1951). The velocity of the sediment accumulation on the Black Sea shelf area in the Quaternary period is 0.0005 mm per year (Козленко, 2015). The difference between tides and ebbs for Black Sea does not exceed 17 cm in the most favourable places, although seasonal variations up to 10 cm are encountered (Korotaev et al., 2001). Surrounded from all sides by continent, the Black Sea is a calm basin. However, there are short-term factors that affect the sea level in certain areas. The effect of the wind leads to an increase in the level of water in individual spots up to 2.83 m (wind coming from the sea) and a decrease of 1.25 m (wind coming from the continent) (Давидов, 1999). Such oscillations of water level were also confirmed on the shore of the Yahorlyk Bay by locals.

Has the sea level changed over a long period of time? Studies below are affirmative about this. In general, during the Holocene, the level of the Black Sea (a lake at the beginning of the Holocene) rose (transgressions were prevailing the regressions), taking land especially actively in the north, where there were flat plains (now the part of the North Black Sea shelf). However, the time of existence of the Yahorlyk settlement belongs to the so-called Phanagorian regression of the Black Sea, when the sea level was up to 5 m below today's one (Янко-Хомбах et al., 2011; АНТОНЮК,

2013). On the contrary, we are witnessing transgression (rising of the sea level) at the present (Коніков, 2004).



**Figure 13:** Geographical outline of the Dnipro mouth region. 1 - Dnipro-Bug estuary; 2 - Yavorlyk Bay. Yavorlyk settlement is marked with orange arrow (Google).

Now we consider the main water bodies in the vicinity of the Yavorlyk settlement, namely the Dnipro-Bug estuary (Fig. 13, 1) and the Yavorlyk Bay. The Dnipro-Bug estuary is a product of the transgression of the Black Sea along the Dnipro and Southern Bug valleys (Чепижко et al., 2007). It has an area of about 1,000 km<sup>2</sup> and has a moderate average depth of 3-5 m (it also has a 12 m deep channel for the ships heading to and out the local ports). There is a complicated and

unstable flow system, which is caused by the flow of river waters (93.8% of discharge by Dnipro, 5.8% by Southern Bug) and sea water with a different salinity (Nesterov, Maderich, 2008). The direction of wind on such a shallow water body is of great importance. The left bank, which is not far from the Yavorlyk settlement, is low, sandy and silty. The bottom is formed by the Holocene alluvial deposits, in some places, up to 15 m in depth (Коніков, 2004).

The Yavorlyk Bay (Fig. 13, 2) is a smaller body of water (340 km<sup>2</sup>) between the Kinburn Peninsula (separating it from the Dnipro-Bug estuary) and the Yavorlyk Kut Peninsula (Марушевський, 2006). From the sea it is separated by a sand spit. The depth is up to 5 m. The bottom is very flat, 1 m of water depth for several hundred meters from the coast (Давидов, 1999). Morphologically, the bottom with adjacent land sections forms an alluvial-sea flat lowland. The bottom is mainly clayey with a small amount (5-7%) of sand fraction. In the shore areas of the bay the erosion processes are observable (Давидов, 1999). As already mentioned, there are several small salt lakes with a muddy bottom in the coastal zone near by the Yavorlyk settlement. The shore is not densely populated or farmed (Миничева et al., 2016).

We cannot help but mention the evidences of the researchers in favour of the direct connection of the Dnipro with the Yavorlyk Bay. Due to the lower sea level, the Yavorlyk settlement was located at least hundreds of meters from the ancient shore, but probably one of the Dnipro's branches (Чепижко et al., 2007), which is documented in historical sources (Латышев, 1906; Одрін, 2008), was not far from there and is still being traced in the form of a chain of lakes and seasonal marshes. This water should solve the problem of fresh water in the settlement and the connection with main cities. It is likely that one of the settlers' occupations was fishing (Одрін, 2008).



**Figure 14:** sand arenas in the Dnipro mouth region: 1. Kakhovka; 2- Kosachelagerna; 3 – Oleshky; 4 – Chalbass; 5 – Zburjivska; 6 – Ivanivka; 7- Kinburn (Погребняк, 1953).

conditions for their expansion, making this place a growing sand desert. The lower Dnipro sands are divided into 7 arenas with different depth of the sand layer and dune relief (Fig.14). The territory of the alluvial plain has undergone significant morphological changes throughout the period that divides us from Ancient Greek times due to the above-mentioned processes (Погребняк, 1953).

However, even though these geologically modern sandy deposits are of local origin, due to sorting, they can differ in mineral and fractional composition from alluvial sands that have not suffered secondary working and deposition by wind (Чепижко et al., 2007; Pettijohn et al., 1987). Dunes reach a height of 5 meters. In the area of the Ivanivka arena, where the settlement is located, they reach a height of not more than 3 m. The aeolian sands there consist of 97-98% quartz. Other minerals (feldspars, tourmaline, limonite, pyrolusite, hematite, pyrite, glauconite, etc.) make up 1-2% (Остапуха, 2010; Сплодитель, 2017). The area of sands exceeds 200 thousand hectares, up to 90 thousand of which were artificially afforested (Остапуха, 2010). The Yahorlyk settlement has been found during the afforestation of the territory.

Data on the mineral and chemical composition of alluvial sands is obtained from the results of the sediment analysis from cores drilled in the 1980s. The share of heavy fraction minerals varies: at the Ancient Dnipro valley 0.056 - 1.35 kg/m<sup>3</sup>; at the bottom of the Dnipro-Bug estuary 0.01-0.5 kg/m<sup>3</sup>; at the bottom of the Yahorlyk Bay 0,0001 - 3,6 kg/m<sup>3</sup>. As it can be seen, the variation in the composition of the heavy fraction is quite significant, especially around the Yahorlyk Bay. It is established that the most abundant heavy fraction minerals of in the region are zircon, rutile, kyanite, sillimanite, ilmenite, garnet, staurolite, epidote, tourmaline, pyroxene, amphibole and apatite (Чепижко et al., 2007). This same association of minerals is detected in the Neweuxinian layers in the Ancient Dnipro valley, which now is on the Black Sea shelf. Researchers noted high content of fine gold, which sometimes reaches 0.692 g / ton (Федорончук et al., 2013).

More recent environmental changes around the settlement are associated with the emergence of a semidesert. As previously mentioned, the forest cover that was characteristic for this bank of the Dnipro in the days of Greek colonization existed also in the Middle Ages (Безусько, 2000), restraining the sand from the movement. Deforestation and widespread grazing of cattle (mostly sheep) have led to the release of sands from the vegetation cover, and the wind has created

Information on the chemical composition of the sand was obtained from geological reports that concluded reconnaissance of raw materials for silica brick production and glass industry in the 1980s. Below is the data from the Shabivske deposit of sand, located directly within the territory in which the samples were collected. As we can see from the Table 1, silica is the main constituent of sand and it contains only a small amount of metal oxides (Хлебников, 1988).

**Table 1:** compositional analysis of sand from “Shabivske” sand deposit (<DL - below detection limit) (Хлебников, 1988).

Oxide	Min (%)	Max (%)	Average (%)
Al <sub>2</sub> O <sub>3</sub>	0,6	4,3	1,2
CaO	0,14	0,84	0,3
Cr <sub>2</sub> O <sub>3</sub>	<DL	<DL	<DL
Fe <sub>2</sub> O <sub>3</sub>	0,2	0,4	0,3
MgO	0,08	0,9	0,34
TiO <sub>2</sub>	0,01	0,2	0,1
MnO	<DL	0,11	0,06
Na <sub>2</sub> O+K <sub>2</sub> O	0,2	0,44	0,32
P <sub>2</sub> O <sub>5</sub>	0,01	0,08	0,03
SO <sub>3</sub>	<DL	0,13	0,02
SiO <sub>2</sub>	91,9	99,0	

We conclude the familiarisation with sandy sediments around the Yavorlyk settlement. As one might notice, the Dnipro river had significant influence on sediment deposition in the region throughout history. Deposits on its terraces, the banks of the Dnipro-Bug estuary and the Yavorlyk Bay, as well as the northern section of the Black Sea shelf, originate from the territories of the Dnipro basin. The environment in which the Yavorlyk settlement was functioning was quite different from the current conditions. In this section, we do not provide a description of sampled sediments that have been collected. Their detailed characteristics and method of sampling, can be found in the section "Sampling".

Therefore, we can summarize the information in the previous section as:

1. Yavorlyk settlement - probably a temporary settlement of the Greek colonists engaged in various crafts (mainly metallurgy). The time of its occupation dates to the 6<sup>th</sup> century BCE, but it is quite possible that it was founded earlier and existed until the middle of the 5<sup>th</sup> century. The site is unique because of its age and craft specialization;

2. The traces of glass production are the most interesting finds on the site. It is necessary to establish whether the glass was produced locally, or the beads were produced using imported glass;

3. By looking at changes in the environment, relevant for this study, it was found that the settlement had available raw material for glass production. In the immediate vicinity there were large deposits of rather clean sands, brought by the Dnipro river. The lime that was commonly used to lower the melting point and to stabilize the glass could be obtained from shell deposits on the sandy beaches of the bay, or from limestones found on the banks of the estuary. The Yahorlyk craftsmen had access to iron oxides, manganese, copper, tin, lead, frequently used in different ancient world regions for colouring, discoloration or opacifying the glass. The question of the flux used remains open, but its kind will be determined during experiments on glass beads from the Yahorlyk settlement. The Woodland provided source of charcoal and probably ash crucially needed for production of glass;

4. The high variability in the mineral and chemical composition of sediments from the surrounding area is explained by different types of sorting during and after the initial deposition. As a result, even if the beads were made locally, their different batches may differ in their chemical composition at the level of minor and trace elements, so it is very important to prepare a representative collection of sediment samples for their further comparison. It is possible that we will be able to determine which kind of sand was preferred by the ancient Greek artisans.

## CHAPTER II. METHODOLOGY OF THE STUDY

This section will describe the progress of the study from the stage of sampling to the stage of systematization of the research results. The selected fragments of glass and collected samples of sediments that were available will be presented. Justification of the selected analytical methods as well as of the way of sample preparation will be done. We will also tackle some theoretical aspects of the chosen techniques since such technical issues will be important when the time to interpret the results comes.

### **2.1 Sampling**

The selection of samples should take place with a clear understanding of the tasks the researcher is facing. It is necessary to adhere to certain criteria of representativeness, regulating the number of samples, their quality and the amount of material to be selected. Here, one may encounter a variety of difficulties. Firstly, working with archaeological materials, especially with materials included in collections of various museums, a researcher will almost always have to select the least possible number of samples because of their cultural value and wish to safeguard objects not only from time but from invasive analyses. Looking for compromises, the set of analytical techniques is complemented with non-invasive, or at least minimally-invasive methods that evolve to powerful tools that can provide information about an object without changing its appearance.

Even if the damage or destruction of the material is not a problem, there are other obstacles. For example, of logistics nature, which are especially acute when there is a necessity to work in the field. Here the main problem is the rational consumption of funds and other resources. It is necessary to constantly put same question: does the desired study result justify the costs?

Bureaucratic obstacles also sometimes stay on the path of researchers. Thus, a big compromise is inevitable which is to minimize the number of specimens under the influence of limiting factors, but still retain its representativeness. The sampling strategy has to be designed to ensure this. It must take into account all the constraints and quite often the final result depends on it. Below you will find the conditions for selecting glass and sediment samples, along with a complete list of each type of samples and their characteristics.

### 2.1.1 Sampling of glass fragments

Several hundred fragments of glass found on Yavorlyk settlement are known. As of 1978, there were more than 200 pieces collected directly at the settlement during the archaeological activities (only fragments of beads not counting other pieces) (Островецьков, 1981). The collection, currently in the possession of the Odessa Archaeological Museum of the National Academy of Sciences of Ukraine, includes more than 150 fragments. Although they are surface finds, they are attributed to the context of the settlement because they are similar to those collected by archaeologists there.

The samples to be analysed in this study come from that collection. They were selected and provided to the research purpose by museum's associate Anzhelika Kolesnichenko. The maximum coverage of all varieties of glass fragments available was the main principle the archaeologist was guided by, which makes the collection fully represented. Twenty-three samples of archaeological glass were selected. They were of different shapes, sizes and colours. Every type of beads is represented at least with one fragment.

Per the previous chapter, the glass beads from the Yavorlyk settlement were divided into 7 archaeological types. Other fragments of glass, which are very different, and which cannot be identified as fragments of beads, have been put in the "non-beads" type. Now we think it is necessary to provide more detailed visual information about each group of samples:

Group 1: Monochromatic, round beads made of semi-translucent blue glass and similar by colour pieces of blue glass. 5 samples are included in this group. While they are characterized by numerous bubbles especially in sections, the beads of this type differ in shades. Beads have a cylindrical, wide aperture, which is usually not placed symmetrically inside;

Group 2: Dark base beads with "eyes". 4 samples are included in this type. Their base is made of dark opaque glass. One of the fragments is rather small, and very difficult to be identified as a bead; They have blue eyes with the green hint. White layer has many bubbles. The aperture is cylindrical;

Group 3: Purple base eyed beads. Two samples represent this group in the set. They are different not only by the colour of the base, which is dark purple, but also by clarity and colour (bright blue) of the eyes and reduced presence of white layer. They do not have so many bubbles as in previous group.

Group 4: It has only one representative (Ya-10). It is detached eye of the bead that seems to be formed in different way. Extreme whiteness of the white layer and clarity of the blue eye when compared to others.

Group 5: Very dark opaque glass bead. Only one sample is included in this type (Ya-9). Its initial diameter could exceed 1 cm. The section surface has bubbles, some holes can be seen on the outer surface. The glass is similar to the base of the dark base eyed beads;

Group 6: Green non-beads. They are fragments of light green of irregular shape, one sample is flat. Part of the samples surface is covered with a lighter, patina-like layer.

Group 7: Biconical colourless beads made of translucent glass. Two samples are included in this type. They have a conical aperture, if one imagines them split in half at the widest plane, then one part will be larger than the other, making them asymmetrical. Bubbles are not noted;

Group 8: Biconical yellow beads made of translucent glass. Four samples are included in this type. Similar in configuration with the previous group, the sections are smooth, sometimes they appear as conchoidal fracture;

Each sample is described in the Table 2 below. The size defined as length for all the beads is the distance between the most distant points along the aperture axis and the width is the distance between the most distant points on the axis perpendicular to the axis of the aperture. If the axis of the aperture cannot be identified, the length is considered to be larger dimension, subsequently the other is the width. Individual traits of each sample and some characteristics not mentioned above are given in the column called "Brief description".

**Table 2:** List of samples of Yadorlyk glass

<b>Sample</b>	<b>Group</b>	<b>Length (mm)</b>	<b>Width (mm)</b>	<b>Brief description</b>
<b>Ya-1</b>	1	7,1	4,7	Half of the bead; asymmetrical aperture (one side is thicker); edge of the aperture has a protrusion; diam. of the aperture - 3,3 mm
<b>Ya-2</b>	1	4,8	4	Smaller size but aperture of the same diameter as the rest of the group; asymmetrical aperture; diam. of the aperture – 4 mm
<b>Ya-3</b>	2	6,7	2,2	Blue part of the "eye"; white layer on the back
<b>Ya-4</b>	1	7,2	3,8	Foliation is visible in section; scratch on surface; protrusion on the edge of the aperture; diam. of the aperture - 3,8 mm
<b>Ya-5</b>	1	6,7	4	Piece of blue glass mass; angular
<b>Ya-6</b>	1	6,2	3,8	Contains three colours: blue translucent, opaque white and dark; similar to eyed beads, may be a fragment of an eyed bead
<b>Ya-7</b>	6	13,9	3,7	Flat, triangular piece of green translucent glass; white layers of different appearance on both sides
<b>Ya-8</b>	6	9,1	5,4	Irregular angular piece of glass mass with purple stains and patina-like layer; similar to Ya-7 in colour
<b>Ya-9</b>	5	9	4,8	Cracks, probably foliation; section area is punctuated with small holes

**Table 2:** List of samples of Yahorlyk glass (cont.)

<b>Sample</b>	<b>Group</b>	<b>Length (mm)</b>	<b>Width (mm)</b>	<b>Brief description</b>
<b>Ya-10</b>	4	4,8	3,5	Eye of the bead; contains blue and white part; dark lines are visible on the surface of white layer; back has dark angular grains; diam. of blue part – 3 mm
<b>Ya-11</b>	2	7	4,5	Eye of the bead with some of the dark base; white layer is porous in appearance; diam. of green - 4 mm
<b>Ya-12</b>	2	9,2	6	Eye of the bead with some of the dark base; green part is big; white layer is porous and thin; diam. of the eye - 8,3 mm, green part - 7,2 mm
<b>Ya-13</b>	2	6,5	5	Eye of the bead with some of the dark base; green part is small; white layer is porous and thick unevenly spread; slight asymmetry of the aperture; diam. of the eye - 6 mm – 8 mm; blue part - 4,3 mm
<b>Ya-14</b>	3	6,3	3	Dark part is made of different lighter glass; white part is visible but very thin; blue and dark parts are in contact; identified as piece of bead only because of the colour and surface
<b>Ya-15</b>	3	6,2	3	Small piece without blue layer; identified as bead only because of colour similarity with others eyed beads
<b>Ya-16</b>	2	4,6	2,2	Small piece of dark glass with some of white; identified as piece of bead only because of colour similarity with others eyed beads
<b>Ya-17</b>	6	9	3,7	Irregular piece of glass mass; light blue colour; one side is vitreous another has patina-like appearance
<b>Ya-18</b>	7	7	11,2	Half of the bead; aperture is conical; asymmetric; the bigger cone has multiple parallel scratches; diam. of aperture - 1,1 mm - 2,2 mm
<b>Ya-19</b>	7	7,4	10	Asymmetrical; very conical aperture; crack
<b>Ya-20</b>	8	6,2	4	Irregular section
<b>Ya-21</b>	8	8	9	About half of a bead, conical aperture; asymmetrical; diam. of aperture 1 – 2 mm
<b>Ya-22</b>	8	7	9,3	Aperture might not be finished; asymmetrical; lighter colour
<b>Ya-23</b>	8	7,8	10	Half of the bead; very conical aperture; asymmetrical; diam. of aperture - 1,5 mm - 2,5 mm

The amount of material and its variety allow us to conclude about the technological level of the Yahorlyk settlement glass industry after studying it. These objects were provided by the Odessa Archaeological Museum without permission to destroy them. Hence, the methodology of the study must be in accord with this condition. The stereomicroscope images of all the glass samples are put in the Annex 1.

## 2.1.2 Sampling of sand

Firstly, we note that the sampling of sand was a difficult task. It was necessary to ensure the representativeness, and since we did not know what sand could be used by ancient man, the coverage of the territory was much larger than the settlement itself. A strategy was developed in agreement with the main limiting factors. It aimed to obtain uncontaminated sand samples from different environments and of different origins.

We must mention that at our disposal there were some samples of sediment from the Yahorlyk settlement (kindly provided by Anjelika Kolesnichenko), which allowed us to judge about the type of sand and fractions present. Unfortunately, due to the fact that material was insufficient, these samples were not representative, and therefore it was decided to re-sample the terrain. In the corresponding place of the geological section of the work we described several types of sediments of the Quaternary period near the Yahorlyk settlement: modern aeolian, ancient aeolian, alluvial, estuarine, and marine (Novodran, 1988; Чекунов et al., 1976). Accordingly, it was necessary to take samples from the banks of the Yahorlyk Bay, the Dnipro-Bug estuary, the dunes of the Ivanivka sand arena, and from quarries. The Figure 15 provides the list of samples collected during field trip to the settlement area. The map shows the locations of the sampling sites (Fig. 15).

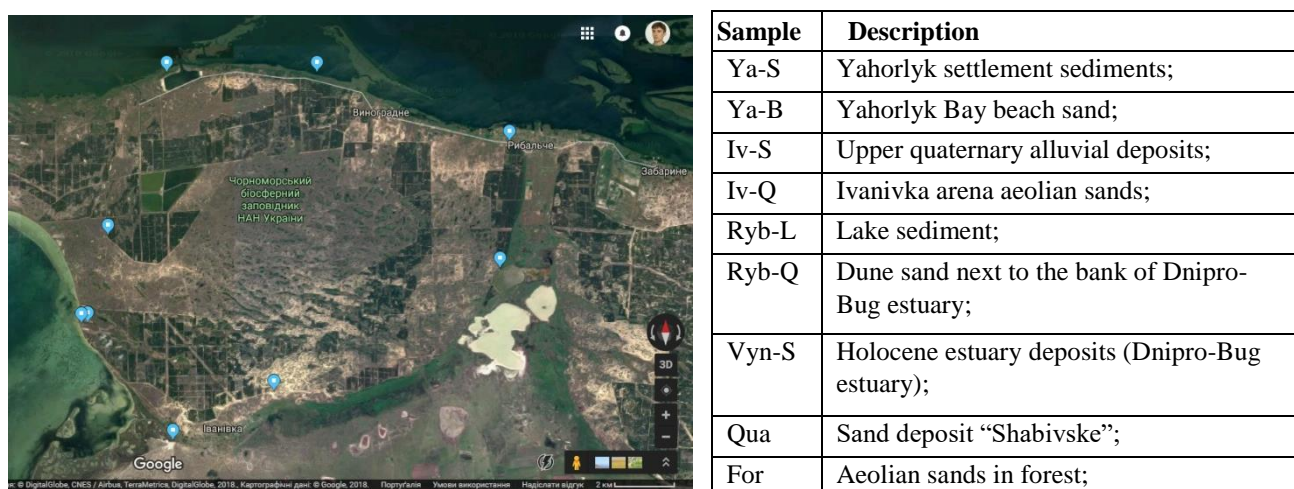


**Figure 15:** The map with pointed places of sampling (left) and the table of sand samples with description (right).

Such composition of samples allows to consider sands of the various ways of deposition, which is very important, because, as it was said in the previous section, the mechanisms of sand sorting determine its mineral composition and, therefore, its chemical composition. As the only purpose of sand study is to find the connection between its chemical composition and the chemical composition of the beads from the Yahorlyk settlement, it is quite obvious that leaving some particular kind of sand out of the research plan may lead to false conclusions.

Equally important is the method of samples procurement. The way of sample collection used took into account the ones used in glass provenance studies (Degryse, et al., 2008) and environment pollution studies (Salminen et al., 1998; Smodis et al., 2003) that used similar analytical methodology. The guiding principles of this protocol are to ensure the representativeness of the data and avoid contamination. Logistic and technical limitations were taken into account. It should be noted that after a closer familiarisation with the field, this protocol has been somewhat modified.

General idea was to find places within above defined areas and dig pits until fine sand comes out. Personal judgement was decisive for picking up the collecting place. It was decided to take samples from places that were looking most stable in terms of sand movement (no samples from top of the dune for example). One of criteria was distance from any current settlement areas or cultivation fields to avoid contamination. The only exception was made for sand quarries because sand there was more likely deposited there for longer period of time than just on the surface of the sand arena.

**Table 3:** Minimum recommended sample size for trace elements analysis based on the biggest estimated grain size in sediments and loose samples (Smodis et.al. 2003).

Estimated largest grain size in sediments and loose samples (mm)	Sample weight (kg)
0.125	0.003
0.252	0.025
0.5)	0.129
1	1
2	5
3	20
5	80
10	300
15	600
25	1,250

One of the most important questions was sample size. Granulometry data of sediment samples collected by the archaeological team has shown that major fractions were 0,5-0,25 mm and 0,25-0,063 mm. Fraction 1-0,5 mm is relatively small and usually does not exceed 5% of total weight of sample (Annex 7). Hence the largest estimated grain size in the sand from the Yahorlyk settlement was thought to be 1 mm. Minimum dry weight of sample should be more than 1 kg (according to Table 3 from IAEA guide). Bigger portion has been taken in field to compensate content of water.

It was determined by the methodology of samples collecting from the river bottom to use a grid 15 by 15 or 20 by 20 m to cover a larger area (Shelton, Capel, 1994), as well as to ensure that the sand does not differ in colour and size from place to place. The pits were dug with the help of metal shovels, which were a gigning tool, and small plastic shovels,



**Figure 16:** Photograph of the Qua-2 sampling pit. The 20 cm ruler is placed for the scale.

which were the tools for collecting the samples (plastic was chosen to contact with the sand, so the metal did not contaminate the samples). The depth of the pits varied between 20 and 80 cm (Fig.16) The configuration of the pitting was different, depending on the terrain. The coordinates were recorded using the Android application “My GPS Coordinates” for the first and last pit made in each

location, which was usually the furthest from the first. The precision of coordinates is up to 24 m. If the sample contains less than 10 samples, coordinates are provided only for the first point. The samples were put in plastic bags with registration of weight. During the work, photographing of the field of sampling and each pit was carried out.

The following Table 4 provides information about each sample taken. Their weight is not given because it has been documented before drying. The degree of humidity varied individually from dry to very wet.

**Table 4:** List of samples from the vicinity of the Yahorlyk archaeological site.

<b>Name of the sample</b>	<b>Coordinates</b>	<b>Number of subsamples</b>	<b>Features of the sample</b>
<b>Ryb-L</b> Rybalchanske lake	46°26'6,99''N 32°13'18,43''E;	2	Subsamples were collected from one pit: one from surface and one from 20 cm below; Sample was taken just on water line
<b>Ryb-Q</b> Rybalche "quarry"	46°28'24.85''N 32°13'33.44''E;	10	Dune used by villagers to take sand; subsamples 1-5 – from the slope, 6-10 – from the "floor" of the "quarry", forming two parallel rows
<b>Vyn-S</b> Vynohradove shore	1. - 46°29'40.09''N 32°8'29.05''E; 4. - 46°29'35.62''N 32°8'28.66''E;	4	Sample from Dnipro estuary; Subsamples 1,2 come from the water line, 3, 4 from the rise after the reed ends 50 m from the shore. 3, 4 - taken from 70-80 cm in depth
<b>Qua</b> The Quarry	46°29'40.2''N 32°4'30.96''E;	5	Shabivske sand deposit; Dnipro estuary bank; Sand is very fine; Subsamples were collected from the top of the artificial hill
<b>For</b> The forest	1 - 46°26'42.66''N 32°2'57.63''E; 10 - 46°26'40.37''N 32°3'3.6''E;	10	Subsamples were collected in one row (every 20 m) from antifire trench (maybe planting trench) on the edge of the planted pine forest
<b>Ya-S</b> Yahorlyk settlement	1. - 46°25'7.66''N 32°2'26.1''E; 10. - 46°25'8,75''N 32°2'23.69''E;	10	Sand from the territory of the settlement between two lakes; grid 15X15 m; 3 rows
<b>Ya-B</b> Yahorlyk beach	1. - 46°25'6.41''N 32°2'15.03''E; 10. - 46°25'0.31''N 32°2'17.29''E;	10	Samples were collected from the sandy cliff formation in one row along the water line
<b>Iv-S</b> Ivanivka south	46°22'59.37''N 32°4'40.59''E;	3	From the seasonal flood area; subsamples are dark
<b>Iv-Q</b> Ivanivka "Quarry"	1.- 46°23'53.2''N 32°7'19.61''E; 10.- 46°23'53.03''N 32°7'18.57''E;	10	Dune sand; non-systematic placing of sampling points; subsamples were taken from the "floor" of the "quarry"

It is believed that this set of samples is representative for this territory. In total, 64 sub-samples were collected with a total weight more than 8.5 kg (wet weight). In any case the results of the sediment analysis will be compared with ones from the already well-known places of the glass

industry in the ancient world, which will make the data conclusive about whether there was or was no glass production on the Yahorlyk settlement.

## **2.2 Justification of selected methodology**

When designing the research methodology, one must focus on getting the answers to the research questions posed in the beginning of the project. In this study, we selected several analytical techniques to answer questions regarding the technology used in Ancient Greek glass industry and to attempt to identify the provenance of the glass from the Yahorlyk settlement.

The results of any study are always more reliable when different complementary techniques can be used. Therefore, we opted to use a multi-analytical approach. We proceed describing the methods of glass and sediment analysis trying to rely on similar studies in order to better understand technical opportunities and limitations in material characterization. Since the laboratory work involves two very different materials to be studied, namely glass and sand, it was decided to describe the methodology separately.

### **2.2.1 Methods of glass analysis**

In this section, the material characterization and provenance study of the glass artefacts will be considered. The study was limited to the non-destructive techniques due to the specific request of the Odesa Archaeological Museum to save the objects. Archaeometry nowadays can offer a variety of methods that can be useful for this material. When studying glass, its chemical composition holds the answers to most questions. It can be used to solve both technological and provenance problems. That makes utilizing of inorganic analytical chemistry techniques inevitable. This includes those that give “bulk” information and micro-analytical ones with spatial resolution. We will start with stereomicroscopy which is a versatile tool for visual characterisation of material. Then micro-X-ray diffraction ( $\mu$ -XRD) is going to help us understand if there are crystalline inclusions inside the glass artefacts and to identify them. Chemical composition will be acquired by means of portable X-ray fluorescence (p-XRF) and variable pressure scanning electron microscope coupled with an energy dispersive spectrometer (VP-SEM-EDS). These two techniques complement information obtained by  $\mu$ -XRD and each other. Their detection limits allow precise quantification of major and minor constituents in glass, besides SEM is irreplaceable for high magnification imaging. Inductively coupled plasma mass spectrometer (ICP-MS) is a powerful tool for provenance studies because it can

offer the chemical composition in what concern to major, minor and trace elements. The addition of a laser ablation system as a way of acquiring the analyte, makes this technique micro-invasive but still within the allowance of this study. All the above-mentioned techniques do not require any specific sample preparation. Glass fragments were studied as they were.

#### *2.2.1.1 Optical microscopy (Stereomicroscopy)*

A stereomicroscope is a relatively simple optical instrument that allows examination of an object at low magnifications. This device was first produced in 17<sup>th</sup> century and has not undergone fundamental change ever since. It has two oculars and uses two optical paths that are joined to receive light from common objective (Nothnagle et al.). Usually this kind of microscope works more with reflected than transmitted light but as a rule both sources are present in the modern models (Schnitzler, Zimmer, 2008). Production of images can be achieved after coupling the microscope to the digital camera. The stereomicroscope is useful when 3D perspective is needed. It works similarly to human vision which is binocular. In this way acquisition of images with 3D effect is possible (Schnitzler, Zimmer, 2008).

If applied to glass studies stereomicroscopy allows the examination of surface and bulk of glass (if it is translucent) objects. During this process it is possible to reach some conclusions about the conservation state of the material and even gather certain information regarding manufacturing technology. It is always useful to know if there is patina layer on the surface, the grade of surface porosity, fracturing, presence of bubbles, their appearance and distribution, presence of grains in the bulk and so on (Wood, 2011). This information can be useful during the investigation of the manufacturing technology or for the application of other techniques (looking for the spots for taking measurements or the opposite to avoid certain areas).

The stereomicroscope was successfully applied in numerous archaeometric studies, mostly as an auxiliary instrument (Lei, Xia, 2015; Neri et al., 2016; Silvestri et al., 2011). It is worth to mention works of Rosemarie Lierke, who studied antique glassware and based on thorough examination of glass appearance and morphology and comparing this data with experiments in glassware production produced valuable theories about Ancient Roman glass industry technologies (Lierke, 2018). Following these and other publications we attempt to make an insight into glass bead production technology that was known to the Yahorlyk artisans.

For this study Leica M205C stereomicroscope was used. Surface observations were carried out at different magnifications (up to 160X). Images were acquired using DFC295HD photo camera.

### 2.2.1.2 Scanning electron microscopy coupled with an energy dispersive spectrometer (SEM-EDS)

Developed in 1930s, the scanning electron microscope is now commonly used as a high resolution (1-5 nm and higher) (Goldstein et al., 2003) observation tool for solid samples. Coupled to an energy dispersive spectrometer this instrument is quite useful for obtaining elemental composition of broad variety of materials including glass (Bell, Garratt-Reed, 2003).

It uses the phenomenon of secondary electrons yield or primary electrons backscattering in order to acquire images of a rectangular area that is divided on certain number of cells – pixels. The beam of (primary) electrons is sharply focused with help of electromagnetic lenses on the area to be analysed (Fig.17).

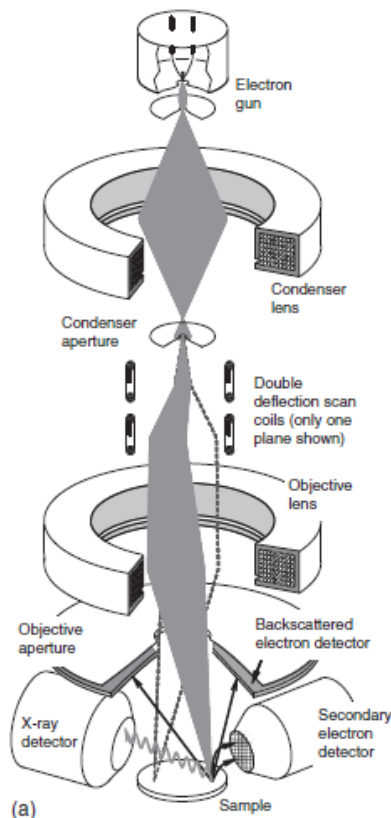


**Figure 17:** Schematic layout of scanning electron microscope (Janssens, 2013).

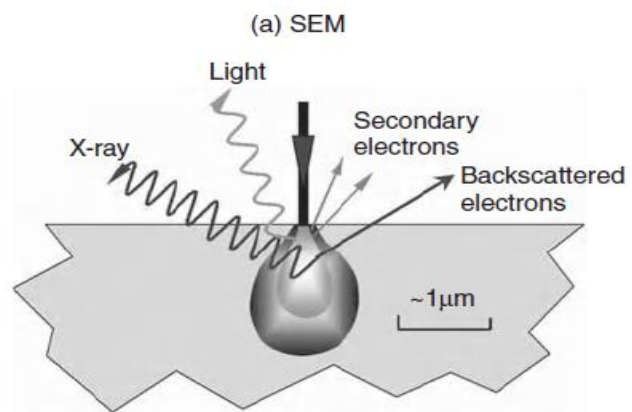


**Figure 18:** Interaction of electrons with semi-infinite sample suitable for SEM (Janssens, 2013).

The interaction between the electron beam and the specimen can cause the emission of different types of secondary particles. Two main processes can occur: scattering and absorption. When inelastic scattering occurs, electrons are ejected from the atoms. They become secondary electrons (SE). Some primary electrons scatter elastically forming backscattered electrons (BSE) (Fig.18). Both these kinds are used for imaging, although there is difference in origin. As a rule, BSE images do not provide as good resolution as SE ones due to the depth they are coming from, but they are irreplaceable for conducting elemental analyses. The scattering efficiency is proportional to the atomic number of the element they are interacting with (Janssens, 2013). In this study we used BSE imaging to collect data

about micromorphology of the face surfaces and sections of glass beads. This imaging technique helped to understand the grade of homogeneity in the samples structure.

But the most important for this study among all kinds of radiation that can be collected from the specimen is the characteristic X-rays radiation. It occurs when the primary electron beam is absorbed by the specimen. This process takes place because core electrons leave their shells. The energy is released when an electron from the empty electronic shell is replaced by another electron from a more outer shell of the same atom. The amount of energy released is equal to the energy difference between the two shells. More important, this difference is characteristic of a chemical element and it is emitted as X-ray. These X-rays are registered by the EDS detectors, that allow to detect and quantify different chemical elements (Bell, Garratt-Reed, 2003).

We used EDS spectra of areas on the surface of beads to obtain their major elemental composition. Point measurements were taken to detect grains of metals compounds that were not dissolved in the glass matrix. Elemental mapping was also used to observe the distribution of different elements.

Nowadays SEM-EDS is one of the most useful techniques for glass analysis. For some studies it plays role of the main one. Elemental analysis can enable the identification of modifiers, colorants and opacifiers that were put in the initial batch along with their ratios (Babalola et al., 2018; Silvestri, 2011).

Following the established non-destructive methodology, the samples were analysed without coating and in variable pressure mode (VP) using a pressure of 40 Pa (low vacuum conditions). VP-SEM-EDS analyses were performed using a Hitachi S3700N SEM coupled to a Bruker XFlash 5010 SDD EDS Detector. The voltage applied was 20 kV. The Esprit 1.9 software was used for a standardless quantification.

### *2.2.1.3 Portable X-ray fluorescence (p-XRF)*

X-ray fluorescence uses same phenomena of atom excitation and substitution of inner shell electrons with outer shell electrons as the SEM-EDS assembly. However, unlike in the SEM-EDS setup, where an electron beam produces secondary X-rays, here energy emission is reached with help of primary X-rays. This provides a spectrum with less background. The first commercial apparatus appeared in 1948 (Beckhoff, 2007). The energy dispersive detector (EDD) plots the energy of the same characteristic rays against intensity (Janssens, 2013). This type of detector was used to study Yavorlyk beads. The handheld version of the apparatus is straightforward in use, and able to provide data with an immediate effect (Fig. 19). The atmosphere x-ray absorption does not allow to detect

presence of light elements ( $Z < 10$ ) but EDS data can give compositional information from Mg to U. The major element quantification has been done by SEM-EDS, but EDXRF detect minor and trace elements. The complementary semi-quantitative data were extremely useful in the beginning of the research, allowing to identify groups of beads and giving preliminary ideas about glass matrix constituents.

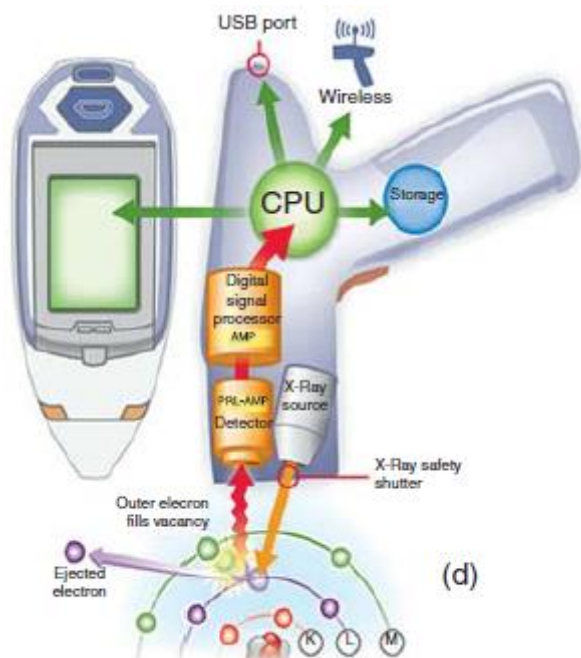


**Figure 19:** Schematic drawing of handheld XRF device (Janssens, 2013).

The XRF instrumentation proved its effectiveness in numerous studies of vitreous materials as a tool for establishing elemental composition (Qin, 2016) and also as an instrument in provenance inquiries (Polikreti et al., 2011).

A Bruker Tracer III SD XRF spectrometer with a SDD multichannel (2024) detector was used. Measurements were taken in the ambient atmosphere for 120 seconds at maximum voltage of 40 kV and current of 35  $\mu\text{A}$ . No filters were applied. Photographing of each spot with help of built-in camera helped documentation of the analyses. Two analyses were made for each sample.

Their size did not allow to take precise point measurements, that is why it was decided to just flip them between measurements. Acquired spectra were processed using the ARTAX software. The generated net areas were normalized to the  $K\alpha$ -Rh counts. The results were then used to make elemental bi-plots in order to determine affinities between different chemical elements and to attempt to establish a link between typology and chemical composition.

#### 2.2.1.4 Micro-X-ray diffraction ( $\mu$ -XRD)

Some X-rays have the wavelength that corresponds to the distance between atomic planes of crystal structure (1,5-4  $\text{\AA}$ ). When they interact with matter they might be partially adsorbed and scattered inelastically (photoionization, Compton scattering) or elastically (Rayleigh scattering). Elastic scattering of X-rays lies in the bottom principle of X-ray diffraction (Warren, 1990): when X-rays are scattered elastically from different parallel planes of crystal structure at certain angles they accomplish the Brag's law ( $n\lambda=2d\sin\theta$ , where  $n$  is number of plane,  $\lambda$  is the wavelength,  $d$  – distance between planes and  $\theta$  – angle of incident beam and scattering) (Ramachandran, Beaudoin, 2001) the

constructive effect increase the intensity of the X-rays in the detector. Since different crystals have different atomic structures, different diffraction patterns are obtained (Warren, 1990). That makes it possible to distinguish between different crystals, irradiating them with monochromatic X-rays. The identification of crystals is based on database values. Different types of apparatus were produced during more than 100 years of contemplation of this phenomenon.

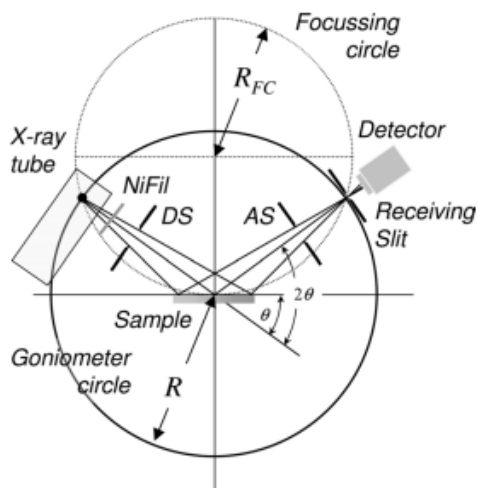


**Figure 20:** Schematic representation of  $\theta/2\theta$  diffraction in Bragg-Brentano geometry (Birkholz, 2006).

Figure 20 represents the layout of typical (Bragg-Brentano geometry) X-ray diffractometer with moving symmetrically the source and detector parts during the analysis. The result is usually a plot of intensity against the angle  $2\theta$ .

As is widely known, glass is not a kind of material with defined crystal structure. XRD analysis of glass feature increasing of background (noise) that impedes interpretation of the results. But glass may contain in its matrix different kinds of crystals due to surface impurities, poor dissolution of ingredients (Janssens, 2013) or glass decay (Gentaz et al., 2012).

The recently developed  $\mu$ -XRD technique allows analyses of individual grains focusing the X-ray beam with sophisticated optics to be up to 50  $\mu\text{m}$  in diameter (Flemming, 2007). This technology was applied to glass beads fragments. Bruker D8 Discover equipment that generated Cu  $K\alpha$  radiation focused with 1 mm collimator was used. Diffractograms were acquired on the  $2\theta$  range from  $3^\circ$  to  $75^\circ$  with step size  $0,05^\circ$  and step time of 1 sec by LYNXEYE detector. DIFFRAC.SUITE EVA software and PDF-2 database was used to interpret the results.

#### 2.2.1.5 Laser ablation inductively coupled plasma mass spectrometry (LA-ICP-MS)

Inductively coupled plasma mass spectrometry (ICP-MS) has become a versatile technique for elemental analysis and isotopic ratio determination. With an extremely high spatial resolution, low detection limits, and short time of analysis it has been a key technique for material characterisation for a few decades. In archaeological material science, where the integrity of analysed object is highly appreciated, the laser ablation (LA) system is the most popular way of sample introduction due to its extremely small invasiveness (Fricker, Günther, 2016). Schematic layout of ICP-MS machine is represented in the Figure 21.

In LA-ICP-MS, the sample is put into the chamber with carrier gas flow (a noble gas, usually He or Ar), a high energy laser beam (193nm, 213nm, 266nm) is ablating the exposed sample surface transforming some part of it into a dry aerosol. The diameter of laser crater (damaged area) is variable but negligible (4-200  $\mu\text{m}$ ) (Janssens, 2013).

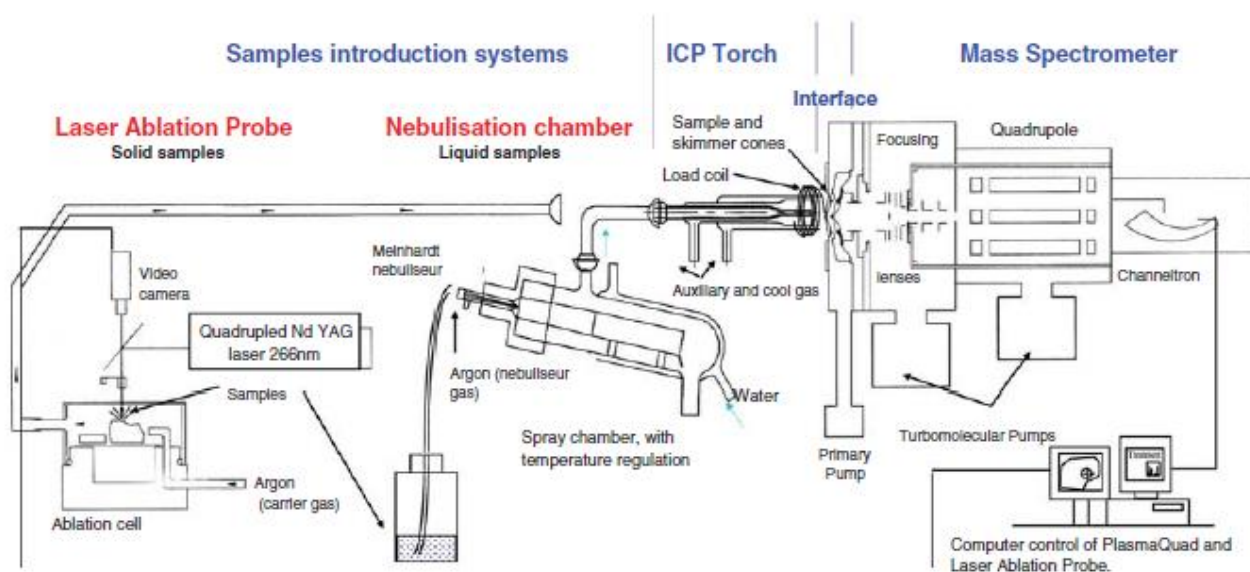


**Figure 21:** Schematic layout of LA-ICP-MS machine (Janssens, 2013).

After that the sample material is directed into torch. It is ionised with help of argon plasma (10000K) that transfers it to the interface with sampler and skimmer cones (to focus the stream). The interface is medium between atmospheric pressure part of the equipment and its vacuum part. It also eliminates all negatively charged and neutral particles and photons (Fricker, Günther, 2016). The so-called mass analyser is the part of ICP mass spectrometer that divides ions according to their mass to charge ratio ( $m/z$ ). There are several ways to do so, in this study the triple quadrupole technology was utilised. Quadrupoles are systems of four conducting rods connected to AC and DC electrical current. The kind of current changes with radiofrequency in a way that opposing rods have same current (AC or DC) making electromagnetic field that stabilises ions moving on spiral trajectory along the way in the middle. The frequency can be adjusted so only ions of certain mass or mass range can reach the detector (Clarke, 2017). In triple quadrupole system the first quadrupole is functioning as a mass filter, allowing only desirable ions reach next the collision/reaction cell which is, in fact, an octopole, where different gases (reactive ( $\text{H}_2$ ,  $\text{O}_2$  or  $\text{NH}_3$ ) or unreactive ( $\text{He}$ )) can be applied to eliminate factor of polyatomic and isobaric interferences. After this “purification” of ions they are transferred into third quadrupole that plays role of the mass analyser itself (Balcaen et al., 2015). The detector part is counting individual ions by electron pulse they make while reach detector, the signal is multiplied and amplified by an electrons cascade. This signal is compared to the one of calibration reference sample, allows determination of absolute concentration of the element in the analyte (Linge, Jarvis, 2009).

This system is a very powerful instrument for establishing elemental composition up to the level of ppt (parts per trillion). The trace elements studies are widely used for revealing the provenance of objects made of different materials. Glass studies are not the exception even though researchers in this field are facing major problems, for example, complexity of glass as a material, that could get same elements from different sources (Pollard, 2008). However, with different grade of success numerous studies have yielded significant amount of information about trace elements content in different glass materials (Freestone et al., 2002; Carter, 2015; Smit et al., 2005). Some of them are very confident about the sand source (Conte et al., 2016). We have to keep in mind the uniqueness of the Yahorlyk settlement context that makes the likelihood of primary glass production be on the high level of probability.

In this study the Agilent 8800 ICP-MS Trip Quad coupled to a CETAC LSX-213 laser ablation system was used. Every sample (in case of polychromatic pieces every colour) was measured four times to ensure the representativity of the data. The working parameters are put in the table below (Table 5).

**Table 5:** Instrumental settings for the analysis of Yahorlyk glass.

Acquisition mode	TRA (time resolved analysis)
Scan type	MS/MS No gas
Plasma parameters:	
RF power	1550 W
RF matching	1,40 V
Sample depth	6,5 mm
Dilution gas	0,6 L/min
Dwell time of isotopes measured:	
2 msec.	<sup>23</sup> Na, <sup>27</sup> Al, <sup>28</sup> Si, <sup>39</sup> K, <sup>43</sup> Ca, <sup>44</sup> Ca, <sup>56</sup> Fe.
5 msec.	<sup>24</sup> Mg, <sup>57</sup> Fe, <sup>63</sup> Cu.
10 msec.	<sup>47</sup> Ti, <sup>55</sup> Mn, <sup>66</sup> Zn, <sup>68</sup> Zn.
20 msec.	<sup>31</sup> P, <sup>51</sup> V, <sup>52</sup> Cr, <sup>59</sup> Co, <sup>60</sup> Ni, <sup>75</sup> As, <sup>85</sup> Rb, <sup>88</sup> Sr, <sup>89</sup> Y, <sup>90</sup> Zr, <sup>93</sup> Nb, <sup>95</sup> Mo, <sup>107</sup> Ag, <sup>118</sup> Sn, <sup>121</sup> Sb, <sup>133</sup> Cs, <sup>137</sup> Ba, <sup>139</sup> La, <sup>140</sup> Ce, <sup>146</sup> Nd, <sup>147</sup> Sm, <sup>153</sup> Eu, <sup>159</sup> Tb, <sup>169</sup> Dy, <sup>166</sup> Er, <sup>169</sup> Tm, <sup>172</sup> Yb, <sup>175</sup> Lu, <sup>197</sup> Au, <sup>208</sup> Pb, <sup>209</sup> Bi, <sup>232</sup> Th, <sup>238</sup> U.
Laser ablation instrumental conditions:	
Laser	Nd/YAG
Wavelength	213 nm
Spot size	100 µm
Laser energy	80%
Laser frequency	20 Hz

**Table 5:** Instrumental settings for the analysis of Yahorlyk glass (cont.).

Laser method	Spot analysis; 600 shots
He flow	1 L/min
Shutter delay	20 sec.
Gas washout	10 sec.

To check the accuracy of the data obtained NIST 610 was used for optimisation and as the reference material. NIST 612 function in the sequence was quality control. The results obtained were processed with GLITTER software where there was an opportunity to discard first few seconds of ablation and check the homogeneity of the signal. CaO data obtained by means of SEM-EDS was used as an internal standard. The resulting table of concentrations underwent averaging and normalisation to 100%. Detection limits of the analyses are placed in the Annex 9.

### 2.2.2 Methods of sand analysis and corresponding sample preparation

As it was said above, to locate the origin of glass one must have data regarding elemental composition of sand from probable raw materials source. Data from famous sites of glass production in the ancient world are widely known and used by scientists worldwide to make suggestions about probable provenance of “raw” glass (Brill,1999; Rehren, Freestone, 2015). The Yahorlyk settlement was located quite far from major known production sites that is why the sand from that area was never in the scope of glass provenance research. Since we want to confirm or disprove local origin of glass found in the Yahorlyk settlement, we are bound to determine elemental composition of sand available there.

This section is meant to describe what has been done for it. Collected samples of sand were transported to the laboratory in plastic bags. The excess of water was removed by drying samples in glass and paper containers at 40°C. During this process it was also reasonable to disaggregate sand and loam or clay clusters. After that about 30 g of each subsample was taken for further analyses. These 30 g of matter were selected after mixing the subsample with subsequent quartering of the subsample mound with the purpose to take substance equally from the centre and margins (these areas might be not identical due to the gravitational sorting of heavy minerals in sand). Every representative part of subsample was cleaned from small particles of plant origin manually and examined under stereomicroscope to ensure its purity. Milling of these parts was necessary to proceed. They were milled into very fine powder with help of (Retsch PM 100) electric mill for 40 min in the agate container with the set of agate balls (2 big or 2 big and 2 small or 2 big and 3 small).

It was decided to establish the elemental composition by means of XRF (major and minor elements) and ICP-MS (trace elements). It is always useful to possess some mineralogical information about analysed material, for this reason XRD analyses were conducted. All steps of the following sample preparation protocols will be placed in the corresponding paragraphs. We will not give here information regarding fundamentals of the techniques mentioned, because it was already given in the section above, instead we are going to note the differences in glass and sand sample processing. They arise from the fact that we are not bound to non-destructiveness or non-invasiveness parameters of analytical methodology applied to archaeological glass.

Sand analysis also involved utilizing the auxiliary techniques such as granulometry (used to check ratio of fractions in samples; was performed on other samples of sand that is not reported in the work (to look at results see Annex 7), thermogravimetical analyses (were conducted for some samples to know the level of impurities and calcium carbonate (shell particles) content (to look at results see Annex 7). The data acquired with help of these techniques sometimes were decisive to choose certain parameters of sampling or sample preparation.

#### *2.2.2.1 X-ray diffraction (XRD)*

Fundamentals of the X-ray diffraction were already described before. Here we only make few remarks about powder method, which is routine approach to analysing earth materials (Louër, 1999). In theory, powder contains crystals oriented differently and hence it will definitely provide signal from all the crystal planes of all phases present due to the homogeneity of the analyte and random (and theoretically proportional) distribution of crystal planes that satisfy Bragg's law (Janssens, 2013). This is the main advantage of powder method to  $\mu$ -XRD, that may not provide signal from random distributed planes. therefore, this method is more appropriate for quantification.

It does not require much preparation after powdering. Particles must be very fine ( $<10\ \mu\text{m}$ ) to avoid biases of representation (Pecharsky, Zavalij, 2009). Approximately 1 g of sample was used to make a disk (or pellet) with pressing by the cover glass the material inside the flat and shallow void on special sample support without gluing or another manipulation.

Bruker D8 Discover was used to perform analyses with the same parameters that were used in the  $\mu$ -XRD configuration. The  $2\theta$  angle range was  $3^\circ$ - $75^\circ$ , the step size  $0,05^\circ$  and step time of 1 sec. DIFFRAC.SUITE EVA software and PDF-2 database from the International Centre for Diffraction Data (ICDD) was used to interpret the results.

#### 2.2.2.2 X-ray fluorescence (XRF)

X-ray fluorescence analyses were also conducted in different way than the ones of beads fragments. First of all, the equipment used was Bruker S2-PUMA Carousel. Its High Sence Ligth Element SDD detector allows to establish elemental composition of the analysed material to ppm level detecting elements from C to Am (Bruker web site). The appropriate way of sample introduction is to press the material in pellets. For this purpose, exactly 10 g (precision 0,0002g) of each subsample was mixed with exactly 1 g of wax (same precision) and pressed by means of the manual hydraulic press for not less than 5 min under the pressure of not less than 22 tons.

Two spectra (for light and for heavy elements) were generated per each sample (of maximum voltage of 20 kV and 40 kV respectively). The current set was 0,241 A for the first spectrum and 0, 411 A for second one. Every measurement acquisition time was 100 sec. All the measurements were performed in vacuum. The values obtained were converted into oxides by built-in operation software of the equipment.

#### 2.2.2.3 Inductively coupled plasma mass spectrometry (ICP-MS)

Even though the mass spectrometer used for analyses of sand was the same, the method of sample preparation was completely different. It was decided to use digested samples in the aqueous acidic solution. In this case aerosol is made in the specially designed nebuliser with Ar as a nebulizing and carrier gas. This aerosol is consequently introduced to plasma torch part where already described process of ionization and mass to charge ratio sorting takes place (Fig. 21).

To prepare samples for experiments a digestion protocol for silica containing materials was inspired by methods used by Ottley, Eggins and Finlay with few modifications (Finlay et al. 2012). Method requires utilizing of a certified reference material that allows to check the accuracy of the data by comparing the data of experiment with one that was certified. This material is treated in the same way as every single sample. This allows to check all the procedure related changes in the samples as well as control reliability of experimental data obtained. For this role Quartz Latite 1a produced by U.S. geological survey was selected. All the steps of protocol were done to empty container that was included to every batch as a contamination control tool. To ensure sufficient quantity of each subsample (100 mg with precision of 5 mg) was weighted in PFA containers with the subsequent drying for over 12 hours at 50 °C. The weights of sample before and after drying were recorded to make possible future quantification. After that, 2 mL of hydrofluoric (HF 50%, OPTIMA grade) and 1 mL of nitric (HNO<sub>3</sub> 65%, Suprapur grade) acids were poured into every container. This

mixture stayed on the hotplate at 150 °C for 48 hours. Evaporation of the mixture until small droplet has left was the next step. Next cycle of digestion was with 2 mL of Aqua Regia (3:1 mixture of respectively hydrochloric (HCl) and nitric (HNO<sub>3</sub>) acids) duration of 24 hours. After that aqueous solution of concentrated nitric acid (1,5 mL of acid and 3 mL of water) was applied. All these steps were interrupted with evaporating sessions when containers were open to let all volatile compounds to leave at the temperature 125 °C. All the reagents were introduced to containers using pipette. Special attention was given to integrity of the mixtures (nothing has to leave the container) and avoiding of contamination. All digested samples after last evaporation session were diluted with 50 mL of Mili-Q water and frozen at -80 °C until the experiment time. It took three digestion sessions to process all of the samples. Three samples were repeated because some of material was lost after opening the container. Three digestion batches were analysed in two runs.

The detection limit was calculated through the analysis of 300 µg/L<sup>-1</sup> multielemental solution and the blank. 11 replicates were made. DL table for every element analysed in each run can be found in the Annex 8. Calibration curve consisted of 14 levels (from blank to 3000 ppm of multielemental solution) and was run prior to the samples. The repetitions of the reference material solution were made to check the drift of the signal.

Same Agilent 8800 ICP-MS Trip Quad equipment was used to analyse samples. Its parameters were different from the ones used in the laser ablation mode they are presented in the Table 6:

**Table 6:** Instrumental settings for the analysis of sand samples.

Scan type	MS/MS
Plasma parameters:	
RF power	1550 W
RF Matching	1,70 V
Sample depth	10 mm
Carrier gas	1,1 L/min
Nebulizer pump	0,10 rps
S/C temperature	2 °C
Measurement parameters	
Acquisition mode	Spectrum
Q2 peak pattern	1 point
Replicates:	3
Sweeps/ Replicate:	10
He	<sup>51</sup> V, <sup>52</sup> Cr, <sup>59</sup> Co, <sup>63</sup> Cu, <sup>66</sup> Zn, <sup>72</sup> Ge, <sup>85</sup> Rb, <sup>88</sup> Sr, <sup>89</sup> Y, <sup>90</sup> Zr
No gas	<sup>90</sup> Zr, <sup>93</sup> Nb, <sup>95</sup> Mo, <sup>107</sup> Ag, <sup>118</sup> Sn, <sup>133</sup> Cs, <sup>137</sup> Ba, <sup>139</sup> La, <sup>140</sup> Ce, <sup>146</sup> Nd, <sup>147</sup> Sm, <sup>153</sup> Eu, <sup>159</sup> Tb, <sup>163</sup> Dy, <sup>166</sup> Er, <sup>169</sup> Tm, <sup>172</sup> Yb, <sup>175</sup> Lu, <sup>182</sup> W, <sup>208</sup> Pb, <sup>232</sup> Th, <sup>238</sup> U

**Table 6:** Instrumental settings for the analysis of sand samples. (cont.)

Dwell time:	
0,5 sec.	<sup>107</sup> Ag, <sup>118</sup> Sn, <sup>133</sup> Cs, <sup>139</sup> La, <sup>140</sup> Ce, <sup>146</sup> Nd, <sup>147</sup> Sm, <sup>153</sup> Eu, <sup>159</sup> Tb, <sup>163</sup> Dy, <sup>166</sup> Er, <sup>169</sup> Tm, <sup>172</sup> Yb, <sup>175</sup> Lu, <sup>182</sup> W, <sup>208</sup> Pb
0,3 sec.	<sup>85</sup> Rb, <sup>88</sup> Sr, <sup>89</sup> Y
0,1 sec.	<sup>51</sup> V, <sup>52</sup> Cr, <sup>59</sup> Co, <sup>63</sup> Cu, <sup>66</sup> Zn, <sup>72</sup> Ge, <sup>93</sup> Nb, <sup>95</sup> Mo, <sup>137</sup> Ba, <sup>232</sup> Th, <sup>238</sup> U
Internal standards (0,1 sec, no gas, He)	<sup>101</sup> Ru, <sup>103</sup> Rh, <sup>193</sup> Ir

Obtained concentrations of the elements were converted from the solution concentration into solid sample concentration expressed in ppm. Certain elements (Cr, Cu, Ge, As, Mo, Ag, Zn, Sn, W) were discarded due to unreliability of the results for majority of samples (due to contamination or CRM data).

Summary for chapter 2:

1. We consider that the set of beads and other fragments selected for the research and the sand sampled in the area make up a representative collection of glass fragments from the Yahorlyk settlement and possible raw material samples. The fact that the glass artefacts are superficial finds has to make us to look at the material with a bit of suspicion which is natural in cases of finds deprived of cultural layer and stratigraphy.
2. All the laboratory processing of both kinds of samples was made avoiding metal tools that can contaminate samples. Therefore, sand samples were manipulated with exclusively plastic or wooden tools. Plastic bags were common storage containers. Exception was made only for process of XRF pellets making. Obviously metal part of the press had to contact with the surface of each sample to be analysed.
3. The methodology selected for the research allows a very detailed comparison of elemental composition of both glass and sand that will make ground for some conclusion about the provenance of the Yahorlyk settlement glass beads. Ancient technology and batch formulae used to make them might be recognised.

## CHAPTER III. RESULTS AND DISCUSSION

The data obtained with each particular method and its interpretation are going to be described below. We start with the results section that is a core of any scientific research. Results allow to build solid conclusions. Interpretation and discussion of the results obtained is following in the structure and it is built in a way that every question put in the beginning will find an answer based on the analysis of the experimental data.

### 3.1 Results

#### 3.1.1 Glass analysis

Some data reduction took place. Only relevant information that helps to answer research questions is put here. The groups of glass colour correspond to the typological groups established in the historical and archaeological context section. Numbers of the groups will be the key in further presentation:

Group 1: Blue translucent glass. Includes samples Ya-1, Ya-2, Ya-4, Ya-5 and Ya-6. Samples Ya-1, Ya-2, Ya-4 are fragments of round beads. Ya-5 and Ya-6 belong to non-beads and put in the same group based on colour;

Group 2: Dark base eyed beads. It includes samples Ya-3, Ya-11, Ya-12, Ya-13 and Ya-16;

Group 3: Purple base eyed beads. Includes samples Ya-14 and Ya-15;

Group 4: It includes sample Ya-10 that is typologically different from all the other eyed beads;

Group 5: Dark monochromatic beads. Only includes sample Ya-9;

Group 6: Green non-beads. Includes samples Ya-7, Ya-8 and Ya-17;

Group 7: Biconical colourless beads. Includes samples Ya-18 and Ya-19;

Group 8: Biconical yellow beads. Includes samples Ya-20, Ya-21, Ya-22 and Ya-23;

The grouping is made on visual inspection. These groups are expected to have distinct differences in their elemental composition. Annex 1 contains stereomicroscope images of entire samples.

##### 3.1.1.1 Optical microscopy (Stereomicroscopy)

The beads were examined from all sides. This applies to both the initial surface and the bead fracturing surface. Certain attention was paid to the surface of the apertures. Below we will focus

on the individual features of each piece, without mentioning the features that have already been specified (like colour, shape and size (this information is put in sampling section)). To somehow organize the presentation, we will organize the description by groups.

Group 1. Samples have differences in the texture of the outer surface. The irregularities are more oblong in the Ya-1 (Fig. 22, a) than in the rest of group (Fig. 22, b).

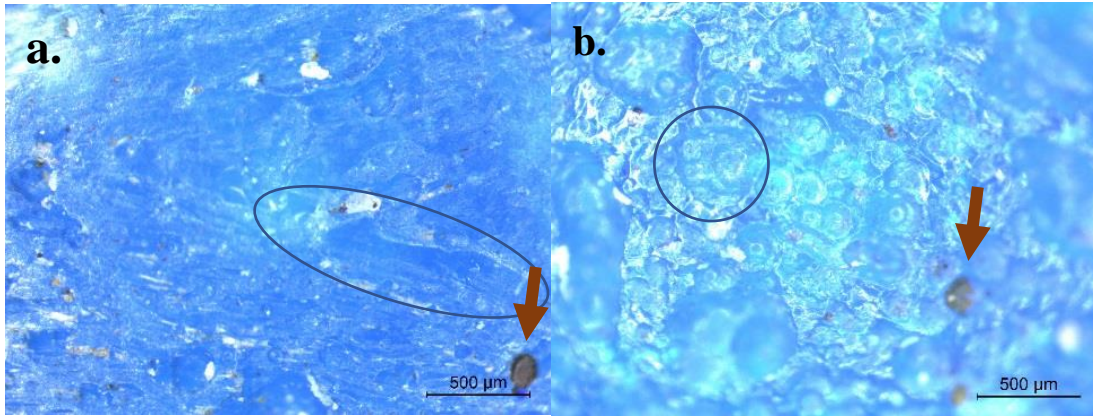


**Figure 22:** Stereomicroscopy images. a - surface of Ya-1 at magnification 50X; b - surface of Ya-2 at magnification 50X. Dark grains are marked with arrows.

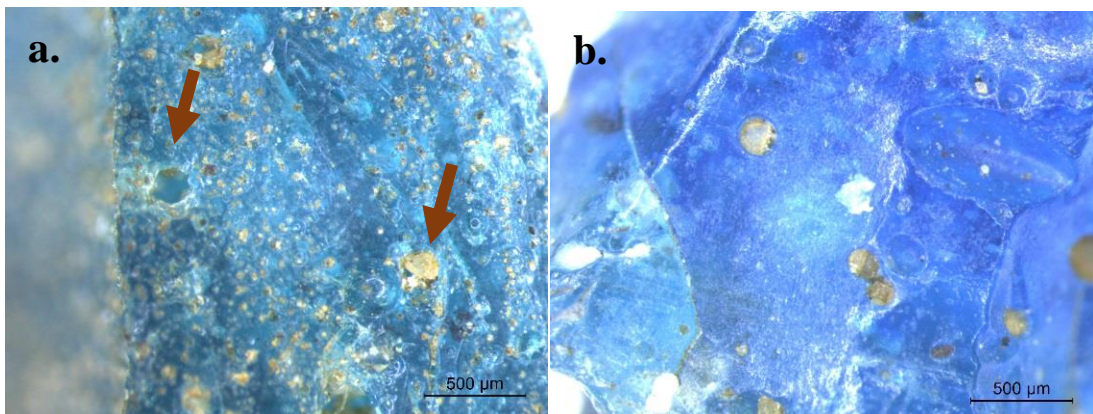


**Figure 23:** Stereomicroscopy images. a - Ya- 4 section surface at magnification 50X. An empty collapsed air bubble (left arrow); a bubble filled with quartz grain (right arrow); b - Ya-5 surface at magnification 50X.

In Figure 22, it is easy to see that the glass mass is quite homogeneous, but it has small dark grains visible within the glass matrix. Extremely noticeable are translucent grains (probably quartz) that occupy places in the rough surface. They are much more numerous in sections and on the surface of the apertures. In Figure 23 (a), one can observe such grains, together with some collapsed bubbles. In addition, there are several cracks of the transversal surface and in depth, which could be generated as glass was cooling down or during a long history of its interaction with the environment. Non-beads within this group have more smooth surfaces. Photos of all samples can be found in the Annex 1.

Group 2. The eyes of these round dark base eyed beads have common features with the previous group. However, these samples, unlike others are polychromatic (Figure 24 shows all the colours and texture of each part).

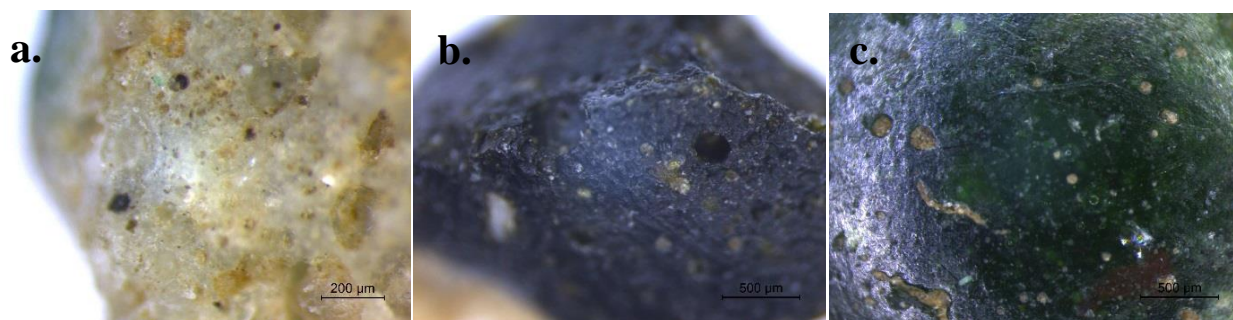


**Figure 24:** Stereomicroscope images. a - Ya-11 white glass (50X); b - Ya-16 dark base glass (50X); c - Ya-12 eye (50X).

The white glass is the hollowest, some bubbles that have not yet collapsed can be seen near the surface. Also, in this glass there are noticeable dark granules, which are rather evenly spread and well sorted (Figure 24, a). The textures of the base and the eye parts are very similar between themselves and with previous group.

Group 3. This group of purple base eyed beads has more even surfaces and clearer glass, especially in the blue parts. The contact zone between the purple and blue glass of sample Ya-14 is shown in Figure 25. Some bubbles under the surface are present in the purple part.

Group 4. Sample Ya-10 has the same eye texture and colour as the previous group. Its white layer has numerous bubbles but they stay intact under the relatively smooth surface.

Group 5. The only representative of this group, sample Ya-9, has surface features similar to group 2. The collapsed bubbles in the section and the aperture surface are larger and more numerous. A small transparent grain of blue colour was also found on the edge of the fragment. Also, the iridescence – the sign of glass alteration due to depletion of the alkaline content of glass, was noticed (Emami et al., 2016) (Figure 26).

Group 6. Green non-beads are different in colour and texture from all the other groups of samples. Their appearance reflects the big amount of bubbles present.

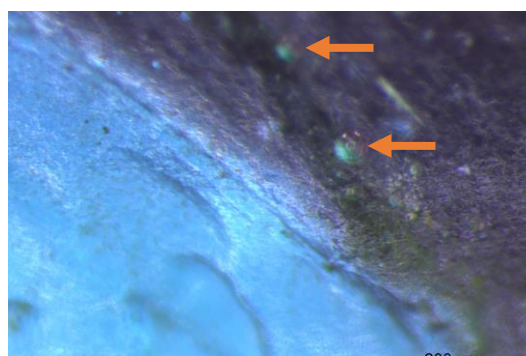


**Figure 25:** Stereomicroscope image of sample Ya-14 at magnification 125X; bubbles underneath the surface are marked with arrows.

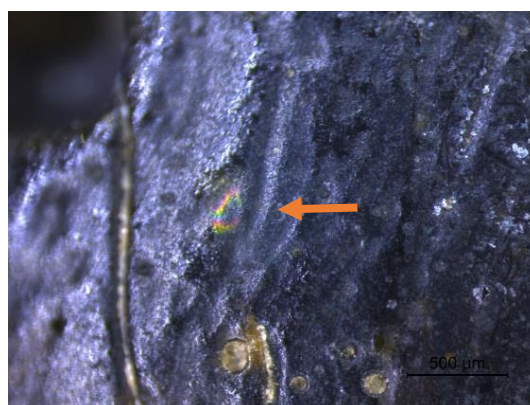


**Figure 26:** Stereomicroscope image of sample Ya-9 (50X); the iridescence effect is marked with an arrow.

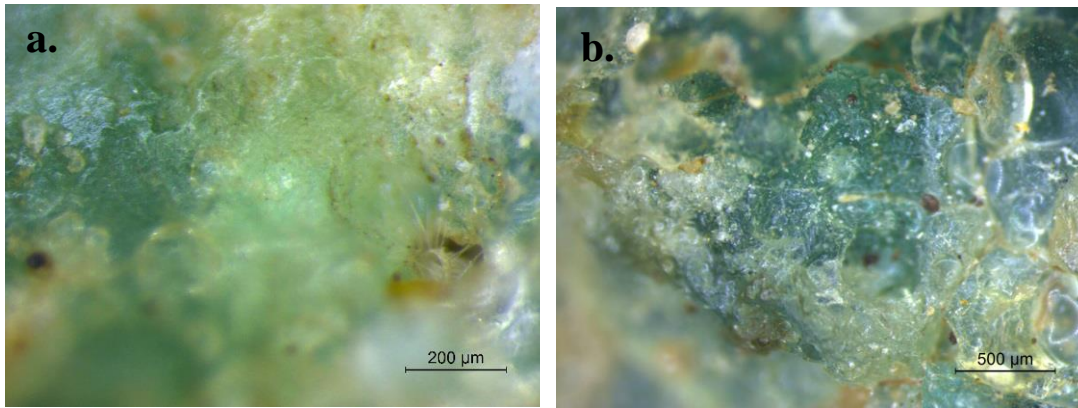


**Figure 27:** Stereomicroscope image of the rough surfaces of green non-beads: a - sample Ya-17 (125X); b - sample Ya-8 with some grains in the matrix (50X).



**Figure 28:** Stereomicroscope image of the light-coloured layer of sample Ya-7. (magnification 50X).

The surface appears to have lighter glass layer. They are probably the consequence of glass alteration. Figure 27 illustrates the look of these fragments. Sample Ya-8 has a purple stain in the depth of a collapsed bubble. The light-coloured layer of Ya-7 does not look like glass (Fig. 28). It has to be considered separately when elemental composition of glass will be acquired.

Group 7. Colourless biconical beads seem to be completely different from the beads of the remaining groups. One of them (sample Ya-18) has multiple scratches, parallel to the aperture, another (sample Ya-19) is covered with very small grains, placed in the irregularities of the surface. Bubbles were not encountered, and roughness is, most likely, of abrasive origin. An important feature of these beads is their transparency. No grains were observed inside the glass matrix (Figure 29).

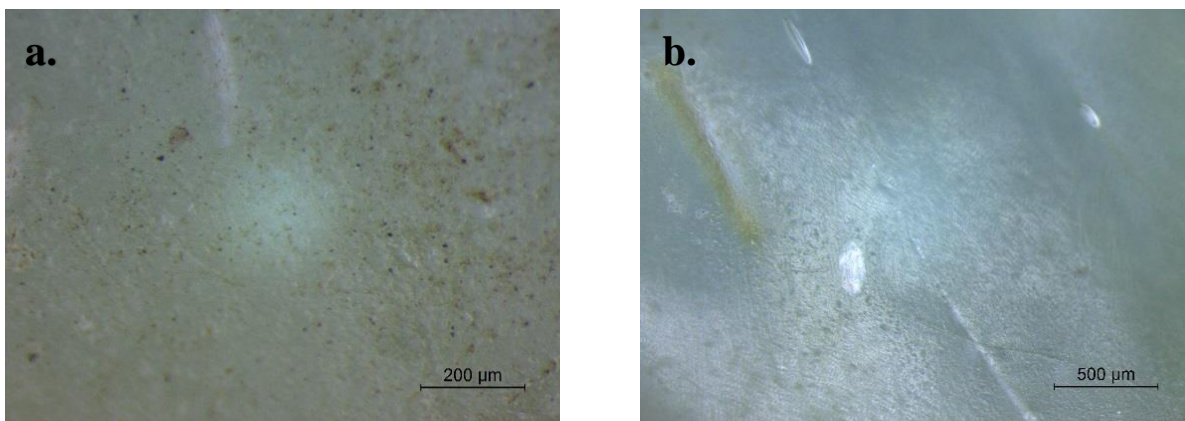


**Figure 29:** Stereomicroscope images. a - surface depositions on sample Ya-19 (120X), b – sample Ya-18 at magnification 50X.

Group 8. Yellow biconical beads differ from the previous group by their yellow tint, but besides that their texture, is rougher. Some have the superficial deposits and in some places there is

an iridescence. Sample Ya-23 under the microscope looks much closer to the colourless group. Disperse and rare dark grains inside the glass mass can occasionally be found (Fig. 30, a).

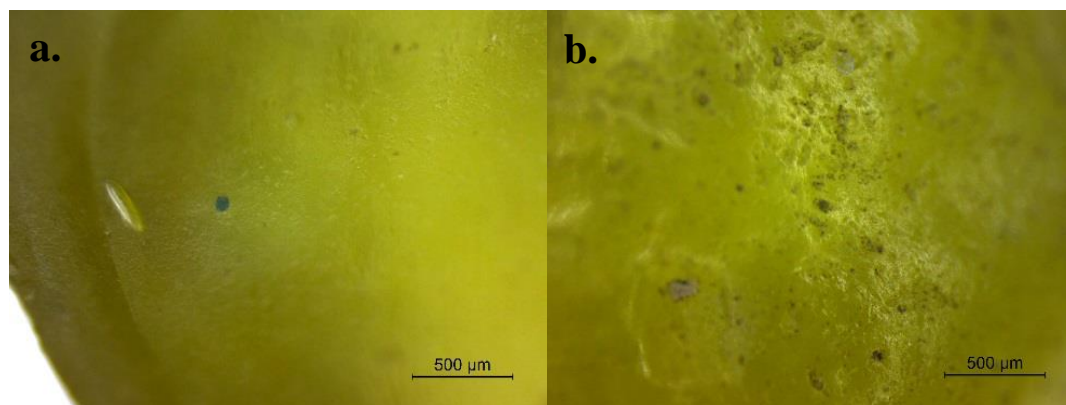


**Figure 30:** Stereomicroscope images. a - dark grain on the surface of sample Ya-22 (50X); b - slight roughness of sample Ya-20 with superficial deposits visible (50X).

To Summarize, the visual examination of glass samples from the Yahorlyk settlement shows that they all spent a long time reacting with soils. A vast majority of them is bearing numerous bubbles that collapsed on the surface, almost every one of them has deposits of loose particles, which are well-fitted in the roughness of the surface (Table 7).

**Table 7:** The summary of stereomicroscope observations of the Yahorlyk glass artefacts. (the number of + corresponds to the relative amount of bubbles; \*- the eye part is free of bubbles).

Group	Transmittance	Colour	Bubbles	Roughness (outer surface)	Visible Alteration
Group 1	Poorly translucent	Blue	+++	Rough	No
Group 2	Opaque	Dark, white, blue	++++	Rough	No
Group 3	Translucent eyes opaque base	Dark purple, white, blue	++*	Smooth	No
Group 4	Translucent eye opaque white layer	White, blue	++++*	Smooth	No
Group 5	Opaque	Dark	++++	Smooth	Yes
Group 6	Poorly translucent	Turquoise, green	+++	Very rough	Yes
Group 7	Translucent	Colourless	+	Smooth	Yes
Group 8	Translucent	Yellow	+	Smooth	Yes

### 3.1.1.2 X-ray fluorescence (Portable XRF)

The semi-quantitative data obtained by means of handheld XRF spectrometer has given the understanding of the major chemical composition of beads and was used as the guideline for all the following research proceedings. All the results are presented in Annex 5. The samples have similar composition in what concern to major elements and remarkable differences in the minor elements content. We also have a chance to compare the dataset from glass with the one from sand made under the same conditions. Elements detected were: Al, As, Br, Ca, Cl, Co, Cr, Cu, Fe, K, Mg, Mn, Mo, Ni, Pb, Rb, S, Si, Sn, Sr, Ti, Zn, and Zr.

Group 1. The distinct feature of this group of blue glass is high Cu content typically more than 20 arb. units although Ya-6 shows only 6,05 arb.units. (Fig. 31). Sample Ya-5 (marked with orange arrow in Fig. 31) is different from the rest of the group as it has one of the highest Co values (0,23

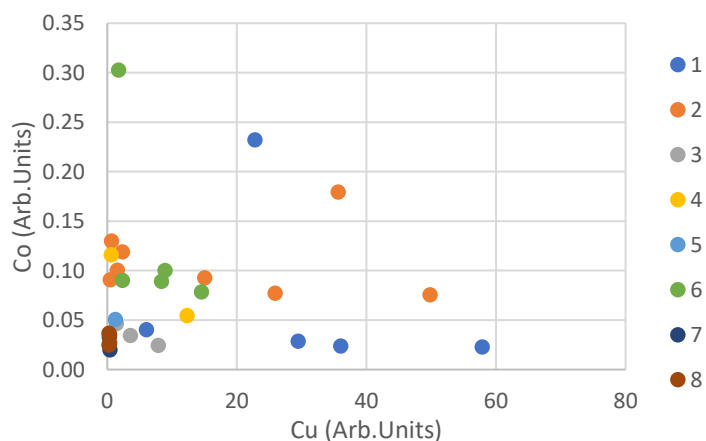


**Figure 31:** Yahorlyk glass Cu against Co binary plot. Every colour is attributed to a specific group. Sample Ya-5 is marked with the arrow.

arb.units), while the rest of the group is relatively depleted in Co. Cl values are one of the highest (0,4-0,7 arb.units). Iron is not so abundant when compared to other groups (always less than 10 arb.units when the maximum of eyed beads is more than 30 arb. units). So is K that shows minimal values for the entire set (to compare see Fig. 32). No Br or Rb was detected for this group. Elements such as Sn and Pb are only present in Ya-2 and Ya-4. Molybdenum was detected in sample Ya-5, whereas antimony was detected in samples Ya-1 and Ya-4 – a unique cases for all the Yahorlyk samples.

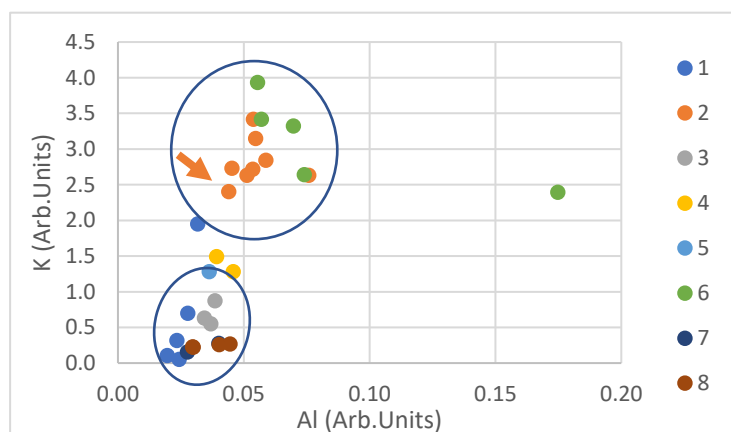


**Figure 32:** Yahorlyk glass Al against K binary plot. Two clusters can be noticed. Sample Ya-3 is marked with an orange arrow.

Group 2. The dark base eyed beads are dominating (sharing this position with group 6) in values for such elements as K and Al (Fig. 32). Ca content is on contrary lower than for the rest of the beads (does not exceed 9 arb.units at the time when the rest of the beads do not

show less than that). As can be seen from the Figure 31, and from the table in the Annex 5, Cu content is elevated for the blue parts of these beads. Together with the other eyed groups, the samples from group 2 have higher amount of Mn than the rest of the samples. Sample Ya-3 groups together with the rest of the group confirming that it is indeed the detached eye of a bead (marked with orange arrow). The Fe content of this group is remarkably higher than in the rest of the bead samples competing only with group 6 (Fig. 33).

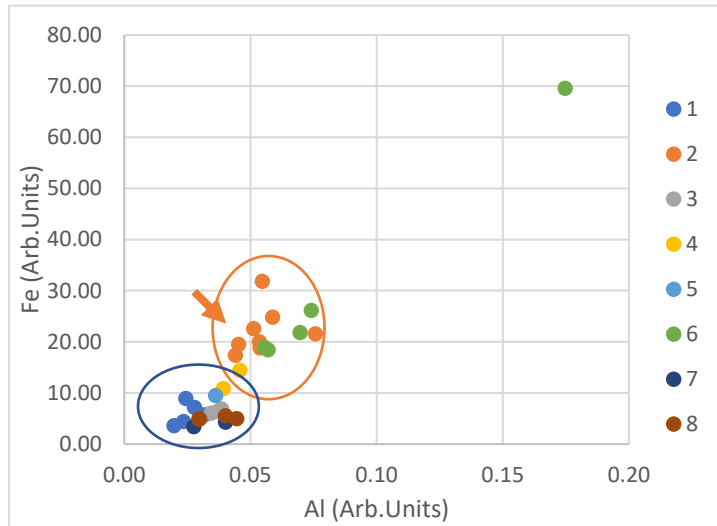


**Figure 33:** Yahorlyk glass Al against Fe binary plot. Sample Ya-3 is marked with the arrow. Two groups can be noticed. Groups 2,6 cluster together in the opposition to groups 1,3,7,8.

Group 3. The most discriminative element for the group of purple beads is Mn. Its values exceed 5 arb. units and are significantly higher than in the rest of the set (Annex 5). In Figures 31 and 32 these samples are grouping with groups 1, 7 and 8. Unlike the previous group, group 3 has significant amounts of Pb (1,57 - 2, 47 arb. units).

Group 4. Sample Ya-10 which is the only representative of the group is different from the rest of the samples most of all by its Pb and Sn content (more

than 6 and 1,8 arb. units respectively) which is more than 2 times higher than the values of these elements in any other sample.

Group 5. Bromine was detected in the dark bead included in this group (sample Ya-9). This element was also found in other dark base eyed beads (group 2), however these groups can easily be distinguished based on the content of major glass elements such as Fe, Al, K (Figures 31, 32). Together with the representative of the group 4 they tend to stay in the middle between high Fe-Al group (orange oval in Fig. 32) and low Fe-Al group (blue oval in the same figure). They repeat this behaviour on the plot of Al against K (Fig. 31).

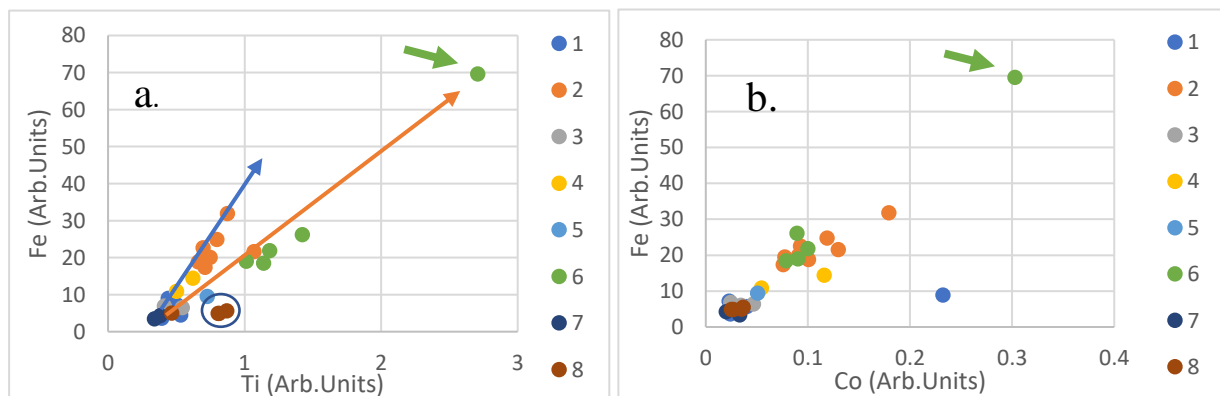


**Figure 34:** h-XRF bi-plots. a - Yahorlyk glass Ti against Fe binary plot; two trendlines are represented with arrows; b - Yahorlyk glass Co against Fe binary plot. Ya-7 light side position is marked with the green arrow.

Group 6. The green non-beads show values higher than beads for elements such as Ti (more than 1 arb. unit) and Rb (0,1-0,2 arb.units). They have approximately equal amounts of K, Fe, and Al as group 2. The light layer of Ya-7 (depicted in Fig. 28) shows the outlying quantities of Fe, Co, Cr, Al, Ti and Zn (marked with the green arrow in Figure 34, a and b). The other side of the sample, which is glass, holds up together with the rest of the group. The trendlines on the Ti against Fe plot can be explained by utilising sand with different Fe-Ti minerals ratio or by intentional addition of iron to the beads that follow blue arrow (Fig. 34, b). It is also visible that Co is strongly related to Fe ( $r= 0,83$ ) with the exception of sample Ya-5 (group 1). Above shown figures demonstrate that light layer of Ya-7 is related to the rest of the group.

Group 7. The biconical colourless beads as can be seen from Figures 31-34 group together with the groups 1 and 3. They show lowest values for Fe (min - 3,41 arb.units) and are also depleted in Ti, Al, K. They seem to be free of sand impurities.

Group 8. The last group of biconical yellow beads is different from previous group having higher Ti values (max 0,87 arb. units (group 7 max - 0,38)) and extremely high Zr values that are much higher than that of the rest of the samples (max - 3,55 arb. units). Sample Ya-23 does not follow this pattern. It is more closer to the group 7. The biplot of Ti against Zr is put below to illustrate the differences between groups 7 and 8 (Fig.35).

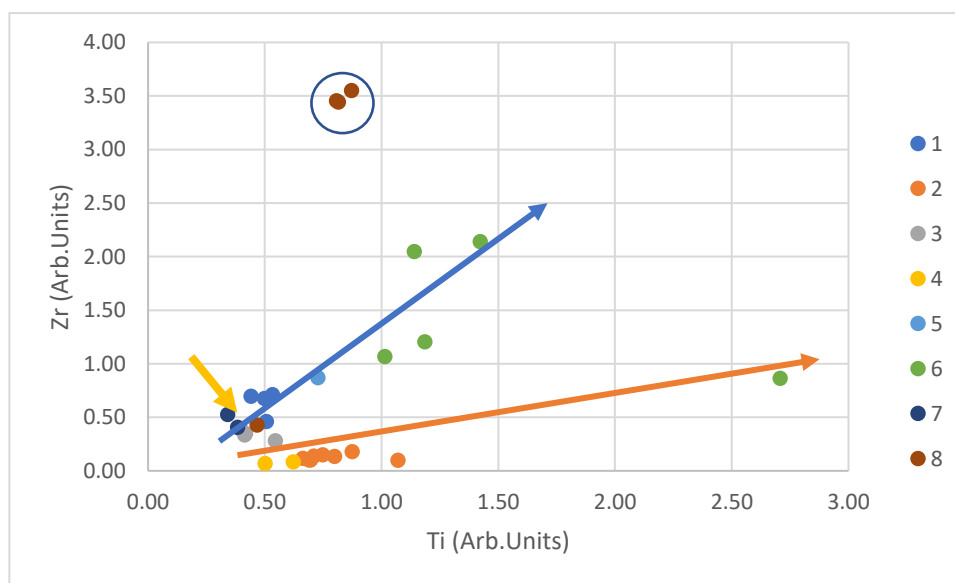


**Figure 35:** Yahorlyk glass Ti against Zr binary plot; two trendlines are represented by arrows, samples from group 8 are in the circle. Sample Ya-23 is marked with the yellow arrow.

As can be seen in Figure 34, groups 1, 5 and 7 cluster together. Groups 2 and 4 form another cluster with different trendline and group 8 is isolated, with the exception of sample Ya-23 (marked with the yellow arrow).

Handheld XRF results show that the typological and visual differences between the groups also translate into compositional differences. However, a bigger division can be made based on transition metal values: groups 1, 3, 7 and 8 are depleted in these metals (Fe, Al, Ti, etc.), while

groups 2 and 6 are relatively enriched in these elements. Groups 4, 5 have intermediate transition metal values but do not display a particularly strong relation with one or another cluster.

### *3.1.1.3 Variable pressure scanning electron microscope coupled with energy dispersive X-ray spectrometry (VP-SEM-EDS)*

In the previous chapter it was established that the variable pressure scanning electron microscope coupled with an energy dispersive spectrometer (VP-SEM-EDS) is a tool capable of producing high resolution images and gathering information about the elemental composition of the material. We begin with the evidences about textures and micromorphology of the Yahorlyk settlement glass fragments. It will be followed by glass matrix EDS analyses that include elemental mapping and area composition analyses. The last part of the presentation will contain consideration of inclusions in the glass matrix that were found. The beads were not analysed from all the sides. Representative side (homogeneous flat area) was taken to be exposed to the microscope. In some cases, the sample was inserted twice to make it possible to analyse all the colours or textures.

#### *Backscattering imaging*

The majority of the artefacts have a rough surface. Sometimes in places of collapsed bubbles there are step-structured internal surfaces that in most of the cases have surface deposits (Figure 36 a, b depicts surfaces of group 1 samples). This kind of surface is inherent to the groups 1 and 2.

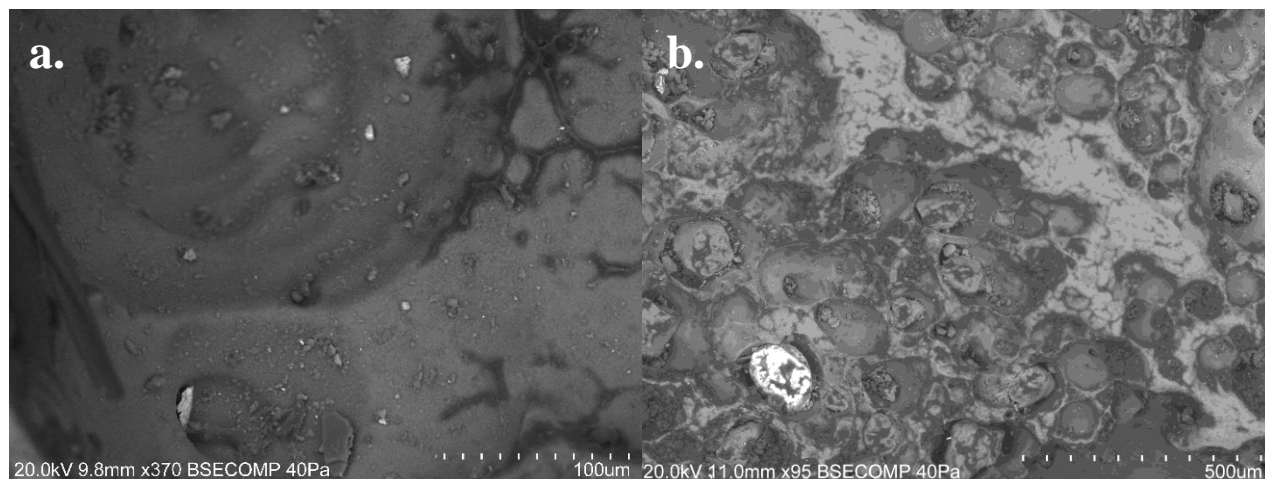


**Figure 36:** VP-SEM images. a - the backscattered image of sample Ya-2 showing step structure inside the collapsed bubble; b. – Ya-1 backscattered image demonstrating the roughness of the surface (light spot is the zircon grain trapped inside one of the collapsed bubbles).

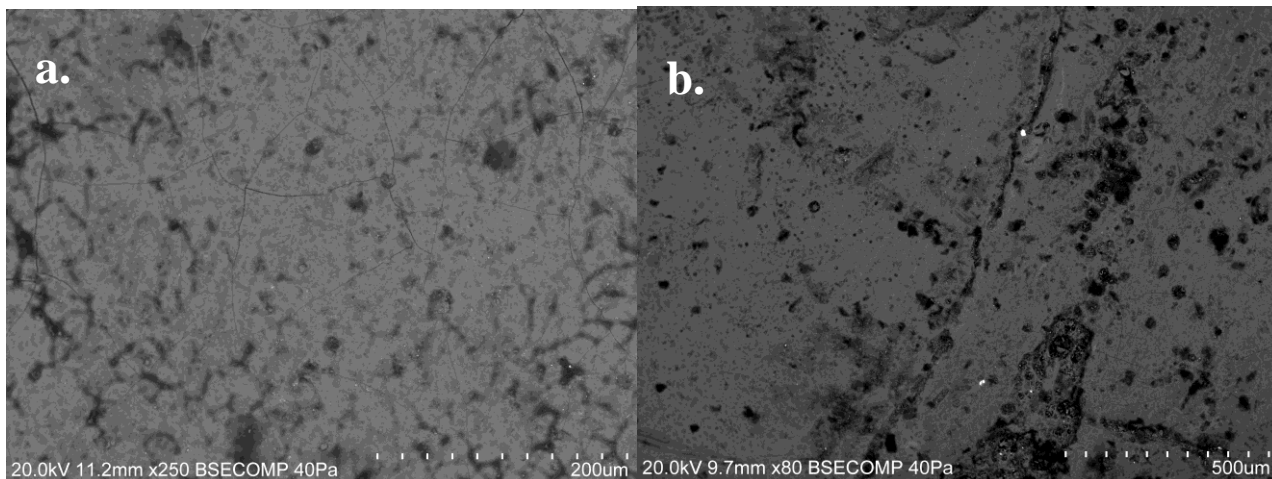


**Figure 37:** VP-SEM images. a - backscattered image of the surface of sample Ya-9; b - backscattered image of the surface of sample Ya-14.

Another type of texture is more abundant on the surfaces of beads from groups 3, 4, 5 and 6. It is less uneven, the total of flat surfaces is bigger. It still features considerable number of pits, collapsed bubbles are smaller. On the surface in some places a network of fine cracks is noticeable (Figure 37 a). This is an evidence of a superficial alteration of glass.

The last type of texture is characteristic of two last groups (namely 7 and 8). It is a relatively smooth surface without bubbles or big cracks. Instead, the network of fine cracks that indicates glass weathering is evident. Figure 38 is representative of this texture.

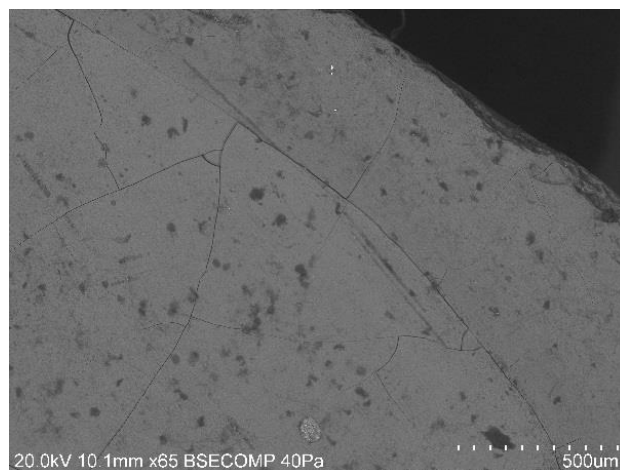


**Figure 38:** The backscattered image of the surface of sample Ya-21. The fine cracks area by the edge.

One must also keep in mind that the eyed beads (groups 2,3,4) are polychromatic, and that the textures of each coloured area within the same sample are not necessarily the same. If one will look at Figure 39, where all three coloured areas of sample Ya-11 can be seen, the slight difference in textures becomes evident (coloured lines help to understand which colour of glass is in each area). While the blue part looks lighter and smoother, there is no visible difference between white and dark parts.

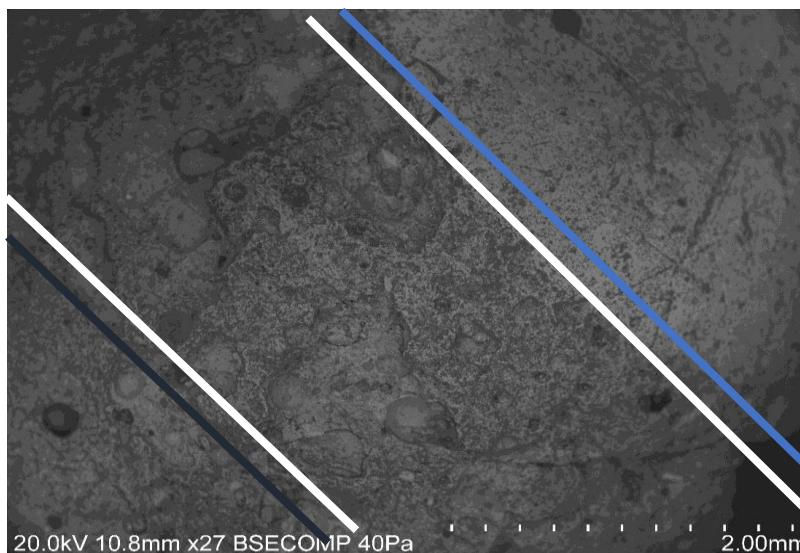


**Figure 39:** Backscattered image of sample Ya-11 representing all three colours. the tilted lines are put to distinguish between them: blue-white - border between blue and white glass; white and dark - border between white and dark parts.

### Micro-analyses by EDS

The areas with the visible differences in intensity of BSE signal, texture or transition zones between different compositions were examined with the mapping tool. Relative difference of elemental composition of different kinds of glass in the eyed beads group and some non-beads was

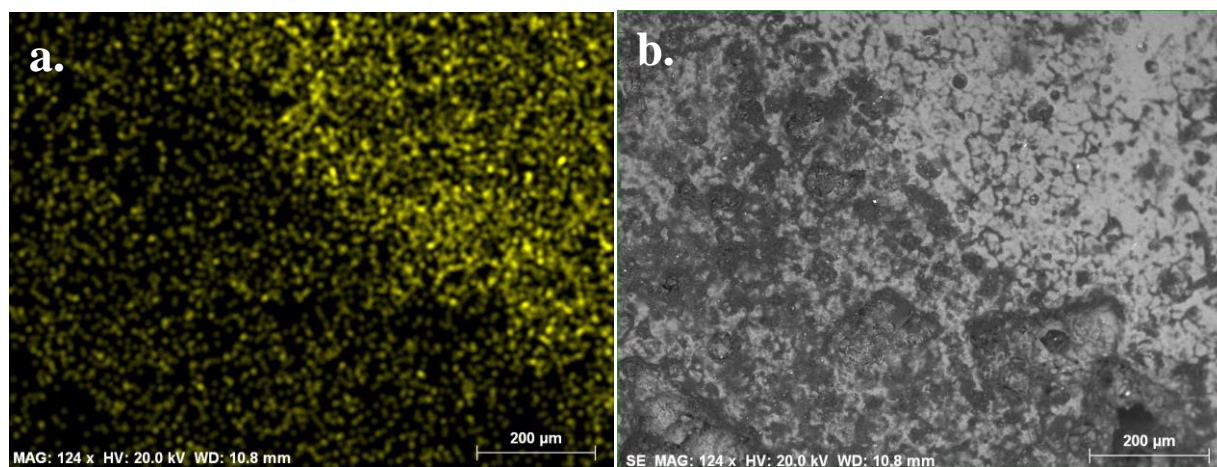


**Figure 40:** VP-SEM-EDS data. a - map of Cu distribution on the surface of sample Ya-11; b - backscattered image of the same area. The blue eye can be identified by different texture and higher amount of Cu.

the objective. It was also possible to check the homogeneity level of the glass matrix. The maps did not reveal any difference between differently coloured parts of eyed beads (groups 2,3 and 4) except the higher copper content in the blue parts. Figure 40 represents typical map of the eyed bead (Ya-11, group 2) with the backscattered image. One can see difference between the blue-green part of the eye and the rest of the bead. It is evident that the right side (the blue-green eye) is enriched in copper, while this element is not present in the remaining parts (dark and white glass) of the bead (Fig. 40).

In case of monochromatic samples (groups 1, 5, 6, 7 and 8) no perceptible inhomogeneity of matrix was registered. To obtain data about the composition two area analyses were made for each

monochromatic and three for each polychromatic sample (one area for each colour). These semi quantitative values allow an insight into the matrix's surface chemistry. We selected always flat areas to ensure same level of the surface response. The Table 8 presents oxides values of major elements present for each area analysed. Specifications of colour are given when the sample is polychromatic or when differences in texture should be noted.

**Table 8:** The VP-SEM-EDS results of selected areas (%), (<DL - below detection limit).

Sample	Area	Na <sub>2</sub> O	MgO	Al <sub>2</sub> O <sub>3</sub>	SiO <sub>2</sub>	P <sub>2</sub> O <sub>5</sub>	SO <sub>3</sub>	Cl	K <sub>2</sub> O	CaO	TiO <sub>2</sub>	MnO	Fe <sub>2</sub> O <sub>3</sub>	CuO
Ya-1	1	5,39	1,05	2,35	78,01	<DL	<DL	1,16	0,6	7,75	0,38	<DL	0,83	2,48
	2	3,33	0,35	1,64	77,83	<DL	0,53	1,13	1,07	11,07	<DL	<DL	<DL	3,05
Ya-2	1	7,57	0,52	1,09	74,35	<DL	0,41	1,19	0,56	10,22	<DL	<DL	<DL	4,08
	2	11,02	0,85	1,35	72,82	<DL	0,47	1,21	0,57	8,51	<DL	<DL	<DL	3,19
Ya-3		3,66	1,46	3,36	71,45	0,7	0,32	1,07	3,52	8,25	<DL	<DL	2,4	3,82
Ya-4	1	5,83	1,67	2,57	74,55	0,19	0,38	1,06	0,95	8,04	<DL	<DL	1,1	3,66
	2	4,51	1,36	2,27	74,89	0,23	0,45	1,22	1,01	8,73	<DL	<DL	1,12	4,22
Ya-5		2,25	<DL	1,85	82,22	<DL	<DL	1,28	<DL	8,89	<DL	<DL	1,29	2,21
Ya-6	1	2,02	1,02	1,86	79,49	0,39	<DL	0,97	2,13	9,8	0,58	<DL	0,88	0,87
	2	5,39	1,12	2,04	77,33	<DL	0,32	0,85	2,49	8,06	0,44	<DL	0,82	1,12
Ya-7	1	13,79	2,32	7,05	60,55	0,66	0,72	<DL	3,61	6,56	0,71	<DL	2,31	1,74
	3	12,24	1,91	6,1	61,76	0,52	0,51	<DL	4,2	7,48	0,6	<DL	2,64	2,03
	Green	8,43	2,08	7,71	66,16	0,66	0,68	0,19	3,84	6,56	0,84	<DL	2,86	<DL
	Light 1	3,62	2,62	24,42	48,45	5,46	0,4	0,25	2,09	3,93	1,14	<DL	7,63	<DL
	Light 2	3,85	2,48	23,04	45,89	5,86	0,44	0,16	2,35	4,42	1,67	<DL	9,86	<DL
Ya-8	1	2	1,4	8,76	63,92	<DL	<DL	<DL	9,12	6,7	1,24	<DL	5,7	1,16
	2	3,19	2,29	6,48	69,95	0,39	<DL	0,17	6,63	5,05	0,59	<DL	3,96	1,28
Ya-9	1	2,6	3,08	5,36	78,58	0,75	0,48	1	1,43	4,66	0,54	<DL	1,53	<DL
	2	2,56	3,48	5,22	77,57	0,95	0,59	1,21	1,5	4,93	0,55	<DL	1,44	<DL
Ya-10	Blue	1,54	3,11	3,51	79,93	1,32	0,59	1,1	1,47	3,71	<DL	<DL	1,12	2,59
	White	3,07	4,95	4,93	77,17	0,96	1,09	0,38	1,76	4,24	<DL	<DL	1,46	<DL
Ya-11	Dark	2,8	0,53	5,02	65,62	0,25	0,36	0,87	4,68	9,82	2,35	<DL	7,69	<DL
	White	7,11	1,69	7,63	63,79	0,75	0,48	0,47	4,59	7,06	1,24	<DL	5,17	<DL
	Blue	13,6	3,3	5,88	61,66	0,97	<DL	0,7	3,31	4,12	0,65	<DL	1,65	4,18
Ya-12	Blue	9,74	4,35	7,37	61,53	0,86	<DL	0,83	3,52	5,15	0,74	<DL	2,82	3,08
	White	13,11	4,31	7,89	59,15	1,24	0,75	0,37	2,95	4,91	0,56	0,62	2,72	1,44
	Dark	4,95	3,7	6,32	71,13	0,79	0,23	0,48	3,69	4,65	0,59	<DL	3,47	<DL
Ya-13	Blue	5,49	2,6	4,68	68,3	1,43	0,33	1,16	3,99	5,35	0,31	0,59	1,98	3,78
	White	4,44	2,29	7,36	67,15	2,82	1,07	1,15	3,91	5,76	0,85	<DL	3,2	<DL
	Dark	0,9	2,62	5,13	73,44	2,31	1,16	1,83	3,05	7,08	<DL	<DL	2,48	<DL
Ya-14	Blue	2,65	0,97	2,82	78,6	<DL	0,65	0,82	1,46	7,68	0,38	0,62	1,26	2,09
	Dark	1,83	0,7	2,92	82,55	<DL	0,81	0,64	1,22	6,98	<DL	1,08	1,29	<DL

**Table 8:** The VP-SEM-EDS results of selected areas (%), (<DL - below detection limit). (cont.)

Sample	Area	Na <sub>2</sub> O	MgO	Al <sub>2</sub> O <sub>3</sub>	SiO <sub>2</sub>	P <sub>2</sub> O <sub>5</sub>	SO <sub>3</sub>	Cl	K <sub>2</sub> O	CaO	TiO <sub>2</sub>	MnO	Fe <sub>2</sub> O <sub>3</sub>	CuO
Ya-15	White	0,9	<DL	1,31	72,91	0,33	0,63	1,07	2,55	13,6	2,19	<DL	4,51	<DL
	Dark 1	0,63	0,04	0,95	82,31	<DL	1,01	0,89	1,44	9,35	0,64	1,49	1,25	<DL
	Dark 2	5,82	0,28	0,8	76,31	<DL	0,62	1,13	1,29	10,82	0,59	<DL	<DL	2,34
Ya-16	Dark	2,65	2,44	6,81	73,88	0,67	0,47	0,92	2,67	5,57	0,8	<DL	3,12	<DL
	White	12,12	3,91	6,07	62,36	2,51	<DL	0,91	3,07	6,54	<DL	<DL	2,51	<DL
Ya-17	Granular	5,64	0,9	9,53	72,09	0,4	<DL	0,41	4,84	3,23	0,52	<DL	2,45	<DL
	Vitreous 1	8,67	1,08	4,32	70,97	<DL	<DL	<DL	3,75	5,66	0,7	<DL	1,78	3,08
	Vitreous 2	7,66	1	3,6	71,38	<DL	<DL	<DL	3,82	6,94	0,62	<DL	1,97	3,02
Ya-18	1	5,26	0,57	1,13	82,84	<DL	0,8	1,1	<DL	8,29	<DL	<DL	<DL	<DL
	2	2,44	1,37	4,33	81,69	<DL	0,56	0,4	1,02	6,82	<DL	<DL	1,37	<DL
Ya-19	1	0,88	0,2	3,19	80,23	0,72	0,83	0,64	1,59	9,17	0,67	<DL	1,87	<DL
	2	0,86	0,45	2,93	80,73	1,01	1,26	0,72	1,16	8,59	0,7	<DL	1,59	<DL
Ya-20		0,29	0,03	1,04	85,02	<DL	<DL	0,79	0,9	10,61	<DL	<DL	1,32	<DL
Ya-21	1	5,05	0,07	0,42	81,54	<DL	<DL	1,42	<DL	10,56	<DL	<DL	0,95	<DL
	2	0,72	0,03	4	79,05	<DL	0,47	0,78	2,44	8,56	0,92	<DL	3,03	<DL
Ya-22	1	0,38	<DL	0,31	87,16	<DL	0,73	1,18	<DL	9,22	<DL	<DL	1,02	<DL
	2	1,74	0,28	3,4	82,21	1,06	1,58	0,78	1,17	5,85	<DL	<DL	1,95	<DL
Ya-23	1	1,03	0,29	1,89	83,11	<DL	0,72	0,92	0,99	9,05	0,67	<DL	1,33	<DL
	2	0,28	0,06	0,74	84,12	<DL	0,64	0,93	0,81	10,32	0,74	<DL	1,37	<DL

As can be seen from the Table 8, the values for main oxides may vary quite a lot within the sample. Sodium oxide has extremely low values comparing to the average amounts of sodium in ancient glasses (for roman ones, for example, it should be not less than 15 %) (Brill, 1999; Degryse, 2014). Moreover, there is neither homogeneity of sodium oxide percentage within the samples nor within the groups of beads. Probably, the surface analysis characteristics of SEM-EDS give us erroneous values because most of the Na was randomly leached. The alteration layer does not allow to obtain adequate composition.

The results of Table 8 can be summarised with regard to the different glass groups.

Group 1: The samples of this group are enriched in Cu (0,87-4,22 %) and have relatively low amounts of Fe (max -1,29%) and Mg (max -1,67%) oxides. Al is in between 1,09% (sample Ya-2) and 2,57% (sample Ya-4). Sample Ya-6 has different amount of K oxide (2,49%) in one of the areas.

Group 2. This group is different due to the high amount of ferric oxide (up to 7, 69% in sample Ya-11 but usually lower – ca. 2-4 %). Al (4-7%), K (2,5 – 4,5 %) and Mg (1,5 - 4,3%) oxides are also elevated comparing to other groups except green non-beads (group 6).

Group 3. The purple base eyed beads are characterized by remarkable MnO content (more than 1% in dark glass areas). These samples practically do not have phosphorus. Instead their content of CaO is one of the highest (7 – 13,6%).

Group 4. Sample Ya-10 in its major element composition is follows the pattern of group 2, except in the case of Fe and K oxides which have lower values (approx. 1,3% and 1,6% respectively).

Group 5. The dark bead (sample Ya- 9) also behaves the same as group 4.

Group 6. Green non-beads are inhomogeneous. Moreover, different areas of the same sample can have different elemental composition; for example, the Al<sub>2</sub>O<sub>3</sub> values of sample Ya-17 are drastically different according to the areas analysed (4% and 9,5% for vitreous and granular sides, respectively). The light layer of Ya-7 has more than 23 % of alumina. This sample also possess the highest content of ferric oxide (more than 9%). Sample Ya-8 shows high values for K<sub>2</sub>O – more than 8%.

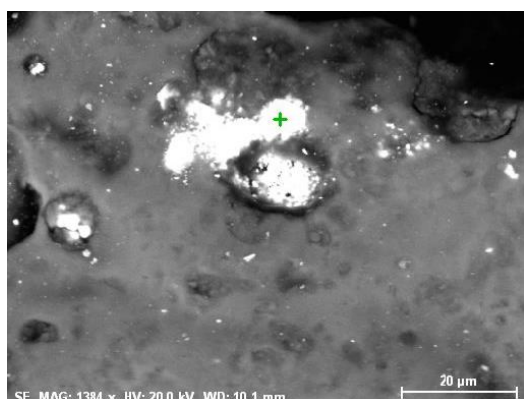
Group 7. Biconical colourless beads are relatively depleted in transition metal oxides but have relatively high amounts of alumina (1,13 – 4,33%). K<sub>2</sub>O concentration are low (just above 1%).

Group 8. The biconical yellow beads are following the same as group 7 pattern.

In this section we only report the values as they have been obtained without the search for defined groups and correlation patterns. The major elements composition obtained by VP-SEM-EDS system is very different from the one reported in the 1980s (beads from the same settlement) and other studies (Brill, 1999; Островерхов, 1981; Petit-Domínguez, 2014).

#### EDS inclusion point analyses

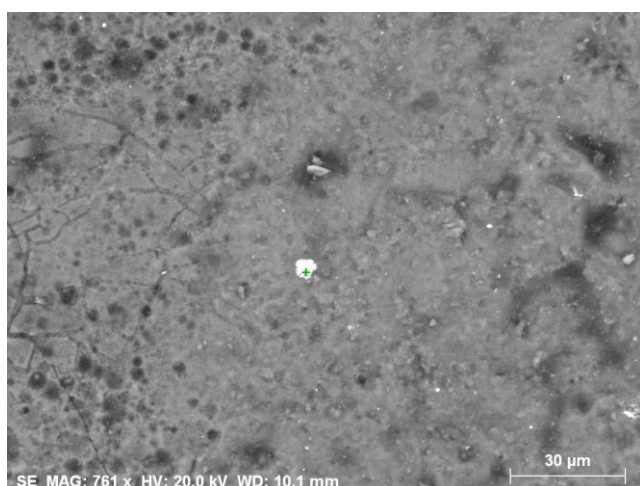
The inclusions found in the glass matrix were analysed by VP-SEM-EDS. Among them the most abundant ones were inclusions of tin, sometimes with the association with other metals, most frequently Cu. They were found in all the groups. The white part of sample Ya-10 (group 4) has numerous inclusions of tin (an example can be seen in Figure 41).



Element	wt.%	norm. wt.%	norm. at.%
Na	4,86	4,86	9,39
Mg	3,39	3,39	6,19
Al	3,76	3,76	6,20
Si	33,08	33,08	52,34
P	1,84	1,84	2,64
Si	1,39	1,39	1,93
Cl	1,46	1,46	1,83
Fe	1,63	1,63	1,29
Sn	48,59	48,59	18,19

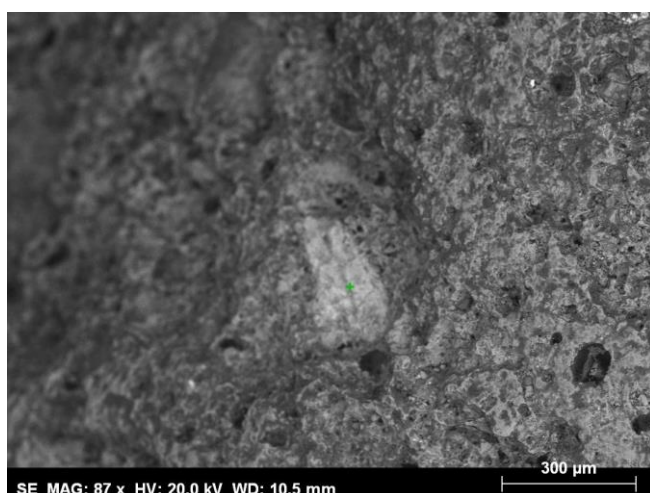
**Figure 41:** Backscattered image of a tin inclusion found in sample Ya-10 and a table generated after quantification of EDS data.

Three inclusions of monazite were detected. The image and the calculated compositional table are placed in the Figure 42. Figure 43 represents one of the apatite inclusions found in the white part of the sample Ya-13 (group 2). More BSE images of Yahorlyk glass can be found in Annex 2.



Element	wt. %	norm. wt. %	norm. wt. %
Na	2,50	2,50	2,50
Mg	1,59	1,59	1,59
Al	3,49	3,49	3,49
Si	39,58	39,58	39,58
P	9,00	9,00	9,00
S	1,01	1,01	1,01
Cl	0,92	0,92	0,92
Ca	5,51	5,51	5,51
Fe	2,08	2,08	2,08
Ag	5,97	5,97	5,97
La	7,17	7,17	7,17
Ce	21,19	21,19	21,19

**Figure 42:** Backscattered image of monazite inclusion detected in sample Ya-15 and a table generated after quantification of EDS data.



Element	wt. %	norm. wt. %	norm. at. %
F	0,03	0,03	0,05
Na	3,58	3,58	5,45
Mg	1,16	1,16	1,67
Al	1,57	1,57	2,03
Si	5,15	5,15	6,43
P	28,08	28,08	31,77
S	0,23	0,23	0,25
Cl	0,97	0,97	0,95
K	0,86	0,86	0,77
Ca	56,29	56,29	49,23
Ti	0,63	0,63	0,46
Fe	1,47	1,47	0,92

**Figure 43:** Backscattered image of apatite inclusion detected in sample Ya-13 and a table generated after quantification of EDS data.

#### 3.1.1.4 X-ray diffraction (Micro XRD)

The diffractograms of Yahorlyk beads do not show the presence of any common crystalline phases that might be used in ancient glassmaking for coloration and/or opacification. Quartz is the most commonly occurring crystalline phase in the diffractograms (15 times out of 34). It is an open question if it is the result of the identification of superficial detrital deposits found in cracks or open

air bubbles or if poor melting resulted in the presence of quartz as a remain of the raw materials used in glass production. We have to mention that no crystalline phases were registered for three samples: Ya-18 (group 7), Ya-20 (group 8) and Ya-22 (group 8).

One of the planes (light coloured) of sample Ya-7 was of particular interest for XRD analysis. It does not look like glass and diffractogram does not look similar either (Fig. 44).

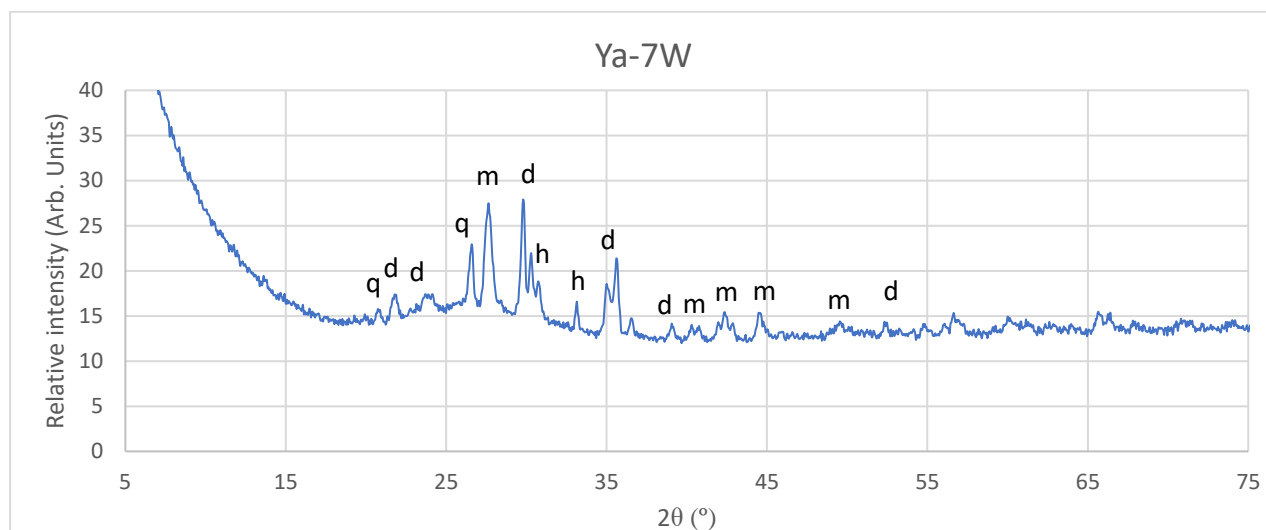


**Figure 44:** X-ray diffractogram of the sample Ya-7 (Light part): q - quartz; d - diopside; m - microcline; h - hematite.

For this sample the presence of quartz (silica), anorthite (Ca-rich plagioclase), diopside (pyroxene) and hematite (iron oxide) is detected. These phases can be present in sands. Remarkable, that quartz seems to be less abundant than the minerals of feldspar group.

### 3.1.1.5 Laser Ablation Inductively Coupled Plasma Mass Spectrometry (LA-ICP-MS)

The LA-ICP-MS results of every sample are going to play the role of the most robust quantitative data of the elemental composition, determining values for elements with concentration on sub ppm level. To visualise the results a joint table with average values per sample (each colour is represented in polychromatic samples) has been produced (Annex 3 and 4). This table is divided into two. The first one contains values for major elements expressed and normalised as respective oxides in percent. The second one contains values of minor and trace elements expressed in ppm. The values of sulphur trioxide and chlorine found in the Annex 3 were added based on the averages of EDS analyses of corresponding areas. In this section we describe tendencies that can be observed in the above-mentioned table. As usual results will be summarized based on sample grouping. Keep in mind that the biggest difference when comparing the VP-SEM-EDS results and the LA-ICP-MS

results is the higher Na<sub>2</sub>O concentration. This result confirms that the glass artefacts of the Yahorlyk settlement suffered glass weathering by selective leaching of the alkaline components.

Group 1. On the sodium against Mg plot the first group clusters together with groups 3, 7 and 8 (Fig. 45). The samples of group 1 all have lower MgO values (usually a bit more than 0,5%) when compared to the groups 2, 4 and 5. The K<sub>2</sub>O values are also low (0,083% -0,64%) except in sample Ya-6 (more than 3%). Content of Cu is within the interval of 1,57% – 3,67% except in sample Ya-6 (0,47%) which was analysed in its darker side. The CaO concentration of samples from this group is always higher than in the other samples (not less than 8,9%). This group is also characterized by low P<sub>2</sub>O<sub>5</sub> values (max.0,44%) higher Cl amounts (up to 1,3%). As it was said in XRF subsection, sample Ya-5 has a higher amount of Co (162 ppm) and this is the maximum value obtained in the set. Sr concentration is always more than 300 ppm.

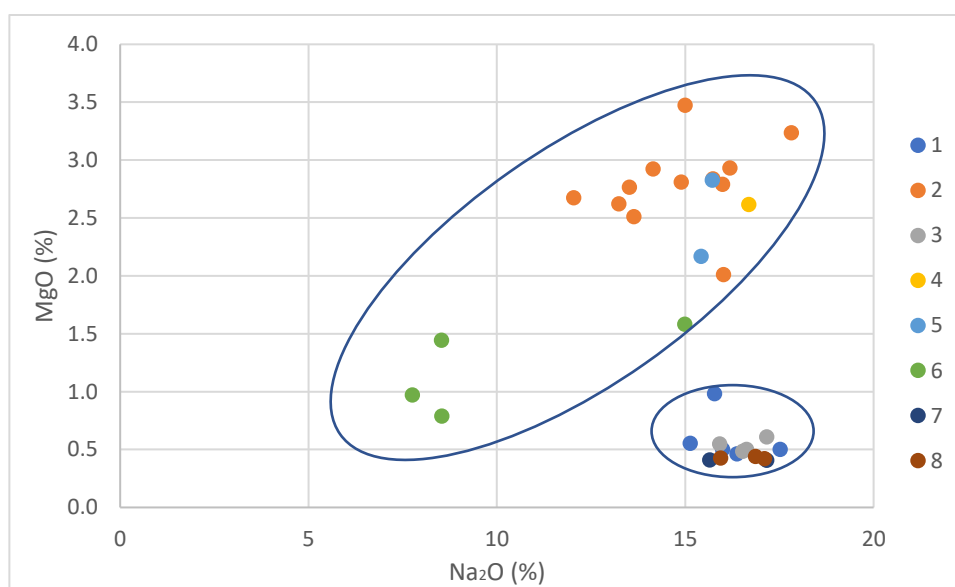


**Figure 45:** The LA-ICP-MS values of Yahorlyk beads binary plot. Na<sub>2</sub>O against MgO. Groups 1,3,7,8 and groups 2,4,5,6 cluster respectively.

Group 2. This group of eyed beads in the plot in the Figure 45 clusters with groups 4 and 5. These beads are enriched in Mg and K which makes up from 2,5 % (sample Ya-3) to 4,7 % (sample Ya-12) of their mass. Iron represented here as ferric oxide is also abundant (1,5 – 2,5%). The blue parts of the eyes are enriched in Cu. This group has the highest concentrations of phosphate (usually more than 0,5%). It also has the highest alumina content (2,7-4,8%). Samples in group 2 have lower Sr (average of 261 ppm) and significantly lower Zr (average 38 ppm) content than the others.

Group 3. The MnO content makes this group unique in the set as it is around 0,8% in the purple parts. These samples do not show high values for Mg, Al, K and Fe oxides (comparable to group 1). Pb and Sn oxides are present in quantities that exceed 1000 ppm (max in white parts – 0,7% Sn<sub>2</sub>O and 0,85% PbO).

Group 4. Sample Ya-10, the only representative of this group, groups together with samples from group 2 when major elements such as iron, aluminum, magnesium and potassium are considered (Figure 46). The ferric oxide is as high as 0,8%. The biggest difference between group 4 and group 2 is the Zr content (139 ppm and never more than 60 ppm, respectively).

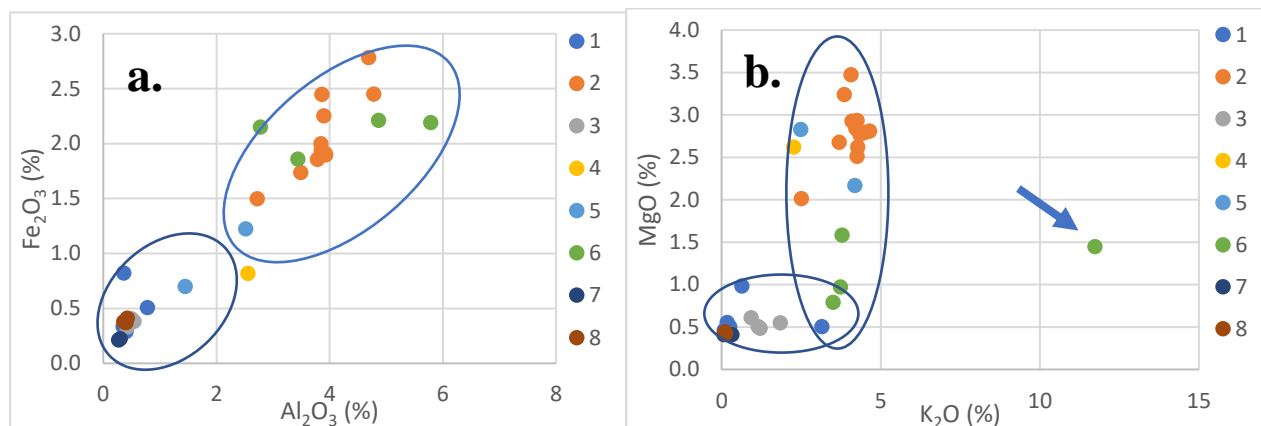


**Figure 46:** the LA-ICP-MS values of Yahorlyk beads binary plots: a -  $\text{Al}_2\text{O}_3$  against  $\text{Fe}_2\text{O}_3$ ; b -  $\text{K}_2\text{O}$  against  $\text{MgO}$ . The two groups can be noted. Sample Ya-8 is marked with the blue arrow (b).

Group 5. As can be seen from figures above (Fig. 45, 46) the representative of this group rather follows the behaviour of the group 2. This sample is remarkable due to the content of Sn and Pb in its white layer (a bit more than 0,9% each). The CaO content is low (3,97 – 4,45%).

Group 6. The green non-beads are more associated with group 2 but are different in the values of Ti (0,33 – 0,43%), Cu (0,47 – 0,9%) and Mg (0,8 – 1,58%). Sample Ya-8 is extremely rich in  $\text{K}_2\text{O}$  - 11,73% (marked with an arrow in the Figure 46 (b)). The samples for this group cluster together and are distinct from other groups in the Fe-Ti and Ti-Zr plots (Fig. 47).

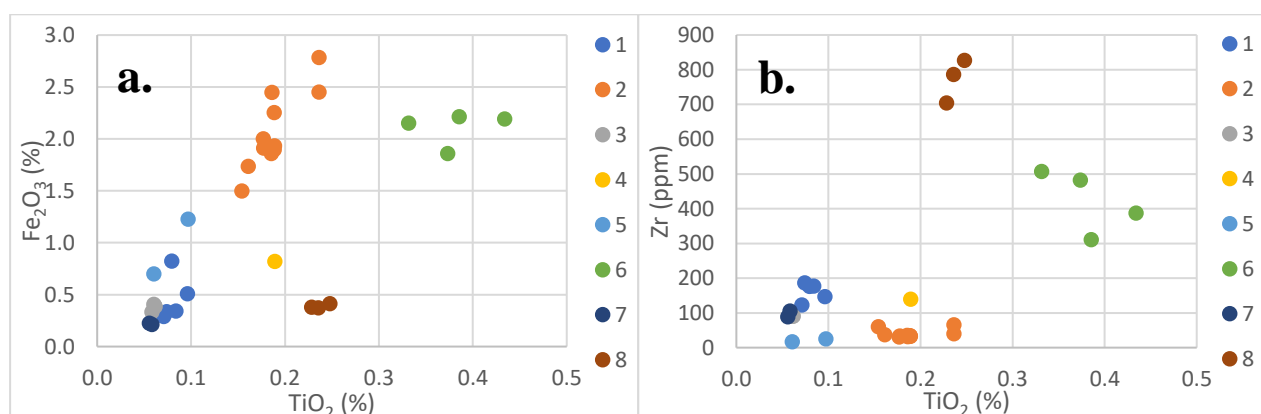


**Figure 47:** the LA-ICP-MS values of Yahorlyk beads binary plots: a -  $\text{TiO}_2$  against  $\text{Fe}_2\text{O}_3$ ; b -  $\text{TiO}_2$  against Zr.

Group 7. Biconical colourless beads usually group with group 1 and 3 on binary plots (Figures 45-47). They are depleted in ferric oxide (0,2%). Values for Mg, Al, K and P oxides are also the lowest for the entire set (none exceeds 0,5%).

Group 8. The last group has many common features with the previous one (contents of Mg, Al, K) but has more ferric oxide (0,37 – 0,41%), TiO<sub>2</sub> (0,23%) and possess the highest concentration of Zr of all the fragments (700 -830 ppm). Due to these numbers it can be separated from all the other beads (Figure 47).

As can be seen from the major element plots, the groups that are considered show distinct differences in the chemical composition. There are two major clusters: groups 1, 3 and 7 and groups 2 and 6 are usually positioned together. Groups 4, 5 and 8 sometimes belong to one or another cluster and in some cases stay separated.

Regarding Rare Earth Elements (REE) concentration all the values of measured elements are reported in the Table 9 found below.

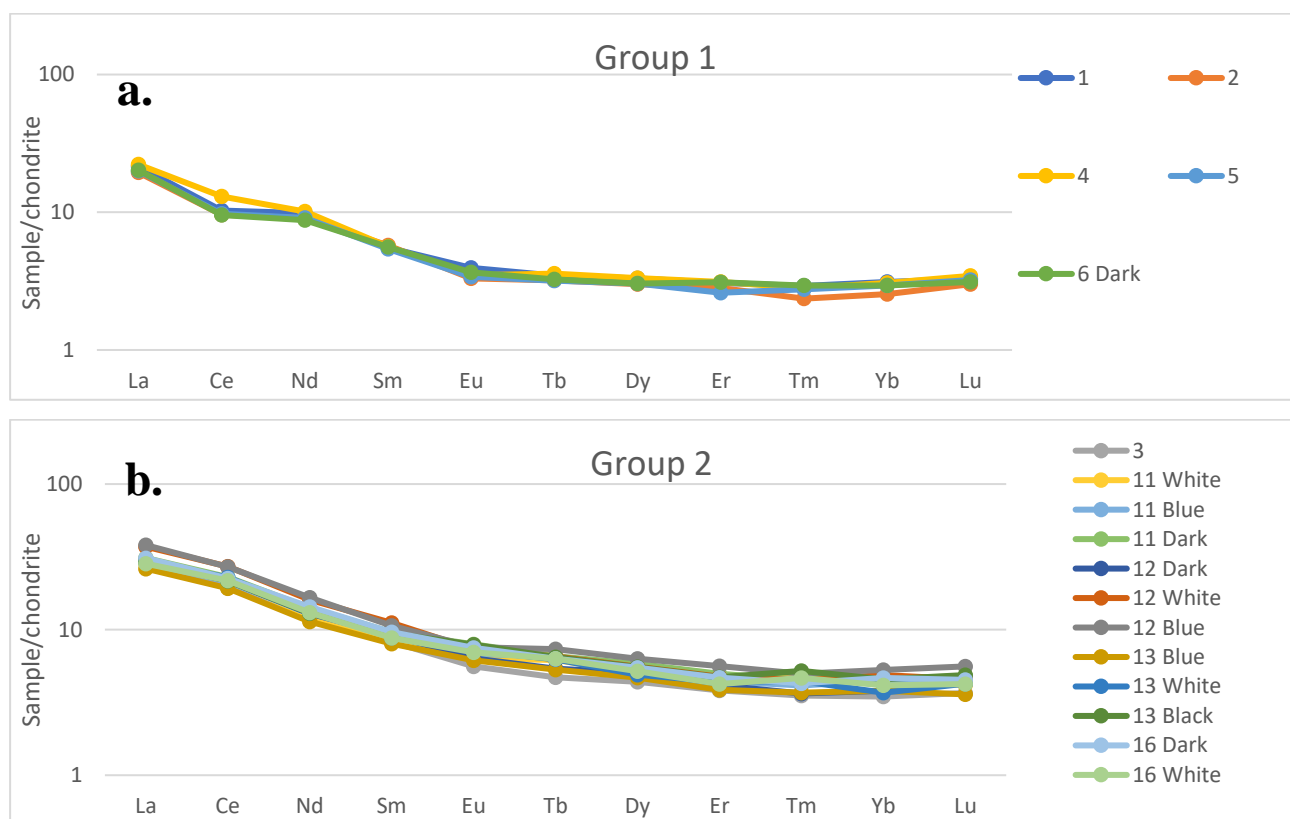
**Table 9:** Yahorlyk glass REE concentrations (ppm), Ce/Ce\* - Ce anomaly; Eu/Eu\* - Eu anomaly.

Sample	La	Ce	Nd	Sm	Eu	Tb	Dy	Er	Tm	Yb	Lu	Ce/Ce*	Eu/Eu*	
1	5,101	6,321	4,516	0,818	0,222	0,125	0,813	0,490	0,072	0,501	0,081	0,58	0,81	
2	4,602	5,888	4,124	0,850	0,186	0,116	0,739	0,450	0,058	0,410	0,074	0,60	0,67	
3	6,940	11,835	5,880	1,224	0,315	0,170	1,079	0,612	0,087	0,559	0,090	0,81	0,79	
4	5,268	7,970	4,618	0,831	0,197	0,129	0,818	0,499	0,070	0,493	0,085	0,71	0,71	
5	4,735	5,984	4,155	0,803	0,191	0,115	0,748	0,417	0,068	0,473	0,079	0,60	0,72	
6	4,793	5,846	4,004	0,828	0,207	0,117	0,746	0,496	0,073	0,473	0,077	0,58	0,76	
7	21,489	40,517	16,948	3,272	0,583	0,437	2,694	1,573	0,231	1,629	0,262	0,90	0,61	
8	20,367	42,370	18,296	3,757	0,692	0,538	3,306	2,083	0,310	2,253	0,359	0,98	0,56	
9	9,755	18,434	8,578	1,662	0,332	0,236	1,492	0,883	0,139	0,856	0,148	0,89	0,61	
10	Blue	2,537	4,667	2,245	0,523	0,160	0,090	0,521	0,299	0,044	0,247	0,036	0,87	0,89
10	White	4,292	8,315	3,866	0,867	0,225	0,155	0,868	0,468	0,069	0,493	0,074	0,91	0,75
11	White	6,735	13,522	5,590	1,219	0,357	0,223	1,246	0,769	0,116	0,744	0,102	0,96	0,84
11	Blue	6,905	13,096	5,857	1,429	0,383	0,237	1,285	0,709	0,102	0,719	0,112	0,90	0,79
11	Dark	7,360	14,085	6,421	1,423	0,445	0,238	1,430	0,798	0,112	0,746	0,118	0,91	0,92
12	Dark	7,039	13,310	5,887	1,351	0,357	0,195	1,235	0,663	0,090	0,613	0,106	0,90	0,80
12	White	8,798	16,611	7,320	1,647	0,411	0,236	1,369	0,759	0,111	0,783	0,112	0,90	0,76
12	Blue	9,022	16,554	7,579	1,573	0,427	0,266	1,551	0,901	0,123	0,852	0,138	0,87	0,79
13	Blue	6,221	11,810	5,178	1,184	0,346	0,191	1,153	0,618	0,091	0,612	0,088	0,91	0,86
13	White	6,919	13,997	6,157	1,304	0,405	0,225	1,204	0,702	0,110	0,594	0,104	0,95	0,91
13	Dark	6,985	13,242	5,931	1,396	0,445	0,234	1,360	0,754	0,129	0,734	0,120	0,90	0,93
14	Blue	5,267	6,392	4,419	0,872	0,214	0,130	0,785	0,495	0,069	0,438	0,068	0,58	0,74
14	Dark	5,333	6,290	4,628	0,917	0,222	0,132	0,828	0,514	0,065	0,445	0,078	0,56	0,74
15	Dark	5,155	6,266	4,416	0,902	0,218	0,132	0,705	0,467	0,061	0,418	0,080	0,58	0,73
15	White	5,197	6,270	4,390	0,873	0,207	0,141	0,781	0,457	0,062	0,418	0,066	0,57	0,70
16	Dark	7,343	13,757	6,539	1,422	0,423	0,228	1,349	0,748	0,106	0,751	0,111	0,88	0,88
16	White	6,724	13,283	5,971	1,300	0,394	0,228	1,272	0,675	0,115	0,667	0,104	0,93	0,88

**Table 9:** Yahorlyk glass REE concentrations (ppm), Ce/Ce\* - Ce anomaly; Eu/Eu\* - Eu anomaly (cont.).

Sample	La	Ce	Nd	Sm	Eu	Tb	Dy	Er	Tm	Yb	Lu	Ce/Ce*	Eu/Eu*
17 Vitreous	15,989	29,398	13,968	2,690	0,517	0,375	2,269	1,453	0,215	1,552	0,250	0,87	0,59
17	13,083	23,313	11,387	2,200	0,471	0,307	1,989	1,223	0,183	1,295	0,225	0,84	0,66
18	4,212	5,792	3,624	0,639	0,187	0,093	0,576	0,337	0,043	0,359	0,053	0,65	0,89
19	4,833	6,059	4,232	0,815	0,207	0,110	0,656	0,395	0,052	0,400	0,064	0,59	0,78
20	5,170	6,805	4,393	0,828	0,231	0,147	1,005	0,755	0,137	0,917	0,171	0,63	0,81
21	4,845	6,461	4,070	0,694	0,219	0,119	0,941	0,728	0,122	0,841	0,174	0,64	0,92
23	4,464	6,105	3,744	0,755	0,179	0,132	0,857	0,676	0,097	0,815	0,154	0,65	0,69

The anomalies of Ce (Ce/Ce\*) were calculated using next equation:  $Ce/Ce^* = 3Cen / (2Lan + Ndn)$ . The anomalies of Eu (Eu/Eu\*) were calculated using next equation:  $Eu/Eu^* = EUn / (Smn/3 * 2 + Tbn/3)$ , where n – chondrite normalised values. The values of Ce anomaly can be divided into two ranges: groups 1, 3, 7 and 8 have  $Ce/Ce^* = 0,58 - 0,71$ , while and groups 2, 4, 5 and 6 have  $Ce/Ce^* = 0,81 - 0,96$ . The Eu anomalies vary significantly within the groups and cannot be used to distinguish between them. The groups also produce different REE patterns. This can be seen from the line plots of chondrite normalised values (after McDonough, Sun, 1995) that represent data for each group of glass fragments (Fig. 47).



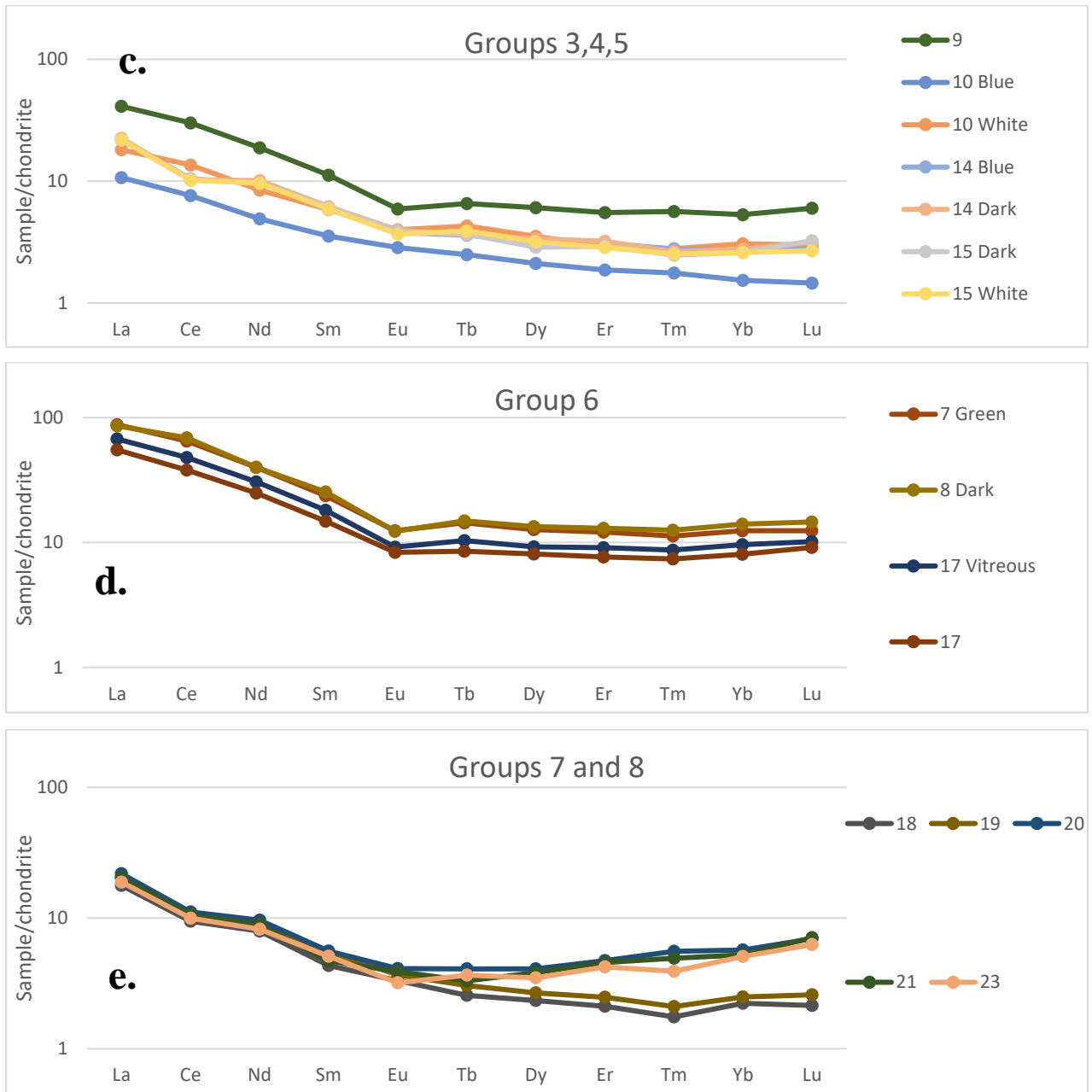


**Figure 48:** Linear plots of chondrite normalised values of REE determined for Yahorlyk glass fragments and divided by groups: a- group 1, b - group 2, c- groups 3 (Ya-14 and 15), 4 (Ya-10), 5 (Ya-9), d - group 6, e - groups 7 (Ya-18 and 19) and 8 (Ya-20, 21 and 23).

The REE signature of the Yahorlyk settlement glass fragments is not uniform for all the samples. Groups seem to be different not just in the concentrations of trace elements but also in the ratios between specific elements. Groups are mostly different by their Ce anomalies. The group 8 (samples Ya-20, Ya-21 and Ya-23) seem to be enriched in heavy REE making the pattern unique. Groups 2 and 6 are very similar in the ratios between the elements but the latter has the highest values of REE. Parts of Ya-10 (group 4) look very distant from one another. Summarizing information, we can say that Yahorlyk glass fragments show three different REE patterns: group 1, 3, 7 with smaller Ce anomalies, groups 2, 4, 5 and 6 with bigger Ce and Eu anomalies and group 8 that is enriched in heavy REE.

### 3.1.2 Sand analyses and their interpretation

#### 3.1.2.1 Powder X-ray diffraction (PXRD)

The X-ray diffraction analyses that were performed by the powder method unveiled the variety of crystalline phases present in sand samples and to a certain extent allowed the semi-quantification of the ratio between these phases. It has to be said, that subsamples that were analysed show high level of homogeneity within the groups and also between them.

Quartz is undoubtedly the main phase in all samples. The small amount of feldspar does not allow to identify the kind of plagioclase or K-Feldspar (Fig. 48). Amphibole, calcite, zircon, rutile and ilmenite were occasionally present in minor amounts. The diffractogram of sample Iv-S shows the presence of clay minerals and mica phases (Table 10). One of the subsamples of Vyn-S seems to contain significant amount of calcite (Table 10). Previously, lumps of rock identified as limestone were found in the sample.

The set of minerals detected with help of X-ray diffraction is very coherent with ones mentioned in literature for this locality (Чепижко et al., 2007; Хлебников, 1988). The Figure 48 (beneath) contains typical diffractogram of the sand considered in this study. Table 10 summarizes all the XRD data gathered from sand samples.

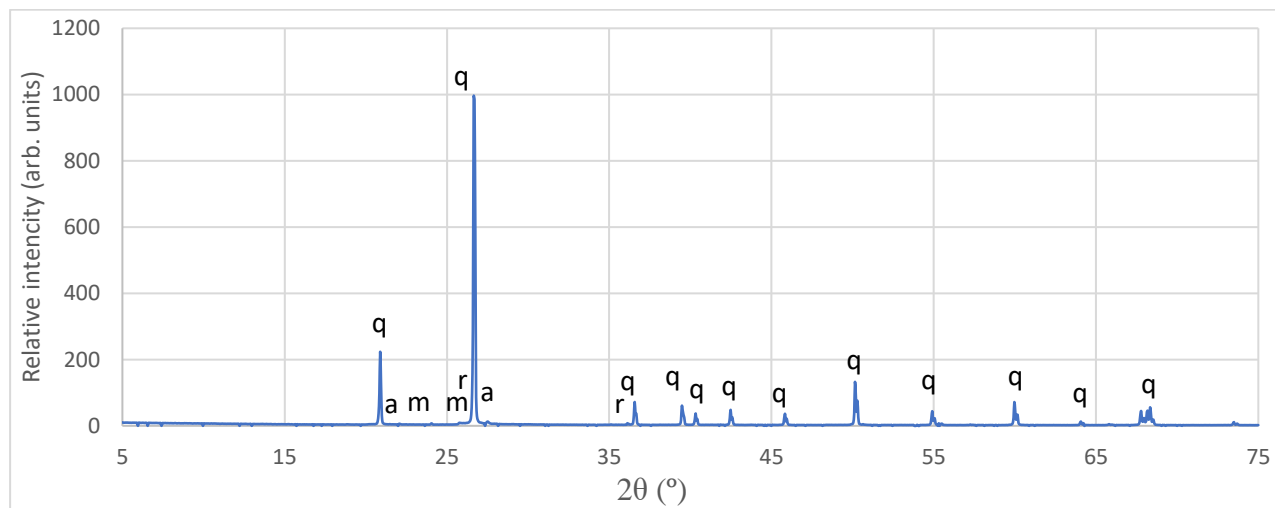


**Figure 49:** IvQ-2 diffractogram: q - quartz, a - albite, m – microcline, r - rutile.

**Table 10:** The results of XRD analyses of Yahorlyk sand samples (+++++ - main constituent; ++++ - very abundant; ++ - small abundance; + - very small abundance; Vtg. – vestigial; - - not detected).

Name	Quartz	K-feldspar	Plagioclase	Mica	Kaolinite	Amphibole	Zircon	Rutile	Ilmenite	Muscovite	Calcite
For	+++++	++	+	-	-	-	Vtg.	-	-	-	-
Iv-Q	+++++	++	+	-	-	Vtg.	-	Vtg.	-	-	-
Iv-S	++++	++	++	++	+	+	-	-	-	-	-
Qua	+++++	++	+	Vtg.	-	Vtg.	-	-	-	Vtg	Vtg.
Ryb-L	+++++	++	+	-	-	-	-	-	-	-	-
Ryb-Q	+++++	++	+	-	-	-	-	-	-	-	Vtg.
Vyn-S	+++++	++	+	-	-	-	-	-	-	-	Vtg.
Ya-B	+++++	++	+	-	-	-	-	-	-	-	-
Ya-S	+++++	++	+	-	-	Vtg.	-	-	Vtg.	-	-

### 3.1.2.2 X-ray fluorescence (XRF)

The percentage of major and minor elements in sand is crucial in the study of possible raw materials used in glass production. The amount of SiO<sub>2</sub> was calculated by subtraction of the sum of all the other oxides from the 100%. Standard deviations were calculated for each value allow to see how dispersed the data is (Table 11).

**Table 11:** The average values of elemental concentrations of Yahorlyk sand samples obtained by XRF.

Name of the sample	SiO <sub>2</sub> %	Al <sub>2</sub> O <sub>3</sub> %	Fe <sub>2</sub> O <sub>3</sub> %	Na <sub>2</sub> O %	K <sub>2</sub> O %	TiO <sub>2</sub> %	CaO %	MgO %	P <sub>2</sub> O <sub>5</sub> %	MnO %	SO <sub>3</sub> %	SrO %	Zr %
Ya-S	95,424	3,233	0,365	0,083	0,215	0,122	0,030	0,236	0,206	0,004	0,029	0,013	0,040
St.dev	0,261	0,102	0,057	0,017	0,076	0,031	0,005	0,025	0,050	0,002	0,004	0,003	0,010
Ya-B	95,516	3,167	0,361	0,092	0,180	0,132	0,045	0,249	0,184	0,005	0,024	0,012	0,034
St.dev	0,117	0,043	0,021	0,020	0,079	0,027	0,017	0,014	0,033	0,001	0,002	0,002	0,008
Iv-Q	95,544	3,215	0,358	0,070	0,176	0,123	0,024	0,223	0,191	0,003	0,024	0,012	0,037
St.dev	0,173	0,082	0,027	0,024	0,064	0,045	0,005	0,012	0,076	0,001	0,003	0,005	0,017
Ryb-Q	93,893	4,075	0,675	0,106	0,348	0,153	0,056	0,383	0,226	0,005	0,021	0,015	0,044
St.dev	1,489	0,865	0,357	0,023	0,101	0,036	0,017	0,169	0,052	0,002	0,002	0,003	0,011
For	95,511	3,291	0,354	0,092	0,209	0,092	0,033	0,243	0,117	0,004	0,025	0,008	0,021
St. dev	0,184	0,089	0,062	0,014	0,035	0,021	0,009	0,014	0,021	0,004	0,003	0,001	0,005
Qua	92,894	4,482	0,608	0,229	0,673	0,217	0,094	0,387	0,305	0,004	0,024	0,022	0,061
St.dev	3,133	1,466	0,380	0,137	0,544	0,135	0,071	0,172	0,184	0,003	0,004	0,014	0,038
Vyn-S	94,468	3,008	0,250	0,091	0,202	0,053	1,505	0,261	0,099	0,002	0,035	0,008	0,017
St.dev	3,030	0,249	0,082	0,030	0,114	0,020	2,930	0,088	0,043	0,001	0,021	0,004	0,009

**Table 11:** The average values of elemental concentrations of Yahorlyk sand samples obtained by XRF.

Name of the sample	SiO <sub>2</sub> %	Al <sub>2</sub> O <sub>3</sub> %	Fe <sub>2</sub> O <sub>3</sub> %	Na <sub>2</sub> O %	K <sub>2</sub> O %	TiO <sub>2</sub> %	CaO %	MgO %	P <sub>2</sub> O <sub>5</sub> %	MnO %	SO <sub>3</sub> %	SrO %	Zr %
Iv-S	77,850	10,123	3,620	1,457	1,930	0,579	1,510	2,200	0,492	0,046	0,067	0,039	0,086
St.dev.	1,004	0,665	0,370	0,204	0,166	0,013	0,220	0,156	0,012	0,009	0,004	0,001	0,003
Ryb-L	95,983	2,905	0,191	0,130	0,200	0,062	0,068	0,256	0,131	0,002	0,039	0,009	0,025
St.dev.	0,499	0,247	0,040	0,008	0,120	0,038	0,050	0,027	0,102	0,000	0,009	0,006	0,022

It is easy to notice, that, as expected, silica is the main constituent of all the samples. Aluminium and iron have, usually, higher concentrations than the rest of the elements, present in the samples. All the samples seem to have quite similar elemental composition except sample Iv-S, that was also different in appearance. This sample was hardly believed to be a possible raw material for glassmaking, and this assumption was confirmed by low concentration of silicon and extremely high concentration (more than 10%) of aluminium and other elements considered to be from detrital sources.

The scatter plots were produced based on the values from all the subsamples (Annex 6). Positive correlation of aluminium with such elements as sodium and potassium ( $r=0,92$ ;  $r=0,96$  respectively) indicates the presence of feldspars (Fig. 50 a, b), which is in strong agreement with the XRD data.

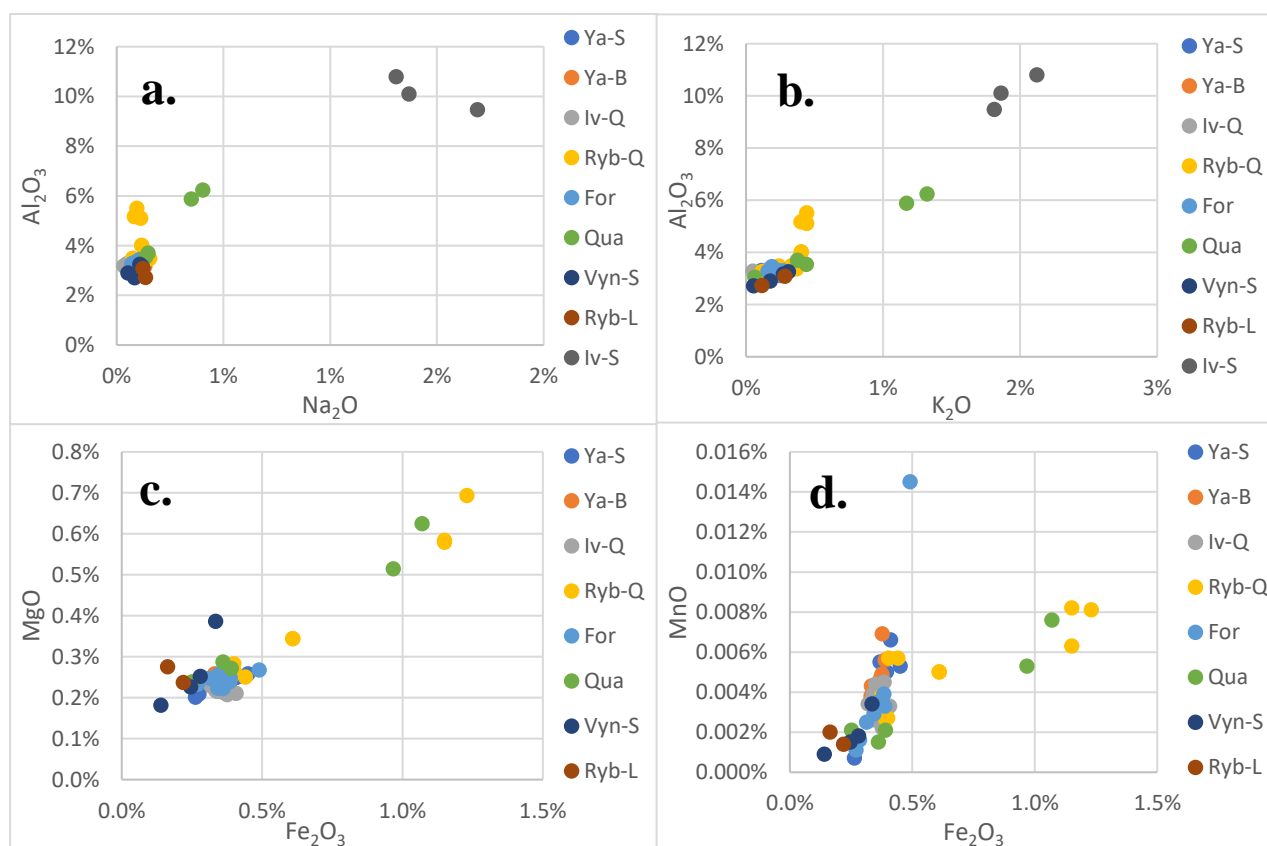


**Figure 50:** Yahorlyk sand binary plots: a - Na<sub>2</sub>O against Al<sub>2</sub>O<sub>3</sub>; b - K<sub>2</sub>O against Al<sub>2</sub>O<sub>3</sub>, c – Fe<sub>2</sub>O<sub>3</sub> against MgO, d – Fe<sub>2</sub>O<sub>3</sub> against MnO. Plots c and d do not include Iv-S sample.

Sample Vyn-S in its first subsample contained lumps of rock previously identified as limestone. The content of calcium for this sample (5,9%) reflects the presence of limestone. These lumps of limestone in one of the subsamples make standard deviations of values for the sample higher than in others.

The iron concentration for most of the samples does not exceed 0.7%. Iv-S sample shows the highest value for Fe<sub>2</sub>O<sub>3</sub>, which is 3,62%. This element has a strong correlation with magnesium and manganese (Fig. 50 c, d) This correlation takes place due to the similar atomic radii and easy substitution of iron by these elements in minerals (Salminen et al., 1998). High silica level and concentrations of Fe<sub>2</sub>O<sub>3</sub> observed in samples Ya-S, Ya-B, For, Ryb-L, Vyn-S, Iv-Q (Table 11) allows one to call these sands suitable for colourless glass making (Jackson, 2005; Хлебников, 1988; Sushkova, Didenko, 1984).

Some samples demonstrate vaguely proportional elevation of values for all evaluated oxides (these samples are Iv-S, Qua and Ryb-Q). A linear plot of major elements present in samples (expressed as respective oxides) can be found in Figure 51. The Iv-S shows divergence with the rest of the samples for such elements as Ca, Mg, Mn (Fig. 51). Vyn-S has high Ca concentration. Ryb-L sample is also different by the amount of Ca and Na oxides. The rest of the samples seem to follow uniform pattern (Fig.51).

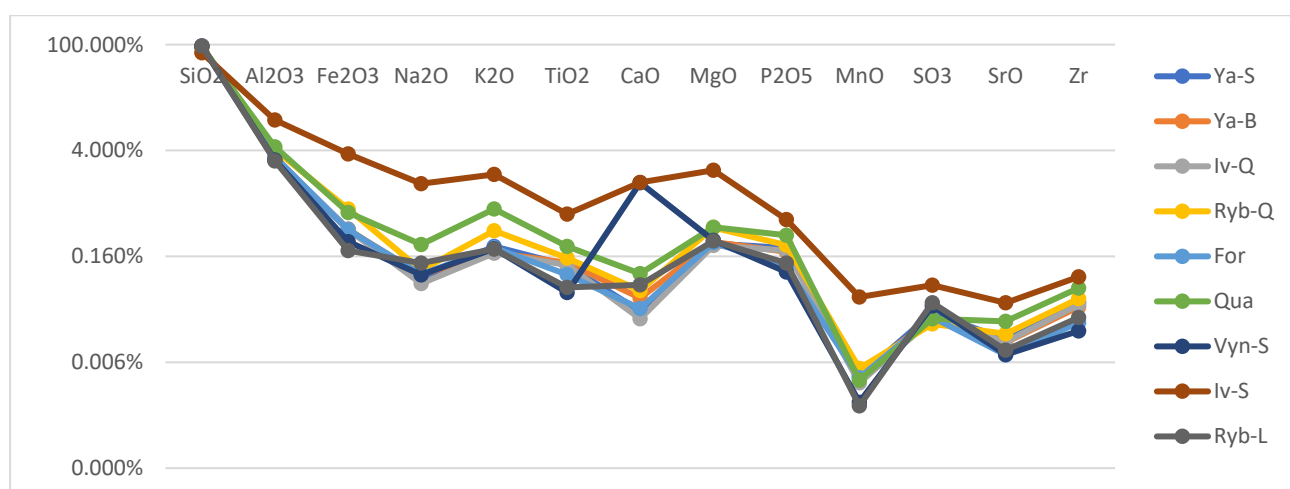


**Figure 51:** The linear graph of element concentrations in sand samples obtained by means of XRF. Logarithmic scale.

The non-quartz fraction of sand seems to be uniform for most of the samples (the constituents keep proportion between themselves regardless their sum concentration). Most of the samples analysed fit to be called possible raw material for glassmaking. The chemical investigation of the Yahorlyk sand is not limited by X-ray fluorescence and major elements. In the upcoming section, more information about trace elements composition will be presented.

### 3.1.2.3 Inductively coupled plasma mass spectrometry (ICP-MS)

We finalize the experimental results presentation with the data obtained with help of ICP-MS. It must be said that certain values of some elements were excluded from the consideration due to quality assurance elimination. The results of samples were calculated as average of all subsamples. Figures we rely on are presented in the table 12:

**Table 12:** Concentrations of trace elements in sand samples obtained by ICP-MS (ppm). Ce/Ce\* - Ce anomaly; Eu/Eu\* - Eu anomaly.

	Ryb-Q	Iv-Q	Ya-B	For	Qua	Iv-S	Ya-S	Vyn-S	Ryb-L
V	6,104	3,944	3,592	3,772	8,127	38,527	4,084	2,722	2,234
Co	0,802	0,396	0,405	0,499	0,855	6,022	0,427	0,300	0,174
Rb	9,059	5,483	5,618	6,758	17,464	52,698	6,067	5,724	4,663
Y	2,616	1,515	1,479	1,431	4,276	14,001	1,551	1,448	1,243
Nb	1,781	1,805	1,678	1,370	3,585	7,920	1,873	0,947	0,801
Cs	0,308	0,167	0,166	0,186	0,381	1,982	0,155	0,144	0,086
Ba	76,479	53,849	56,030	65,735	155,034	223,748	55,906	57,265	51,562
La	3,770	2,163	2,171	2,329	6,637	18,639	3,137	2,767	2,182
Ce	8,983	5,409	5,633	5,201	14,002	39,281	7,046	5,633	4,656
Sm	0,696	0,358	0,373	0,336	1,108	3,290	0,356	0,323	0,256
Eu	0,137	0,069	0,069	0,080	0,240	0,666	0,075	0,073	0,058
Tb	0,082	0,041	0,043	0,045	0,142	0,440	0,054	0,052	0,042
Dy	0,464	0,248	0,255	0,259	0,815	2,526	0,255	0,240	0,196
Er	0,275	0,165	0,166	0,157	0,491	1,470	0,153	0,137	0,118
Tm	0,039	0,024	0,024	0,024	0,075	0,217	0,023	0,020	0,017
Yb	0,274	0,175	0,177	0,166	0,513	1,412	0,156	0,135	0,122
Lu	0,042	0,027	0,027	0,026	0,082	0,218	0,024	0,021	0,019
Pb	2,697	2,240	2,997	2,491	4,488	10,935	2,517	1,833	1,763
Th	1,050	0,662	0,675	0,660	1,765	5,460	0,697	0,592	0,459
U	0,290	0,244	0,238	0,207	0,537	1,074	0,196	0,182	0,158
Ce/Ce*	1,10	1,17	1,21	1,07	1,00	0,99	1,08	0,97	1,02
Eu/Eu*	0,63	0,61	0,59	0,74	0,68	0,63	0,63	0,67	0,66

The Table 12 shows that samples Iv-Q, Ya-B, Ya-S, For, Vyn-S and Ryb-L make close group with relatively similar values of the elements. Sample Ryb-L shows the lowest values for all the REE. The Iv-S sample shows highest concentrations for all the elements present in the table. To visualise differences in REE patterns the line plot of chondrite normalized values was produced (Fig. 52). Samples demonstrate relatively similar Ce and Eu anomalies (0,97 – 1,21 and 0,59 – 0,74 respectively). Chondrite normalisation and calculation of Ce and Eu anomalies was analogous to the glass data treatment.

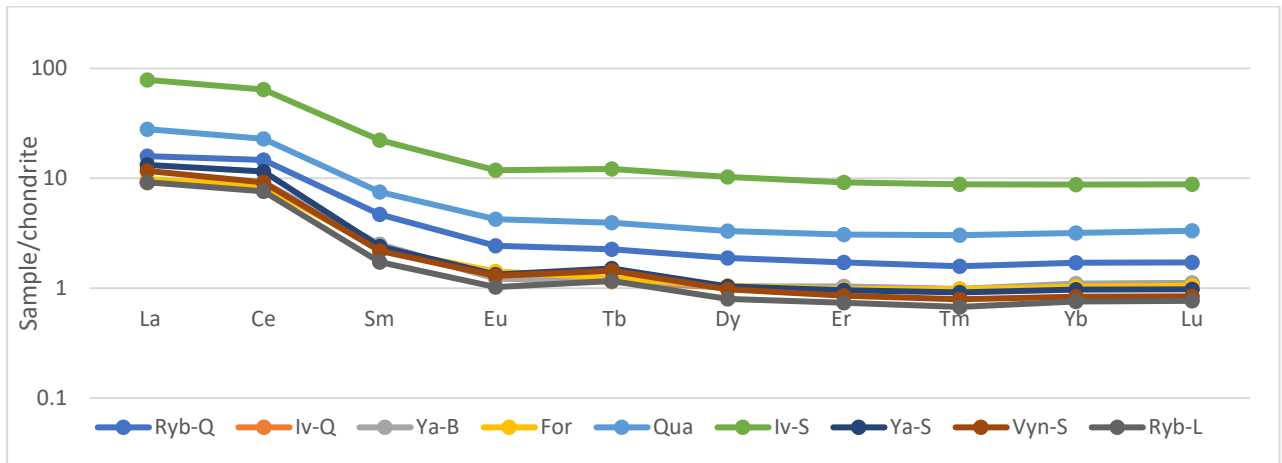


**Figure 52:** The line graph of chondrite normalised values of REE of sand samples.

It is evident that the collected sediments have same pattern of REE. Two exceptions have to be made: samples Vyn-S and Ryb-L seem to be more enriched in Tb. This can be explained by their proximity to the aquatic environments (estuary and lake respectively) (Piper, 1974). This pattern will be compared with the ones of glass fragments in order to make suggestions about provenance of the second ones.

### 3.2. Discussion

Any sort of interpretation of the experimental results has to be done in strong agreement with the context of the material studied. Obtaining the answers on each question put in the beginning is the purpose of current section. We structure it in the same way i.e. by the issue or question that must be answered. The secondary structuring within the subsections is made by the group of artefacts. Glass beads and other fragments from the Yahorlyk settlement, as it was said before, is an extremely diverse sample. It seems that each object despite the similarities in type has its own production history. We attempt to dismantle every thread from the ball that makes the Yahorlyk archaeological site such a unique place for ancient glass industry.

#### 3.2.1. Glass batch

For the ancient glass industry, the usual way for the manufacture of glass was the use of sand. However, sometimes scientists point out that quartz pebble, which is a much purer source of silica, could also be used for this craft (Smirniou et al., 2018). From the chemical composition of fragments

from the Yahorlyk settlement it is possible to exclude such raw material, since beads (and non-beads) have a certain amount (at least 22 ppm and more than 800 ppm as maximum) of zirconium and even more of other metals (aluminium, titanium) which are the indicators of the use of sand (Aerts et al., 2003; Degryse, 2014). Moreover, the strong correlation between K and Al (Fig. 33) should indicate the contamination of quartz sand by clay minerals or feldspar that was detected by XRD.

In the previous section, the difference in minor element content between the so-called translucent (groups 1, 3, 7 and 8) and opaque (groups 2, 6, sometimes 4 and 5) objects allows us to assume that different sands were used for their manufacturing. One of these sands was, apparently, quite clean from impurities of other minerals, while the other had a more abundant fraction of feldspar; the same can be deduced for heavy minerals fraction (although iron was probably added intentionally to some samples and the impurities associated with it can impact the trace metals distribution in the glass). The origin of the sands will be discussed separately in the section assigned to the origin of artefacts.

For the classification of archaeological glass, a very important point is the source of alkali, serving as the network modifiers (Goffe, 2007). As already mentioned, their source could be of mineral or plant origin. The difference between the glass made with the addition of natron and ash can be pointed by the total content of MgO and K<sub>2</sub>O, which for the natron glass will not exceed 1.5% and, on the contrary, will be greater than the indicated value for the flux of plant ash origin. As one can see from the table in the Annex 3 the magnesium and potassium oxides do not exceed such a level in the so-called translucent groups (groups 1, 3, 7 and 8) and always exceeds it in some of the groups of opaque objects (groups 2 and 4). The difference between these two sources of flux is visualized on the ternary graph below (Fig. 53).

As it can be seen, the above-mentioned samples with low content of magnesium and potassium (groups 1, 3, 7 and 8) can be attributed to natron soda-lime glass, while the groups 2, 4, 5 and 6 are grouped within plant ash soda-lime glass range. Sample Ya-6 (group 1) is different from the rest of the group falling into plant ash soda-lime glasses area. One sample (Ya-8, group 6), having a much higher relative content of potassium oxide, falls into a group of mixed soda-potash glass unlike the rest of the group 6 representatives that are together in the plant ash soda lime glasses area. This last samples can be the evidence of using of different plants for making ash (Ya-8) or glass recycling (Ya-6 and Ya-8).

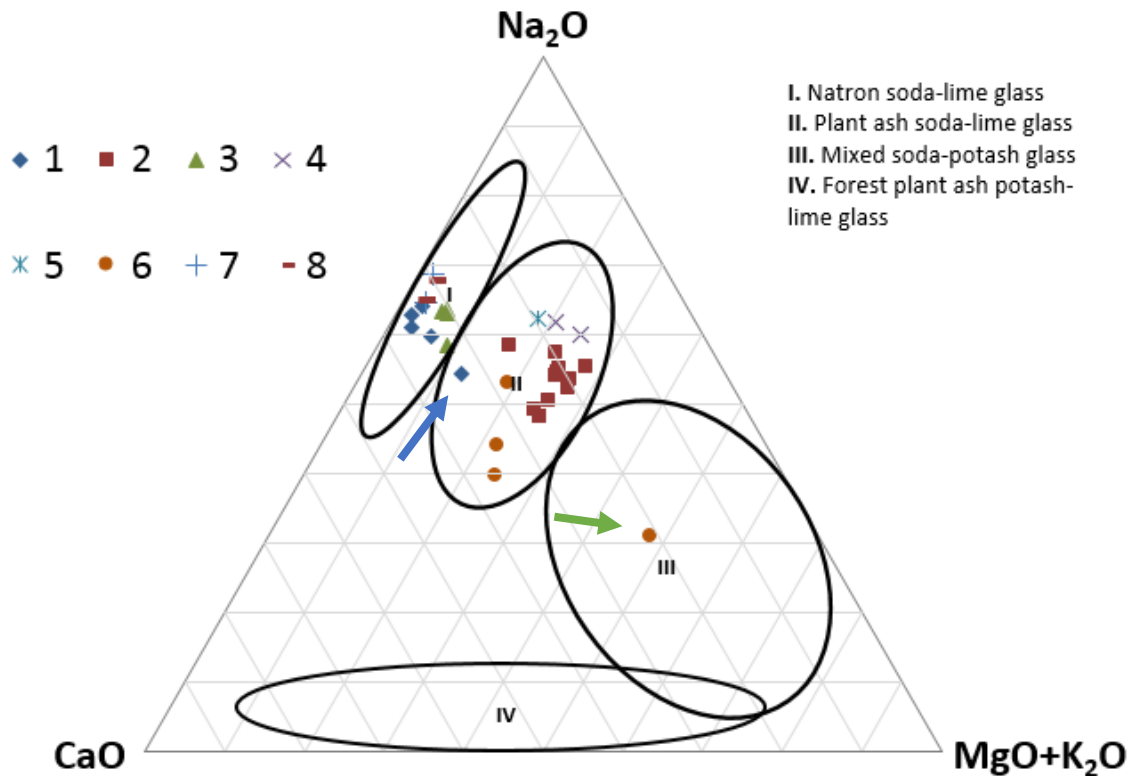


**Figure 53:** Ternary plot of the system CaO-Na<sub>2</sub>O-MgO+K<sub>2</sub>O. Glass families are put after Gratuze, Janssens, 2004. Sample Ya-8 is marked with a green arrow. Sample Ya-6 is marked with a blue arrow. Data of from the LA-ICP-MS analyses.

Natron, as already mentioned, has a mineral origin. It is interesting, that for samples that are very likely to be made with its addition the high level of chlorine is inherent. The well-known deposits exploited in antiquity are mostly concentrated in Egypt. The Egyptian natron is not pure hydrated carbonate, it also contains halite and sulphates (Henderson, 1985). The composition of various halophyte types ash reveals variability of the elemental composition and, as experiments show, does not depend on geographic location (Tite et al., 2006). The great variability in the quantities of potassium and magnesium for samples of opaque groups corresponds to this generalization. Halophytes are also characteristic biotas for the modern coast of the Yahorlyk Bay (Марушевський et al., 2006).

Lime, as the most widespread glass stabilizer in the ancient world, is also an important component of the glass matrix. The source of lime could be mineral (limestone) or shells, which, like the limestone, are composed of calcium carbonate (Henderson, 1985; Degryse, 2014). It is believed that the content of strontium is lower in limestone than in shells (Li, Henderson, 2016; Degryse, 2014), but studies show that the variability can be quite high and depends on the characteristics of the environment and microenvironment, the shell species and the age of the limestone deposits (Kulp et al., 1952; Marcano et al., 2015). Correlation between calcium oxide and strontium values is weak ( $r = 0.58$ ). However, if we take the task of finding a correlation coefficient

for the “translucent” (groups 1, 3, 7 and 8) and “opaque” (groups 2, 4, 5 and 6) samples separately, then its value increases to  $r = 0.74$  and  $r = 0.68$ , respectively (Fig. 54).

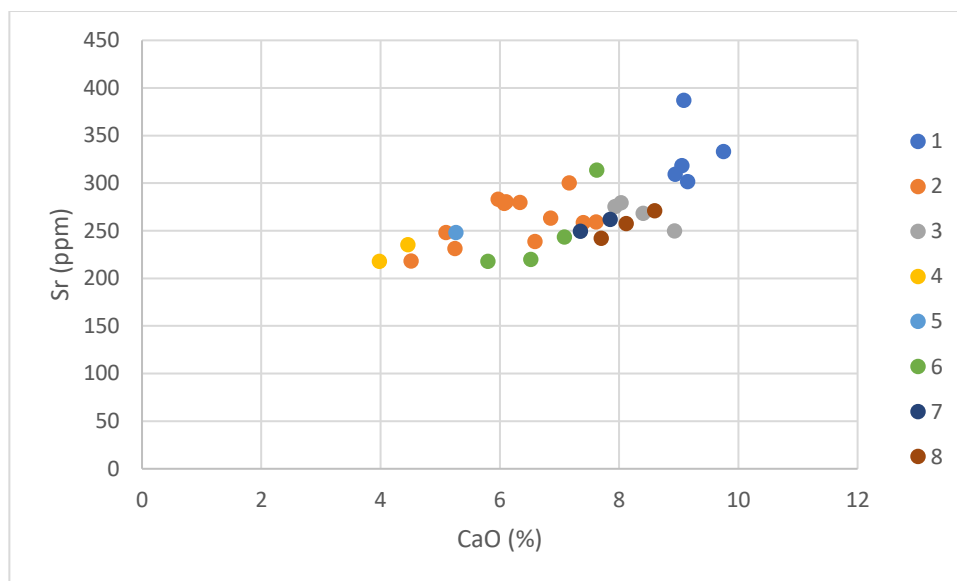


**Figure 54:** Yahorlyk glass scattered biplot of CaO against Sr. Data of the LA-ICP-MS analyses.

It is easy to notice that in this case the “translucent” groups (1, 3, 7 and 8) cluster more closely on the plot in opposition to “opaque” (groups 2, 4, 5 and 6) ones. Differences in correlation can be explained by different sources of CaO. Calcium is likely to be introduced into the glass also from the ashes of certain plants (Tite et al., 2006). Some of its amount can come into the glass mass from the plagioclases. The ratio between calcium and strontium will be different for each of these materials. On the shore of the Yahorlyk Bay one can find compact clusters of shell (Марушевський et al., 2006).

The three most important components of glass - glass former, glass modifier and glass stabilizer - make up from 77 to 97% of the total mass of oxides in the samples from the Yahorlyk settlement (table in the Annex 3). The proportion of these three main components remains approximately equal. Figure 54 is presenting relationships between major components of glass batch (Fig. 54).

The normalized to 100% oxides values of these three components show standard deviations of 1.45% for sodium, 1.85% for silicon and 1.47% for calcium oxides. This suggests that despite the difference in the source of alkali and alkali-earth oxides the glass from the Yahorlyk settlement belongs to the common "school" of glassmaking. In addition, this may be the evidence of the relative simultaneity of production, perhaps even the same executors.

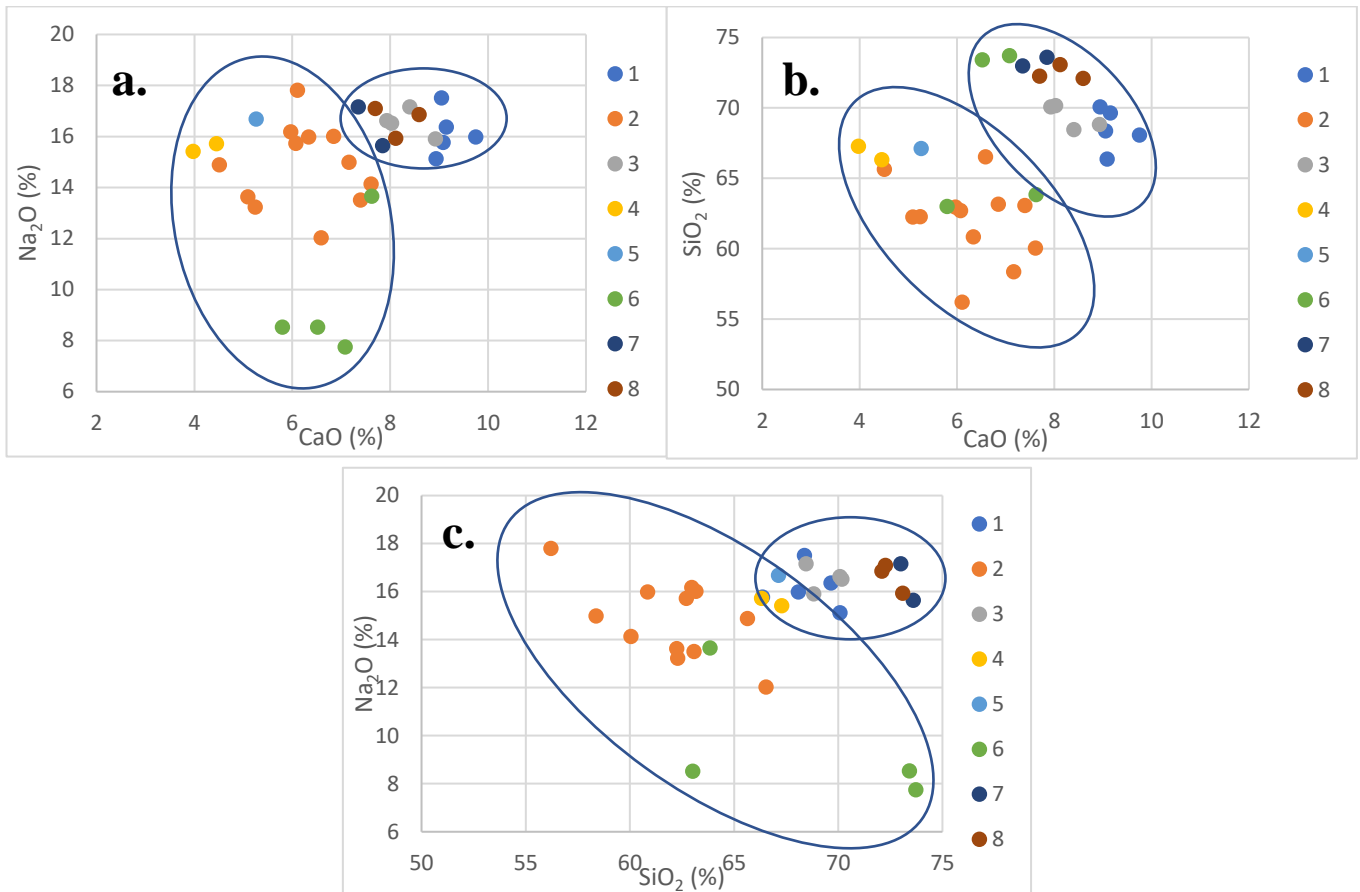


**Figure 55:** Yahorlyk glass biplots: a- CaO against Na<sub>2</sub>O; b- CaO against SiO<sub>2</sub>; c - SiO<sub>2</sub> against Na<sub>2</sub>O. Clustering of groups 1,3,7,8 on one side and 2,4,5,6 on the other is observable.

It is very possible that some glass recycling has taken place. Samples from group 2 and 6 show concentrations of Cu, Pb and Sn higher than 100 ppm that can indicate presence of cullet in the initial batch. It could have been used to lower the melting point of the batch. Co in Ya-5 (group 1) also can be a sign of recycling (Henderson, 2013).

### 3.2.2. Technology of producing glass beads

The furnace temperature regime is an important characteristic of the technological process. Available data on the ratio of the three main components of the glass allows to find out the temperature at which this glass was made. Because of the similar ratio between the three main components in all the samples, the furnace temperature range is rather narrow - 800-1000 °C (Fig. 56).

The results of two samples (Ya-8, Ya-17) indicate that the temperature of their vitrification should be 1300 and 1500 °C, respectively, which was unattainable for the ancient Greeks. It is likely that the reason for this positioning is in the low content of Na<sub>2</sub>O. Instead, the Ya-8 has a rather high K<sub>2</sub>O level (different plant ash and/or mineral impurity), which makes it impossible to adequately

represent the sample in the phase diagram of the system, because  $K_2O$  acts as a flux as well. It is very possible that melting temperature of the fragments containing more  $K_2O$  (plant ash soda-lime glass groups (2, 4, 5 and 6)) was different due to the same reason. Apparently, Ya-17 simply lost the portion of alkali due to their leaching and is also unsuitable for presentation. Both of its sides showing similar values of sodium oxide (7,7 – 8,5%). The temperature of the manufacture of the remaining samples is within the limits available to Greek or Scythian artisans, who smelted iron at the settlement, and iron smelting involved the highest operating temperatures of that time (Rehren, Pusch, 2005). The redox conditions of the furnace will be discussed in the “Colour” subsection because they can be reconstructed by the final colour of the beads.

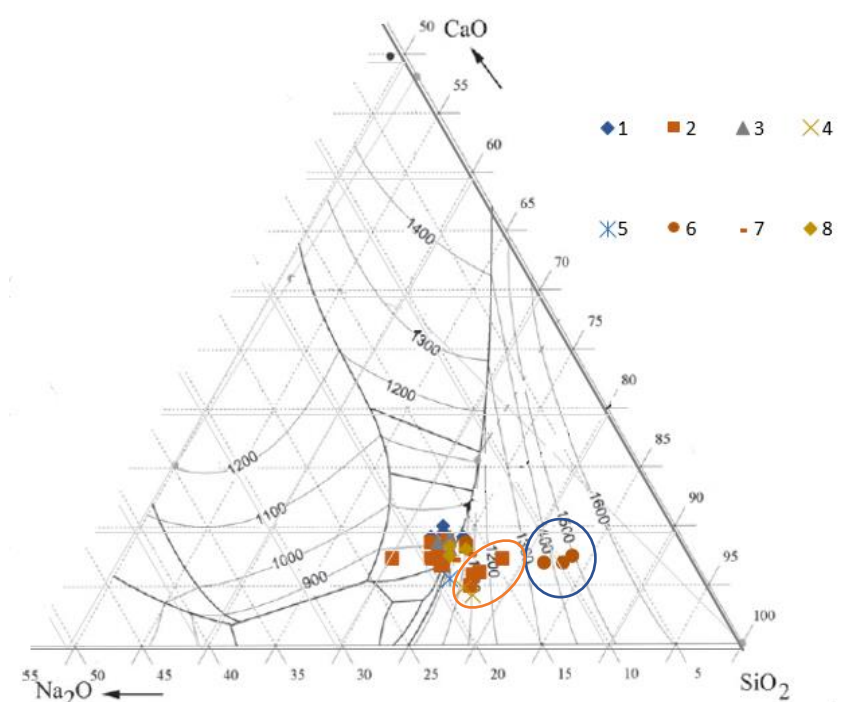


**Figure 56:** Phase diagram of the system  $SiO_2$ - $Na_2O$ - $CaO$  (after Shugar, Rehren, 2002) showing the minimum melting points for Yahorlyk samples. Samples of group 6 (blue oval) are positioned in the area of high temperatures due to depletion in sodium oxide. Groups 2, 4 and 5 (orange oval) have significant amount of  $K_2O$  to shift their positions left in the range of 800-1000°C.

The objects from the Yahorlyk settlement were made using more than one manufacturing method. The difference in shape, symmetry, and the nature of the apertures indicates at least two different types of beads forming. Rounded beads could be formed around a metal or ceramic rod in series. In this case, a cylindrical aperture and a certain asymmetry in the relation to it were formed (wound method) could be seen. The characteristics of this method are the protrusions of glass around one of the apices. The biconical bead hole had to be pierced with another tool that would have left a conic aperture after it. The biconical beads from the Yahorlyk settlement were, probably, formed in the special moulds and the apertures were made individually (mould method) (Острроверхов, 1981; Beck, 1928). For the manufacture of beads with eyes it was necessary to prepare three colours. The high degree of similarity in the elemental composition of beads suggests that the glass for their

manufacture was the same, it was already split and followed the transformations that occurred with the addition of colorants. The base could have been made in the same way as in the case of round beads, and the eye was formed by the gradual dropping of white glass first, and then blue. Some samples of this type are showing the irregularities of the eye shape, which may be a sign of low viscosity during the overlay. In case of sample Ya-10, the ornament was formed spirally (Алексева, 1975; Beck, 1928). All these forming processes had to pass within the temperature of working range of glass, before it became rigid.

### 3.2.3. Colour

So far, we have been discussing only the major components of glass, which form, modify and stabilize it. Meanwhile, other properties of glass often depend on components that make up less than 10% of its mass. In this section, we will focus on the colour scheme of a set of fragments from the Yahorlyk settlement, and the components that define this characteristic. Colour may also depend on temperature and redox level of the furnace. Sometimes the cooling process can also affect the colour of the final product (Moncke et al., 2014).

All samples of blue and blue-green colour have a discriminative feature - they all have a significant percentage of copper in their composition (ranging from 0.30% in green non-beads to 4.13% in blue parts of the eyed beads). From the beginning of the glass industry, copper was known as a colorant (Rehren, Freestone, 2015). Copper in the oxidising conditions forms  $\text{Cu}^{2+}$  ions that give the glass a blue colour (Moncke et al., 2014). This pure colour can be observed in a group of round blue beads (group 1). To reach the blue colour, it was also possible to use cobalt (Smirniou, Rehren, 2013), but it is practically absent in the beads (the largest amounts are 162 ppm in sample Ya-5 and 59 ppm in sample Ya-12, the rest of the samples show values smaller than 10 ppm).

Iron, provided the predominance of  $\text{Fe}^{2+}$  ions, can also give a blue hue (Goffer, 2007). However, the proportion between  $\text{Fe}^{2+}$  and  $\text{Fe}^{3+}$  (that gives yellow) ions usually makes the glass have a green tint (Moncke et al., 2014; Pollard, Heron, 2008; Ceglia et al., 2014). Due to the high content of iron and other components, the beads eyes, with exception of samples Ya-10 and Ya-14 (groups 4 and 3 respectively), are distinguished by a deeper, opaquer colour that is close to the green. In the Figure 57 the difference in the content of iron and copper in the glass samples is visualised.

As can be seen, samples Ya-7, Ya-8 and Ya-17 (group 6) have more iron than copper, so their colour is different from all other specimens. We can conclude that both Fe and Cu ions have

influenced the final hue of the group 6 samples. We cannot elucidate Fe and Cu ion ratios with the available data.

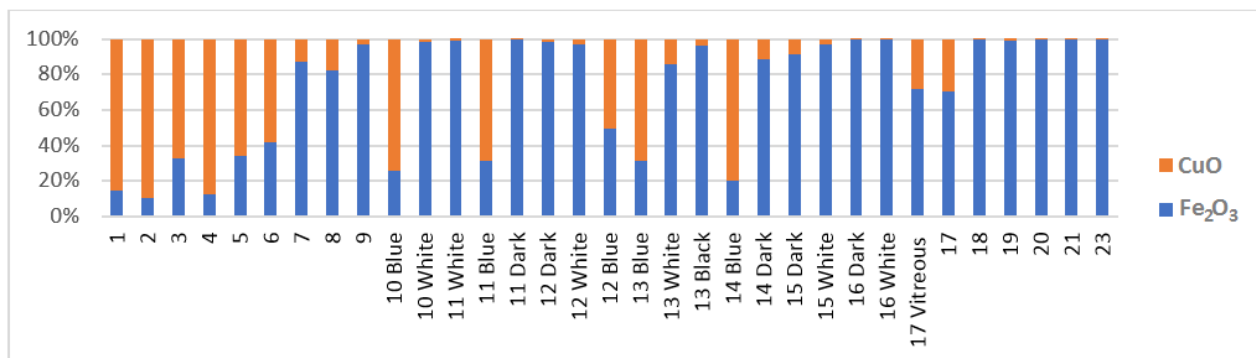


**Figure 57:** proportion of Fe (expressed as ferric oxide) and Cu (expressed as cupric oxide) shown as the normalized to 100%. Cu is prevailing in blue coloured glass (samples 1-6 and blue parts of the eyes), Fe in green (samples Ya-7, Ya-8 and Ya-17).

Ferric iron ions can provide the yellow tint of the glass of group 8, indicating an oxidizing atmosphere. Experiments show that obtaining a yellow shade does not require such a high temperature and time as for the acquisition of blue or green hues (Jackson, 2005). The participation of other colouring agents as lead antimonate, uranium or silver (Janssens, 2013; Goffer, 2007) is excluded as the respective elements are present only in trace concentrations. The iron content in these samples is also low (about 0.4%), but it is still twice as high as in colourless beads (group 7). In addition, a high level of titanium and zirconium suggests that there was a selectivity of the source of sand, or intentional adding of heavy fraction minerals with high content of the mentioned elements. We are not able to say if it was a deliberate addition. For the comparison, the yellow colour is also attributed to iron at similar concentrations (Oikonomou, Tryantafyllidis, 2018).

After getting acquainted with the data of LA-ICP-MS regarding the colourless beads (group 7), the absence of any impurities (the level of iron does not exceed 0.25%) is noticeable. This soda glass was made without the addition of manganese, which in small quantities neutralizes iron (Moncke et al. 2014). Therefore, the transparency and absence of a yellow tint can be attributed to the redox environment of the furnace, which retained the proportion of iron ions.

The dark colour of archaeological glass, in the literature, is usually attributed to elements such as manganese and iron. The presence of manganese ions impact either a very dark purple or a very dark green colour to glass. At the appropriate concentration, these colours become very intense and look black when the piece is sufficiently thick (Moncke et al., 2014; Janssens, 2013; Goffer, 2007). To obtain this dark colour with iron, it is not necessary to adhere to its high concentration. Sometimes even samples with only a few percent iron have a dark colour. This can be achieved by the very reduced atmosphere of the furnace with the addition of fresh wood to the charcoal during

the manufacture of glass (Ceglia et al., 2014). For samples Ya-9, Ya-11, Ya-12, Ya-13 and Ya-16 it seems that this method was used to make the base on which the eye decoration was added. However, it is obvious that this does not apply to samples Ya-14 and Ya-15. For these two samples, there is a characteristic higher level of manganese, which, however, does not exceed 1%. The base of these beads is much lighter (Fig. 58) than the samples that owe their colour to iron. Bright violet colour is documented for concentration of manganese about 1% (Moncke et al., 2014). Obviously, the exact thickness and opacity of the sample plays the role of an intensifier.

For the acquisition of white colour by ancient artisans, several substances were used. Calcium antimonate, used by the Egyptians to produce opaque white colour (Swann et al., 1990), could not be used to make parts of the Yahorlyk samples, since Sb was only found in trace amounts and no crystals enriched in both Sb and Ca were found by VP-SEM-EDS. An alternative could be bone ash. There is a rather strong correlation between the main elements that form the bone ash - calcium and phosphorus oxides ( $r = 0.8$ ) for the eyed beads of group 2.

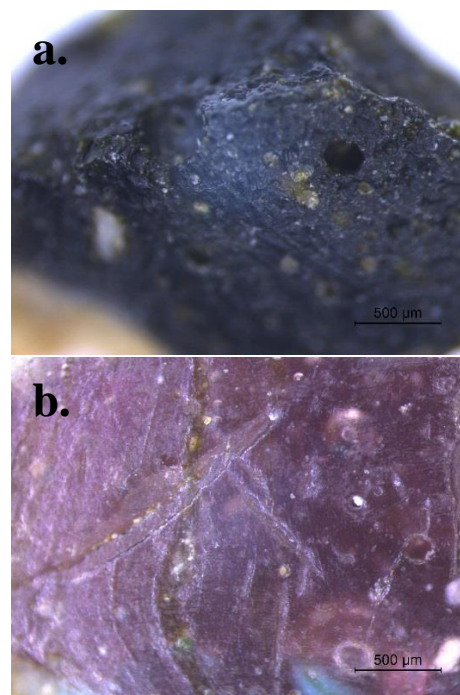


**Figure 58:** Comparison of appearance of two kinds of base glass that was used in eyed beads: a - Ya16 (50X magnification); b - Ya-14 (50X magnification).

Sample	P <sub>2</sub> O <sub>5</sub> (%)	CaO (%)	CaO/P <sub>2</sub> O <sub>5</sub>
11 White	1,218	7,396	6,068
11 Blue	0,715	5,246	7,328
11 Dark	0,811	5,968	7,355
12 Dark	0,647	4,510	6,962
12 White	1,487	7,163	4,814
12 Blue	0,736	6,106	8,256
13 Blue	0,758	5,096	6,722
13 White	1,248	7,614	6,101
13 Black	0,795	6,337	7,961
16 Dark	0,767	6,072	7,916
16 White	1,399	6,589	4,707
	Corr	0,80	

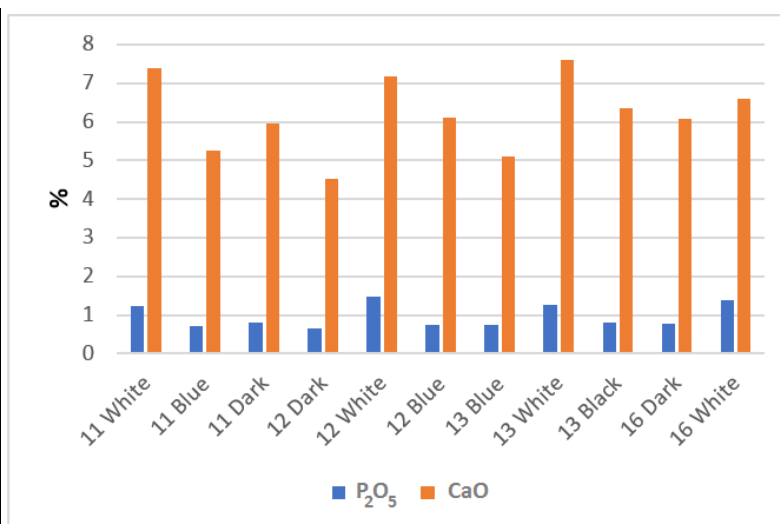


**Figure 59:** The relationship between Ca and P oxides in the beads of group 2. Values of each oxide concentration together with calculated ratios and correlation coefficient are put in the table on the left.

Apatite inclusions found by means of SEM-EDS also support this option. Not all the amount of calcium and phosphorus can be attributed to the possible use of bone ash since these elements

can also be added as glass stabilizer and with the plant ash flux. However, when comparing the white parts with the remaining colours of the eyed beads, it becomes apparent that the amount of both elements is significantly higher (by about 0.5% for phosphorus and 1-1.5% for calcium) in the white sections (Fig. 59). The correlation of these elements within the group 2 is fundamentally different from the correlation of all considered samples, which is negative ( $r = -0.5$ ). In our opinion, it is likely that the bone ash is part of the formula of all three parts of the group 2 eyed beads. In the dark and blue parts it can play the role of opacifier and in white it is present also as a colorant (Biek, Bayley, 1979; Towle, Henderson, 2007).

However, not all samples with a white colour are suitable for such explanation. Samples Ya-10 and Ya-15 have elevated levels of tin and lead (up to 1% each). Widely used in the ancient world, the lead tin oxide (lead stannate) provides yellow colour and opacity to the glass (Agua et al. 2017). Perhaps, each oxide was introduced separately from one another without forming the compound. But there is a possibility that this compound was disintegrated to respective oxides after overheating at 1100 °C (Eastaugh et al., 2008; Heck et al. 2003). Tin oxide makes the glass opaque and white (Eastaugh et al., 2008). Bubbles, which are present in large quantities in the white part of the Ya-10, add a cloudy effect.

It has already been noticed that between translucent groups (1, 3, 7 and 8) and opaque ones (2, 4, 5 and 6) there is a difference in elemental composition, but despite the much larger amount of impurities, it is likely that this glass owes its opaque appearance not only to them. Bubbles also contribute to opacity, and it is also possible that some grains (quartz, apatite, iron) were deliberately introduced into the matrix maintaining solid state during the production of glass and providing the desired level of opacification (Goffer, 2007).

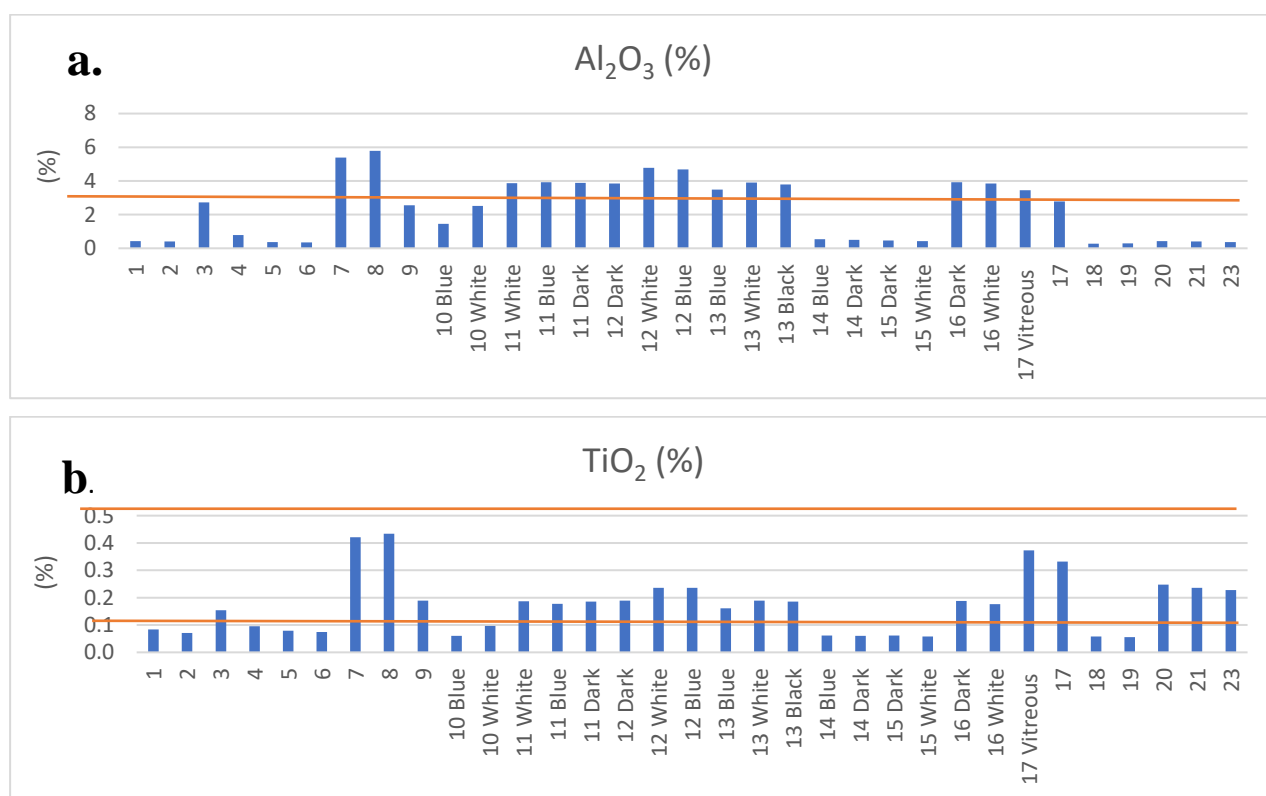
#### 3.2.4. Possible raw materials

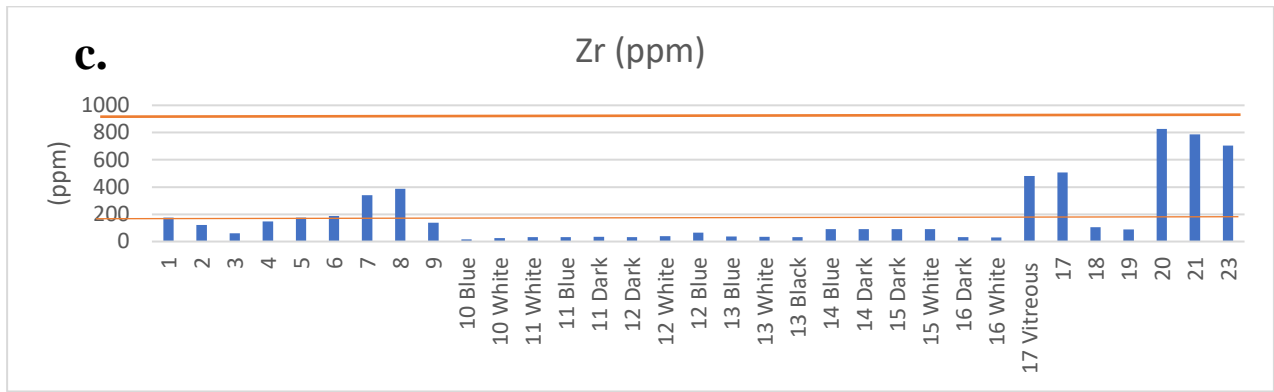
In this section, we will discuss the origin of glass fragments from the Yavorlyk settlement. It is already clear that the raw material for the manufacture of the glass beads does not have the same origin. In this work, we will make a comparison of the beads' elemental composition with that of sand from the vicinity of the archaeological site. When making an attempt to link glass with the source of sand one must always keep in mind the fundamental differences between them, namely, the presence of other substances among the necessary ingredients of the glass batch. We must track only components of glass that depend on sand. Together with the recording of the common and distinctive features between the sand and the glass fragments, we will go from the main components

to the rare earth elements, comparing the studied fragments with data available in the literature regarding other glass objects from well-known centres of the glass industry.

To visualize the compatibility of the sands and artefacts, bar graphs of the amount of metal oxides in the beads (obtained with LA-ICP-MS) with the minimum and maximum values found in sand (obtained with XRF) (orange lines) were generated (Fig. 60).

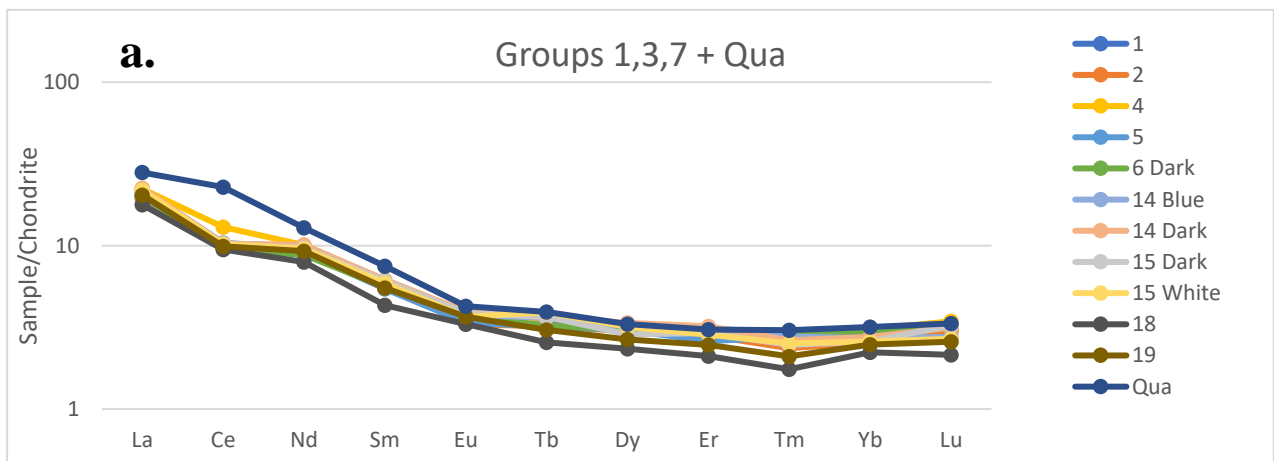
While the graphs a and b show that “translucent groups” (1, 3, 7 and 8) do not converge with values of sand, in the third (c) one, it is evident the lack of Zr in “opaque groups” (2, 4 and 6) as well as in biconical colourless (group 7) and purple base eyed beads (group 3). There is not enough to compare with even the most depleted sample of sand. Regarding the fluctuations in the amount of zircon on the shore and bottom of the Yahorlyk Bay it was already spoken in the geoenvironment section (Чепижко, 2007). Therefore, we cannot rely solely on this data because gravitational sorting could change the concentration of zircon in sand in one direction or another. Also, grains of zircon may stay suspended in the matrix of glass and might not give signal to the ICP operating in laser ablation point analysis mode.





**Figure 60:** The concentrations of elements from La-ICP-MS analyses of Yahorlyk glass compared with such found in sands by means of XRF (orange lines for min and max value): a -  $\text{Al}_2\text{O}_3$  (the max value of sand is 10,8% - not depicted), b -  $\text{TiO}_2$ , c - Zr. The groups: group 1 - Ya-1, Ya-2, Ya-4, Ya-5 and Ya-6; group 2 - Ya-3, Ya-11, Ya-12, Ya-13 and Ya-16; group 3 - Ya-14 and Ya-15; group 4 - Ya-10; group 5 - Ya-9; group 6 - Ya-7, Ya-8 and Ya-17; group 7 - Ya-18 and Ya-19; group 8 - Ya-20, Ya-21 and Ya-23.

It is more reliable to compare glass and sand by the values and ratios of rare earth metals. First of all, it is necessary to find out how close are samples of sand from the vicinity of the Yahorlyk settlement and fragments of glass found on it. Variation within the groups REE signature when they are chondrite normalised and plotted was noted in the previous section (Results of LA-ICP-MS). After comparing the samples of sand with beads, it became clear that the sample Qua is best suited to the profile of the beads, and the Iv-S pattern is best suited for comparison with non-beads of group 6. The rest of the sand samples, although having similar signatures, are rather depleted in the quantities of REE. Below one can find normalized to chondrite comparable profiles of sand and the glass fragments from the Yahorlyk settlement.



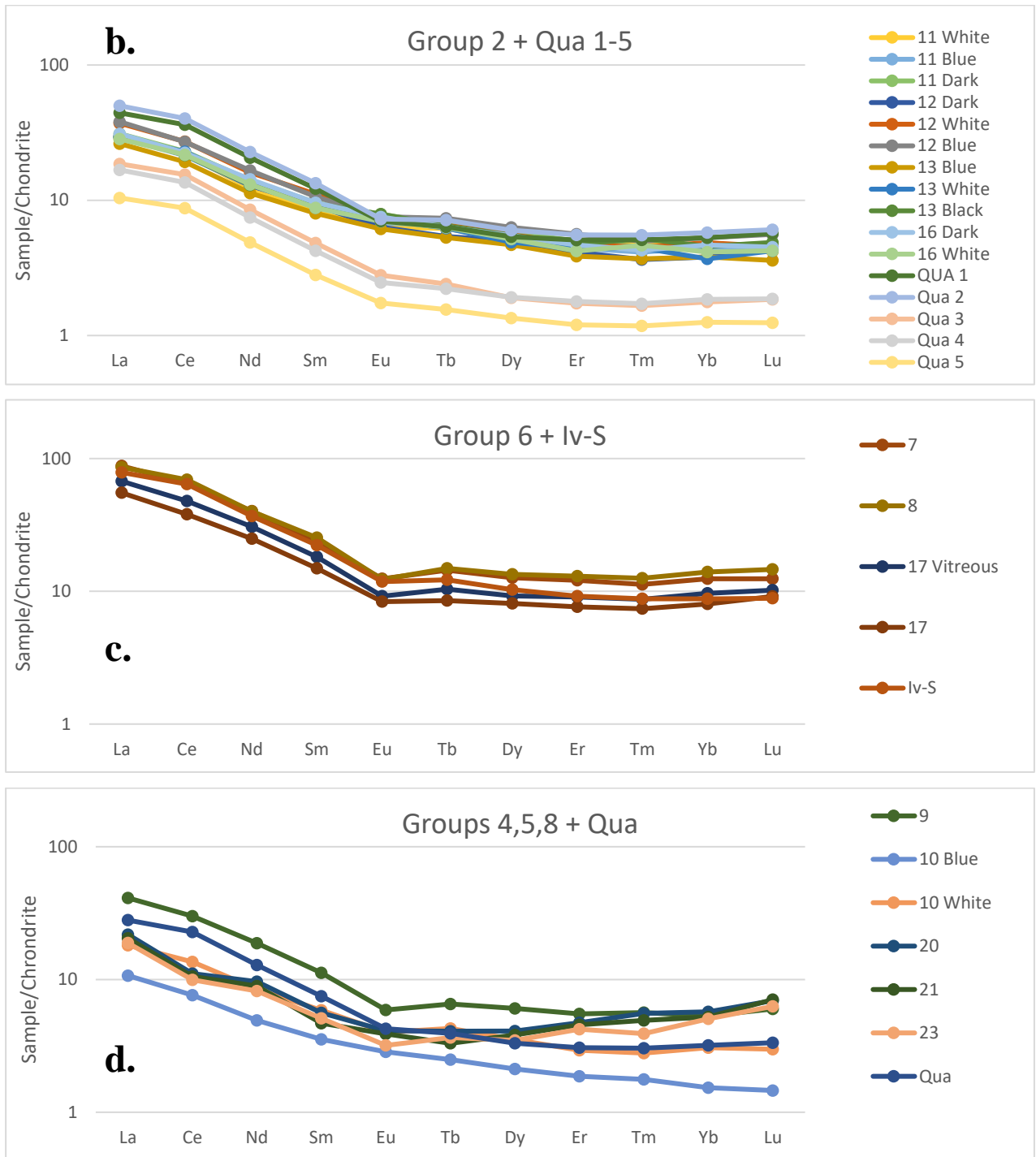


**Figure 61:** Chondrite normalised linear plots of Yadorlyk glass and sand: a - groups 1,3,7 in comparison to Qua sample of sand; b - group 2 in comparison to all the Qua subsamples; c - group 6 in comparison to Iv-S sample of sand; d - groups 4,5,8 in comparison to Qua sample of sand. The groups: group 1 – 1,2,4,5,6; group 2 – 3,11,12,13,16; group 3 – 14,15; group 4 – 10; group 5 – 9; group 6 – 7,8,17; group 7 – 18,19; group 8 – 20,21,23.

On the graph a, we see that so-called translucent groups demonstrate a discrepancy with the sand sample in the Ce region. Their difference in the magnitude of the anomaly is quite significant (approximately 0,35). Most of opaque beads are matched with a Qua sand sample profile, which is shown on the graph not as a mean value of aliquots but split in its subsamples. This has been done for a better perception and demonstration that there are also slight differences between the sand subsamples. The anomalies values for Qua sample are:  $Ce/Ce^* = 1$ ,  $Eu/Eu^* = 0,68$ . The first value

is similar to what groups 2, 4, 5 and 6 show but the second one shows the divergence (0,73 - 0,94 for glass fragments) with this sample. Some samples (Ya-13 and Ya-16 White from group 2) have a barely noticeable positive anomaly of Tm. Group 6 is distinguished by higher concentration of rare-earth elements. In general, they repeat the profile of the group 2, but in order to compare them with sand, an Iv-S sample with matching values of REE concentrations was used. For some of them smaller values of Eu negative anomaly are characteristic (min 0,55). The last graph contains samples that are not depicted in the previous ones. The difference between the biconical yellow group from all others glass fragments and from other samples of sand is undoubted. In addition, sample Ya-23 is also different from the other two. Sample Ya-9 has the common features with the depicted sand pattern but is considerably enriched in the REE. It looks like differently coloured parts of the Ya-10 were made from different raw materials. However, the white part is close to the opaque eyed group only with depleted REE values.

Ce is a rather redox-sensitive element. In seawater, it is deposited depending on the salinity. The ability of cerium to exist in two valent states with the preference of IV for lower salinity and III for higher making in this way positive and negative anomalies with respect to La and Nd. Also, the ratio may change from the depth, activity of microorganisms and weathering of already formed deposits (Shelds-Zhou, 1998; Shields-Zhou, Stille, 2001). During the weathering heavy rare-earth elements decrease in the level (Shelds-Zhou, 1998). Positive Ce anomalies and negative Eu that we observe in the sand can be a consequence of the redox state of the magma (Trail et al. 2012). Such anomalies and the general profile of normalized to chondrite values (enrichment in LREE when compared to HREE) is considered to be typically continental (Whitehouse, Kamber, 2002)).

The close values of the anomalies and the similarity of the profile suggests that the sets of opaque eyed beads and also the blue-green non-beads are made of local sand. True, there is some depletion of beads compared to the sand in the region of LREE. This can be explained by the inclusive state of monazite in the glass: monazite has an extremely high melting point of more than 2000 °C (Hikichi, Nomura, 1987), so it remains solid in the melt matrix (as seen with VP-SEM-EDS in several glass beads) (Annex 2); in the case of acid digestion, monazite disintegrates and its signal can give higher values for LREE than the ones of the glass made of it and analysed by LA-ICP-MS. Incomplete coherence in the HREE region may be due to over-evaluation of the values that takes place for the Qua sample.

Now, let us focus on finding the place of beads from the Yahorlyk settlement among other published artefacts originating from about the same time period (8-4<sup>th</sup> centuries BC from Pieria (Blomme et al., 2017), and the late bronze age (14<sup>th</sup>-11<sup>th</sup> centuries BC from Egypt and Mesopotamia (Shortland et al., 2007)). Shortland has offered to distinguish Egyptian (Amarna, Malkata) and

Mesopotamian glass (Nuzi, Tell Brak) with a combination of  $1000 \cdot \text{Zr}/\text{TiO}_2$  and Cr/La ratios. The chart below shows the values of the corresponding samples (Fig. 62).

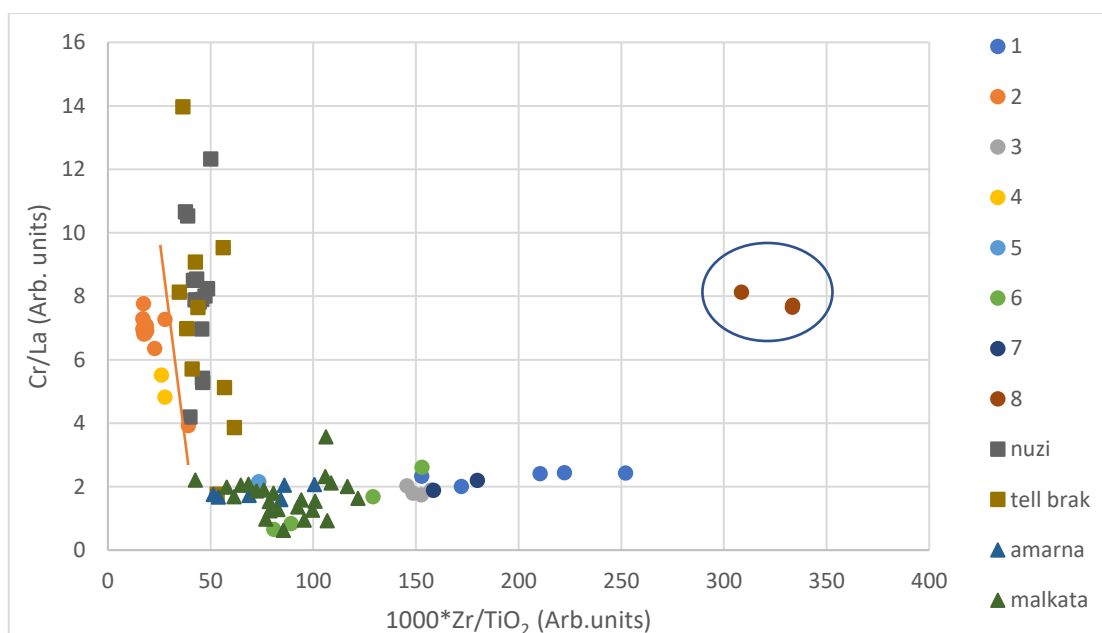


**Figure 62:**  $1000 \cdot \text{Zr}/\text{TiO}_2$  against Cr/La binary plot of Yahorlyk glass (rounds) compared with the ones reported in Shortland et al. 2007. Nuzi and Tell Brak are Mesopotamian sites (squares) while Amarna and Malkata are Egyptian (triangles). Group 8 is in the blue circle. The orange line is separating groups 2 and 4 from the Mesopotamian samples.

As we can see groups 1, 3 and 7 have common features with Egyptian specimens, one can also find green non-beads (group 6) in the same area. The dark base eyed (group 2) ones, even though they have a parallel vector with Mesopotamian, have a slightly lower ratio of zircon to titanium. Hence, they are different from all the samples present at the graph. The biconical yellow (group 8) beads group separately as well, both ratios are relatively high in their case. It supports the suggestion that the high content of titanium and zirconium in these beads is a deliberate addition. They are grouped together again with all colourless (group 7) ones and “translucent” (groups 1 and 3) in general in the caesium against lanthanum plot (Fig. 63 a). Here we can see that beads from Greece form a dense group together with blue and some other groups of translucent beads. Blue-green non-beads (group 6) do not belong to any of the groups and are scattered. The Mesopotamian glass is clearly separated from opaque beads that are grouped around the Qua sample of sand. The latest plot to be considered is Lu / Th.

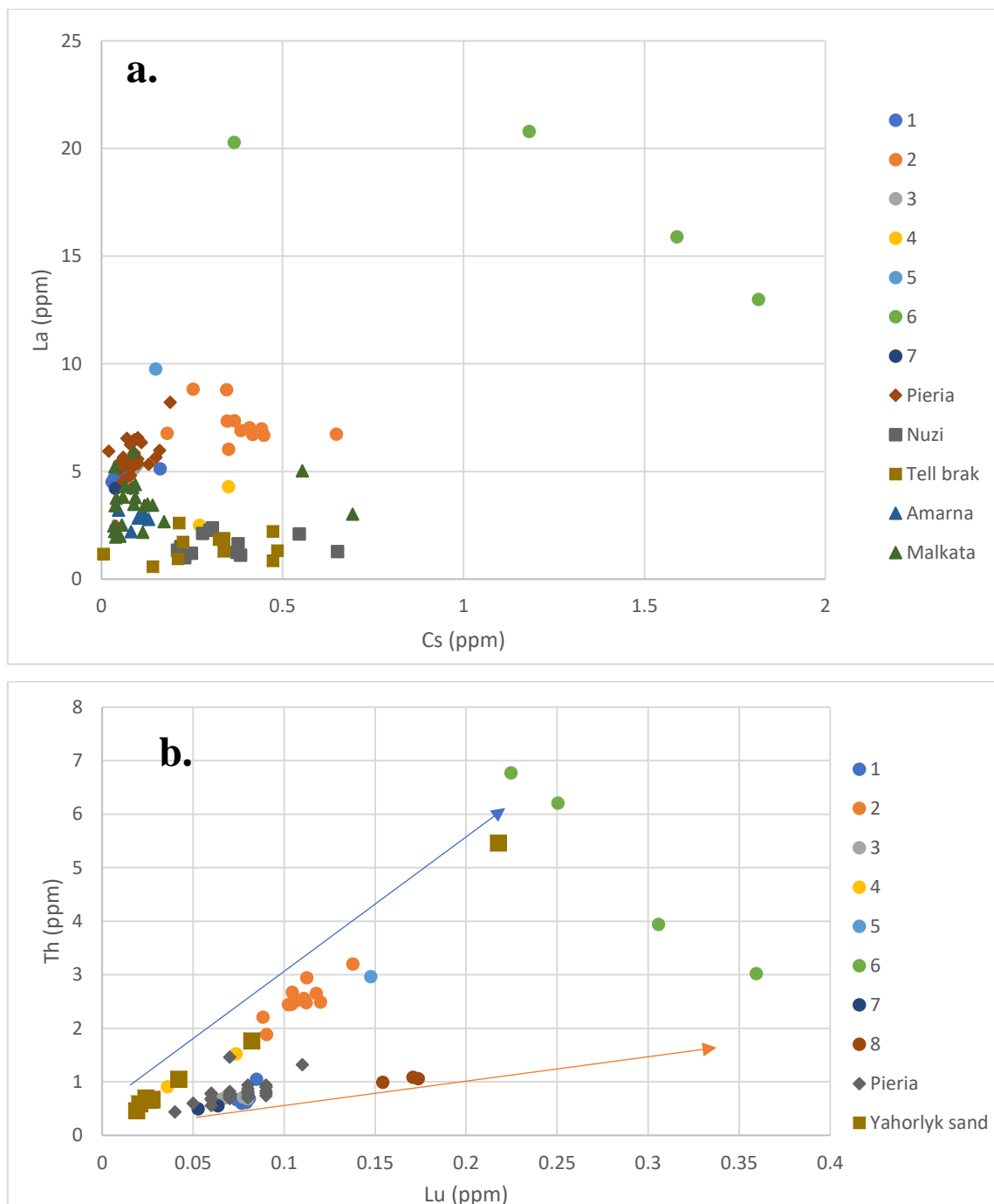


**Figure 63:** Binary plots of Yahorlyk glass compared with the ones reported in Shortland et al. 2007 and Blomme et al., 2017: a – Cs-La plot (group 8 is absent due to the absence of Cs values); b – Lu-Th plot with two different trend lines (one follows sand samples (blue arrow), another Pieria samples (orange arrow)). Pieria is a Greek site (diamonds). Nuzi and Tell Brak are Mesopotamian (squares) sites while Amarna and Malkata – Egyptian (triangles).

It shows a clear separation of samples on those that correlate with the sand and those that correlate with the Greek beads. Sample Ya-9 is an outlier, biconical yellow beads form a distinct dense group, but on a common trend line with the rest of translucent and Greek ones. It can also be noted here that most of sand samples, that make a close, depleted in REE group can be used as markers to make a trendline. It is possible that this sand values are the result of sorting that began in the 19<sup>th</sup> century, which led to a higher percentage of quartz in the sand than it once had.

Thus, based on the all gathered information, we can suggest local origin for samples of dark base eyed beads and blue-green non-beads (groups 2 and 6). Samples of round blue and associated with them blue non-beads, biconical colourless and yellow, and in addition, samples Ya-14 and Ya-15 (groups 1, 3, 7 and 8) are proposed to be associated with the Greek objects having a common primary glass-making centre at Syro-Palestine coast (Blomme et al., 2017). Samples Ya-9 and Ya-10, depending on the situation, behave in a coherent manner with an opaque group of eyed beads or individually. This might be caused by recycling or unusual selection of the raw material.

## CONCLUSIONS AND FUTURE WORK

Questions of provenance, technology and raw materials selection for the set of glass fragments from the Yahorlyk settlement that were discussed throughout the previous chapter can be answered now with different grade of insight. Reliability of the results was assured by the multianalytical approach. Data obtained by means of XRF gave an idea about bulk composition of both glass and sand samples. In case of sand samples, the analyses performed on different equipment also allowed to get the precise major elements composition. VP-SEM-EDS area analysis was used to obtain quantifiable information about glass elemental composition but superficial alteration of glass due to the loss of alkali made the results inadequate to represent the bulk composition of material. In this study we relied on the LA-ICP-MS data about glass matrix. Quantitative information about sand composition was based on XRF (major elements) and ICP-MS (trace elements). VP-SEM-EDS (point analyses) and  $\mu$ -XRD were the sources of information about particles suspended in the matrix. Powder XRD was crucial for mineralogical characterisation of sand samples.

Since the question of provenance was rated the most important in the work, it is appropriate to start generalisation with this topic. Prior to this study, it was established that the Yahorlyk settlement was a glass working site (besides other crafts). All the beads considered were plausibly made there, judging by the archaeological remains. The research indicates the presence of both kinds of objects: made of local sand (groups 2 and 6) and the ones that were made of imported glass (groups 1, 3, and 7) (associated with Levant coast). The provenance of the samples Ya-9 (group 5) and Ya-10 (group 4) as well as biconical yellow beads (samples Ya-20, 21, 22, 23, group 8) remains unknown. It is possible that their REE signatures were affected by recycling (groups 4 and 5) or by very specific selection of sand (reach in heavy fraction minerals) (group 8). That makes this group different from the very similar biconical colourless beads (group 7). The addition of a certain amount of cullet is also possible for the case of the beads that were made from local sand (groups 2 and 6). It is suggested that the glass that was used to produce fragments of groups 1, 3 and 7 is of Levant coast origin.

Two samples of sand show close signature to the glass fragments: sample Qua and sample Iv-S. Sample Qua is very fine white sand that did not need to be ground before the batch making. This type of sand is the closest match with group 2 (dark base eyed beads). Sample Iv-S is very fine dark sediment enriched in REE which makes it comparable with the samples from the group of green non-beads (group 6). In any case, it is possible to say that Greek artisans knew well the terrain and selected the very fine raw material with the idea about the final product.

All the artefacts were made with closely calculated batch formula maintaining  $\text{SiO}_2$ - $\text{Na}_2\text{O}$ - $\text{CaO}$  ratios on the same level which can suggest the link between the people involved in the primary production overseas and the ones, who made the glass locally. The beads were made in two different

ways (by winding and moulding), the eyes were also made differently (by dropping glass sequentially (groups 2 and, probably, 3) or shaped by some tool (group 4).

Regarding the colourants used to produce glass it was established that the blue glass was coloured by the addition of  $\text{Cu}^{2+}$  ions that were incorporated into the glass matrix under oxidising conditions of the furnace. Dark glass was, probably, obtained by the reducing conditions of furnace and some iron (converted into  $\text{Fe}^{2+}$  ions) that was added to the batch. The yellow colour also relies on the content of iron (in  $\text{Fe}^{3+}$  form) (probably added with a heavy fraction sand minerals) and oxidizing conditions. Glass with the purple hue was, probably, made by the addition of manganese. Colourless glass was achieved just with careful selection of raw materials and not very oxidizing conditions of the furnace. The white glass of the Yahorlyk settlement has to do with two substances: bone ash and tin oxide that was probably added with lead. We are not able to say more about the relationship between lead and tin oxides, namely is they were forming a single compound before melting or not. It is also very unusual for the centuries that are discussed. The nature of archaeological finds that has been studied here does not allow to rely on their origin and there is a chance that some of the artefacts come from later times, which might be the case of groups 3 and 4. It is a question if the imported glass was coloured during the production on the primary site or during the production of beads on the Yahorlyk settlement site.

The Yahorlyk settlement seems to be the site of both glassworking and glassmaking. Artisans used new raw materials, could adjust colour with chemical agents and by furnace conditions. They were capable of producing beads in different ways. They had some links with the Eastern Mediterranean and were probably covering the needs of population placed very distant from the big primary production sites of ancient world. The use of different flux for groups 2, 4, 5 and 6, which were made using soda plant ash, fits well into this picture, because, located on the remote coast, artisans, though they had access to Mediterranean glass, did not have access to natron flux that was becoming the most popular variety of flux in the ancient world.

The methodology of the study seems to be reliable and applicable to the other cases of probable glassmaking sites. Probably results were even more reliable if the same ICP-MS mode was applied to both kinds of samples – glass and sand.

It would be interesting to broaden the number of the sites for comparison of glass artefacts and try to look for the Yahorlyk glass elsewhere. The experiments of making glass from the actual samples Qua and Iv-S can provide material to reconstruct glassmaking technology in full. In parallel it is proposed to study halophytes of the Yahorlyk bay and their ash. In any case this study contributes to the geography of ancient glass industry adding on the map one more remote point with the description of methods used by ancient people and their links to the main centres of the industry.

## REFERENCES

- Aerts, A., Velde, B., Janssens, K., Dijkman, W. (2003) Change in silica sources in Roman and post-Roman glass. *Spectrochimica Acta Part B*. Vol. 58, pp. 659–667.
- Agua, F., Conde, J.F., Kobylińska, U., Kobyliński, Z., García-Heras, M., Villegas, M.A. (2017) Chemical–physical characterisation of Early Iron Age glass beads from Central Europe. *Boletín de la Sociedad Española de Cerámica y Vidrio*. Vol. 56, issue 3, pp. 119-130.
- Babalola, A.B., Dussubieux, L., McIntosh, S.K., Rehren, T. (2018) Chemical analysis of glass beads from Igbo Olokun, Ile-Ife (SW Nigeria): New light on raw materials, production, and interregional interactions. *Journal of Archaeological Science*, Vol. 90, pp. 92-105.
- Balcaen, L.I.L, Bolea-Fernandez, E., Resano, M. Vanhaecke, F. (2015) Inductively coupled plasma - Tandem mass spectrometry (ICP-MS/MS): A powerful and universal tool for the interference-free determination of (ultra)trace elements - A tutorial review. *Analytica Chimica Acta* Vol. 894, pp. 7-19.
- Bardman, N.G.L., Hammond, J. (ed.) (1982) *The Cambridge Ancient History. The Expansion of the Greek World, Eight to Sixth Centuries B.C.* Vol.3 Part 3, Cambridge University press, 530 pp.
- Beck, H.C. (1928) *Classification and Nomenclature of Beads and Pendants*. *Archaeologia*, Volume 77, pp. 1-76.
- Beckhoff, B., Kanngießer, B., Langhoff, N., Wedell, R., Wolff H. (2007) *Handbook of Practical X-Ray Fluorescence Analysis*. Springer Science & Business Media, 863 pp.
- Bell, D.C., Garratt-Reed, A.J. (2003) *Energy Dispersive X-ray Analysis in the Electron Microscope*. 1st Edition. Garland Science, 160 pp.
- Bezborodov, M.A., Ostroverkhov, A. S. (1978) A glass-making workshop in the Northern Black sea region in the sixth century B.C. Translated from *Steklo i Keramika*, no. 2, pp. 32-33.
- Biek, L., Bayley, J. (1979) Glass and other vitreous materials. *World Archaeology*, 11, 1, pp. 1-25.
- Birkholz, M. (2006) *Thin Film Analysis by X-Ray Scattering*. Willey-VCH Verlag GmbH & Co., Weinheim 378 pp.
- Blagovolin, N. S. (1984) *The Northern Black Sea Lowlands and Crimea. Geomorphology of Europe* Ed. by C. Embleton, Palgrave, London pp. 387-392.
- Blomme, A., Degryse, P., Dotsika, E., Ignatiadou, D., Longinelli, A., Silvestri, A. (2017) Provenance of polychrome and colourless 8th–4th century BC glass from Pieria, Greece: A chemical and isotopic approach. *Journal of Archaeological Science*. Vol. 78, pp. 134-146.
- Bobrov, O.B., Gurskiy, D.S., Malyuk, B.I. et al. (2006) *Ukraine: Carpathians and Ukrainian shield. Geological excursion book*. Ukrainian state geological institute, 154 pp.
- Brill, R.H. (1972) Some chemical observations on the cuneiform glassmaking texts. *Annales du 5e Congrès de l'Association Internationale pour l'Histoire du Verre*. Liège: Edition du Secrétariat Général, pp. 329-351.

- Brill, R.H. (1999) Chemical analyses of early glasses. Vol.1 catalogue of samples. Corning museum of glass, Corning, 336 pp.
- Brill, R.H. (1999) Chemical analyses of early glasses. Vol.2 tables of analyses. Corning museum of glass, Corning, 554 pp.
- Bruker company web-site, digital source: <https://www.bruker.com/products/x-ray-diffraction-and-elemental-analysis/x-ray-fluorescence/s2-puma/technical-details.html>
- Carter, A.K. (2015) Beads, Exchange Networks and Emerging Complexity: A Case Study from Cambodia and Thailand (500 bce–ce 500). *Cambridge Archaeological Journal*. Vol. 25, issue 4, pp. 733-757.
- Ceglia, A., Nuyts, G., Cagno, S., Meulebroeck, W., Baert, K., Cosyns, P., Nys, K., Thienpont, H., Janssens, K., Terry, H. (2014) A XANES study of chromophores: the case of black glass. *Analytical methods* Vol. 6, 8, pp. 2662 – 2671.
- Chadima, S.A., McCormick, K.A., Schulz, L.D., Haggart, T.N. (2003) X-ray diffraction analysis of post-cretaceous sand and gravel units in southeastern South Dakota. *Akeley-Lawrence Science Center, University of South Dakota, Vermillion*, 17 pp.
- Christodoulou, S. (2016) The History of Ancient Olbia in the Northern Black Sea Region, *Balkan Studies, Thessaloniki* vol. 51 pp. 215-242.
- Claesson, S., Bibikova, E., Shumlyanskyy, L., Dhuime, B., Hawkesworth, C.J. (2014) The oldest crust in the Ukrainian Shield – Eoarchean U–Pb ages and Hf–Nd constraints from enderbites and metasediments. *Geological Society, Special Publications* 389, London, pp. 227-259.
- Clarke, W. (2017) Mass spectrometry in the clinical laboratory: determining the need and avoiding pitfalls. In: *Mass Spectrometry for the Clinical Laboratory*. Ed. by: H. Nair, W. Clarke, Academic Press pp. 1-15.
- Conte, S., Arletti, R., Mermati, F., Gratuze, B. (2016) Unravelling the Iron Age glass trade in southern Italy: the first trace-element analyses. *European Journal of Mineralogy*. Vol. 28, 2, pp. 409 – 433.
- Degryse, P. (ed.) (2014) *Glass making in Greco-Roman world. Results of the ARCHGLASS project*. Leuven university press. Leuven, 190 pp.
- Degryse, P., Schneider, J. (2008) Pliny the Elder and Sr–Nd isotopes: tracing the provenance of raw materials for Roman glass production. *Journal of Archaeological Science* Vol. 35, issue 7, pp.1993-2000.
- Eastaugh, N., Walsh, V., Chaplin, T., Siddall, R. (2008) *Pigment Compendium: A Dictionary and Optical Microscopy of Historical Pigments*. Routledge, 958 pp.
- Eisen, G. (1916) The Characteristics of Eye Beads from the Earliest Times to the Present. *American Journal of Archaeology* Vol. 20, No. 1, pp. 1-27.
- Emami, M., Nekouei, S., Ahmadi, H., Pritzel, C., Trettin, R. (2016) Iridescence in Ancient Glass: A Morphological and Chemical Investigation. *International journal of applied glass science* Vol. 7, issue1, pp. 59-68.

- Esipchuk, K.Y., Sheremet, Y.M., Sveshnikov, K.I. (1993) Rare metal granites and related rocks of the Ukrainian shield. *Bull. Geol. Soc. Finland*. Vol. 65, Part II, pp. 131-141.
- Fellows, P.M., Spears, D.A. (1978) The determination of feldspars in mudrocks using an X-Ray powder diffraction method. *Clays and Clay Minerals*, Vol. 26, 3, pp. 231-236.
- Finch, A.A., Allison N. (2007) Coordination of Sr and Mg in calcite and aragonite. *Mineralogical Magazine*. Vol. 71, 5, pp. 539-552.
- Flemming, R. (2007) Micro X-ray diffraction ( $\mu$ XRD): A versatile technique for characterization of Earth and planetary materials. *Canadian Journal of Earth Sciences*. Vol. 44, 9, pp. 1333-1346.
- Freestone, I.C., Ponting, M., Hughes, M.J. (2002) The origins of Byzantine glass from Maroni Petrera, Cyprus. *Archaeometry*, Vol. 44, 2, pp. 257-272.
- Fricker, M.B., Günther, D. (2016) Instrumentation, Fundamentals, and Application of Laser Ablation-Inductively Coupled Plasma-Mass Spectrometry. In: *Recent Advances in Laser Ablation ICP-MS for Archaeology*. Ed. by Dussubieux, L., Golitko, M., Gratuze B. Natural science in Archaeology. Springer-Verlag, Berlin, Heidelberg, pp.1-19.
- Gagarin, M. (ed.) (2010) *Oxford encyclopaedia of ancient Greece and Rome*. Vol. 1 Oxford University Press, 251-256 pp.
- Gentaz, L., Lombardo, T., Chabas, A., Verney-Carron A. (2012) Impact of neocrystallisations on the SiO<sub>2</sub>-K<sub>2</sub>O-CaO glass degradation due to atmospheric dry depositions. *Atmospheric Environment*. Vol. 55, pp. 459-466.
- Goffer, Z. (2007) *Archaeological chemistry*. 2<sup>nd</sup> edition, John Wiley & Sons, Inc., 654 pp.
- Goldstein, J., Newbury, D.E., Joy, D.C., Lyman, C.E., Echlin, P., Lifshin, E., Sawyer, L., Michael, J.R. (2003) *Scanning Electron Microscopy and X-Ray Microanalysis*. Third Edition Springer Science and Business Media LCC, 709 pp.
- Grad, M., Tripolsky, A.A. (1995) Crustal structure from P and S seismic waves and petrological models of the Ukrainian shield. *Tectonophysics* Vol. 250, issue 1: 89-112.
- Graham, A. J. (1999) *Colony and the mother city in ancient Greece*. Special edition for Sandpiper Books Ltd. Manchester university press, 259 pp.
- Graham, A.J., (ed.) *Collected papers on Greek Colonization*. (2001) Brill, Leiden, Boston, 414 pp.
- Greaves A. (2010) Milesians in the Black Sea: Trade, Settlement and Religion. *Black Sea Studies*. Vol. 6, pp. 9-22.
- Heck, M., Rehren, T., Hoffmann, P. (2003) The production of lead-tin yellow at Merovingian Schleithem (Switzerland). *Archaeometry*. Vol. 45, 1, pp. 33-44.
- Henderson, J. (1985) The raw materials of early glass production. *Oxford Journal of Archaeology*. Vol. 4, issue 3, pp. 267-291.
- Henderson, J. (2013) *Ancient Glass: An Interdisciplinary Exploration*, Cambridge University Press, 433 pp.
- Herodotus, *The Histories* (1920) with an English translation by A. D. Godley. Cambridge. Harvard University Press. – digital version.

- Hikichi, Y., Nomura, T. (1987) Melting Temperatures of Monazite and Xenotime. *Journal of the American ceramic society*. Vol. 70, issue 10, pp. 252-253.
- Jackson, C.M. (2005) Making colourless glass in the roman period. *Archaeometry* 47, 4, pp. 763–780.
- Janssens, K. (ed.) (2013) *Modern methods for analyzing archaeological and historical glass*. Vol. 1. John Wiley and Sons, Ltd., 711 pp.
- Kalliopi, N., Henderson, J. (2006) Glass Analyses from Mycenaean Thebes and Elateia: Compositional Evidence for a Mycenaean Glass Industry, *Journal of Glass Studies* 48, pp. 71-120.
- Karlsson, S., Bäck, L.G., Kidkhunthod, P., Lundstedt, K., Wondraczek, L. (2016) Effect of TiO<sub>2</sub> on optical properties of glasses in the soda-lime-silicate system. *Optical Materials Express*. Vol. 6, issue 4, pp. 1198-1216.
- King, C.A.M. (1951) Depth of disturbance of sand on sea beaches by waves. *Journal of Sedimentary Petrology*, Vol. 21, issue 3, pp. 131-140.
- Koleini, F., Prinsloo, L. C., Biemond, W. M., Colomban, P., Ngo, A. T., Boeyens, J. C. A. & van der Ryst, M. M. (2015) Towards refining the classification of glass trade beads imported into Southern Africa from the 8th to the 16th century AD. *Journal of Cultural Heritage*, Vol. 19, pp. 435-444.
- Korotaev, G., Saenko, O.A., Koblinsky, C.J. (2001) Satellite altimetry observations of the Black Sea level. *Journal of Geophysical Research Atmospheres* 106, C1, pp. 917-934.
- Kulp, J.L., Turekian, K., Boyd, D.W. (1952) Strontium content of limestone and fossils. *July Geological Society of America Bulletin*. Vol. 63, 7, pp. 701-716.
- Lei, Y., Xia, Y. (2015) Study on production techniques and provenance of faience beads excavated in China. *Journal of Archaeological Science* Vol. 53, pp.32-42.
- Li, Q., Henderson, J. (2016) *Recent Advances in the Scientific Research on Ancient Glass and Glaze*. World Scientific, 572 pp.
- Lierke, R., (2018) web-site. Digital source: <http://www.rosemarie-lierke.de/English/english.html>
- Linge, K.L., Jarvis, K. (2009) Quadrupole ICP-MS: Introduction to Instrumentation, Measurement Techniques and Analytical Capabilities. *Geostandards and Geoanalytical Research* 33, 4, pp. 445-467.
- Linnik, P.M., Zubenko I.B. (2000) Role of bottom sediments in the secondary pollution of aquatic environments by heavy-metal compounds. *Lakes and reservoirs*. Vol. 5, Issue1, pp. 11-21.
- Louër, D. (1999) Powder X-Ray Diffraction, Applications. In: *Encyclopedia of Spectroscopy and Spectrometry*. Ed by: J.C. Lindon. Academic Press. pp.1865-1875.
- Marcano, M.C., Frank, T.D., Mukasa, S.B., Lohmann, K.C., Taviani, M. (2015) Diagenetic incorporation of Sr into aragonitic bivalve shells: implications for chronostratigraphic and palaeoenvironmental interpretations. *The depositional record*. Vol. 1, issue1, pp. 38-52.

- Margvelashvily, N., Maderich, V., Zheleznyak, M. (1999) Simulation of radionuclide fluxes from the Dnieper-Bug Estuary into the Black Sea. *Journal of Environmental Radioactivity*. Vol. 43, Issue 2, pp. 157-171.
- Matoshko, A.V., Gozhik, P.F. Ivchenko, A.S. (2002) The fluvial archive of the Middle and Lower Dnieper (a review). *Netherlands Journal of Geosciences*. Vol. 8, issue 13-4, pp. 339-355.
- McComb, J. Q., Rogers, C., Han, F.X., Tchounwou P.B. (2014) Rapid screening of heavy metals and trace elements in environmental samples using portable X-ray fluorescence spectrometer, A comparative study. *Water Air Soil Pollut*. Vol. 225, issue 12, 2169.
- McReynolds, T.E., Skaggs, S. A., Schroeder, P.A (2008) Feldspar and Clay Mineralogy. In: *Woodland Pottery Sourcing in the Carolina Sandhills*. Ed. by: J.M. Herbert T.E. McReynolds. Research Report 29. Research Laboratories of Archaeology, University of North Carolina, Chapel Hill, pp. 108-121.
- Möncke, D., Papageorgiou, M., Winterstein-Beckmann, A., Zacharias, N. (2014) Roman glasses coloured by dissolved transition metal ions: redox reactions, optical spectroscopy and ligand field theory. *Journal of Archaeological Science*. Vol. 46, pp. 23-36.
- Morris, H. C. (1900) *The history of colonization. From the ancient times to the present day*. The Macmillan company, New York, London, Vol.1 465 pp.
- Neri, E., Morvan, C., Colomban, P., Guerra, M.F., Prigent, V. (2016) Late Roman and Byzantine mosaic opaque “glass-ceramics” tesserae (5th-9th century). *Ceramics International*. Vol. 42, issue 16, pp. 18859-18869.
- Nesterov, A.A., Maderich, V.S., (2008) Modeling of hydrodynamics and transport processes in the Dnieper–Bug estuary. *Physical Oceanography*, Vol. 18, 6. pp. 345-356. Translated from *Morskoi Gidrofizicheskii Zhurnal*, No. 6, pp. 66–77.
- Noonan T. S. (1973) *The Grain Trade of the Northern Black Sea in Antiquity*. *The American Journal of Philology* Vol. 94, No. 3 pp. 231-242.
- Nothnagle, P.E., Chambers, W., Davidson, M.W. (2018) *Introduction to Stereomicroscopy digital source*.
- Novodran, V.S., Goloshchapova A.I., Nasad, A.G., Nasad, N.P., (1988) *State Geological Map of Ukraine in the scale 1:200 000, map sheets L-36-XIV (Ochakiv) L-36-XV (Kherson)* Ministry of Ecology and Natural Resources of Ukraine, digital version.
- O’Hea, M. (2005) *Greeks And Glass: The Role Of Hellenistic Greek Settlements In The Eastern Mediterranean In Glass Production And Consumption*. *Proceedings of the 25th anniversary symposium of the Australian archaeological institute at Athens*. *Mediterranean Archaeology* Vol. 19/20, pp. 141-150.
- Oikonomou, A., Beltsios, K., Zacharias, N., Triantafyllidis, P. (2012) Technological and provenance study of archaic glassy materials from Rhodes island. *Proceedings of the 39th International Symposium for Archaeometry, Leuven*, pp. 245-250.
- Oikonomou, A., Triantafyllidis, P. (2018) An archaeometric study of Archaic glass from Rhodes, Greece: Technological and provenance issues. *Journal of Archaeological Science: Reports*. In Press.

- Oppenheim A. L. (1973) Towards a History of Glass in the Ancient Near East. *Journal of the American Oriental Society* Vol. 93, issue: 3, pp. 259-266.
- Pecharsky, V., Zavalij, P. (2009) *Fundamentals of Powder Diffraction and Structural Characterization of Materials*, Second Edition, Springer, 744 pp.
- Petit-Domínguez, M. D., Giménez, R. G., de Soto, I. S., Rucandio, I. (2014) Chemical and statistical analysis of roman glass from several northwestern Iberian archaeological sites. *Mediterranean Archaeology and Archaeometry*, Vol. 14, 2, pp. 221-235.
- Pettijohn, F.J., Potter, P.E., Siever, R. (1987) *Sand and Sandstone*. Second edition. Springer Science & Business Media, 553 pp.
- Piper, D.Z. (1974) Rare earth elements in the sedimentary cycle: a summary. *Chem. Geol.* Vol. 14, pp. 285-304.
- Pliny the Elder, *The Natural History*. (1855) Translated and commented by J. Bostock, M.D., F.R.S. H.T. Riley, Esq., B.A. London. Taylor and Francis, Red Lion Court, Fleet Street. – digital version.
- Polikreti, K., Murphy, J.M.A., Kantarelou, V., Karydas, A. G. (2011) XRF analysis of glass beads from the Mycenaean palace of Nestor at Pylos, Peloponnesus, Greece: new insight into the LBA glass trade. *Journal of Archaeological Science* Vol. 38, Issue 11, pp. 2889-2896.
- Pollard, A.M., Heron C. (2008) *Archaeological chemistry 2<sup>nd</sup> edition*, The Royal Society of Chemistry 443 pp.
- Qin, Y., Wang, Y., Chen, X., Li, X. (2016) The research of burning ancient Chinese lead-barium glass by using mineral raw materials. *Journal of Cultural Heritage* 21, pp. 796-801.
- Ramachandran, V. S. Beaudoin, J. J. (2001) *Handbook of Analytical Techniques in Concrete Science and Technology: Principles, Techniques, and Applications*. Noyes Publications, 964 pp.
- Rehren, T., Freestone, I.C. (2015) Ancient glass: from kaleidoscope to crystal ball. *Journal of Archaeological Science*. Vol. 56, pp. 233-241.
- Rehren, T., Pusch, E.B. (2005) Late Bronze Age Glass Production at Qantir-Piramesses, Egypt. *Science* 308, pp. 1756-1758.
- Roberts, J. (2007) *Oxford dictionary of classical world*. Oxford University press, 858 pp.
- Robinson, A., Spadini, G., Cloetingh, S., Rudat, J. (1995) Stratigraphic evolution of the Black Sea: inferences from basin modelling. *Marine and Petroleum Geology*. Vol. 12, Issue 8, pp. 821-835.
- Ross, D.A., Stoffers, P., Trimonis, E.S. (1978) Black sea sedimentary framework. *Deep Sea Drilling Project. Initial Reports* Vol. 42, part 3, pp. 359-372.
- Salminen, R., (ed.) (1998) *FOREGS Geochemical Atlas of Europe*, chief-editor digital source.
- Salminen, R., Tarvainen, T., Demetriades, A. et al. (1998) *Foregs Geochemical Mapping Field Manual*, Geological Survey Of Finland. Guide 47, Espoo, 42 pp.
- Schnitzler, H., Zimmer, K.P. (2008) Advances in stereomicroscopy. *Proc. SPIE* Vol. 7100: *Optical Design and Engineering*, 12 pp.

- Schuiling, R.D. Feenstra, A. (1980) Geochemical behaviour of vanadium in iron—titanium oxides. *Chemical Geology*. Vol. 30, issues 1–2, pp. 143-150.
- Shcherbak N.P., Bartnitsky E.N., Bibikova E.V., Boiko V.L. (1984) Age and Evolution of the Early Precambrian Continental Crust of the Ukrainian Shield. In: Kröner A., Hanson G.N., Goodwin A.M. (eds) *Archaean Geochemistry*. Springer, Berlin, Heidelberg. pp. 251-261.
- Shelton, L.R., Capel, P.D. (1994) Guidelines for Collecting and Processing Samples of Stream Bed Sediment for Analysis of Trace Elements and Organic Contaminants for the National Water-Quality Assessment Program, U.S. Geological Survey Open-File Report 94-458, Sacramento, digital source.
- Shields-Zhou, G.A. (1998) Stratigraphic Trends in Cerium Anomaly in Authigenic Marine Carbonates and Phosphates: Diagenetic Alteration or Seawater Signals? *Mineralogical Magazine*. Vol. 62, 3, pp. 1387-1388.
- Shields-Zhou, G.A., Stille, P. (2001) Diagenetic constraints on the use of cerium anomalies as palaeoseawater redox proxies: An isotopic and REE study of Cambrian phosphorites. *Chemical Geology*. Vol. 175, 1-2, pp. 29-48.
- Shortland, A., Rogers, N., Eremin, K. (2007) Trace element discriminants between Egyptian and Mesopotamian Late Bronze Age glasses. *Journal of Archaeological Science*. Vol. 34, issue 5, pp. 781-789.
- Shugar, A., Rehren, T. (2002) Formation and composition of glass as a function of firing temperature. *Glass Technology*. Proc. XIX Int. Congr. Glass, Edinburgh, pp. 145–150.
- Silvestri, A., Molin, G., Pomeroy, V. (2011) The stained glass window of the southern transept of St. Anthony's Basilica (Padova, Italy): study of glasses and grisaille paint layers. *Spectrochimica Acta Part B: Atomic Spectroscopy*. Vol. 66, issue 1, pp. 81-87.
- Smirniou, M., Gratuze, B., Asderaki, E., Nikolaou E. (2018) Chemical compositional analysis of glass from the north cemetery of ancient Demetrias (Thessaly). *Journal of Archaeological Science: Reports*. In Press.
- Smirniou, M., Rehren, T. (2013) Shades of blue – cobalt-copper coloured blue glass from New Kingdom Egypt and the Mycenaean world: a matter of production or colourant source? *Journal of Archaeological Science*. Vol. 40, issue 12, pp. 4731-4743.
- Smit, Z., Janssens, K., Bulska, E., Wagner, B., Kos, M., Lazar, I. (2005) Trace element fingerprinting of facon-de-Venise glass. *Nuclear Instruments and Methods in Physics Research*. Vol. 239, 1-2, pp. 94-99.
- Smodiš, B., Annareddy, V.R.R., Rossbach, M. (2003) Collection and preparation of bottom sediment samples for analysis of radionuclides and trace elements. International Atomic Energy Agency, Vienna, 130 pp.
- Solovev, S. (1999) *Ancient Berezan: The Architecture, History and Culture of the First Greek Colony in the Northern Black Sea*. Brill, Leiden, 148 pp.
- Starostenko, V., Gintov, O., Kutas R., Pashkevich, I (2010) Geodynamics of lithosphere as one of the crucial factors of mineral deposits formation of Ukraine. *Геофизический журнал*. Vol. 32, issue 4, 162-165 pp.

- Stern, E.M. (1999) Ancient Glass In Athenian Temple Treasures. *Journal of Glass Studies* Vol. 41, pp. 19-50.
- Stern, M.E. (2007) Ancient Glass in a Philological Context. *Mnemosyne Fourth Series*, Vol. 60, issue 3, pp. 341-406.
- Sushkova, S. G., Didenko, E. A. (1984) Complete chemical analysis of sand with a SiO<sub>2</sub> concentration of less than 95%. *Glass and Ceramics*. Vol. 41, issue 7, pp. 313–315.
- Švecová B., Vařák P., Vytykáčová S., Nekvindová P., Macková A., Malinský P., Böttger R. (2017) A study of the behaviour of copper in different types of silicate glasses implanted with Cu<sup>+</sup> and O<sup>+</sup> ions. *Nuclear Instruments and Methods in Physics Research, Section B: Beam Interactions with Materials and Atoms*. Vol. 406, pp. 193-198.
- Swann, C.P., McGovern, P.E., Fleming, S.J. (1990) Colorants used in ancient Egyptian glassmaking: Specialized studies using PIXE spectrometry. *Nuclear Instruments and Methods in Physics Research Section B: Beam Interactions with Materials and Atoms*. Vol. 45, issues 1–4, pp. 311-314.
- Thybo, H., et al. (2003) Upper lithospheric seismic velocity structure across the Pripyat Trough and the Ukrainian Shield along the EUROBRIDGE'97 profile. *Tectonophysics*, 371, pp. 41-79.
- Tite, M.S., Shortland, A., Maniatis, Y., Kavoussanaki, D., Harris, S.A. (2006) The composition of the soda-rich and mixed alkali plant ashes used in the production of glass. *Journal of Archaeological Science*. Vol. 33, pp. 1284-1292.
- Towle, A., Henderson, J. (2007) The Glass Bead Game: Archaeometric evidence for the existence of an Etruscan glass industry. *Etruscan Studies*: Vol. 10, pp. 47-66.
- Trail, D., Watson, E.B., Tailby, N.D. (2012) Ce and Eu anomalies in zircon as proxies for the oxidation state of magmas. *Geochimica et Cosmochimica Acta*. Vol. 97, 15, pp. 70-87.
- Tsetskhladze, G. (ed.) (1998) The Greek colonisation of the Black sea area (*Historia – Einzelschriften*) Franz Steiner Verlag, 336 pp.
- Turmanidze, M. (2005) Beads from the Fifth-Century BC Greek Necropolis of Pichvnari. *Collection de l'Institut des Sciences et Techniques de l'Antiquité Année 2005* 979 pp. 283-292.
- Warren, B. E. (1990) X-ray Diffraction. Courier Corporation, 381 pp.
- White M. E. (1961) Greek Colonization. *The Journal of Economic History* Vol. 21, No. 4: 443-454 pp.
- Whitehouse, M.J., Kamber, B.S. (2002) On the overabundance of light rare earth elements in terrestrial zircons and its implication for Earth's earliest magmatic differentiation. *Earth and Planetary Science Letters*. Vol. 204, issues 3–4, pp. 333-346.
- Wood, M. (2011) A Glass Bead Sequence for Southern Africa from the 8 Th to the 16 Th Century AD *Journal of African Archaeology* Vol. 9, 1, pp. 67-84.
- Wright, L.D. (1977) Sediment transport and deposition at river mouths: A synthesis. *GSA Bulletin* 88, issue 6, pp. 857-868.

- Алексеева, Е.М. (1975) Античные бусы Северного Причерноморья. Археология СССР. Свод археологических источников. Ред. Б.А. Рыбаков. Наука, Москва, Т. Г1-12, 120 сс.
- Алексеева, Е.М. (1978) Античные бусы Северного Причерноморья. Археология СССР. Свод археологических источников. Том 2. Ред. Б.А. Рыбаков. Наука, Москва, Т. Г1-12, 122 сс.
- Антонюк, О.С. (2013) Основні особливості коливання рівня чорного моря за історичний час. Ужгородський національний університет. Говерла, Ужгород, 6 сс.
- Безусько, Л.Г., Безусько, А.Г. (2000) До питання про поширення лісів у нижньому подніпров'ї у пізньому голоцені : (за палінологічними даними). Наукові записки НаУКАМА. Том 18, сс. 4-11.
- Білецький, В.С., (ред.) (2004) Мала гірнича енциклопедія. Донбас, Донецьк, Т.1, 640 сс.
- Білецький, В.С., (ред.) (2007) Мала гірнича енциклопедія. Донбас, Донецьк, Т.2, 652 сс.
- Білецький, В.С., (ред.) (2013) Мала гірнича енциклопедія. Донбас, Донецьк, Т.3, 644 сс.
- Буйских, С.Б., Островерхов А.С. (1978) Работы на Ягорлыцком поселении. Археологические открытия 1977 года. Наука, Москва, 304 с.
- Виноградов, Ю. А., Фоняков, Д. И. (2000) Коллекция металлических предметов с Ягорлыцкого поселения. Археологические Вести № 7, сс. 96-105.
- Водно-болотні угіддя України. Довідник (2006) ред. Г.Б. Марушевський, І.С. Жарук. Чорноморська програма Ветландс Інтернешнл, Київ, 312 сс.
- Гаврилюк Н.О. (2008) Торгівля між греками та скіфами у VI—IV ст. до н.е. Надчорномор'я: студії з історії та археології (з IX ст. до н.е. по XIX ст. н.е.). Інститут історії України НАН України, Вип. 1, сс. 60-70.
- Гайдукевич, В.Ф. (1955) История античных городов Северного Причерноморья. Античные города Северного Причерноморья. Античные города Северного Причерноморья (ред. Гайдукевич В.Ф., Максимова М.И.) Издательство Академии Наук СССР, Москва, Ленинград, Т.1: 23-147 сс.
- Галибин, В.А. (2001) Состав стекла как археологический источник, Институт истории материальной культуры Российской Академии Наук, Санкт-Петербург, 212 сс.
- Гречко, Д. С. (2010). Курганы конца VI—середины V вв. до н. э. Нижнего Побужья: греки или скифы? Древности. Харьковский историко-археологический ежегодник. ООО «НТМТ», Харьков, 9, сс.116-135.
- Давидов О.В. (1999) Фізико-географічні особливості берегів з вітровою присухою на Чорному морі Вісник Одеського Національного університету, Географічні та геологічні науки, Том 4, випуск 5, сс. 76 – 80.
- Дараган, М. Н. (2010) О датировке амфоры аз погребения № 2 Репяховой Могилы Античный мир и археология, Саратов, Вып. 14. С. 175—202.
- Загний, Г.Ф., Островерхов, А.С., Черняков, Т.И., (1977) Исследования у Ягорлыцкого залива. Археологические открытия 1976 года. Наука, Москва, 294 с.

- Зограф А. Н. (1955) Денежное обращение и монетное дело Северного Причерноморья. Античные города Северного Причерноморья (ред. Гайдукевич В.Ф., Максимова М.И.) Издательство Академии Наук СССР, Москва, Ленинград, Т.1: сс. 148-164.
- Иессен А.А. (1947) Греческая колонизация Северного Причерноморья ее предпосылки и особенности. Государственный Эрмитаж, Ленинград, 93 сс.
- Карышковский, П.О. (1988) Монеты Ольвии. Очерк денежного обращения Северо-Западного Причерноморья в античную эпоху.: Наукова думка, Киев, 168 сс.
- Козленко М.В. (2015) Скорости осадконакопления как индикатор тектонических процессов в пределах северо-западного шельфа черного моря. Геология и полезные ископаемые мирового океана, № 4, 42, сс. 70-85.
- Коніков Є.Г. (2004) Екзогеодинамічна модель умов осадконакопичення і формування берегових геосистем північно-західної частини Чорного моря протягом останніх 18000 років. Вісник Одеського національного університету. Том 9, 4: Географічні та геологічні науки. сс.161-179.
- Крижицкий, С.Д. (ред.) Археология украинской ССР (1985) Наукова думка, Киев, Т.2: 592 сс.
- Крижицький С.Д. (2010) Ольвія. Енциклопедія історії України: Ред. В. А. Смолій Інститут історії України. Наукова думка, Київ, Т. 7: 728 с.
- Крижицький, С.Д., Буйських С.Б., Бураков А.В., Отрешко В.М. (1989) Сельская округа Ольвии. Институт Археологии АН УССР, Наукова думка, Киев, 242 сс.
- Лاپин, В.В. (1966). Греческая колонизация Северного Причерноморья. Наукова думка, Киев, 241 сс.
- Латышев, В.В. (1906) Жития св. епископов Херсонских : Исследование и тексты : тип. Имп. акад. наук, 1906 Петербург, 81 с.
- Марченко, К. К. (1980) Модель греческой колонизации Нижнего Побужья. Вестник Древней Истории. № 1. сс. 131–143.
- Махортих, С., Тупчієнко, І. (2011) Скіфські кургани біля села Молдовки на Кіровоградщині. Записки Наукового товариства ім. Т.Г. Шевченка Том 235 (ССXXXV). Праці Археологічної комісії. Ред. М. Бандрівський сс.487-503.
- Миничева, Г.Г., Соколов, Е.В., Швець, А.В. (2016) Оценка природно-антропогенного статуса прибрежно-аквального комплекса Ягорлыцкого залива. Наукові записки Тернопільського національного педагогічного університету імені Володимира Гнатюка. Серія: Біологія. № 3-4, сс. 74-84.
- Назаров, В.В. (2003) Березанське поселення. Енциклопедія історії України. Ред. В. А. Смолій. Інститут історії України. Наукова думка, Київ, Т. 1: 688 с.
- Одрін, О. (2010) Ключові проблеми сучасного стану дослідження скіфо-грецьких торгівельних відносин: до постановки питання. Елліністичні студії : Зб. спогадів та наук. пр. пам'яті Наталії Олексіївни Терентьевої. Ред. О.П. Реєнт. Інститут історії України НАН України, сс. 286-298.

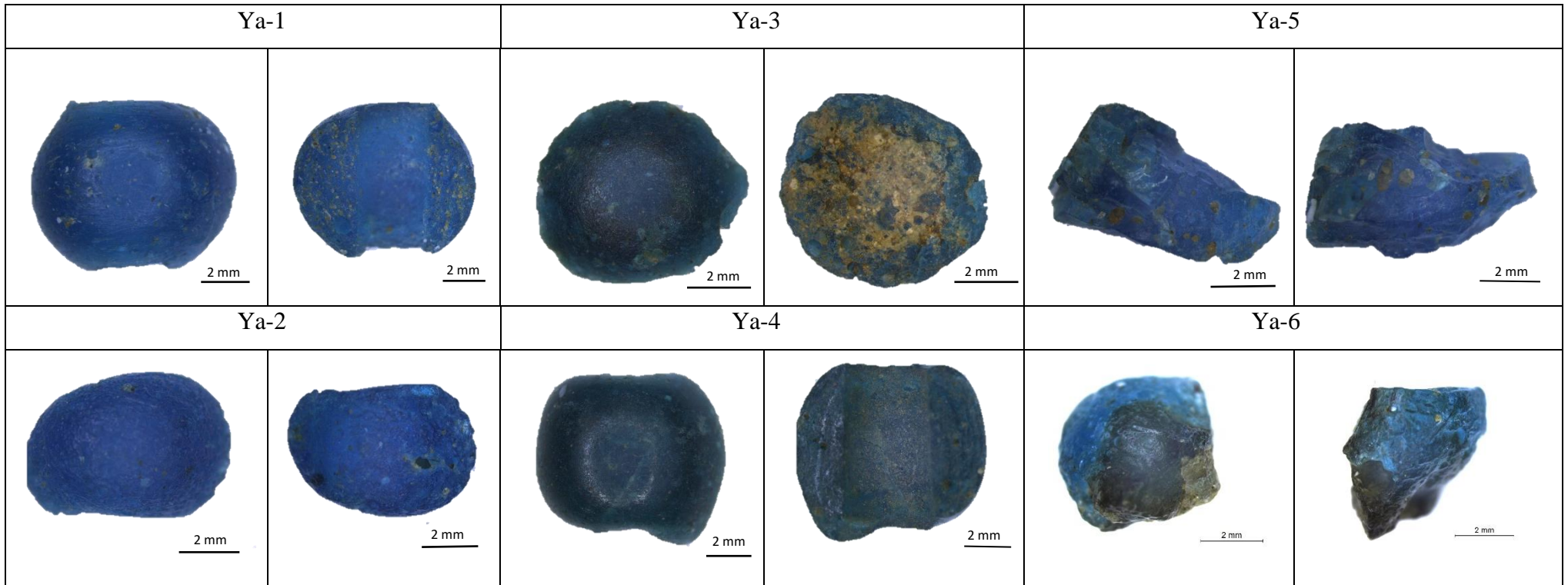
- Одрін, О.В. (2008) Ольвійське рибальство VI–III ст. до н.е. з Надчорномор'я у IX ст. до н.е. – на початку XIX ст.: студії з історії та археології. Ред. Н.А. Ярको. Інститут історії України НАНУ, Київ, сс. 71-89.
- Оленковский, Н.П. (2013) Семь исторических чудес Херсонщины. Херсон, 54 сс.
- Ольговський, С. Я. (2012) Виїзний промисел скіфських ливарників. Сіверщина в історії України. № 5, сс. 52-55.
- Остапуха, С.В. (2010) Сучасний санітарний стан соснових насаджень на нижньодніпровських пісках. Науковий вісник НЛТУ України. Том 20, 13, сс. 58-61.
- Островерхов А.С. (1978) Про чорну металургію на Ягорлицькому поселенні. Археологія, 28, сс. 25-36.
- Островерхов, А.С. (1974) Ягорлицькое поселение. Археологические открытия 1973 года. Наука, Москва, 323 сс.
- Островерхов, А.С. (1978) Антична склоробна майстерня на Ягорлицькому поселенні. Археологія 1978, 25, Наукова думка, Київ 49-58 сс.
- Островерхов, А.С. (1981) Древнейшее античное производство стеклянных бус в Северном Причерноморье. Советская археология, 1981, 4: 214-228 pp.
- Петренко, В. Г. (1978) Украшения Скифии VII-III вв. до н. э. Археология СССР. Свод археологических источников. Ред. Б.А. Рыбаков. Наука, Москва, 144 сс.
- Погребняк, П.С. (1953) Нижнеднепровские пески и проблема их освоения. Природа 8, сс 56-61.
- Рубан, В.В. (1983) Керамика Ягорлицького поселення из собрания Херсонского музея. Советская археология. Наука, Москва 1983, 1, сс. 285-290.
- Сплодитель, А.О. (2017) Ландшафтознавче обґрунтування оптимізації діяльності національних природних парків України (на прикладі національних природних парків «Нижньосульський» та «Олешківські піски»). Дисертація. Інститут географії Національної Академія Наук України. Київ, 495 сс.
- Федорончук, Н.О., Сучков, І.О., Мудров, І.О., Гончарова І.О. (2013) Літолого-фаціальні та мінералогічні передумови накопичення тонкого золота у Новоевксинських відкладах Дніпровського жолоба (північно західний шельф Чорного моря). Геология и полезные ископаемые мирового океана 2, 32, сс. 64-75.
- Фиалко, Е. Е. (2010) Погребения амазонок из могильника Мамай-Гора. Stratum plus. №3 сс. 188-196.
- Хлебников, А.Н. (1988) Детальная разведка Шабовского месторождения песков для силикатного кирпича в Голопристанском районе Херсонской обл. УССР, 1986-1987 гг. 50540 - номер зберігання в геоінформ. України. – digital source.
- Чекунов, А.В., Веселов, А.А., Гилькман, А.И. (1976) Геологическое строение и история развития Причерноморского прогиба. Наукова думка, Киев, 165 сс.

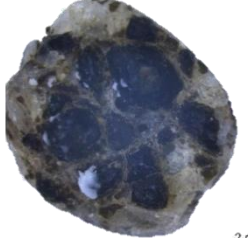
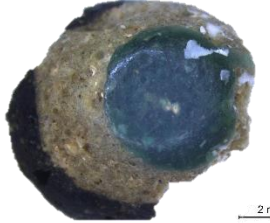
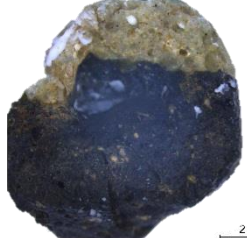
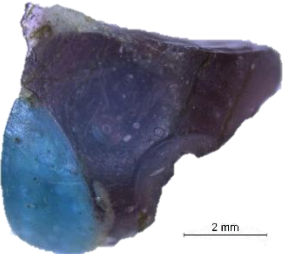
- Чешижко, А.В., Сучков И.А. et al. (2007) Услови́я осадконакоплення в районі Дніпро-Бугського лимана Ягорлыцького за́лива и подводного склону за́падно́й части́ Кинбу́рнско́й ко́сы в голо́цене. Ві́сник Оде́ського націо́нального універсі́тету. Сері́я: Географі́чні та геологі́чні нау́ки. Том 12, 8, сс. 244–251.
- Шуйський, Ю. Д., Вихованець Г.В., Муркалов, О.Б. (2005) Сучасна динаміка берегів о. Зміїний та її вплив на навколишню акваторію чорного моря. Ві́сник Оде́ського націо́нального універсі́тету. Том 10, 4, сс. 108 -122.
- Янко-Хомбах, В.В., Смынтына, Е.В., Каду́рин, С.В., Ларченков, Е.П., Мотненко, И.В., Какаранза, С.В., Киосак Д.В., (2011) Ко́лебания́ у́ровня́ чорного́ моря́ и адаптаціо́нная стратегі́я дре́внего́ чело́века́ за́ последние́ 30 ты́сяч ле́т. Геоло́гия и по́лезные і́скопае́мые мі́рового́ океа́на 2, сс. 61-94.
- Яценко, Г., Кирьянов, М., Калашник, Г., Гайовський, О., Сливко, Є., Яценко, І., Соломатіна, Л. (2009) Мінералогі́чні особливості́ рудоно́сних порі́д чо́хла Кі́ровоградського́ бло́ка Украї́нського́ щита́ на при́кладі́ териге́нно-глинисто́ї алмазоно́сної́ формаці́ї. Мінералогі́чний збі́рник, 59, вип. 1, сс. 144-159.

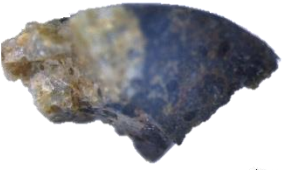
## ANNEXES

Annex 1.

1. Stereomicroscope images of glass samples. Every sample is represented by two photographs face surfaces of beads are always on the left and section surfaces are always on the right. For non-beads two opposite surfaces are depicted. (All the scale bars are 2 mm (Ya-16 – 1 mm)).



Ya-7		Ya-8		Ya-9	
					
Ya-10		Ya-11		Ya-12	
					
Ya-13		Ya-14		Ya-15	
					

Ya-16		Ya-17		Ya-18	
 1 mm	 1 mm	 2 mm	 2 mm	 2 mm	 2 mm
Ya-19		Ya-20		Ya-21	
 2 mm	 2 mm	 2 mm	 2 mm	 2 mm	 2 mm
Ya-22		Ya-23			
 2 mm	 2 mm	 2 mm	 2 mm		

Annex 2.  
Selected BSE images.

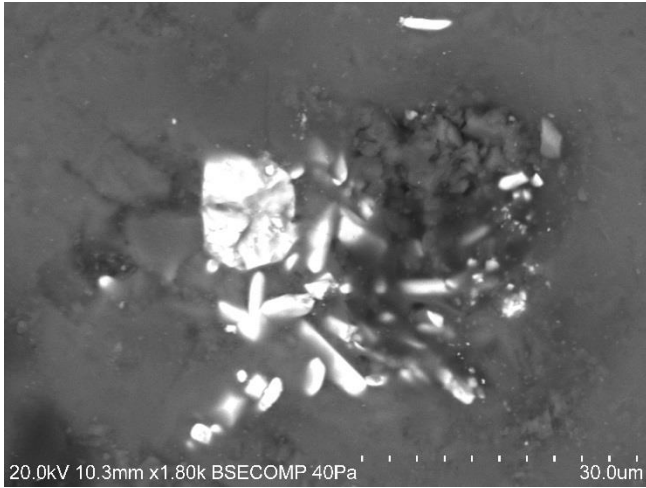


*Image 1. Ya-3 point 1 inclusion of tin.*

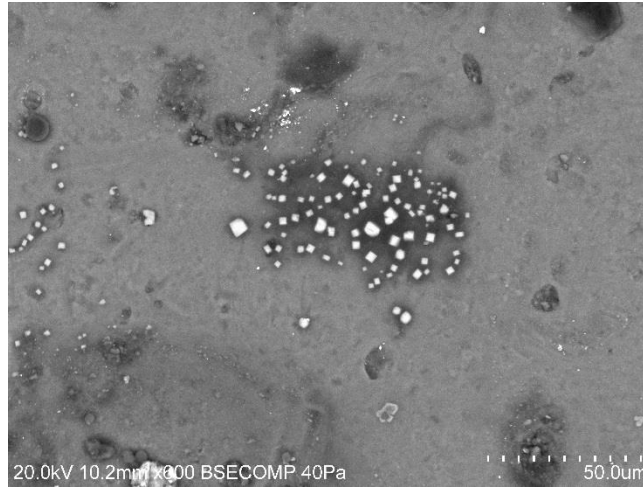


*Image 2. Ya-5 point 3 surface deposition of sylvite.*

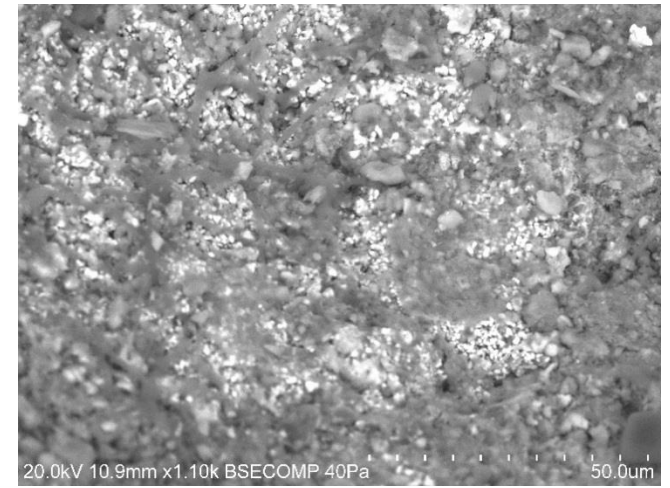


*Image 3. Ya-7 light layer; high content of Fe and Ca.*

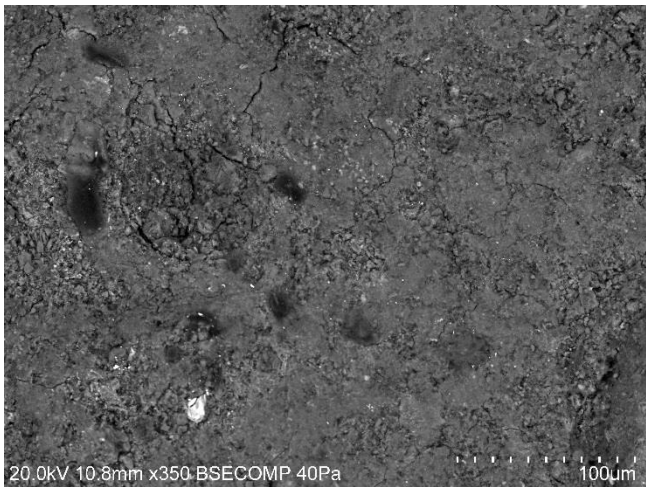


*Image 4 Ya-7 light layer; area 1.*

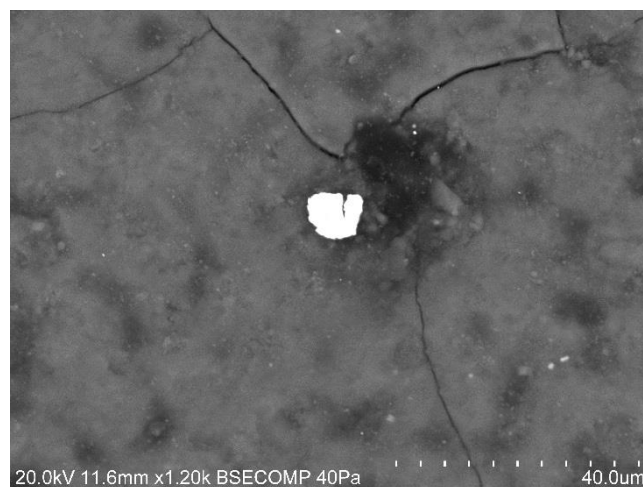


*Image 5. Ya-9 Acanthite superficial deposition.*

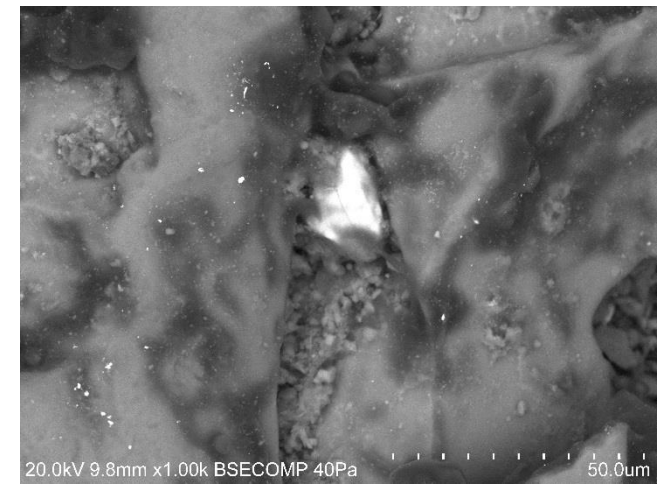


*Image 6. Ya-7 grain of zircon and superficial deposits in the crack of matrix.*

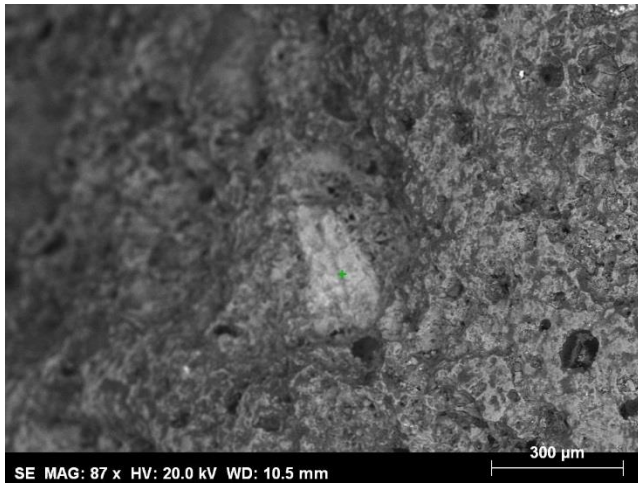


*Image 7. Ya-13 apatite inclusion.*

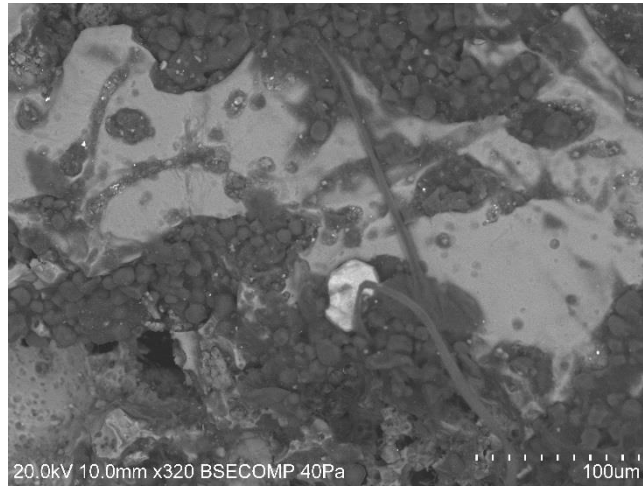


*Image 8. Ya-13 ilmenite and light elements superficial depositions.*

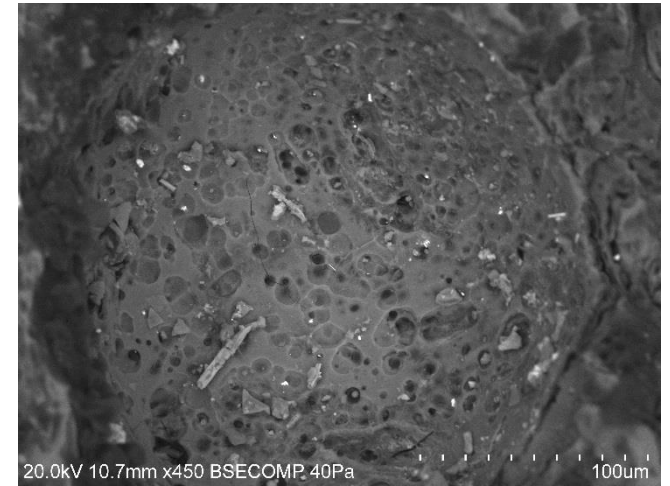


*Image 9. Ya-15 collapsed bubble with multiple depositions (Pb, Sn, Fe, Mn).*

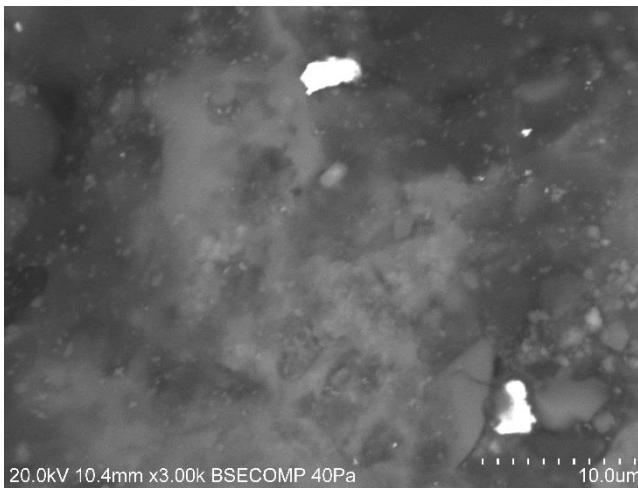


*Image 10. Ya-17 superficial depositions of pure gold (up) and silver (bottom).*

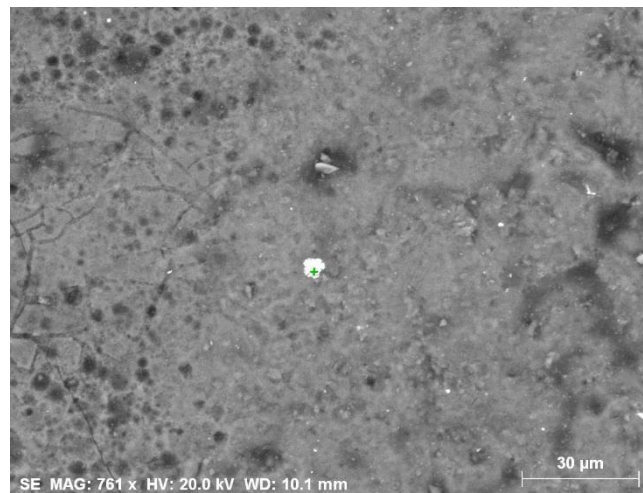


*Image 11. Ya-15 monazite inclusion.*

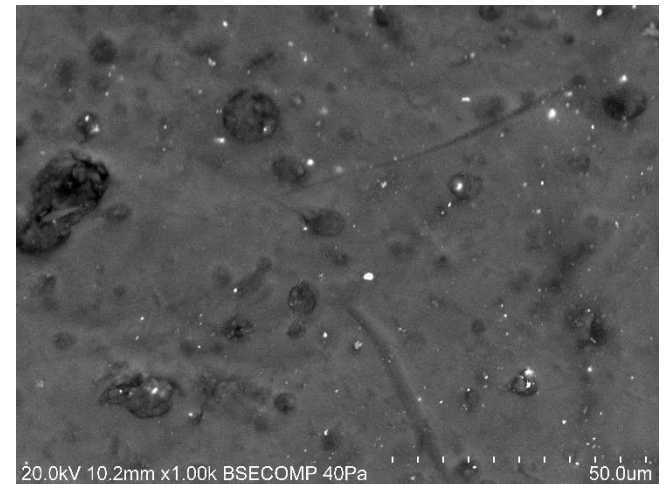


*Image 12. Ya-10 multiple inclusions of tin.*

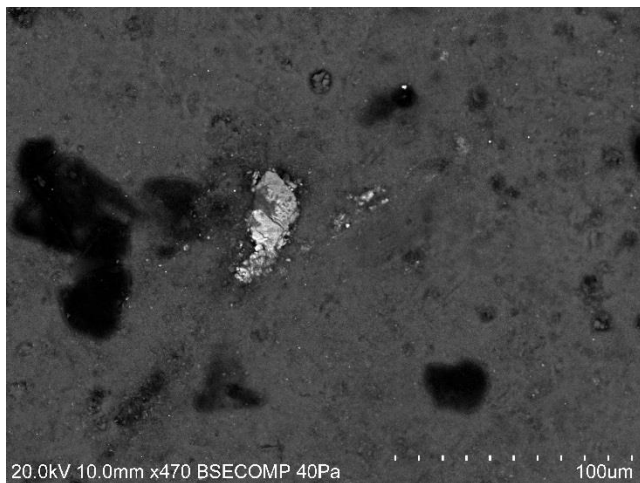


*Image 13. Ya-14 blue part; barite inclusion.*

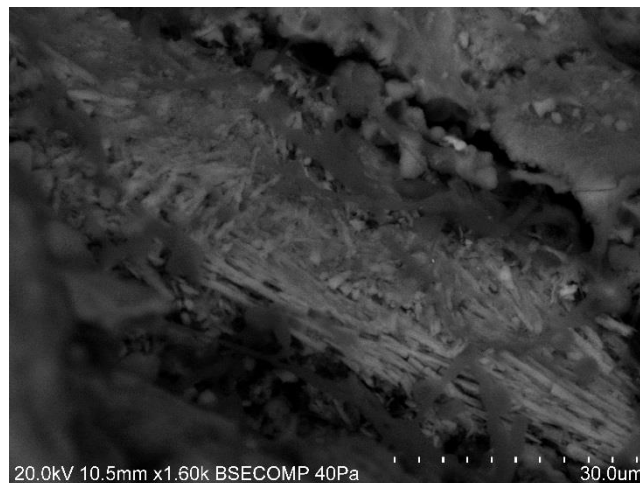


*Image 14. Ya-16 apatite; possibly a superficial deposit.*

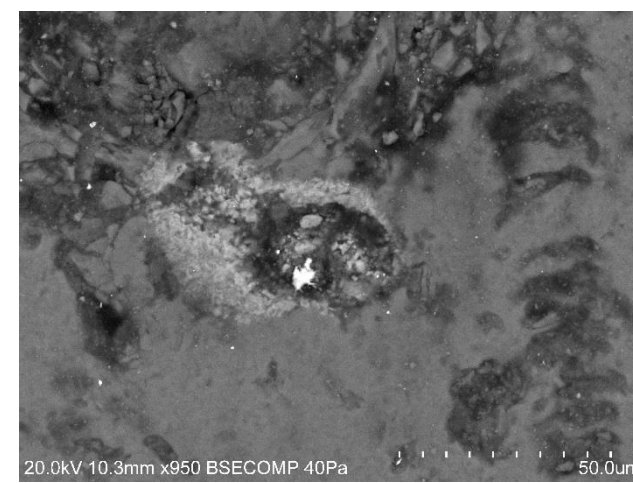


*Image 15. Ya-17 Vitreous side; titanium inclusion with some Nb impurities.*

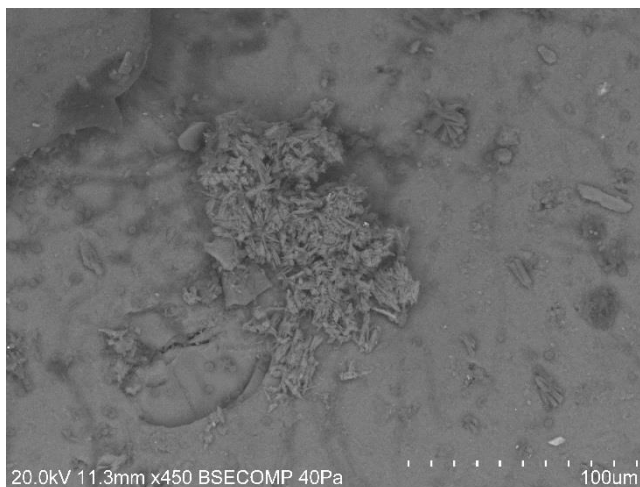


*Image 16. Ya-8 superficial deposits of mirabilite or thenardite.*

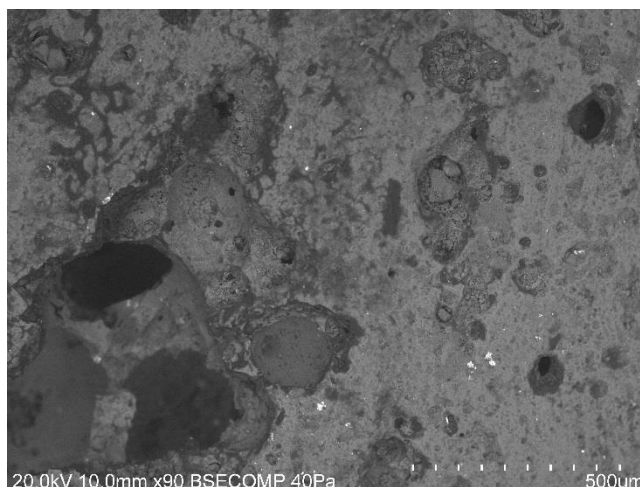


*Image 17. Ya-12 inclusions of tin in the matrix.*

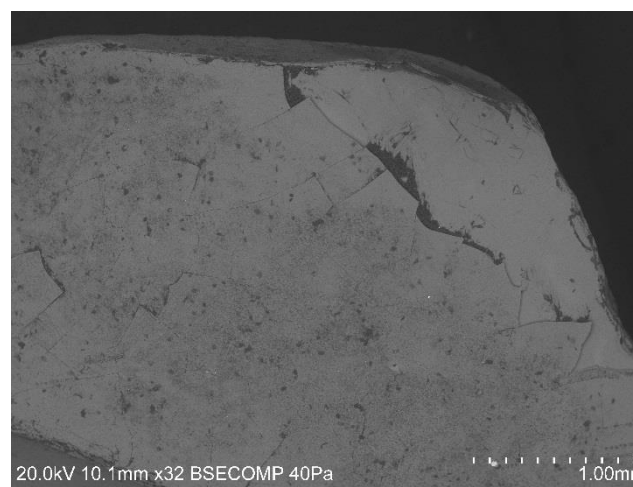


*Image 18. Ya-21 layers of altered surface.*

Annex 3.

LA-ICP-MS results table of major elements represented as respective oxides Values of SO<sub>3</sub> and Cl are taken from SEM-EDS results. <DL – below detection limit of SEM-EDS.

	Na <sub>2</sub> O (%)	MgO (%)	Al <sub>2</sub> O <sub>3</sub> (%)	SiO <sub>2</sub> (%)	P <sub>2</sub> O <sub>5</sub> (%)	K <sub>2</sub> O (%)	CaO (%)	TiO <sub>2</sub> (%)	MnO (%)	Fe <sub>2</sub> O <sub>3</sub> (%)	CuO (%)	SnO <sub>2</sub> (%)	PbO (%)	SO <sub>3</sub> (%)	Cl (%)
Ya-1	17,514	0,501	0,422	68,378	0,033	0,261	9,053	0,084	0,014	0,341	1,962	0,010	0,002	0,257	1,106
Ya-2	15,127	0,553	0,400	70,077	0,051	0,177	8,941	0,071	0,010	0,288	2,553	0,066	0,061	0,423	1,147
Ya-3	16,012	2,011	2,718	63,158	0,509	2,508	6,850	0,154	0,041	1,497	3,062	0,123	0,130	0,264	0,887
Ya-4	15,774	0,984	0,780	66,359	0,168	0,640	9,084	0,096	0,022	0,509	3,674	0,047	0,110	0,446	1,232
Ya-5	16,370	0,462	0,365	69,649	0,025	0,083	9,151	0,079	0,011	0,823	1,572	0,003	0,003	<DL	1,316
Ya-6	15,985	0,501	0,350	68,076	0,037	3,156	9,751	0,074	0,012	0,336	0,470	0,014	0,002	0,175	0,994
Ya-7	14,986	1,582	4,862	61,946	0,443	3,791	7,912	0,385	0,077	2,212	0,704	0,158	0,070	0,693	<DL
Ya-8	8,529	1,445	5,784	63,013	0,212	11,731	5,798	0,434	0,066	2,193	0,479	0,033	0,044	<DL	0,083
Ya-9	16,684	2,618	2,557	67,127	0,518	2,270	5,264	0,189	0,054	0,819	0,029	0,002	0,001	0,586	1,215
Ya-10 Blue	15,420	2,167	1,451	67,283	0,672	4,193	3,977	0,061	0,059	0,699	2,016	0,120	0,009	0,637	1,176
Ya-10 White	15,718	2,825	2,515	66,315	0,561	2,492	4,456	0,097	0,300	1,225	0,024	0,924	0,934	1,142	0,395
Ya-11 White	13,512	2,766	3,863	63,078	1,219	4,347	7,397	0,186	0,075	2,447	0,020	0,001	0,005	0,502	0,497
Ya-11 Blue	13,234	2,621	3,921	62,286	0,716	4,276	5,247	0,177	0,303	1,911	4,132	0,193	0,005	<DL	0,890
Ya-11 Dark	16,181	2,932	3,879	62,959	0,811	4,263	5,968	0,186	0,075	1,921	0,004	<DL	0,001	0,218	0,531
Ya-12 Dark	14,889	2,809	3,850	65,631	0,648	4,657	4,511	0,189	0,082	1,934	0,035	0,002	0,008	0,224	0,468
Ya-12 White	14,994	3,473	4,779	58,373	1,488	4,074	7,163	0,236	0,499	2,450	0,079	0,139	0,533	1,095	0,536
Ya-12 Blue	17,810	3,236	4,687	56,201	0,740	3,863	6,107	0,236	0,350	2,783	2,884	0,005	0,009	<DL	0,989
Ya-13 Blue	13,634	2,510	3,492	62,249	0,758	4,265	5,097	0,161	0,265	1,736	3,818	0,507	0,006	0,310	1,103
Ya-13 White	14,141	2,924	3,897	60,037	1,248	4,098	7,615	0,189	0,144	2,253	0,384	0,043	0,017	1,418	1,514
Ya-13 Black	15,986	2,791	3,784	60,842	0,796	4,515	6,337	0,185	0,075	1,857	0,077	0,003	0,002	1,040	1,639
Ya-14 Blue	17,159	0,609	0,542	68,453	0,075	0,936	8,401	0,062	0,169	0,383	1,531	0,006	0,006	0,717	0,899
Ya-14 Dark	16,627	0,502	0,500	70,073	0,066	1,156	7,930	0,060	0,783	0,407	0,054	0,036	0,107	0,919	0,728
Ya-15 Dark	16,518	0,484	0,472	70,165	0,067	1,209	8,030	0,061	0,736	0,395	0,038	0,042	0,094	0,866	0,769
Ya-15 White	15,907	0,549	0,425	68,825	0,289	1,845	8,926	0,058	0,031	0,333	0,012	0,785	0,850	0,416	0,704
Ya-16 Dark	15,729	2,837	3,931	62,701	0,767	4,222	6,073	0,188	0,071	1,897	0,003	<DL	0,001	0,509	1,003

LA-ICP-MS results table of major elements represented as respective oxides Values of SO<sub>3</sub> and Cl are taken from SEM-EDS results. <DL – below detection limit of SEM-EDS (cont.).

	Na <sub>2</sub> O (%)	MgO (%)	Al <sub>2</sub> O <sub>3</sub> (%)	SiO <sub>2</sub> (%)	P <sub>2</sub> O <sub>5</sub> (%)	K <sub>2</sub> O (%)	CaO (%)	TiO <sub>2</sub> (%)	MnO (%)	Fe <sub>2</sub> O <sub>3</sub> (%)	CuO (%)	SnO <sub>2</sub> (%)	PbO (%)	SO <sub>3</sub> (%)	Cl (%)
Ya-16 White	12,036	2,674	3,846	66,524	1,400	3,696	6,589	0,177	0,069	1,999	0,005	<DL	0,004	<DL	0,914
Ya-17 Vitreous	7,752	0,970	3,441	73,720	0,135	3,738	7,082	0,373	0,042	1,859	0,743	0,008	0,004	<DL	<DL
Ya-17	8,534	0,788	2,776	73,408	0,065	3,506	6,519	0,332	0,038	2,152	0,909	0,010	0,004	<DL	0,838
Ya-18	17,160	0,408	0,274	72,990	0,029	0,077	7,348	0,058	0,008	0,213	<DL	<DL	<DL	0,660	0,730
Ya-19	15,646	0,410	0,301	73,592	0,027	0,323	7,847	0,056	0,008	0,224	0,002	<DL	<DL	0,922	0,599
Ya-20	16,863	0,441	0,425	72,091	0,044	0,110	8,593	0,248	0,010	0,412	0,001	<DL	<DL	<DL	0,639
Ya-21	15,935	0,427	0,405	73,083	0,043	0,123	8,117	0,236	0,010	0,371	0,001	<DL	<DL	0,198	0,933
Ya-23	17,102	0,420	0,362	72,255	0,046	0,115	7,698	0,228	0,010	0,379	0,001	<DL	<DL	0,541	0,736

## Annex 4.

LA-ICP-MS results for trace elements (All the values are in ppm. (<DL) – below detection limit. Colour specification is done where needed).

	V	Cr	Co	Ni	Zn	As	Rb	Sr	Y	Zr	Nb	Mo	Ag	Sb	Cs	Ba
Ya-1	4,971	12,295	1,275	4,788	9,562	10,216	3,385	318,439	5,587	176,771	1,448	0,126	7,120	6,167	0,057	36,176
Ya-2	4,557	9,207	1,229	5,372	8,888	23,194	1,710	309,111	4,943	122,233	1,242	0,065	6,032	8,006	0,030	30,028
Ya-3	20,721	27,215	9,204	54,972	76,264	81,432	7,538	263,012	6,040	60,394	2,280	0,194	16,134	8,942	0,185	83,744
Ya-4	6,429	12,258	1,871	6,216	19,099	59,179	6,367	386,979	5,349	146,895	1,687	0,165	12,317	9,609	0,167	51,872
Ya-5	4,615	11,535	162,479	10,211	6,344	9,995	0,974	301,638	5,188	176,543	1,369	86,757	2,789	43,697	0,035	30,049
Ya-6	4,209	11,633	1,220	4,645	12,517	21,579	12,689	333,219	5,483	186,552	1,261	0,098	0,051	10,369	0,058	37,685
Ya-7	38,584	7,854	7,006	20,578	389,479	6,637	33,945	447,029	15,170	310,542	6,676	0,278	0,302	2,226	0,614	416,026
Ya-8	42,969	16,854	8,984	19,280	372,216	11,696	47,927	217,885	19,184	387,169	7,594	0,339	0,030	6,797	0,368	295,058
Ya-9	12,972	21,040	2,329	6,257	34,377	5,020	10,671	247,913	8,666	139,032	3,111	0,103	0,267	0,634	0,150	133,205
Ya-10 Blue	8,377	12,232	6,194	67,112	100,447	22,560	12,720	217,896	2,990	16,859	0,954	0,341	1,875	3,718	0,275	107,560
Ya-10 White	10,920	23,653	5,072	27,771	266,675	15,056	14,801	235,312	4,528	25,216	1,600	0,247	1,230	11,590	0,351	85,754
Ya-11 White	31,140	49,072	8,076	58,419	220,327	6,735	14,050	258,366	7,063	31,755	2,856	0,369	1,343	0,511	0,649	121,662
Ya-11 Blue	30,124	48,782	9,467	74,580	127,787	98,780	13,383	231,365	7,077	33,247	2,661	0,318	12,097	21,494	0,463	120,001
Ya-11 Dark	32,408	50,906	6,725	35,788	82,986	2,047	10,876	282,884	7,792	35,105	2,719	0,179	0,076	0,115	0,367	111,194
Ya-12 Dark	29,668	54,608	8,398	45,769	80,512	2,253	13,977	218,150	6,435	32,584	2,770	0,189	0,309	0,210	0,409	103,347
Ya-12 White	36,848	61,322	11,602	66,058	120,009	11,913	12,394	299,982	7,579	40,144	3,381	0,432	0,740	1,730	0,346	158,196
Ya-12 Blue	34,628	65,583	59,226	111,933	123,042	10,317	10,839	280,205	8,767	65,438	3,423	0,340	11,850	0,477	0,259	168,894
Ya-13 Blue	26,255	39,492	8,822	100,710	114,301	102,681	11,551	247,918	6,233	36,577	2,441	0,471	8,853	37,489	0,362	121,287
Ya-13 White	30,878	47,249	9,205	58,559	116,788	23,695	13,204	258,998	6,620	34,080	2,806	0,440	1,524	5,035	0,386	138,202
Ya-13 Black	32,196	49,927	7,114	39,058	92,146	3,826	15,477	279,694	7,260	33,114	2,721	0,336	1,179	0,432	0,442	106,201
Ya-14 Blue	6,252	10,652	3,678	7,763	30,212	14,248	8,302	268,355	5,533	90,033	1,064	0,452	3,970	5,568	0,084	47,798
Ya-14 Dark	8,072	9,288	4,049	5,583	16,015	4,506	12,100	275,377	5,438	92,010	1,046	0,734	0,328	1,182	0,100	75,077
Ya-15 Dark	7,412	9,205	3,852	5,255	14,486	4,554	11,479	279,204	5,416	90,740	1,048	0,770	0,362	1,332	0,091	72,588
Ya-15 White	4,974	9,839	1,419	5,098	16,706	2,111	11,501	249,845	5,366	91,916	1,043	0,118	1,260	3,617	0,082	46,699
Ya-16 Dark	31,747	49,948	6,585	33,802	78,409	1,779	9,623	278,627	7,376	33,039	2,695	0,149	0,038	0,104	0,347	108,535
Ya-16 White	28,765	46,683	7,276	48,787	97,085	4,777	9,430	238,486	6,636	30,516	2,703	0,143	0,077	0,329	0,417	110,187

LA-ICP-MS results for trace elements (All the values are in ppm. (<DL) – below detection limit. Colour specification is done where needed) (Cont.)

	V	Cr	Co	Ni	Zn	As	Rb	Sr	Y	Zr	Nb	Mo	Ag	Sb	Cs	Ba
Ya-17 Vitreous	32,890	26,778	5,434	15,216	122,235	10,893	64,548	243,432	13,572	481,773	6,117	0,687	0,995	6,376	1,600	207,307
Ya-17	26,296	34,145	4,457	12,997	65,933	9,746	65,615	219,824	12,174	506,797	5,481	0,381	2,700	10,503	1,828	175,484
Ya-18	4,550	9,248	0,839	1,801	5,415	1,091	0,843	249,378	4,001	104,937	1,031	0,085	0,149	0,123	0,038	27,473
Ya-19	4,120	9,101	0,875	2,156	4,087	1,606	1,184	261,748	4,491	88,267	0,968	0,071	0,075	0,088	<DL	28,562
Ya-20	10,001	39,865	1,294	2,999	5,324	1,667	1,019	270,830	7,082	826,379	4,239	0,178	0,089	0,647	<DL	35,225
Ya-21	9,858	37,072	1,229	2,826	5,807	2,242	1,125	257,430	6,983	785,726	4,215	0,159	0,116	0,696	<DL	34,329
Ya-23	9,838	36,255	1,161	2,916	6,785	1,409	1,091	241,895	6,252	704,313	3,820	0,192	0,097	0,672	<DL	31,718

LA-ICP-MS results for trace elements (All the values are in ppm. (<DL) – below detection limit. Colour specification is done where needed) (Cont.)

	La	Ce	Nd	Sm	Eu	Tb	Dy	Er	Tm	Yb	Lu	Au	Bi	Th	U
Ya-1	5,101	6,321	4,516	0,818	0,222	0,125	0,813	0,490	0,072	0,501	0,081	0,402	0,138	0,686	2,149
Ya-2	4,602	5,888	4,124	0,850	0,186	0,116	0,739	0,450	0,058	0,410	0,074	0,176	0,637	0,669	1,984
Ya-3	6,940	11,835	5,880	1,224	0,315	0,170	1,079	0,612	0,087	0,559	0,090	0,747	5,552	1,882	0,938
Ya-4	5,268	7,970	4,618	0,831	0,197	0,129	0,818	0,499	0,070	0,493	0,085	0,234	0,747	1,048	1,825
Ya-5	4,735	5,984	4,155	0,803	0,191	0,115	0,748	0,417	0,068	0,473	0,079	0,299	1,939	0,618	2,192
Ya-6	4,793	5,846	4,004	0,828	0,207	0,117	0,746	0,496	0,073	0,473	0,077	0,061	0,585	0,600	2,312
Ya-7	21,489	40,517	16,948	3,272	0,583	0,437	2,694	1,573	0,231	1,629	0,262	0,017	0,114	5,977	1,899
Ya-8	20,367	42,370	18,296	3,757	0,692	0,538	3,306	2,083	0,310	2,253	0,359	0,016	1,026	6,773	1,630
Ya-9	9,755	18,434	8,578	1,662	0,332	0,236	1,492	0,883	0,139	0,856	0,148	<DL	0,087	2,963	0,971
Ya-10 Blue	2,537	4,667	2,245	0,523	0,160	0,090	0,521	0,299	0,044	0,247	0,036	0,138	1,398	0,905	0,927
Ya-10 White	4,292	8,315	3,866	0,867	0,225	0,155	0,868	0,468	0,069	0,493	0,074	0,026	0,904	1,522	0,744
Ya-11 White	6,735	13,522	5,590	1,219	0,357	0,223	1,246	0,769	0,116	0,744	0,102	0,724	0,243	2,444	0,652
Ya-11 Blue	6,905	13,096	5,857	1,429	0,383	0,237	1,285	0,709	0,102	0,719	0,112	0,444	2,318	2,480	0,644
Ya-11 Dark	7,360	14,085	6,421	1,423	0,445	0,238	1,430	0,798	0,112	0,746	0,118	0,033	0,037	2,653	0,814
Ya-12 Dark	7,039	13,310	5,887	1,351	0,357	0,195	1,235	0,663	0,090	0,613	0,106	0,045	0,025	2,513	0,614

LA-ICP-MS results for trace elements (All the values are in ppm. (<DL) – below detection limit. Colour specification is done where needed) (Cont.)

	La	Ce	Nd	Sm	Eu	Tb	Dy	Er	Tm	Yb	Lu	Au	Bi	Th	U
Ya-12 White	8,798	16,611	7,320	1,647	0,411	0,236	1,369	0,759	0,111	0,783	0,112	0,115	0,187	2,946	0,768
Ya-12 Blue	9,022	16,554	7,579	1,573	0,427	0,266	1,551	0,901	0,123	0,852	0,138	2,617	0,115	3,198	0,804
Ya-13 Blue	6,221	11,810	5,178	1,184	0,346	0,191	1,153	0,618	0,091	0,612	0,088	0,434	2,329	2,208	0,647
Ya-13 White	6,919	13,997	6,157	1,304	0,405	0,225	1,204	0,702	0,110	0,594	0,104	0,128	0,591	2,673	0,895
Ya-13 Black	6,985	13,242	5,931	1,396	0,445	0,234	1,360	0,754	0,129	0,734	0,120	0,626	0,110	2,490	0,802
Ya-14 Blue	5,267	6,392	4,419	0,872	0,214	0,130	0,785	0,495	0,069	0,438	0,068	0,241	0,186	0,711	1,226
Ya-14 Dark	5,333	6,290	4,628	0,917	0,222	0,132	0,828	0,514	0,065	0,445	0,078	<DL	0,128	0,714	1,352
Ya-15 Dark	5,155	6,266	4,416	0,902	0,218	0,132	0,705	0,467	0,061	0,418	0,080	<DL	0,140	0,682	1,303
Ya-15 White	5,197	6,270	4,390	0,873	0,207	0,141	0,781	0,457	0,062	0,418	0,066	0,016	1,224	0,684	1,191
Ya-16 Dark	7,343	13,757	6,539	1,422	0,423	0,228	1,349	0,748	0,106	0,751	0,111	0,017	0,023	2,558	0,771
Ya-16 White	6,724	13,283	5,971	1,300	0,394	0,228	1,272	0,675	0,115	0,667	0,104	0,219	0,084	2,449	0,592
Ya-17 Vitreous	15,989	29,398	13,968	2,690	0,517	0,375	2,269	1,453	0,215	1,552	0,250	0,027	0,150	3,941	1,709
Ya-17	13,083	23,313	11,387	2,200	0,471	0,307	1,989	1,223	0,183	1,295	0,225	0,180	0,265	3,021	1,663
Ya-18	4,212	5,792	3,624	0,639	0,187	0,093	0,576	0,337	0,043	0,359	0,053	0,018	0,041	0,494	1,176
Ya-19	4,833	6,059	4,232	0,815	0,207	0,110	0,656	0,395	0,052	0,400	0,064	0,014	0,029	0,552	1,294
Ya-20	5,170	6,805	4,393	0,828	0,231	0,147	1,005	0,755	0,137	0,917	0,171	0,067	<DL	1,086	1,450
Ya-21	4,845	6,461	4,070	0,694	0,219	0,119	0,941	0,728	0,122	0,841	0,174	<DL	0,139	1,057	1,333
Ya-23	4,464	6,105	3,744	0,755	0,179	0,132	0,857	0,676	0,097	0,815	0,154	0,035	0,039	0,990	1,288

## Annex 5.

Yahorlyk glass portable XRF analyses table (all the values are expressed in arb.units).

		Al	Ca	Cl	Co	Cr	Cu	Fe	K	Mn	Ni	Pb	S	Si	Sn	Sr	Ti	Zn	Zr
Ya-1		0,02	10,27	0,47	0,03	0,03	29,49	4,44	0,32	0,17	1,91	0,04	0,08	2,15	0,03	1,17	0,53	0,15	0,71
Ya-2		0,02	9,35	0,50	0,02	0,03	36,05	3,61	0,10	0,14	2,22	0,67	0,08	1,96	0,19	0,99	0,39	0,20	0,40
Ya-3	Eye side	0,04	9,81	0,54	0,08	0,04	49,82	17,37	2,40	0,42	2,11	1,72	0,07	2,55	0,80	0,89	0,71	0,26	0,14
Ya-4		0,03	12,10	0,59	0,02	0,04	57,90	7,18	0,70	0,25	1,72	1,19	0,06	2,45	0,15	1,35	0,51	0,16	0,46
Ya-5		0,02	10,59	0,59	0,23	0,03	22,79	8,94	0,05	0,17	2,23	0,11	0,06	2,68	0,04	1,12	0,44	0,14	0,70
Ya-6		0,03	10,53	0,45	0,04	0,04	6,05	5,73	1,95	0,18	2,18	0,11	0,07	2,71	0,02	1,20	0,50	0,14	0,68
Ya-7	Green glass	0,07	8,52	0,05	0,10	0,02	8,92	21,86	3,32	0,60	1,60	0,84	0,08	2,18	0,44	1,39	1,18	0,70	1,21
Ya-7	Light layer	0,17	7,81	0,11	0,30	0,16	1,75	69,57	2,39	0,54	1,44	0,23	0,06	1,38	0,23	0,46	2,71	0,15	0,87
Ya-8		0,06	4,95	0,14	0,09	0,02	2,33	18,97	3,93	0,43	1,62	0,44	0,05	1,98	0,25	0,73	1,01	0,51	1,07
Ya-9		0,04	6,01	0,50	0,05	0,03	1,27	9,47	1,28	0,49	1,62	0,07	0,06	2,38	<DL	1,01	0,73	0,12	0,87
Ya-10	Base side	0,05	5,21	0,37	0,12	0,04	0,63	14,41	1,28	1,21	2,34	7,21	0,12	2,23	1,86	0,89	0,62	0,26	0,08
Ya-10	Eye side	0,04	5,29	0,39	0,05	0,02	12,34	10,89	1,49	1,49	2,38	6,71	0,09	2,74	1,81	0,75	0,50	0,29	0,07
Ya-11	Base side	0,05	6,90	0,43	0,09	0,05	0,49	20,01	2,71	0,62	1,71	0,09	0,08	1,77	0,03	1,05	0,75	0,19	0,15
Ya-11	Eye side	0,05	7,15	0,41	0,08	0,06	25,93	19,49	2,73	1,42	1,83	0,22	0,08	1,83	0,23	0,89	0,69	0,29	0,10
Ya-12	Base side	0,06	5,45	0,37	0,12	0,05	2,33	24,83	2,84	1,33	1,67	0,46	0,06	1,78	0,35	0,91	0,80	0,20	0,14
Ya-12	Eye side	0,05	7,93	0,46	0,18	0,07	35,67	31,87	3,15	2,95	1,72	0,91	0,05	2,00	0,46	0,96	0,87	0,30	0,18
Ya-13	Base side	0,05	7,70	0,54	0,10	0,05	1,54	18,84	3,41	0,62	1,71	0,06	0,08	2,15	0,03	1,06	0,66	0,19	0,12
Ya-13	Eye side	0,05	8,22	0,40	0,09	0,05	15,02	22,59	2,63	1,07	1,72	0,20	0,09	1,74	0,19	0,92	0,70	0,25	0,10
Ya-14	Base side	0,03	9,82	0,39	0,03	0,01	3,59	6,07	0,63	5,12	2,04	2,42	0,09	2,50	0,33	1,06	0,42	0,08	0,35
Ya-14	Eye side	0,04	11,70	0,47	0,02	0,02	7,90	6,86	0,87	4,93	2,12	1,58	0,10	3,43	0,28	1,09	0,41	0,11	0,33
Ya-15		0,04	10,11	0,43	0,05	0,03	1,41	6,45	0,55	5,78	2,93	2,09	0,12	2,79	0,22	1,06	0,54	0,11	0,28
Ya-16		0,08	8,62	0,56	0,13	0,07	0,68	21,56	2,63	0,73	4,16	<DL	0,13	2,32	<DL	0,93	1,07	0,23	0,10
Ya-17	Vitreous	0,06	8,25	0,10	0,08	0,04	14,57	18,47	3,42	0,37	1,91	0,15	0,05	3,21	0,04	0,72	1,14	0,36	2,05
Ya-17	Rough	0,07	4,45	0,17	0,09	0,10	8,38	26,14	2,64	0,31	1,77	0,11	0,06	2,50	0,03	0,70	1,42	0,28	2,14
Ya-18		0,03	11,22	0,30	0,03	0,03	0,33	3,42	0,15	0,14	1,70	<DL	0,10	3,09	<DL	1,13	0,34	0,05	0,53
Ya-19		0,04	10,53	0,29	0,02	0,02	0,40	4,29	0,27	0,17	1,78	<DL	0,11	2,99	<DL	1,17	0,38	0,08	0,41

Yahorlyk glass portable XRF analyses table (all the values are expressed in arb.units).

		Al	Ca	Cl	Co	Cr	Cu	Fe	K	Mn	Ni	Pb	S	Si	Sn	Sr	Ti	Zn	Zr
Ya-20		0,03	11,29	0,39	0,03	0,05	0,38	4,92	0,23	0,15	1,78	<DL	0,06	3,26	<DL	1,11	0,81	0,05	3,45
Ya-21		0,04	11,25	0,40	0,04	0,07	0,26	5,55	0,26	0,16	1,70	<DL	0,05	3,21	<DL	1,13	0,87	0,04	3,55
Ya-22		0,03	11,23	0,34	0,02	0,09	0,25	4,91	0,22	0,14	1,72	<DL	0,05	3,13	<DL	1,13	0,81	0,07	3,46
Ya-23		0,04	9,61	0,33	0,04	0,03	0,38	4,99	0,27	0,17	1,88	<DL	0,10	3,17	<DL	0,82	0,47	0,09	0,43

## Annex 6.

XRF results of sand analyses (samples split in subsamples; all the values are in percent (%)).

number	Name of the sample	SiO <sub>2</sub>	Al <sub>2</sub> O <sub>3</sub>	Fe <sub>2</sub> O <sub>3</sub>	Na <sub>2</sub> O	K <sub>2</sub> O	TiO <sub>2</sub>	CaO	MgO	P <sub>2</sub> O <sub>5</sub>	MnO	SO <sub>3</sub>	SrO	Zr
1	Ya-S-1	95,347	3,300	0,370	0,086	0,113	0,156	0,037	0,267	0,229	0,004	0,033	0,014	0,044
2	Ya-S-2	95,761	3,130	0,367	0,051	0,152	0,088	0,033	0,231	0,128	0,006	0,022	0,008	0,023
3	Ya-S-3	95,339	3,280	0,410	0,063	0,248	0,111	0,030	0,249	0,191	0,007	0,025	0,012	0,035
4	Ya-S-4	95,319	3,250	0,383	0,082	0,253	0,144	0,032	0,232	0,221	0,006	0,023	0,014	0,042
5	Ya-S-5	95,029	3,340	0,450	0,089	0,225	0,175	0,034	0,258	0,294	0,005	0,026	0,018	0,057
6	Ya-S-6	95,483	3,190	0,367	0,083	0,277	0,102	0,020	0,212	0,183	0,003	0,033	0,012	0,036
7	Ya-S-7	95,155	3,360	0,393	0,080	0,308	0,113	0,031	0,273	0,198	0,005	0,035	0,012	0,037
8	Ya-S-8	95,757	3,070	0,275	0,096	0,073	0,142	0,028	0,209	0,252	0,002	0,030	0,016	0,051
9	Ya-S-9	95,763	3,110	0,263	0,111	0,247	0,077	0,023	0,201	0,140	0,001	0,029	0,010	0,027
10	Ya-S-10	95,288	3,300	0,375	0,089	0,258	0,114	0,034	0,229	0,220	0,005	0,031	0,014	0,044
Average	Ya-S	95,424	3,233	0,365	0,083	0,215	0,122	0,030	0,236	0,206	0,004	0,029	0,013	0,040
St. dev		0,261	0,102	0,057	0,017	0,076	0,031	0,005	0,025	0,050	0,002	0,004	0,003	0,010
11	Ya-B-1	95,326	3,260	0,375	0,092	0,298	0,098	0,040	0,262	0,177	0,005	0,023	0,011	0,032
12	Ya-B-2	95,348	3,210	0,388	0,101	0,230	0,115	0,035	0,248	0,232	0,006	0,027	0,015	0,045
13	Ya-B-3	95,612	3,110	0,376	0,069	0,067	0,180	0,041	0,265	0,198	0,007	0,022	0,013	0,039
14	Ya-B-4	95,634	3,160	0,368	0,062	0,176	0,123	0,053	0,222	0,143	0,004	0,022	0,009	0,024
15	Ya-B-5	95,610	3,150	0,369	0,096	0,093	0,147	0,023	0,242	0,197	0,004	0,021	0,012	0,037
16	Ya-B-6	95,574	3,180	0,370	0,070	0,130	0,120	0,088	0,240	0,160	0,005	0,026	0,010	0,028
17	Ya-B-7	95,525	3,170	0,331	0,132	0,099	0,172	0,047	0,258	0,187	0,004	0,028	0,012	0,036
18	Ya-B-8	95,454	3,120	0,332	0,100	0,263	0,138	0,040	0,251	0,217	0,004	0,024	0,014	0,043
19	Ya-B-9	95,441	3,160	0,367	0,096	0,229	0,117	0,048	0,261	0,199	0,004	0,026	0,013	0,039
20	Ya-B-10	95,637	3,150	0,331	0,102	0,214	0,109	0,036	0,236	0,125	0,004	0,025	0,008	0,023
Average	Ya-B	95,516	3,167	0,361	0,092	0,180	0,132	0,045	0,249	0,184	0,005	0,024	0,012	0,034
St. dev		0,117	0,043	0,021	0,020	0,079	0,027	0,017	0,014	0,033	0,001	0,002	0,002	0,008

XRF results of sand analyses (samples split in subsamples; all the values are in percent (%)). (Cont.).

n	Name of the sample	SiO <sub>2</sub>	Al <sub>2</sub> O <sub>3</sub>	Fe <sub>2</sub> O <sub>3</sub>	Na <sub>2</sub> O	K <sub>2</sub> O	TiO <sub>2</sub>	CaO	MgO	P <sub>2</sub> O <sub>5</sub>	MnO	SO <sub>3</sub>	SrO	Zr
21	Iv-Q-1	95,597	3,260	0,342	0,079	0,211	0,075	0,018	0,219	0,138	0,003	0,025	0,009	0,025
22	Iv-Q-2	95,365	3,240	0,407	0,095	0,222	0,133	0,020	0,210	0,224	0,003	0,022	0,014	0,045
23	Iv-Q-3	95,633	3,090	0,351	0,054	0,097	0,167	0,022	0,240	0,253	0,004	0,023	0,016	0,051
24	Iv-Q-4	95,610	3,230	0,335	0,072	0,264	0,069	0,030	0,217	0,120	0,004	0,021	0,008	0,021
25	Iv-Q-5	95,491	3,340	0,376	0,107	0,157	0,090	0,021	0,236	0,122	0,002	0,030	0,007	0,021
26	Iv-Q-6	95,741	3,190	0,319	0,034	0,217	0,075	0,031	0,228	0,111	0,003	0,026	0,007	0,019
27	Iv-Q-7	95,154	3,280	0,384	0,048	0,208	0,190	0,022	0,238	0,354	0,005	0,024	0,022	0,073
28	Iv-Q-8	95,564	3,280	0,346	0,097	0,050	0,166	0,031	0,219	0,176	0,003	0,023	0,011	0,034
29	Iv-Q-9	95,711	3,120	0,340	0,052	0,168	0,110	0,026	0,215	0,184	0,004	0,023	0,012	0,036
30	Iv-Q-10	95,575	3,120	0,376	0,066	0,170	0,154	0,019	0,207	0,230	0,003	0,021	0,014	0,046
Average	Iv-Q	95,544	3,215	0,358	0,070	0,176	0,123	0,024	0,223	0,191	0,003	0,024	0,012	0,037
St. dev		0,173	0,082	0,027	0,024	0,064	0,045	0,005	0,012	0,076	0,001	0,003	0,005	0,017
31	Ryb-Q-1	95,113	3,340	0,403	0,099	0,333	0,110	0,051	0,261	0,209	0,006	0,020	0,014	0,041
32	Ryb-Q-2	95,320	3,270	0,374	0,115	0,118	0,163	0,039	0,244	0,262	0,004	0,021	0,017	0,053
33	Ryb-Q-3	94,047	4,010	0,609	0,117	0,403	0,135	0,055	0,344	0,200	0,005	0,023	0,014	0,039
34	Ryb-Q-4	95,033	3,480	0,387	0,155	0,239	0,132	0,038	0,248	0,212	0,003	0,018	0,014	0,041
35	Ryb-Q-5	94,818	3,360	0,441	0,088	0,367	0,170	0,043	0,250	0,343	0,006	0,022	0,022	0,070
36	Ryb-Q-6	95,030	3,490	0,399	0,075	0,331	0,102	0,047	0,282	0,173	0,003	0,022	0,012	0,034
37	Ryb-Q-7	92,131	5,170	1,150	0,082	0,400	0,180	0,071	0,584	0,163	0,008	0,020	0,011	0,029
38	Ryb-Q-8	91,381	5,510	1,230	0,095	0,442	0,221	0,089	0,693	0,249	0,008	0,018	0,017	0,047
39	Ryb-Q-9	94,047	4,010	0,609	0,117	0,403	0,135	0,055	0,344	0,200	0,005	0,023	0,014	0,039
40	Ryb-Q-10	92,014	5,110	1,150	0,113	0,442	0,177	0,076	0,579	0,249	0,006	0,019	0,017	0,048
Average	Ryb-Q	93,893	4,075	0,675	0,106	0,348	0,153	0,056	0,383	0,226	0,005	0,021	0,015	0,044
St. dev		1,489	0,865	0,357	0,023	0,101	0,036	0,017	0,169	0,052	0,002	0,002	0,003	0,011
41	For-1	95,494	3,280	0,348	0,071	0,218	0,105	0,024	0,258	0,140	0,003	0,023	0,009	0,026
42	For-2	95,501	3,260	0,383	0,100	0,246	0,080	0,041	0,238	0,099	0,004	0,025	0,007	0,017
43	For-3	95,520	3,290	0,284	0,106	0,271	0,071	0,036	0,250	0,119	0,002	0,022	0,008	0,022

XRF results of sand analyses (samples split in subsamples; all the values are in percent (%)). (Cont.).

n	Name of the sample	SiO <sub>2</sub>	Al <sub>2</sub> O <sub>3</sub>	Fe <sub>2</sub> O <sub>3</sub>	Na <sub>2</sub> O	K <sub>2</sub> O	TiO <sub>2</sub>	CaO	MgO	P <sub>2</sub> O <sub>5</sub>	MnO	SO <sub>3</sub>	SrO	Zr
44	For-4	95,493	3,280	0,363	0,099	0,221	0,093	0,020	0,241	0,131	0,004	0,022	0,009	0,025
45	For-5	95,340	3,380	0,387	0,098	0,188	0,114	0,031	0,248	0,147	0,003	0,026	0,010	0,028
46	For-6	95,572	3,280	0,361	0,103	0,166	0,088	0,039	0,222	0,109	0,004	0,030	0,008	0,019
47	For-7	95,185	3,450	0,490	0,108	0,187	0,097	0,030	0,267	0,116	0,015	0,027	0,008	0,021
48	For-8	95,546	3,310	0,313	0,081	0,227	0,083	0,046	0,247	0,094	0,003	0,028	0,007	0,017
49	For-9	95,549	3,280	0,343	0,086	0,159	0,131	0,039	0,223	0,131	0,003	0,023	0,009	0,024
50	For-10	95,913	3,100	0,270	0,073	0,203	0,059	0,022	0,232	0,082	0,001	0,027	0,006	0,014
Average	For	95,511	3,291	0,354	0,092	0,209	0,092	0,033	0,243	0,117	0,004	0,025	0,008	0,021
St. dev		0,184	0,089	0,062	0,014	0,035	0,021	0,009	0,014	0,021	0,004	0,003	0,001	0,005
51	Qua-1	89,921	5,880	0,967	0,350	1,170	0,386	0,162	0,514	0,487	0,005	0,023	0,036	0,099
52	Qua-2	89,124	6,240	1,070	0,403	1,320	0,341	0,182	0,624	0,515	0,008	0,032	0,038	0,104
53	Qua-3	94,724	3,700	0,361	0,148	0,374	0,120	0,043	0,287	0,172	0,002	0,023	0,013	0,034
54	Qua-4	94,715	3,540	0,390	0,135	0,440	0,140	0,047	0,271	0,234	0,002	0,023	0,016	0,047
55	Qua-5	95,983	3,050	0,251	0,109	0,063	0,099	0,038	0,238	0,116	0,002	0,020	0,008	0,022
Average	Qua	92,894	4,482	0,608	0,229	0,673	0,217	0,094	0,387	0,305	0,004	0,024	0,022	0,061
St. dev		3,133	1,466	0,380	0,137	0,544	0,135	0,071	0,172	0,184	0,003	0,004	0,014	0,038
56	Vyn-S-1	89,991	2,900	0,335	0,053	0,176	0,064	5,900	0,386	0,101	0,003	0,066	0,012	0,013
57	Vyn-S-2	96,697	2,710	0,140	0,085	0,054	0,025	0,035	0,181	0,039	0,001	0,028	0,003	0,005
58	Vyn-S-3	95,587	3,250	0,246	0,109	0,308	0,054	0,037	0,226	0,123	0,002	0,027	0,009	0,023
59	Vyn-S-4	95,597	3,170	0,280	0,119	0,272	0,070	0,047	0,252	0,135	0,002	0,022	0,009	0,025
Average	Vyn-S	94,468	3,008	0,250	0,091	0,202	0,053	1,505	0,261	0,099	0,002	0,035	0,008	0,017
St. dev		3,030	0,249	0,082	0,030	0,114	0,020	2,930	0,088	0,043	0,001	0,021	0,004	0,009
60	Iv-S-1	76,931	10,800	3,980	1,310	2,120	0,565	1,290	2,300	0,481	0,036	0,062	0,038	0,087
61	Iv-S-2	78,922	9,470	3,240	1,690	1,810	0,584	1,510	2,020	0,505	0,052	0,068	0,040	0,089
62	Iv-S-3	77,697	10,100	3,640	1,370	1,860	0,589	1,730	2,280	0,491	0,051	0,071	0,039	0,083
Average	Iv-S	77,850	10,123	3,620	1,457	1,930	0,579	1,510	2,200	0,492	0,046	0,067	0,039	0,086
St. dev		1,004	0,665	0,370	0,204	0,166	0,013	0,220	0,156	0,012	0,009	0,004	0,001	0,003

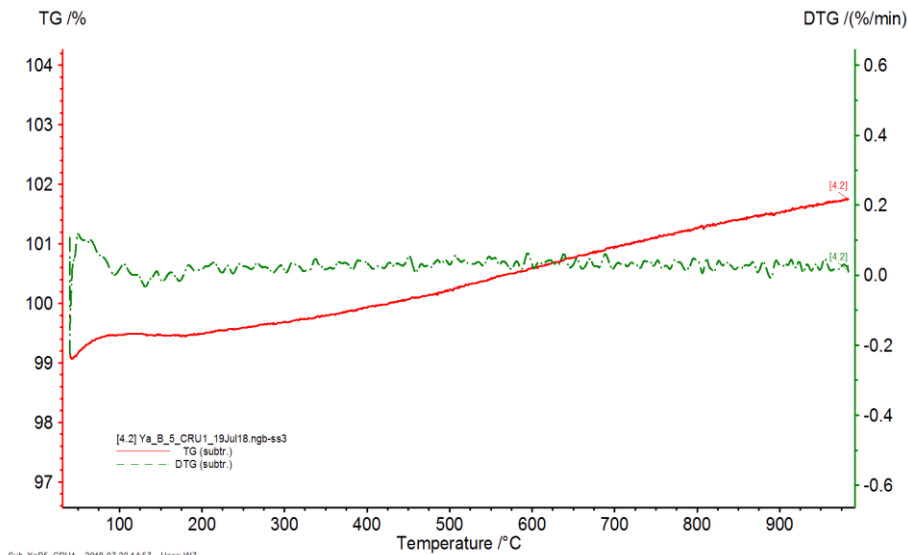
XRF results of sand analyses (samples split in subsamples; all the values are in percent (%)). (Cont.).

n	Name of the sample	SiO <sub>2</sub>	Al <sub>2</sub> O <sub>3</sub>	Fe <sub>2</sub> O <sub>3</sub>	Na <sub>2</sub> O	K <sub>2</sub> O	TiO <sub>2</sub>	CaO	MgO	P <sub>2</sub> O <sub>5</sub>	MnO	SO <sub>3</sub>	SrO	Zr
63	Ryb-L-1-2cm	96,336	2,730	0,163	0,136	0,115	0,036	0,103	0,275	0,059	0,002	0,032	0,005	0,009
64	Ryb-L-1-20cm	95,630	3,080	0,219	0,124	0,284	0,089	0,032	0,237	0,203	0,001	0,046	0,014	0,041
Average	Ryb-L	95,983	2,905	0,191	0,130	0,200	0,062	0,068	0,256	0,131	0,002	0,039	0,009	0,025
St. dev		0,499	0,247	0,040	0,008	0,120	0,038	0,050	0,027	0,102	0,000	0,009	0,006	0,022
Total average		94,168	3,757	0,569	0,165	0,338	2,966	0,204	0,366	0,201	0,006	0,028	0,014	2,968
Total St. Dev.		3,936	1,578	0,719	0,296	0,411	0,113	0,789	0,423	0,106	0,009	0,011	0,008	0,021

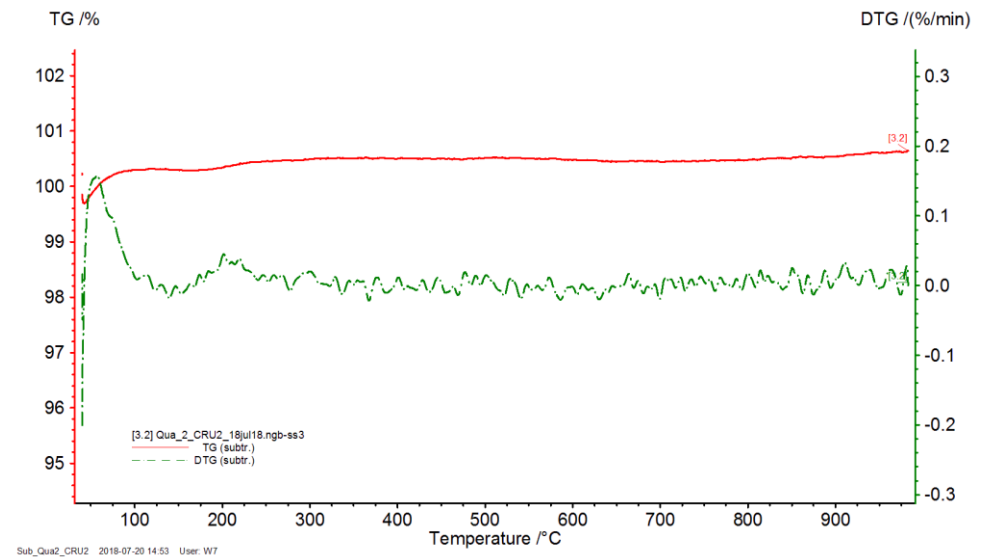
## Annex 7.

### Auxiliary analyses.

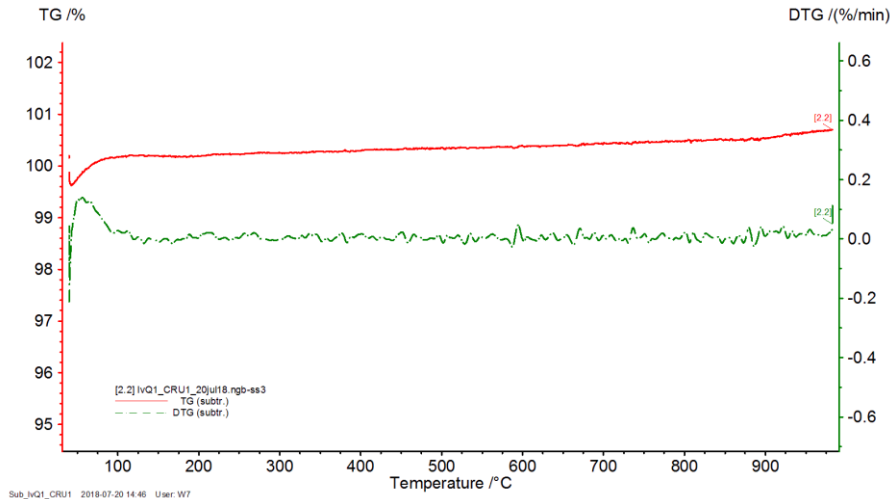
The purpose of this appendix is reporting the results of auxiliary analyses of sand samples. We used Thermal Gravimetric Analysis TGA to find the absolute values of such components of sand as shell and fine organic particles of plant origin. This technique is based on loss of the sample weight due to decomposition and loss of certain components that can be deduced by their temperature of decomposition which is displayed on weight/temperature graph. Four subsamples were selected to be analysed: Qua-2 as the one that had the most of plant particles, Ya-B-5 as the one from the beach to check the presence of shell, Iv-Q-1 as the subsample of aeolian sand and Iv-S-1 as the one of undefined nature. Samples were introduced in form of fine powder; their initial weights were registered. The temperature program was next: temperature range: 40-1000 °C, step 10 °C per minute, nitrogen atmosphere. Graphs below (1-4) represent the change of weights of samples (red and blue lines). The only sample that has shown countable loss of weight was Iv-S-1 (4). It lost 2 % of total weight in the wide range of temperatures (400-600°C) that is not a clear indicator of material that has gone. The rest of the samples did not lose practically any weight hence there was no significant amount of shell or plant particles in the samples.



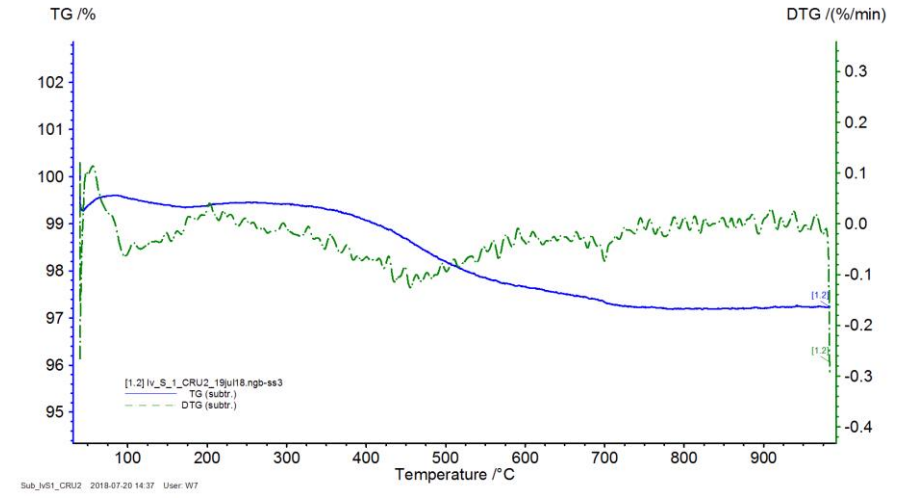
1. Ya-5



2. Qua-2



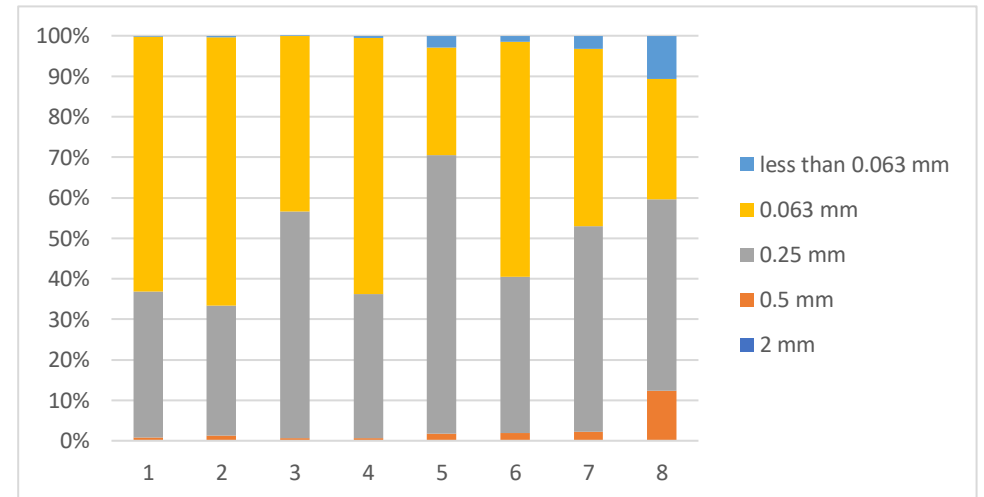
3. Iv-Q-1



4. Iv-S-1

Another kind of analysis that was helpful for developing the sampling strategy was granulometric analysis. In short, it is a sieving of the sample through the special set of sieves with registration of weight of every fraction obtained. The analysis was performed with samples never reported in the main body of the work. This data helped to establish the sample size for the subsequent sampling of desired areas. Below one can find the table and graph with the weights obtained, sizes of fractions and their proportions in every sample. The samples demonstrate that sand grains mostly vary between 0,063 mm and 0,5 mm.

	initial total weight (g)	2 mm (g)	0.5 mm (g)	0.25 mm (g)	0.063 mm (g)	less than 0.063 mm (g)
Ya-1	604,85	0	4,76	217,41	380,3	1,69
Ya-2	565,76	0	7,06	182,05	374,9	1,74
Ya-3	366,73	0	2,24	205,12	159,07	0,24
Ya-4	430,71	0	2,99	152,88	272,09	2,1
Ya-5	298,59	0,09	5,24	205,28	78,79	8,93
Ya-6	319,31	0,14	6,05	122,94	185,29	4,55
Ya-7	241,79	0,08	5,13	122,68	105,76	7,83
Ya-8	133,62	0	16,49	62,98	39,71	14,23
<b>total</b>	<b>2961,36</b>	<b>0,31</b>	<b>49,96</b>	<b>1271,34</b>	<b>1595,91</b>	<b>41,31</b>



## Annex 8.

## Detection limits of ICP-MS sand analyses. (DL-detection limit)

First run		Second run	
Element	DL (ppb)	Element	DL (ppb)
V	0,01644	V	0,08896
Cr	0,11213	Cr	0,40089
Co	0,01013	Co	0,01784
Cu	0,06233	Cu	0,16571
Zn	0,16737	Zn	0,99404
Ge	0,07041	Ge	0,04136
As	0,01176	As	0,02591
Rb	0,02594	Rb	0,03291
Sr	0,03019	Sr	0,07092
Y	0,00234	Y	0,00615
Zr	0,00287	Zr	0,00562
Zr	0,01770	Zr	0,00752
Nb	0,02175	Nb	0,06686
Mo	0,00534	Mo	0,07576
Ag	0,61608	Ag	0,00663
Sn	0,00796	Sn	0,00496

First run		Second run	
Element	DL (ppb)	Element	DL (ppb)
Cs	0,00661	Cs	0,00395
Ba	0,02363	Ba	0,25287
La	0,00049	La	0,00209
Ce	0,00050	Ce	0,00490
Nd	0,00112	Nd	0,00241
Sm	0,00060	Sm	0,00030
Eu	0,00031	Eu	0,00066
Tb	0,00024	Tb	0,00084
Dy	0,00111	Dy	0,00240
Er	0,00104	Er	0,00107
Tm	0,00016	Tm	0,00080
Yb	0,00038	Yb	0,00008
Lu	0,00026	Lu	0,00035
W	0,32792	W	0,76598
Pb	0,02312	Pb	0,03685
Th	0,00299	Th	0,00472
U	0,00223	U	0,00136

Annex 9.

The Detection limits of LA-ICP-MS glass analyses (ppm).

Sample		Na	Mg	Al	Si	P	K	Ca	Ti	V	Cr	Mn	Fe	Co
1		3,8550	0,1665	0,4320	19,7225	2,8650	1,8775	31,5475	0,1534	0,0088	0,1173	0,0873	0,8013	0,0286
2		3,0833	0,1337	0,3157	16,5300	2,3733	1,4900	26,4267	0,1450	0,0074	0,0984	0,0679	0,6563	0,0245
3		3,2600	0,1378	0,3695	17,7000	2,5575	1,5900	27,9100	0,1383	0,0074	0,1025	0,0746	0,6893	0,0259
4		3,2075	0,1355	0,3535	16,3625	2,4175	1,5450	26,3000	0,1347	0,0075	0,0978	0,0725	0,6553	0,0247
5		3,2400	0,1430	0,3393	17,5300	2,5333	1,5633	27,9067	0,1210	0,0085	0,1035	0,0722	0,6867	0,0250
6		5,4800	0,3010	0,7013	27,7475	3,9575	2,9300	46,2750	0,2115	0,0138	0,1618	0,1275	1,1600	0,0429
7		2,9425	0,1073	0,2818	15,0150	2,1950	1,4700	29,4100	0,1081	0,0068	0,0925	0,0692	0,6838	0,0204
8		3,3350	0,1493	0,3485	17,6475	2,5100	1,6050	27,1700	0,1413	0,0078	0,1043	0,0773	0,6978	0,0265
9		3,4350	0,1355	0,3793	17,5525	2,5825	1,6400	29,0775	0,1603	0,0081	0,1041	0,0780	0,6998	0,0267
10	Blue	3,6250	0,1858	0,4168	18,0475	2,5300	1,8425	28,5700	0,1240	0,0096	0,1060	0,0821	0,7558	0,0280
	White	3,3650	0,1553	0,3913	16,4650	2,3825	1,6775	26,4425	0,1432	0,0078	0,0987	0,0752	0,6963	0,0263
11	Blue	2,5925	0,1360	0,3425	12,8975	1,8675	1,4400	21,9525	0,1260	0,0067	0,0768	0,0592	0,5733	0,0213
	Dark	5,7600	0,1967	0,5443	28,5667	4,3000	2,9533	56,5433	0,2607	0,0137	0,1777	0,1307	1,3667	0,0381
	White	17,7600	1,0870	2,3470	92,0167	13,1533	9,9667	153,8067	0,6743	0,0431	0,5383	0,4113	3,9533	0,1418
12	Blue	2,5975	0,0916	0,2550	12,9850	1,9550	1,3725	25,8550	0,1219	0,0060	0,0805	0,0606	0,6378	0,0172
	Dark	3,9000	0,1720	0,4593	20,3075	2,8625	1,9125	31,5775	0,1537	0,0088	0,1168	0,0875	0,8045	0,0297
	White	2,1275	0,0906	0,2528	10,8475	1,5800	1,0360	17,3450	0,0667	0,0049	0,0644	0,0475	0,4400	0,0166
13	Blue	3,9050	0,2173	0,5058	19,6700	2,8000	2,1125	32,7725	0,1325	0,0091	0,1166	0,0911	0,8510	0,0309
	Dark	7,4125	0,3875	0,9935	36,3925	5,3250	3,9750	61,1775	0,3548	0,0214	0,2193	0,1720	1,6050	0,0583
	White	5,6800	0,3163	0,7417	27,9733	4,0633	3,0733	46,8833	0,2523	0,0155	0,1663	0,1300	1,2233	0,0443
14	Blue	3,7525	0,2018	0,4805	18,8450	2,6150	1,9400	30,6225	0,1220	0,0085	0,1097	0,0852	0,7883	0,0308
	Dark	3,7200	0,1908	0,4618	19,2050	2,7175	1,9175	29,9425	0,1500	0,0093	0,1100	0,0845	0,7540	0,0294
15	Dark	5,0433	0,2333	0,6060	24,6600	3,6333	2,5200	41,0000	0,2257	0,0102	0,1493	0,1140	1,0340	0,0375
	White	6,4950	0,2858	0,7693	31,9775	4,6525	3,2150	52,7100	0,2293	0,0142	0,1955	0,1463	1,3450	0,0523
16	Dark	2,9900	0,1388	0,3568	14,8800	2,1800	1,5000	24,1300	0,1084	0,0072	0,0904	0,0660	0,6293	0,0237
	White	5,7400	0,2570	0,6708	28,1775	4,2375	2,8325	46,9625	0,2695	0,0122	0,1720	0,1267	1,1845	0,0444

		Na	Mg	Al	Si	P	K	Ca	Ti	V	Cr	Mn	Fe	Co
17	Vitreous	2,7500	0,1213	0,3115	14,9200	2,1300	1,3625	23,6200	0,0955	0,0063	0,0859	0,0623	0,5755	0,0211
		1,7875	0,0617	0,1750	8,9550	1,3300	0,9103	17,5650	0,0709	0,0041	0,0549	0,0419	0,4230	0,0124
18		3,1075	0,1330	0,3508	16,5575	2,3825	1,5125	25,8150	0,0982	0,0068	0,0957	0,0720	0,6408	0,0239
19		4,9800	0,2128	0,5315	27,2550	3,8450	2,4500	42,7050	0,1783	0,0113	0,1560	0,1130	1,0440	0,0394
20		7,8275	0,3198	0,8778	42,1050	5,9875	3,8425	65,5175	0,2658	0,0142	0,2465	0,1805	1,6750	0,0612
21		20,9500	1,1273	2,9500	108,1600	15,6325	11,6950	186,4400	0,6345	0,0521	0,6268	0,4940	4,8350	0,1730
22		77,1600	4,2100	10,2975	395,3675	56,7250	43,2850	671,5875	3,5700	0,1845	2,3125	1,7600	17,7025	0,6125
23		9,0075	0,4845	1,1995	44,2100	6,3050	4,8125	74,2575	0,4015	0,0188	0,2665	0,2008	1,9475	0,0683

The Detection limits of LA-ICP-MS glass analyses (ppm). (cont.)

		Ni	Cu	Zn	As	Rb	Sr	Y	Zr	Nb	Mo	Ag	Sn	Sb
1		0,0850	0,1393	0,1978	0,1690	0,0297	0,0058	0,0025	0,0052	0,0013	0,0109	0,0167	0,0129	0,0232
2		0,0714	0,1337	0,1283	0,1503	0,0242	0,0052	0,0019	0,0043	0,0012	0,0097	0,0115	0,0087	0,0177
3		0,0678	0,1473	0,1483	0,1533	0,0237	0,0058	0,0024	0,0040	0,0014	0,0119	0,0141	0,0073	0,0201
4		0,0648	0,1355	0,1188	0,1598	0,0242	0,0049	0,0019	0,0051	0,0012	0,0130	0,0099	0,0110	0,0186
5		0,0713	0,1507	0,1537	0,1480	0,0253	0,0053	0,0015	0,0042	0,0015	0,0103	0,0127	0,0087	0,0195
6		0,1230	0,2110	0,2743	0,2725	0,0470	0,0092	0,0034	0,0084	0,0017	0,0176	0,0211	0,0163	0,0339
7		0,0620	0,0982	0,1195	0,1315	0,0226	0,0041	0,0020	0,0034	0,0014	0,0000	0,0113	0,0088	0,0193
8		0,0744	0,1248	0,1503	0,1580	0,0255	0,0058	0,0025	0,0054	0,0017	0,0101	0,0137	0,0103	0,0173
9		0,0697	0,1325	0,1231	0,1548	0,0264	0,0047	0,0021	0,0047	0,0011	0,0113	0,0129	0,0105	0,0190
10	Blue	0,0798	0,1340	0,1748	0,1640	0,0294	0,0060	0,0026	0,0054	0,0021	0,0075	0,0135	0,0095	0,0238
	White	0,0745	0,1115	0,1335	0,1510	0,0273	0,0045	0,0020	0,0047	0,0017	0,0000	0,0112	0,0124	0,0179
11	Blue	0,0582	0,0978	0,1118	0,1313	0,0224	0,0036	0,0019	0,0037	0,0009	0,0086	0,0094	0,0102	0,0178
	Dark	0,1120	0,1813	0,2333	0,2630	0,0443	0,0083	0,0029	0,0112	0,0020	0,0185	0,0202	0,0163	0,0443
	White	0,3893	0,5613	0,6417	0,8657	0,1486	0,0224	0,0146	0,0165	0,0109	0,0441	0,0687	0,0557	0,1104
12	Blue	0,0499	0,0994	0,1180	0,1160	0,0198	0,0036	0,0018	0,0050	0,0010	0,0000	0,0116	0,0094	0,0178
	Dark	0,0823	0,1160	0,1798	0,1733	0,0304	0,0061	0,0021	0,0041	0,0017	0,0000	0,0149	0,0111	0,0226
	White	0,0447	0,0695	0,1032	0,0972	0,0173	0,0031	0,0014	0,0033	0,0013	0,0096	0,0074	0,0071	0,0129

		Ni	Cu	Zn	As	Rb	Sr	Y	Zr	Nb	Mo	Ag	Sn	Sb
13	Blue	0,0819	0,1595	0,1776	0,1880	0,0338	0,0066	0,0024	0,0045	0,0021	0,0100	0,0142	0,0182	0,0263
	Dark	0,1638	0,2855	0,3335	0,3683	0,0627	0,0105	0,0047	0,0108	0,0023	0,0324	0,0342	0,0394	0,0441
14	Blue	0,0757	0,1310	0,1706	0,1753	0,0312	0,0054	0,0016	0,0057	0,0016	0,0000	0,0135	0,0071	0,0242
	Dark	0,0750	0,1393	0,1415	0,1713	0,0314	0,0062	0,0020	0,0041	0,0022	0,0093	0,0126	0,0113	0,0211
15	Dark	0,0993	0,1820	0,2377	0,2433	0,0407	0,0081	0,0032	0,0074	0,0037	0,0108	0,0150	0,0151	0,0249
	White	0,1328	0,2193	0,3278	0,2938	0,0516	0,0087	0,0040	0,0077	0,0029	0,0164	0,0251	0,0331	0,0363
16	Dark	0,0675	0,1253	0,1186	0,1453	0,0248	0,0044	0,0017	0,0037	0,0000	0,0073	0,0092	0,0114	0,0169
	White	0,1221	0,1995	0,3045	0,2645	0,0499	0,0096	0,0043	0,0086	0,0019	0,0315	0,0238	0,0206	0,0339
17	Vitreous	0,0579	0,0930	0,1379	0,1300	0,0214	0,0042	0,0013	0,0044	0,0012	0,0083	0,0104	0,0082	0,0177
17		0,0398	0,0640	0,0840	0,0754	0,0131	0,0029	0,0014	0,0024	0,0008	0,0028	0,0068	0,0051	0,0119
18		0,0650	0,1027	0,1026	0,1468	0,0240	0,0053	0,0013	0,0048	0,0011	0,0078	0,0134	0,0116	0,0186
19		0,1147	0,1620	0,2058	0,2415	0,0392	0,0081	0,0028	0,0083	0,0025	0,0133	0,0236	0,0105	0,0303
20		0,1683	0,2635	0,3453	0,3705	0,0609	0,0110	0,0057	0,0146	0,0054	0,0169	0,0330	0,0212	0,0476
21		0,5080	0,6388	1,1948	1,0435	0,1888	0,0364	0,0134	0,0296	0,0118	0,0736	0,0842	0,0511	0,1435
22		1,6700	2,1225	3,2350	3,9400	0,6468	0,1146	0,0382	0,1106	0,0306	0,2188	0,3303	0,2833	0,4203
23		0,2020	0,3243	0,2910	0,4370	0,0755	0,0124	0,0054	0,0120	0,0042	0,0000	0,0305	0,0304	0,0542

The Detection limits of LA-ICP-MS glass analyses (ppm). (cont.)

		Cs	Ba	La	Ce	Nd	Sm	Eu	Tb	Dy	Er	Tm	Yb	Lu
1		0,0256	0,0245	0,0023	0,0032	0,0100	0,0097	0,0052	0,0000	0,0076	0,0050	0,0015	0,0114	0,0024
2		0,0210	0,0170	0,0016	0,0000	0,0000	0,0000	0,0048	0,0000	0,0065	0,0000	0,0011	0,0068	0,0020
3		0,0212	0,0210	0,0027	0,0016	0,0000	0,0000	0,0047	0,0012	0,0071	0,0043	0,0000	0,0083	0,0022
4		0,0209	0,0208	0,0014	0,0014	0,0000	0,0000	0,0032	0,0011	0,0055	0,0039	0,0014	0,0086	0,0020
5		0,0217	0,0207	0,0021	0,0012	0,0000	0,0000	0,0043	0,0019	0,0064	0,0047	0,0011	0,0062	0,0025
6		0,0366	0,0296	0,0029	0,0025	0,0099	0,0164	0,0060	0,0017	0,0107	0,0057	0,0030	0,0000	0,0042
7		0,0181	0,0109	0,0014	0,0011	0,0000	0,0097	0,0047	0,0000	0,0000	0,0049	0,0012	0,0085	0,0025
8		0,0218	0,0220	0,0018	0,0000	0,0075	0,0000	0,0050	0,0012	0,0094	0,0056	0,0000	0,0069	0,0020
9		0,0217	0,0144	0,0021	0,0017	0,0000	0,0113	0,0044	0,0013	0,0097	0,0000	0,0015	0,0000	0,0023

The Detection limits of LA-ICP-MS glass analyses (ppm). (cont.)

		Cs	Ba	La	Ce	Nd	Sm	Eu	Tb	Dy	Er	Tm	Yb	Lu
10	Blue	0,0233	0,0181	0,0029	0,0020	0,0000	0,0000	0,0033	0,0019	0,0047	0,0045	0,0000	0,0064	0,0032
	White	0,0225	0,0154	0,0024	0,0000	0,0000	0,0098	0,0037	0,0012	0,0059	0,0064	0,0015	0,0054	0,0023
11	Blue	0,0179	0,0121	0,0018	0,0009	0,0000	0,0072	0,0030	0,0011	0,0000	0,0043	0,0013	0,0054	0,0018
	Dark	0,0358	0,0314	0,0041	0,0034	0,0000	0,0000	0,0064	0,0029	0,0101	0,0000	0,0021	0,0216	0,0042
12	Blue	0,0162	0,0115	0,0012	0,0000	0,0065	0,0068	0,0041	0,0013	0,0039	0,0031	0,0017	0,0069	0,0021
	Dark	0,0247	0,0198	0,0016	0,0000	0,0112	0,0084	0,0059	0,0000	0,0065	0,0054	0,0013	0,0073	0,0033
	White	0,0135	0,0091	0,0015	0,0008	0,0059	0,0047	0,0026	0,0006	0,0026	0,0031	0,0009	0,0000	0,0015
13	Blue	0,0269	0,0216	0,0017	0,0000	0,0083	0,0078	0,0052	0,0000	0,0068	0,0054	0,0013	0,0059	0,0031
	Dark	0,0503	0,0350	0,0043	0,0000	0,0165	0,0000	0,0087	0,0020	0,0153	0,0068	0,0032	0,0090	0,0050
	White	0,0375	0,0300	0,0030	0,0020	0,0133	0,0000	0,0071	0,0019	0,0152	0,0080	0,0026	0,0137	0,0044
14	Blue	0,0245	0,0246	0,0026	0,0012	0,0070	0,0089	0,0031	0,0013	0,0058	0,0033	0,0020	0,0111	0,0030
	Dark	0,0241	0,0196	0,0023	0,0023	0,0093	0,0000	0,0052	0,0014	0,0057	0,0046	0,0019	0,0084	0,0020
15	Dark	0,0331	0,0352	0,0022	0,0017	0,0084	0,0141	0,0052	0,0000	0,0087	0,0078	0,0024	0,0139	0,0028
	White	0,0426	0,0403	0,0033	0,0025	0,0160	0,0215	0,0097	0,0029	0,0166	0,0088	0,0041	0,0164	0,0044
16	Dark	0,0192	0,0135	0,0013	0,0013	0,0000	0,0000	0,0045	0,0000	0,0000	0,0031	0,0015	0,0069	0,0019
	White	0,0370	0,0212	0,0015	0,0020	0,0211	0,0126	0,0064	0,0068	0,0057	0,0066	0,0014	0,0159	0,0034
17	Vitreous	0,0185	0,0155	0,0012	0,0010	0,0052	0,0078	0,0030	0,0010	0,0039	0,0039	0,0010	0,0057	0,0020
		0,0113	0,0123	0,0014	0,0008	0,0000	0,0000	0,0023	0,0008	0,0000	0,0028	0,0008	0,0054	0,0009
18		0,0201	0,0141	0,0013	0,0000	0,0000	0,0073	0,0040	0,0000	0,0051	0,0000	0,0015	0,0080	0,0019
19		0,0339	0,0234	0,0029	0,0023	0,0108	0,0125	0,0069	0,0025	0,0105	0,0079	0,0000	0,0087	0,0033
20		0,0517	0,0512	0,0042	0,0038	0,0192	0,0257	0,0097	0,0043	0,0000	0,0099	0,0031	0,0170	0,0043
21		0,1463	0,1046	0,0141	0,0000	0,0551	0,0592	0,0318	0,0125	0,0428	0,0264	0,0068	0,0401	0,0184
22		0,5118	0,3123	0,0447	0,0366	0,2390	0,2250	0,1241	0,0473	0,0860	0,2060	0,0000	0,2350	0,0508
23		0,0596	0,0439	0,0050	0,0000	0,0170	0,0000	0,0121	0,0035	0,0220	0,0106	0,0030	0,0193	0,0065

The Detection limits of LA-ICP-MS glass analyses (ppm). (cont.)

		Au	Pb	Bi	Th	U
1		0,0105	0,0289	0,0216	0,0000	0,0000
2		0,0084	0,0218	0,0165	0,0000	0,0000
3		0,0098	0,0240	0,0175	0,0000	0,0000
4		0,0097	0,0218	0,0191	0,0000	0,0000
5		0,0100	0,0221	0,0177	0,0000	0,0000
6		0,0206	0,0347	0,0345	0,0000	0,0000
7		0,0134	0,0226	0,0223	0,0000	0,0000
8		0,0092	0,0223	0,0182	0,0000	0,0000
9		0,0123	0,0223	0,0198	0,0000	0,0000
10	Blue	0,0083	0,0245	0,0210	0,0000	0,0000
	White	0,0108	0,0296	0,0197	0,0000	0,0000
11	Blue	0,0116	0,0167	0,0186	0,0000	0,0000
	Dark	0,0198	0,0403	0,0456	0,0000	0,0000
	White	0,0807	0,1258	0,1292	0,0000	0,0000
12	Blue	0,0157	0,0189	0,0211	0,0000	0,0000
	Dark	0,0130	0,0236	0,0217	0,0000	0,0000
	White	0,0055	0,0151	0,0112	0,0000	0,0000

		Au	Pb	Bi	Th	U
13	Blue	0,0147	0,0249	0,0281	0,0018	0,0000
	Dark	0,0291	0,0436	0,0493	0,0000	0,0000
	White	0,0196	0,0324	0,0405	0,0000	0,0000
14	Blue	0,0130	0,0232	0,0237	0,0000	0,0000
	Dark	0,0145	0,0258	0,0231	0,0000	0,0000
15	Dark	0,0172	0,0370	0,0289	0,0000	0,0000
	White	0,0254	0,0543	0,0384	0,0000	0,0000
16	Dark	0,0089	0,0210	0,0173	0,0000	0,0000
	White	0,0220	0,0371	0,0322	0,0000	0,0000
17	Vitreous	0,0088	0,0189	0,0153	0,0000	0,0000
		0,0067	0,0121	0,0135	0,0000	0,0000
18		0,0115	0,0223	0,0173	0,0000	0,0000
19		0,0147	0,0321	0,0284	0,0000	0,0000
20		0,0273	0,0588	0,0422	0,0000	0,0000
21		0,0987	0,1362	0,1443	0,0000	0,0000
22		0,2236	0,5068	0,5365	0,0000	0,0000
23		0,0334	0,0579	0,0606	0,0000	0,0000